EMID-702169

DEPARTMENT OF ENERGY

Environmental Management Los Alamos Field Office (EM-LA)
Los Alamos, New Mexico 87544

RECEIVED
JUN 29 2022
NMED Hazardous Waste Bureau

EMLA-2022-BF100-02-001

June 29, 2022

Mr. Rick Shean
Bureau Chief
Hazardous Waste Bureau
New Mexico Environment Department
2905 Rodeo Park Drive East, Building 1
Santa Fe, NM 87505-6313

Subject: Submittal of Interim Measures Final Report for Soil-Vapor Extraction of Volatile Organic Compounds from Material Disposal Area L, Technical Area 54, Revision 1

Dear Mr. Shean:

Enclosed please find two hard copies with electronic files of the "Interim Measures Final Report for Soil-Vapor Extraction of Volatile Organic Compounds from Material Disposal Area L, Technical Area 54, Revision 1." Enclosure 1 includes an electronic copy of a redline strikeout version of the report that incorporates all changes made in response to the New Mexico Environment Department's (NMED's) draft comments dated July 17, 2019, on the interim measures (IM) final report, submitted August 6, 2018. Responses to NMED's comments were submitted on February 8, 2022, and an updated version of the comment responses is included as Enclosure 2. This report compares the work performed with requirements in the "Interim Measure Work Plan for Soil-Vapor Extraction of Volatile Organic Compounds from Material Disposal Area L, Technical Area 54, Revision 1," submitted in September 2014 (LA-UR-14-26472).

This report is being issued with the approved administrative record title containing the phrase "Final Report." However, based on recent communications with NMED, aspects of the IM will continue as described in the Recommendations section of the report. The report presents vapor monitoring data collected from 2018 through 2021 that indicate the continuing effectiveness of the IM.

If you have any questions, please contact David Diehl at (505) 551-2496 (david.diehl@em-la.doe.gov) or Cheryl Rodriguez at (505) 414-0450 (cheryl.rodriguez@em.doe.gov).

Sincerely,

ARTURO DURAN

Digitally signed by ARTURO DURAN
Date: 2022.06.21 16:39:55 -06'00'

Arturo Q. Duran
Compliance and Permitting Manager
U.S. Department of Energy
Environmental Management
Los Alamos Field Office

Enclosure(s): Two hard copies with electronic files:

1. Interim Measures Final Report for Soil-Vapor Extraction of Volatile Organic Compounds from Material Disposal Area L, Technical Area 54, Revision 1 (EM2022-0290)
2. Revised Response to NMED Draft Comments on Interim Measures Final Report for Soil-Vapor Extraction of Volatile Organic Compounds from Material Disposal Area L, Technical Area 54, Dated July 17, 2019 (EM2022-0037)

cc (letter and enclosure[s] emailed):
Laurie King, EPA Region 6, Dallas, TX
Raymond Martinez, San Ildefonso Pueblo, NM
Dino Chavarria, Santa Clara Pueblo, NM
Steve Yanicak, NMED-DOE-OB
Chris Catechis, NMED-RPD
Jennifer Payne, LANL
Phillip Stauffer, LANL
Stephen Hoffman, NA-LA
William Alexander, N3B
Emily Day, N3B
David Diehl, N3B
Michael Erickson, N3B
John Hopkins, N3B
Kim Lebak, N3B
Joseph Legare, N3B
Dana Lindsay, N3B
Pamela Maestas, N3B
Joseph Murdock, N3B
William O'Neill, N3B
Troy Thomson, N3B
M. Lee Bishop, EM-LA
John Evans, EM-LA
Thomas McCrory, EM-LA
Michael Mikolanis, EM-LA
David Nickless, EM-LA
Lee Ocker, EM-LA
Cheryl Rodriguez, EM-LA
emla.docs@em.doe.gov
n3brecords@em-la.doe.gov
Public Reading Room (EPRR)
PRS website

Revised Response to NMED Draft Comments on Interim Measures Final Report for Soil-Vapor Extraction of Volatile Organic Compounds from Material Disposal Area L, Technical Area 54 Dated July 17, 2019

INTRODUCTION

To facilitate review of this response, the New Mexico Environment Department's (NMED's) comments are included verbatim. The U.S. Department of Energy (DOE) Environmental Management Los Alamos Field Office responses follow each NMED comment.

GENERAL COMMENTS

NMED Comment

1. *The Permittee has demonstrated that the SVE system is capable of removing VOC mass from the upper vadose zone. During 10 months of operation in 2015, the two SVE units reportedly removed approximately 553 kg (1217 lb) of total organic vapor mass. Effluent concentrations from both SVE-East and SVE-West reportedly decreased with time for all analytes. The permittee reports that a comparison of April 2015 mass estimates with those of the baseline 2014 estimates suggests substantial (~30%) SVE-induced mass reductions. NMED notes that reduction in VOC mass presented as a percentage of the total initial mass is unnecessary, inaccurate, and irrelevant because of the uncertainties associated with estimating the baseline VOC mass and the difficulty of quantifying continuing contributions to the plume by leaking containers.*

DOE Response

1. DOE concurs that the soil-vapor extraction (SVE) system is capable of removing volatile organic compound (VOC) mass from the upper vadose zone. This is the primary goal of the interim measure, to ensure that significant new leakage can be removed from the mesa before any impact to groundwater can occur.

   On the second point, DOE has removed the mass estimates.

NMED Comment

2. *The Permittee has demonstrated that the SVE system is capable of decreasing maximum VOC concentrations within the plume areas influenced by the system (i.e, the upper 300 ft bgs). Subsurface pore-gas sampling data collected during and after operation of the SVE reportedly indicate an overall reduction in concentration of VOCs when compared to 2014 baseline conditions. Some exceptions do exist. Boreholes 54-02089 and 54-24238, located in the eastern source region, both show an increase in VOC concentrations in response to SVE.*

DOE Response

Increased VOC concentrations were observed in shallow ports following SVE that occurred from January through November 2015. As discussed in the meeting with NMED on January 22, 2020, these increased VOC concentrations are likely associated with ongoing releases of VOCs from Material Disposal Area (MDA) L. There is not enough data to suggest that the increased leakage from 54-02089 and 54-24238 are in response to the SVE. There are two reasons we believe the increases seen in these two boreholes are not caused by the SVE system. First, based on measured concentrations in the source regions through time, we know that the subsurface drums and containers have continued to leak VOCs over the past 30+ years. Second, the pressure perturbation from the SVE units in the vicinity of the two wells (>75 ft from the SVE unit) showing increased concentrations during and after SVE are quite small, an unlikely driver for forcing new leakage.

NMED Comment

3. *The Permittee has demonstrated that the SVE system is not capable of reducing the extent of the vapor plume so that the plume remains well-contained within the upper vadose zone. Plume containment in the upper vadose is necessary to protect groundwater while final remedies are selected and implemented at the site. The Permittee presents two lines of evidence to demonstrate that the 10-month operation of the SVE system was successful at containing the plume. First, the concentration gradient of VOCs appears to have been reversed to an upward direction in some wells. Second, the overall VOC concentrations in the vapor plume area located within the tuff have generally decreased in response to SVE. However, some monitoring wells do not show a gradient reversal and the lateral and vertical extent of the plume does not appear to have been much reduced. Also, concentrations of several VOCs in deep monitoring well 54-24399 were detected above Tier-1 screening levels in 2017 pore-gas samples, even without using the double packer system required by NMED's July 19, 2016 Disapproval letter for Interim Measures Progress Report for Soil-Vapor Extraction of Volatile Organic Compounds from Material Disposal Area L, Technical Area 54. VOC concentrations in well 54-24399 may indicate that contaminants continue to migrate downward and that the current SVE system, which is only pilot-scale, is not capable of reducing contaminant concentrations below the tuff.*

DOE Response

One purpose of the SVE interim measure (IM) at MDA L is to ensure that significant new leakage in the source region is not allowed to impact groundwater. As noted in NMED comment #1, this goal has been achieved by the IM SVE system. The latest data (2021 periodic monitoring report [PMR]) show that concentrations in the deepest part of the Bandelier Tuff have decreased by half, and that the lateral edges of the plume are pulling back from the maximum extent. Continued operation of the SVE units in the future should help achieve continued reductions in concentrations in the deeper parts of the Bandelier Tuff.

Please see response to comments 4 and 5 below about monitoring in the basalt.

SPECIFIC COMMENTS

NMED Comment

4. Section 1.1 Background, page 2:

Permittee Statement: *Concentrations in the subsurface VOC plume are generally highest within 150 ft belowground surface (bgs) and decrease significantly with depth to the top of the Cerros del Rio basalts. Concentrations measured in the basalt are quite low, with values less than 1 ppmv.*

NMED Comment: *2016 pore gas monitoring results for borehole 54-24399, completed within the basalt, exceed 1 parts per million volume (ppmv) for multiple analytes. Revise the statement for accuracy and identify the analytes that exceed 1 ppmv in the basalt.*

DOE Response

The sentence in the executive summary will be modified to read "Concentrations measured in the basalt from 2017 through 2021 are quite low, with values less than 1 ppmv."

Installation of the permanent packer in 54-24399 appears to have reduced cross-contamination from the surface, resulting in lower concentrations in samples from 54-24399 and historical results from this vapor monitoring well may have been biased high due to VOCs moving down the previously open borehole during atmospheric high pressure periods. This idea is supported by the relatively high concentrations of benzene, toluene, ethylbenzene, xylene (BTEX) compounds from vehicle traffic at the surface found in data from 54-24399.

NMED Comment

5. Section 4.4 Monitoring Well 54-24399, page 11.

NMED has determined that the vapor samples collected at monitoring well 54-24399 are likely not representative of true VOC concentrations within the basalt. The borehole was initially drilled to investigate the presence of perched water and later repurposed for vapor monitoring. In the past, a dual packer system was successfully used to isolate a short section of basalt directly below the well casing from the rest of the 90' section of open borehole. The dual packer assembly was abandoned after claims of being damaged by a section of cavernous voids made up of sharp basalt and was replaced with a single packer placed within the well casing. NMED has previously directed the Permittee to return to using a dual packer system to isolate and sample distinct vertical intervals of basalt within the open borehole. NMED notes that even if a dual packer were to be used, borehole 54-24399 is still not an acceptable monitoring point to track the advancement of the VOC contamination plume in the basalt towards groundwater because the Permittee has not completely characterized the well. The Permittee was directed in NMED's July 19, 2016 Disapproval letter for Interim Measures Progress Report for Soil-Vapor Extraction of Volatile Organic Compounds from Material Disposal Area L, Technical Area 54 to submit a work plan to recharacterize well 54-24399. The Permittee has not complied. Additionally, the Permittee has reported that because of the large voids in the basalt, it is unlikely that borehole 54-24399 was sealed between the formation and the casing, potentially creating a short circuit from the base of the Bandelier Tuff to the 566.7-ft monitoring point. Therefore, the Permittee must submit a work plan for a replacement deep vapor monitoring well to determine vertical extent of the VOC vapor plume. The borehole must be drilled just short of the water table and be capable of sampling discreet intervals in isolation from the rest of the borehole.

DOE Response

As discussed in the meeting with NMED on January 22, 2020, monitoring data from the two angled vapor monitoring wells within the Cerros del Rio basalt (54-01015 and 54-01016) support the concept that VOC concentrations within the basalt are well mixed and relatively uniform because of the nature of transport processes (advection and dispersion within factures and highly porous interflow rubble zones [Stauffer et al. 2019]).

The recommendation that NMED agreed to in the January 2020 meeting is to retain vapor monitoring well 54-24399 and keep it within the current sentry borehole monitoring program (twice a year). Data from 54-24399 coupled with data from nearby and deeper ports within the basalt should provide adequate characterization of VOC concentrations within the basalt and response to potential future SVE operations. These recommendations are based on our current conceptual model for vapor-phase flow and transport within the basalt, as published in “Evidence for High Rates of Gas Transport in the Deep Subsurface” (Behar et al. 2019), and illustrated in the figure below.

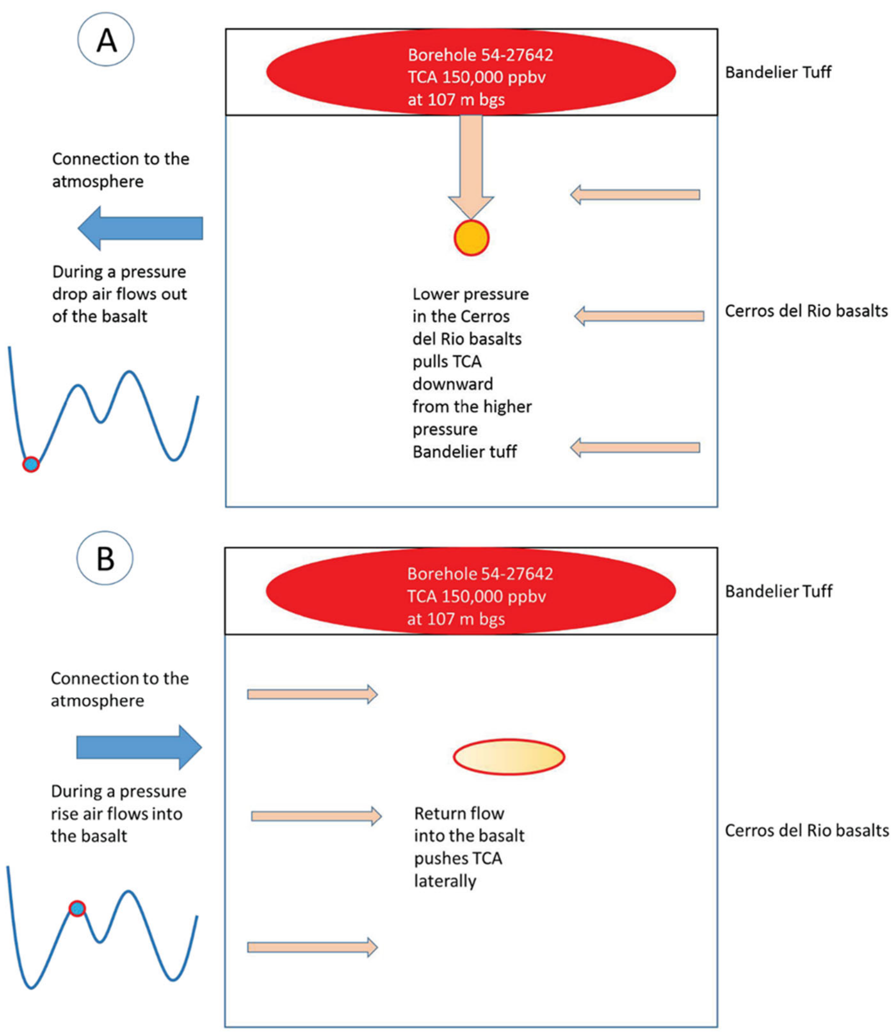

NMED Comment

6. ***Section 5.0 Numerical Analysis, page 15:***

   The Permittee conducted site-scale modeling in support of decision analysis undertaken at MDA-L, primarily to demonstrate that the current SVE system is capable of remediating a sudden release of solvents and that such remediation could happen over a relatively short period (2 yr of SVE). The Permittee did not provide the modeling information such as numerical modeling input parameters, including uncertainties and technical defensibility, along with modeling results (i.e., predictions) that reflect new data inputs. As a result, NMED cannot review or approve the modeling results presented in the Final Report nor evaluate the Permittee's recommendations for activating the SVE system based on modeling results. Activation of the SVE system must be based on actual soil vapor data.

DOE Response

DOE concurs that detection of a sudden release and associated changes in VOC concentrations would be entirely based on actual soil vapor data.

We will be monitoring pore gas in the sentry boreholes semiannually. We propose that if the concentration of total VOCs in any sentry borehole are above 2000 ppmv for three consecutive monitoring periods, the SVE system will be restarted within 1 year. The 2000 ppmv trigger is based on historic data during times when the plume in the source region regularly maintained 3000 ppmv with no apparent risk to groundwater. The 2000 ppmv total VOC trigger is thus conservative from a historical perspective. Currently, maximum VOC in the latest sampling rounds (2021) is on order of 500 ppmv or less.

The modeling results are used for insight into the potential impacts of a significant new release, the ability of the SVE system to mitigate a significant new release, and the timeframe associated with detection and response. The use of simulations to predict the behavior of the SVE system is supported by similar work in a variety of other fields, including petroleum engineering, groundwater management, and nuclear waste management. Simulations were developed by a team with extensive experience using state-of-the-art tools. A published, peer-reviewed version of the SVE modeling is presented in "An Investigation of Plume Response to Soil Vapor Extraction and Hypothetical Drum Failure" (Behar et al. 2019). DOE will include an appendix in the next version of the IM report summarizing modeling details. DOE is also available to meet with NMED to further explain the assumptions and details of the modeling and can provide input files, executables, and guidance should NMED wish to run the simulations on their own computer systems. DOE will continue to use the model results to guide our understanding of how the SVE system interacts with the subsurface because this is the only scientific tool available that incorporates the physics of three-dimensional time-dependent plume changes from both pumping and natural diffusive processes. DOE will add Appendix F to the "Interim Measures Final Report for Soil-Vapor Extraction of Volatile Organic Compounds from Material Disposal Area L, Technical Area 54, Revision 1" to include more modeling details.

NMED Comment

7. ***Section 8.0 Recommendations, page 20:***

   a) ***Sampling schedule:*** *NMED concurs with the Permittee's recommendation to conduct semiannual monitoring of sentry boreholes to allow early detection of potential container failure and monitoring of peripheral boreholes once every two years to monitor for evidence of plume expansion.*

DOE Response

DOE concurs.

b) Activation of the SVE system: *Until the vertical extent of the VOC contamination in the basalt is determined, a more conservative approach to protection of human health and groundwater from VOCs at MDA-L must be followed. The Permittee must revise the recommendations for activating the SVE system to use the Tier 1 pore gas concentrations presented in Table 4.3-1, which correspond to applicable groundwater standards. The Permittee must also conduct an evaluation of the vapor intrusion pathway including comparison of site data to the most recent NMED vapor intrusion screening levels and incorporate the evaluation as appropriate into recommendations for activating the SVE system.*

DOE Response

The purpose of the SVE IM at MDA L is to ensure that significant new leakage in the source region is not allowed to impact groundwater. As noted in NMED comment #1, this goal has been achieved by the IM SVE system. DOE will operate the SVE systems annually moving forward. DOE will also continue to base more aggressive operation of the SVE (2000 ppmv) on historic measurements of the source region that do not appear to have put groundwater at risk. DOE is eager to work with NMED to design a Tier II threshold for MDA L similar to the Tier II approach designed for MDA C, but including relevant physics and chemistry at MDA L. The MDA L Tier II approach will need to include the breathing basalt and three-dimensional effects that limit the ability of VOC to migrate to depth.

Additionally, in PMRs, the vapor-phase monitoring data will be compared with NMED's vapor intrusion screening levels presented in Table A-1 of the NMED Risk Assessment Guidance for Site Investigations and Remediation (https://www.env.nm.gov/hazardous-waste/guidance-documents/).

NMED Comment

8. *VOC concentrations at MDA-L have been measured above Tier-1 screening levels and at depths in excess of 500 feet bgs. The existing SVE units pull subsurface gas from the open uncased part of the boreholes, from 65 to 215 ft bgs in the east SVE well and 65 to 115 ft bgs in the west SVE well. Results from the 10-month operation of the SVE system indicate that the system is capable of reducing VOC concentrations at depths up to 350' bgs. However, the long-term effectiveness of SVE on VOCs at depths greater than 300'bgs has not been clearly demonstrated. 2017 pore gas data from the deepest monitoring ports at location 54-27642 (up to 340.5 ft bgs) show VOC concentrations rebounding to above 2014 baseline conditions. VOC concentrations measured in borehole 54-24399 at depths of 567 ft bgs and 588 ft bgs show no response to the SVE system. Additionally, the Permittee's report that data from the gas-phase tracer test conducted in the Cerros del Rios basalts indicate that tight coupling between the atmosphere and the subsurface pressure in the basalt enhances vapor diffusivity, moves contaminants more rapidly in all directions, and may shorten the arrival time of contaminants at the regional aquifer. Therefore, the Permittee must modify the current interim measures system to extract VOCs from deeper in the mesa by adding two additional boreholes. The two existing shallow SVE boreholes will continue to provide focused extraction in the higher concentration zones while extraction in two deeper boreholes will provide additional protection to the ground water resource by retarding migration of VOCs to greater depths and reducing maximum VOC concentrations in the basalt. The Permittee should incorporate adaptive management principles into the design of the system so that the focus of extraction can be varied in response to*

vapor monitoring results that indicate an increase in contamination (e.g., drum failure in a shaft or increased contaminant levels at depth via vapor plume migration).

DOE Response

As discussed in the January 22, 2020, meeting with NMED, DOE believes that additional deep vapor-extraction wells in the Cerros del Rio would not improve groundwater protection better than extraction in higher concentration/higher mass portions of the vapor plume above the basalt. Protecting the groundwater beneath MDA L can be accomplished through suction applied to an open section of borehole reaching from approximately 60 ft below ground surface (bgs) to near the bottom of the Qbt 1g. Additionally, deeper suction could pull higher concentrations toward the deeper extraction interval, which would be detrimental to the overall goal of preventing VOCs from impacting the regional aquifer.

The current SVE system should be sufficient to protect groundwater from a significant new release until a final remedy is designed and implemented through the corrective measures evaluation (CME)/ corrective measures implementation (CMI) process. It is recommended that additional information that supports this approach be included in the strategy presented either in a revision to the August 2018 Interim Measures Final Report.

See responses to NMED comments #3 and #7, which both relate to the difference between the SVE IM and the upcoming CME/CMI for MDA L.

REFERENCES

2019 Stauffer, P.H., T. Rahn, J.P. Ortiz, L.J. Salazar, H. Boukalfa, H.R. Behar, and E.E. Snyder, March 2, 2019. “Evidence for High Rates of Gas Transport in the Deep Subsurface,” *Geophysical Res.* Let, 46. doi.org/10.1029/2019GL082394. (Stauffer et al. 2019)

2019 Behar, H.R., E.E. Snyder, S. Marczak L.J. Salazar, B. Rappe, G. Fordham, S.P. Chu, D. Strobridge, K.H. Birdsell, T.A. Miller, K.C. Rich, and P.H. Stauffer, February 14, 2019. “An Investigation of Plume Response to Soil Vapor Extraction and Hypothetical Drum Failure,” *Vadose Zone J.,* 18(1), doi: 10.2136/vzj2018.04.0080. (Behar et al. 2019)

June 2022
EM2022-0290

Interim Measures Final Report for Soil-Vapor Extraction of Volatile Organic Compounds from Material Disposal Area L, Technical Area 54, Revision 1

Newport News Nuclear BWXT–Los Alamos, LLC (N3B), under the U.S. Department of Energy Office of Environmental Management Contract No. 89303318CEM000007 (the Los Alamos Legacy Cleanup Contract), has prepared this document pursuant to the Compliance Order on Consent, signed June 24, 2016. The Compliance Order on Consent contains requirements for the investigation and cleanup, including corrective action, of contamination at Los Alamos National Laboratory. The U.S. government has rights to use, reproduce, and distribute this document. The public may copy and use this document without charge, provided that this notice and any statement of authorship are reproduced on all copies.

EM2022-0290

Interim Measures Final Report for Soil-Vapor Extraction of Volatile Organic Compounds from Material Disposal Area L, Technical Area 54, Revision 1

June 2022

Responsible program director:

Printed Name	Signature	Title	Organization	Date
Michael Erickson		Program Director	RCRA Remediation Program	June 20, 2022

Responsible N3B representative:

Printed Name	Signature	Title	Organization	Date
Troy Thomson		Program Manager	N3B Environmental Remediation Program	June 20, 2022

Responsible DOE-EM-LA representative:

Printed Name	Signature	Title	Organization	Date
Arturo Q. Duran	ARTURO DURAN Digitally signed by ARTURO DURAN Date: 2022.06.29 13:00:34 -06'00'	Compliance and Permitting Manager	Office of Quality and Regulatory Compliance	

EXECUTIVE SUMMARY

This interim measures (IM) final report summarizes the results from 10 mo of continuous soil-vapor extraction (SVE) operation at two vapor-extraction wells at Material Disposal Area (MDA) L, Technical Area 54. The SVE-West system began operation on January 9, 2015, and the SVE-East system began operation on January 26, 2015. Both the East and West systems were turned off for the winter on November 18, 2015. During the period of operation, the two SVE units removed 553 kg (1217 lb) of total organic vapor mass. The mass was primarily removed from within an approximately 150-ft radius surrounding the extraction wells. Following the initial 10-mo SVE operation, short duration (2-d) rebound testing was performed in 2016. A final 25-d rebound test on SVE-East was performed in June 2017. These rebound tests were performed to provide additional insight into plume behavior and to create a data set for model validation.

Baseline and annual pore-gas monitoring samples were collected from 185 pore-gas sampling ports in 28 boreholes within and surrounding MDA L. Quarterly pore-gas monitoring samples were collected from a subset of ports in 14 boreholes located within a 150-ft radius of the SVE units through August 2017. Beginning in 2019, monitoring followed recommendations developed in the IM to sample 28 boreholes every other year while sampling 7 sentry wells twice a year. Pore-gas sampling results confirm SVE operation has reduced the concentrations at most sampling ports to below their baseline values. The radius of influence of both SVE wells is at least 150 ft, increasing the previous estimates from shorter duration SVE testing.

This report is being submitted with the approved administrative record title containing the phrase “Final Report.” However, based on communications with the New Mexico Environment Department (NMED), aspects of the IM will continue as described in the recommendations discussed below.

Revision 1 of this report incorporates revisions based on NMED draft comments dated July 17, 2019, and vapor-monitoring data collected from 2018 to 2021 that show the effectiveness of the IM. Data collected during the IM has been analyzed and used to calibrate and validate a three-dimensional numerical model of the site. The numerical model was used to explore scenarios of hypothetical future releases at the site and present suggestions to support the selection and design of a final remedy for MDA L. Recommendations include the following:

1. Conduct semiannual monitoring of boreholes located in the source region (“sentry boreholes”) to allow early detection of potential container failure. Boreholes 54-27641 and 54-24240 on the western side of MDA L are sentry boreholes. On the eastern side of MDA L, boreholes 54-24238, 54-24241, and 54-27642 and open borehole 54-24399 are sentry boreholes. Peripheral borehole 54-02089 was added to the sentry borehole sampling network in 2020 because of an increase in concentrations over the last several sampling events.
2. Monitor peripheral boreholes once every 2 yr for evidence of plume expansion or contraction.
3. Conduct semiannual monitoring of deep borehole 54-24399 to further characterize long-term trends of volatile organic compound (VOC) concentrations in the basalt and to provide data needed to support the Corrective Measures Evaluation process (e.g., updating the conceptual model for transport and developing Tier II screening levels and cleanup goals).
4. Operate the SVE units to continue efficient VOC mass removal. Operation of the SVE units will initially be in the spring and fall seasons, and effluent data will be used to determine the duration of each extraction cycle. The operation schedule of the SVE units may be modified, with NMED concurrence, to adapt to changing subsurface concentration data and will continue until a final remedy is implemented at MDA L.

5. Activate the eastern SVE unit if, at any time, total VOC concentrations in any ports in the eastern sentry boreholes rise above 2000 ppmv with a trend of consistent increase with each consecutive measurement for ports to depths of 100 ft, and adapt the eastern SVE system as necessary to run as continuously as possible until concentrations drop below 2000 ppmv.
6. Activate the western SVE unit if, at any time, total VOC concentrations in any ports in the western sentry boreholes rise above 2000 ppmv, with a trend of consistent increase with each consecutive measurement for ports to depths of 100 ft, and adapt the western SVE system as needed to run as continuously as possible until concentrations drop below 2000 ppmv.
7. Report all monitoring data and SVE operations details in a single report to be submitted annually to NMED. This report will replace the current MDA L Periodic Monitoring Report and be renamed to indicate the addition of the SVE operations details.

CONTENTS

Figures

Tables

Appendixes

Plate

1.0 INTRODUCTION

This interim measures (IM) final report summarizes results from a soil-vapor extraction (SVE) operation at two extraction wells at Material Disposal Area (MDA) L, Technical Area 54 (TA-54), within the boundaries of Los Alamos National Laboratory (LANL or the Laboratory). These activities were conducted in accordance with the "Interim Measures Work Plan for Soil-Vapor Extraction of Volatile Organic Compounds from Material Disposal Area L, Technical Area 54, Revision 1" (hereafter, the IMWP) (LANL 2014, 261843). The IMWP was submitted to the New Mexico Environment Department (NMED) on September 15, 2014, in response to requirements in NMED's "Approval with Modifications, Interim Measures Work Plan for Soil-Vapor Extraction of Volatile Organic Compounds from Material Disposal, Area L," dated July 17, 2014 (NMED 2014, 525053). The IMWP had the following objectives:

- Remove volatile organic compound (VOC) mass from the subsurface
- Reduce maximum VOC concentrations
- Contain the vapor plume within the Bandelier Tuff units

The activities in the IM focus on removing mass from the VOC vapor plume beneath MDA L to protect groundwater until final remedies are implemented at the site. VOC mass removal is a proactive step that will reduce both vapor concentrations and the extent of the subsurface vapor plume. Because there is uncertainty related to plume migration in the deep basalt toward the regional aquifer, SVE was recommended as a method for containing the vapor plume within the Bandelier Tuff during the IM.

The IMWP also states that "the Laboratory plans to run the interim measure for an initial 1-yr extraction period, evaluate the data, and make a decision about continuing the interim measure. A decision to continue the interim measure will be based on multiple metrics, including extraction efficiency, plume evolution, and available budget. If SVE is continued, a similar decision strategy will be revisited annually until a final remedy is implemented."

Following 6 mo of operation, a progress report was submitted to NMED on September 28, 2015 (LANL 2015, 600930). In May, 2016, LANL submitted to NMED an annual progress report (LANL 2016, 601484).

Revision 1 of this report incorporates revisions based on NMED draft comments dated July 17, 2019 (NMED 2019, 700515) and vapor-monitoring data collected from 2018 to 2021 that show the effectiveness of the IM. The data in the original IM report were collected from August 2014 to August 2017. Though initial plans were to run the SVE IM for a full year, concerns over damage to the system caused by freezing of condensation in the winter months led to modification of the plan, and the SVE units were shut down in November 2015. Following the initial 10 mo SVE operation, short duration (2-d) rebound testing was performed in 2016 with the goal of gathering more data on plume behavior. A final 25-d rebound test was undertaken in June 2017 using the eastern SVE unit.

Remediation of the vapor plume by SVE is included as part of the recommended final remedy in the "Corrective Measures Evaluation Report for Material Disposal Area L, Solid Waste Management Unit 54-006, at Technical Area 54, Revision 2" (hereafter, the CME report) to meet the remedial action objective of preventing groundwater from being impacted above a regulatory standard by the transport of volatile organic compounds (VOCs) to groundwater through soil vapor (LANL 2011, 205756). The depth to regional groundwater beneath MDA L is on the order of 285 m (935 ft), whereas the vapor plume is predominantly within the Bandelier Tuff in the upper 90 m (300 ft) of the subsurface. The tuff units beneath the surface at MDA L are underlain by a thick (nearly 150-m [500-ft]) sequence of Cerros del Rio basalts. There is uncertainty regarding the long-term transport of vapors downward through the basalt toward the water table. Therefore, it is desirable to contain the plume above the basalt. The SVE IM is a proactive step to remove VOC mass, to decrease maximum VOC concentrations within the plume, to reduce the current extent of the vapor plume so it remains well-contained within the upper tuff units, and to gather design information for a potential final corrective measures remedy. The CME report was withdrawn by the U.S. Department of Energy (DOE) in October 2016 (DOE 2016, 601899) based on an updated schedule of environmental cleanup activities at TA-54. The 2011 CME report will be updated and resubmitted in the future in accordance with the revised schedule.

To better characterize the transport properties of the Cerros del Rio basalts, a gas-phase tracer test was implemented in conjunction with the SVE IM. Results from the tracer test in the Cerros del Rio basalts yield estimates of effective diffusivity that are orders of magnitude above simple porous diffusion. The enhanced diffusivity is a result of tight coupling between the atmosphere and the subsurface pressure in the basalt. The impact of enhanced vapor diffusivity in the basalt is to move contaminants more rapidly in all directions. This may shorten the arrival time of contaminants at the regional aquifer; however, because of later spreading in three dimensions, the mass flux to a given location at the top of the regional aquifer could be reduced relative to that predicted with a simpler one-dimensional diffusion calculation. Variability in VOC data from boreholes in the basalts suggests that a more complex conceptual model may be needed to explain transport through this horizon.

1.1 Background

MDA L operated from the early 1960s to 1986 as the designated disposal area for nonradiological liquid chemical wastes, including containerized and uncontainerized liquid wastes; bulk quantities of treated aqueous waste; batch-treated salt solutions and electroplating wastes, including precipitated heavy metals; and small-batch quantities of treated lithium hydride. Waste was disposed of in 1 pit, 3 impoundments, and 34 shafts (Plate 1).

Disposal Shafts 1 through 34 were dry-drilled directly into the Tshirege Member of the Bandelier Tuff. The shafts range from 3 to 8 ft in diameter and from 15 to 65 ft in depth. The 34 disposal shafts were used to dispose of containerized and uncontainerized liquid chemical wastes and precipitated solids from the treatment of aqueous waste. Before 1982, containerized liquids were disposed of without the addition of absorbents. Small containers were typically dropped into a shaft. Larger drums were lowered by crane and arranged in layers of one drum in a 3- or 4-ft-diameter shaft, four to five drums in a 6-ft-diameter shaft, or six drums in an 8-ft-diameter shaft. The space around the drums was filled with crushed tuff, and a 6-in. layer of crushed tuff was placed between each layer of drums. Uncontainerized liquid wastes were also disposed of in the shafts. Between 1982 and 1985, only containerized wastes (including organic and inorganic liquids, precipitated heavy metals, and stabilized heavy metals) were disposed of in the shafts. These shafts are the primary source for the subsurface VOC vapor plume that is present beneath MDA L (LANL 2011, 205756).

Soil-vapor monitoring boreholes located within and around MDA L have been used to characterize the nature and extent of the subsurface vapor plume at the site since 1986. Figure 1.1-1 shows the pore-gas monitoring boreholes at MDA L. Concentrations in the subsurface VOC plume are generally highest within 150 ft below ground surface (bgs) and decrease significantly with depth to the top of the Cerros del Rio basalts. Concentrations measured in the basalt from 2017 through 2021 are quite low, with values of all measured VOCs at less than 1 ppmv.

The CME report used a two-tiered screening approach to identify the VOCs present at high enough concentrations within the vapor plume to potentially impact groundwater above a regulatory standard if they migrated to groundwater (LANL 2011, 205756). The analysis found vapor concentrations for

1,1,1-trichloroethane (1,1,1-TCA); trichloroethene (TCE); tetrachloroethene (PCE or PERC); methylene chloride; 1,2-dichloropropane (1,2-DCP); 1,1-dichloroethene (1,1-DCE); 1,2-dichloroethane (1,2-DCA); and 1,4-dioxane present within the tuff units at concentrations that exceed their Tier II screening levels (LANL 2011, 205756). However, the one-dimensional diffusion assumptions used in the Tier II screening analysis are not consistent with field measurements of barometric pumping and VOC concentration variability in the basalt.

The hydrogeologic framework for the contaminated subsurface at MDA L is based on years of data collection, including results from a 2006 pilot SVE test at the site (LANL 2006, 094152). The current IM used the same two wells that were used during the pilot test: SVE-East and SVE-West (Figure 1.1-1). Data gathered in 2006 and subsequent analysis (Stauffer et al. 2007, 097871; Stauffer et al. 2011, 255584) were used to create three-dimensional (3-D) numerical simulations that provided expected total mass removal from the two SVE units during the IM.

2.0 OPERATION OF SVE UNITS

2.1 Description of SVE Units

The two SVE systems have a main blower unit rated to 129 standard cubic feet per minute (scfm) at vacuum equal to 42.5 kPa (120 in. of water), a knock-out trap for liquid, various in-line flow and pressure-measurement instruments, and an off-gas stack to the atmosphere (Figure 2.1-1). The SVE blower systems are 11-ft long × 3-ft wide skid-mounted Model 4L SVE Blower Package systems provided by Catalytic Combustion Corp. of Bloomer, WI (Figure 2.1-2).

The SVE units pull subsurface gas from the open uncased part of the boreholes, 65 to 215 ft bgs on the east SVE well and 65 to 115 ft bgs on the west SVE well. Condensed liquid (water) is removed in the SVE unit knock-out tank, and the effluent gas is filtered with a rough particulate filter to protect the blower from large particulate material that may be present. Untreated effluent gas from each SVE unit is then discharged through a stack located 21 ft above ground surface. Samples representative of the extracted gas are collected from a sample port (SP1) located between the blower and the exhaust stack. Each unit is equipped with a manual air dilution valve (V1) that is closed at all times (Figure 2.1-1).

The gas-flow rate is measured at each wellhead using a Dwyer Series PE Orifice Plate Flow Meter (Model PE-H-2) equipped with a Dwyer 0–25 in. of water Magnehelic Differential Pressure Gage. Flow rate is calculated using the measured differential pressure across the orifice plate, line pressure, and temperature using a formula provided by the manufacturer of the flow meter (Appendix A, on CD included with this document). This calculation is also corrected for a local atmospheric pressure of 80 kPa. Output from the calculation are in scfm. Readings from the differential pressure gage, pipeline temperature, and pressure are recorded by the operator and used to calculate the instantaneous flow rate per Detailed Operating Procedure ER-DOP-20242, “Soil Vapor Extraction System Setup, Operation, and Monitoring Procedure.” During the first 3 wk of operation, each system was monitored 7 d/wk. Following the first 3 wk of operation, each system was inspected and monitored by the operator a minimum of 4 d (Mondays through Thursdays) each week.

2.2 Data Collection Methods and Results

SUMMA canisters were used for both SVE gas effluent and subsurface pore-gas sampling. Evacuated canisters were attached to valved T-ports and allowed to equilibrate to atmospheric pressure before sealing. All SUMMA samples were analyzed by an independent analytical laboratory, Eurofins Air Toxics, Inc., using U.S. Environmental Protection Agency (EPA) Method TO-15. Eurofins Air Toxic is a National

Environmental Laboratory Accreditation Program–certified laboratory. The data are entered into the Environmental Information Management (EIM) database and undergo a secondary validation. EIM is the official database for environmental data collected by both the Laboratory and NMED. Table 2.2-1 lists the organic compounds analyzed by EPA Method TO-15 from samples collected from the effluent streams of the active SVE units and subsurface pore-gas sampling ports. Analytical results from samples collected during SVE operation are presented in Appendix B (on CD included with this document).

All data analyzed by Eurofins Air Toxics using the EPA Method TO-15 are reported to the Laboratory in units of ppbv. To convert from ppbv to ppmv, one divides by 1000. Both ppmv and ppbv are used in this report. Concentrations expressed as ppmv or ppbv are independent of temperature or pressure. NMED has also requested that the Laboratory provide concentrations in μg/m^3, and these units are included in Appendix B. To convert between the two units, one must know the molecular weight of the contaminant and that of air as well as the density of air, which is a function of temperature and pressure. Air is a mixture of many gases but can be approximated as having a molecular weight of 29 g/mol. The primary VOC at MDA L, TCA, has a molecular weight of 133 g/mol. Assuming the density of air on the mesa (top elevation, average atmospheric pressure, and temperature of 2072 m, 80 kPa, and 10°C: 6800 ft, 11.6 psi, and 50°F) is approximately 1 kg/m^3, a concentration of 1000 ppmv TCA can be converted to μg/m^3 as follows:

1000 ppmv = 1000 moles TCA/1e6 moles air

1000 moles TCA * 133 g/mol * 1e6 μg/g = 133.e9 μg TCA

1e6 moles Air * 29 g/mol * 1 m^3/kg * 1e-3 kg/g= 29,000 m^3

yielding

133.e9 μg/29,000 m^3 = 4.6e6 μg/m^3

Within Laboratory databases, units of ppbv provided by the analytical laboratory are converted to μg/m^3 using the assumption of constant gas density at standard pressure and temperature (101.325 kPa, 25°C) with conversion factors for each compound based on individual molecular weights. Because the actual pressures and temperatures are not constant for each measured sample, this required assumption of the conversion from ppbv to μg/m^3 introduces an error into the μg/m^3 values that could be up to 20% (Stauffer et al. 2007, 097871).

2.2.1 Effluent Gas from SVE Units

Effluent gas from each SVE system was sampled in accordance with the sampling plan outlined in the IMWP (LANL 2014, 261843). Section 12[2] of ER-DOP-20242 outlines the steps taken to collect the gas sample from sampling port SP1 on each unit (Figure 2.1-1). Data were collected by connecting tubing from port SP1 to the SUMMA canister. Port SP1 was then opened, followed by opening of the SUMMA canister valve. Samples were collected in SUMMA canisters more frequently early in the operation of the system. As operation of the system continued and the vapor concentrations of VOCs were observed to level out, the sampling frequency decreased. Section 2.3.1 of this report presents the SVE effluent sampling schedule.

2.2.2 Calculation of Mass Removal from SVE Effluent and Gas Flow Rate

Calculation of mass removal is based on two principles: numerical integration of the flow rate and concentration data and interpolation of the results to the desired date. Numerical integration is based on the trapezoid method, and the interpolation is always linear. No results are extrapolated beyond the last measurement.

The first step in the numerical integration is the calculation of the volume of the gas pumped. The flow rate versus time curves are integrated, producing two curves of volume pumped versus time: one each for the SVE-East and SVE-West units. Total pumped volume versus time is produced by adding the SVE-East and SVE-West curves. The addition process includes interpolation of the results from the SVE-West volume versus time curve to time concurrent with data collection used to generate the SVE-East curve. This is necessary because the SVE-West and SVE-East flow rate and concentration data are not measured at exactly the same time.

In the second step, concentration versus time columns are (virtually) constructed, transferred to the concentration versus volume scale (using volume pumped values from the first step) and numerically integrated, producing total mass removed. The “concentration” in this process may be a concentration of the individual compound or a total concentration (sum of all VOC concentrations). Finally, the SVE-West and SVE-East mass removal curves are added together using interpolation. Example calculations for effluent mass removal are included in Appendix C.

VOC concentrations from SUMMA samples are reported by the analytical laboratory in ppbv units. Laboratory values are stored in the EIM database as “Laboratory Result.” The EIM database recalculates the ppbv concentrations to $\mu g/m^3$ values using molar mass, and standard temperature and pressure (101.325 kPa, 25°C). Recalculated values (in $\mu g/m^3$) are stored by the database as “Reported Result,” and these data were used to calculate total mass removed.

2.2.3 Subsurface Pore-Gas Sampling

Subsurface pore-gas sampling during the active SVE and rebound phases of the IM was performed from April 2015 to August 2017 in accordance with Standard Operating Procedure EP-ERSS-SOP-5074, “Sampling Subsurface Vapor.” Current subsurface pore-gas sampling is performed under “Sampling Subsurface Vapor,” N3B-SOP-ER-2008.

Baseline (Quarter 4 2014) and annual monitoring samples were collected from pore-gas sampling ports in 28 boreholes (Table 2.2-2). Quarterly samples were collected from a subset of ports in 14 boreholes located within a 150-ft radius of the SVE units (Table 2.2-3).

Sampling involves a set of steps for each well and port. This process begins when a well is opened and a radiological control technician (RCT) monitors the well for radioactivity. If the activity levels are less than 20 $\mu Ci/m^3$, each port is opened and the RCT monitors the area above each port within 2 in. of the opening. If any ports are found to be higher than 20 $\mu Ci/m^3$, the port is allowed to breathe and then is monitored again. Next, the sampling team records static subsurface pressure with a handheld digital manometer. Once static pressure has been measured, the sample port is connected to the sample train shown in Figure 2.2-1.

The sample train consists of tubing that connects the sample port to a pair of isolation valves. The isolation valves allow the SUMMA canister to be bypassed during purging. The sample train continues past the isolation valves into a Sierra Instruments Top-Trak Mass Flow Meter that displays the purge rate and total purge volume in standard liters per minute. The flow meter is connected to a Brailsford & Company single-head portable pump that produces a flow rate of 4 to 5 L/min. Exhaust from the pump is routed through a Geotech MultiRAE portable screening instrument that measures CH_4, O_2, VOC, and CO_2. The MultiRAE is the final piece of the sample train, and exhaust from this instrument is allowed to vent to the atmosphere.

After the sampling train is assembled, the isolation valves are opened (SUMMA is closed at this point), and the sample port is purged for 10 min at a flow rate of 4 to 5 L/min. At the beginning of purge, the ambient surface air concentrations of CH_4, O_2, VOC, and CO_2 are recorded on a purge form. After 10 min, CH_4, O_2, VOC, and CO_2 readings are taken and recorded every minute for 3 min. If readings are stable and within 10% of one another, the pump is turned off and the isolation valves are closed. Next, the valve on the SUMMA canister is opened and the vacuum pressure is checked to ensure the SUMMA canister is at the required initial vacuum. The isolation valve on the sample port side of the sampling train is then opened to allow subsurface gas to flow into the SUMMA canister. Once the pressure gauge equilibrates back from the lower SUMMA suction pressure to ambient pressure, the SUMMA valve is closed. The time of the sample collection is recorded in the log book, on the purge form, on the chain of custody, and on the identification tag of the sample. At the completion of each sampling day, the SUMMA samples were taken to the Laboratory's Sample Management Office for shipment to the analytical laboratory.

In some cases, sample ports were determined to be either fully blocked or partially blocked. In an effort to ensure data quality, ports that were either fully or partially blocked on two consecutive sampling events were assumed to be adversely impacted and were subsequently removed from the sampling plan.

2.2.4 Subsurface Pore-Gas Sampling at Borehole 54-24399

Borehole 54-24399 is the deepest borehole at MDA L with an open interval in the Cerros del Rio basalts. A dedicated packer system and sampling line are used to collect samples at borehole 54-24399. In the past, a drill rig was used for lowering and raising a single and double packer system into the borehole. Because of issues with packer destruction on sharp basalt, the Laboratory installed a permanent packer in August 2016 (Figure 2.2-2).

The permanent packer was placed with its bottom at 566.7 ft bgs within the casing of the wellbore. To sample borehole 54-24399, the packer is inflated with pure nitrogen (99.99%) from a surface port to the desired inflation pressure according to the manufacturer's specification. The sample train is then connected to one of the two ports on the surface completion (Figure 2.2-3). The packer has two sample ports, one pulling air from 566.7 ft bgs and one pulling air from 587.8 ft bgs. The port labeled "Sample" is open to 587.8 ft bgs while the port labeled "Tracer" is open to 566.7 ft bgs (Figure 2.2-3). There is also an OMEGA PX429-015AI-EH extra-high-accuracy 0–15 psi (±0.05%) pressure transducer mounted on the top of the packer that is open to a feed-through port to monitor pressure immediately below the packer at 566.7 ft bgs (Figure 2.2-4). This transducer is connected to the surface through a grey wire shown in Figure 2.2-3 and is connected to a data logger and records 6-min averages of pressure. The pressure transducer was used to demonstrate the close coupling between the atmosphere and the subsurface pressure within the basalt. A schematic of the packer completion is shown in Figure 2.2-5 and includes rock types as seen in the video log (August 2015) of borehole 54-24399 (Appendix D, on DVD included with this document). The depth to the bottom of the casing was revised from 568 ft to 566.7 ft bgs after review of the video log and original drilling log (LANL 2005, 092591).

2.3 Gas Sampling Schedule

2.3.1 Effluent Sampling from SVE Units, 2015–2017

Gas samples were collected in SUMMA canisters from the two SVE systems effluent sample ports (SP1) according to the following schedule:

1. Day 1 and Day 2 of operation: Four samples were collected each day.
2. Next 3 wk: One sample was collected each day (closure of the Laboratory prevented collection of one daily sample during this period).

3. Next 9 to 11 wk: One sample was collected weekly (generally on Wednesday of each week).
4. Beginning April 15, 2015, for SVE-West and May 6, 2015, for SVE-East: One sample was collected monthly on the first Wednesday of each month.
5. Monthly sampling of the SVE system effluent continued until the SVE units were shut down in November 2015.
6. Short duration, 2-d rebound sampling (SVE-West April, June, August 2016; SVE-East April, June, November 2016) included a minimum of five SUMMA samples collected for each test.
7. The 25-d rebound test on SVE-East, June 5–29 2017, collected 14 SUMMA samples with higher frequency in the first 4 d.

2.3.2 Subsurface Pore-Gas Data

Baseline subsurface samples were collected from pore-gas sampling ports in 28 boreholes from late August to early October 2014. Annual sample collection at these 28 boreholes was repeated in February 2016 and February 2017. In addition, 8 quarters of subsurface samples from 14 boreholes located within a 150-ft radius of the SVE wells were collected in April 2015, July 2015, November 2015, May 2016, August 2016, November 2016, May 2017, and August 2017. Analytical results are included in Appendix B. Blockages and radiological screening results prevented sampling at some ports during annual and quarterly sampling. Tables 2.2-2 and 2.2-3 show the ports from wells sampled during each round, and notes are included to indicate why certain samples could not be collected. If a port failed because of blockage or partial blockage for two quarters in a row, the port was removed from the sampling plan.

2.4 Summary of SVE System Operations

The SVE-West system operated from January 9, 2015, to November 18, 2015, at an average flow rate of 99.3 scfm. During this period, the system was operational 99.0% of the available time. The system shut down five times: on January 24, 2015, because of a site wide power failure; on February 23, 2015, because of ice buildup in the water knock-out tank; and on August 8, October 21, and October 22, 2015, when lightning caused power outages in the area. The SVE-West system was also shut down for very short periods for maintenance.

The SVE-East system operated from January 26, 2015, to November 18, 2015, at an average flow rate of 97.5 scfm. During this period, the system was operational 99.0% of the available time. The system shut down four times: on February 23, 2015, because of ice buildup in the water knock-out tank; and on August 8, October 21, and October 22, 2015, when lightning caused power outages in the area. The SVE-East system was also shut down for very short periods for maintenance.

Water has condensed in the knock-out tank of both systems during periods of cold weather. Generally, water vapor in extracted pore gas condenses and is captured in the knock-out tank when the ambient air temperature drops below freezing for an extended period of time. More water was generated in the SVE-West unit probably because it is shaded in winter and does not warm from exposure to the sun. Approximately 200 gal. of condensed water was generated through November 2015 from the operation of both SVE units. The condensed water was characterized as nonradioactive and nonhazardous and was disposed of at the Laboratory's Sanitary Wastewater System Consolidation treatment facility.

3.0 SUMMARY OF SUBSURFACE PORE-GAS BASELINE RESULTS

Baseline pore-gas samples were collected in August and September 2014 from 185 individual gas sampling ports in 28 boreholes within and surrounding MDA L. These data were used to estimate the total plume mass of two primary constituents: 1,1,1-TCA and TCE. These constituents were selected because they have historically constituted more than 60% of the estimated plume mass (Stauffer et al. 2005, 090537; Stauffer et al. 2007, 097871; LANL 2011, 205756; Stauffer et al. 2011, 255584). The mass of 1,1,1-TCA and TCE was calculated using 3-D data-interpolation techniques described more fully by Weston Solutions, Inc. (Weston 2015, 600886). Assumptions in this technique include fixed subsurface water saturation within each geological unit, fixed Henry's Law partitioning into subsurface pore water, fixed sorption parameters, and a small component (0.05%) of organic carbon within the subsurface. Given these assumptions, the baseline 1,1,1-TCA plume mass in September 2014 was estimated to be 740 kg (1628 lb), while the TCE plume mass was estimated to be 343 kg (755 lb).

4.0 SUMMARY OF SOIL VAPOR EXTRACTION RESULTS

4.1 Effluent Mass Removal

From January 9, 2015, to November 18, 2015, the combined VOC mass removal from the two SVE units is calculated to be 553 kg (1217 lb), thus achieving the mass removal goal in the IMWP. Figure 4.1-1 shows the cumulative VOC mass removal versus time for both SVE units as well as the cumulative volume of pore gas pumped from the subsurface by both SVE units. The slopes of both the mass removal and volume pumped curves changed when the SVE-East unit became active on January 26, 2015.

Figure 4.1-2 shows the rate of mass removal for the combined extraction from both SVE units in pounds per week. The activation of SVE-East on January 26, 2015, resulted in an increase in mass removal from 35 lb/wk to nearly 60 lb/wk. The mass-removal rate then decreased over time to 23 lb/wk in July 2015. By November 2015, the rate decreased to about 17 lb/wk. The long tail in the mass removal curve shows the SVE systems continue to be effective after 10 mo of operation.

Table 4.1-1 lists the mass removed for each detected organic compound during SVE operations. Out of 62 analytes measured using the TO-15 panel, only 24 have reported detections in the SVE effluent. Of the total 1217 lb removed, 1,1,1-TCA was the highest constituent at over 44% (541 lb); TCE composed 21% of the mass extracted (259 lb); Freon-113 (1,1,2-trichloro-1,2,2-trifluoroethane) was third at 10% (117 lb); and PCE was the fourth most prevalent component in the effluent at 9% (110 lb). Other compounds with significant mass removal include 1,2-DCA (46 lb); 1,1-DCE (34 lb); 1,2-DCP (29 lb); and chloroform (24 lb). Together these constituents composed 95% of the total extracted mass.

Tables 4.1-2 and 4.1-3 list the flow rates for SVE-West and SVE-East, respectively. These flow rates were calculated using observed wellhead pressures and orifice plate pressure differentials as described in section 2.1. Flow rate data for SVE-West and SVE-East are included in Appendix E (on CD included with this document).

4.2 Concentrations in the SVE Effluent

Concentration reductions in the effluent from the two SVE units are presented in Figure 4.2-1. The five analytes with the greatest mass removal (TCA, TCE, PCE, 1,2-DCA, and Freon-113) were selected to illustrate the decreases in concentrations in the effluent with time. Effluent concentrations from both systems decrease with time for all analytes, with larger decreases in concentrations seen for SVE-West. On both east and west sides of the site, PCE concentrations are reduced by smaller fractions of their initial values than are other constituents, possibly related to stronger liquid partitioning for PCE. The larger reduction in all concentrations on the west side of MDA L is likely because the SVE-West system is located closer to the western source region than is the SVE-East system to the eastern source region (Figure 1.1-1).

Figure 4.2-2 shows how the molar ratios of these compounds evolved during the 10 mo of continuous SVE operation and during rebound tests through June 2017. Molar ratio is defined as the number of moles of a given compound divided by the total number of moles of organics measured in the TO-15 suite. Because ppbv is a measure of molar volumetric concentration (volume fraction per total volume) and volume is directly proportional to the number of moles, molar ratio is derived by dividing the ppbv of a given analyte by the sum of all measured analytes in ppbv at a given port (see Appendix B for the lists of analytes found at each port). Initially, for SVE-West, TCE decreased rapidly as a mole fraction of the plume while PCE increased. Beginning around August 2015, TCE reached a steady percentage while TCA began to drop with a further increase of PCE molar fraction. For SVE-East, small changes occurred in the percentages of the major constituents, with TCA decreasing and TCE; 1,2-DCA; and PCE increasing while Freon-113 appeared to maintain a relatively constant mole fraction.

4.3 Subsurface Plume Changes Relative to Baseline 2014

Figure 4.3-1 plots individual concentrations for seven analytes from each port in the boreholes around SVE-East and SVE-West that were sampled for both the baseline 2014 and the November 2015 events (553 points in total). Data in this plot are for 1,1,1-TCA; TCE; PCE; 1,2-DCA; 1,1-DCE; 1,2-DCP; and methylene chloride. Dashed black lines above and below the red 1:1 line show typical ±30% uncertainty in reproducibility of subsurface gas concentration measurements. Baseline 2014 concentrations are plotted on the horizontal axis and November 2015 concentrations are plotted on the vertical axis. Figure 4.3-1 shows the decreasing trend in concentrations that occurred during the first 10 mo of SVE operation. If the SVE system had no impact on subsurface concentrations, the data would plot on or close to the 1:1 line shown in red in the figure. However, most of the points fall below the 1:1 line, indicating the SVE system has reduced the concentrations at the majority of sample ports below their baseline values. Points are colored by borehole, indicating the boreholes that are the most impacted. In this figure, several points from boreholes 54-02089 (purple triangles) and 54-24238 (green circles) are labeled to highlight increasing concentration during the SVE IM.

Figure 4.3-2 shows how concentrations of the same seven analytes described in the previous paragraph responded over three quarters of sampling. The green points from April 2015 have slightly more scatter around the 1:1 line, while July 2015 and November 2015 both show the majority of the measurements to be well below the 2014 baseline sampling concentrations. Shown in the figure are the increases in concentration of several VOCs in borehole 54-24238 during 2015.

4.3.1 Weston Data Interpolations

Figures 4.3-3 and 4.3-4 show images of the 1,1,1-TCA plume generated by data interpolation for the baseline 2014 and April 2015 data, respectively (Weston 2015, 600887). Data are shown with dots, while the interpolation is shown on a contoured color scale with both color contour lines and contour shading. The contour intervals are based on multiples of Tier I screening values used in the CME report (LANL 2011, 205756). Tier I screening uses only Henry's Law partitioning to determine if a given vapor concentration exceeds groundwater standards, assuming the vapor is in contact with groundwater (Table 4.3-1). The post-SVE image (Figure 4.3-4) shows a decrease in both the spatial extent of most individual concentration contours and the magnitude of concentrations of the 1,1,1-TCA plume.

Figures 4.3-5 and 4.3-6 show similar information for TCE (Weston 2015, 600887). Again, the extent of a given contour is reduced, and for TCE, maximum concentration contours are absent in the interpolated data set for April 2015. For example, the highest concentration of TCE in Figure 4.3-5 on the west side of the site is well into the 250 times (red) color shading, while in April 2015 (Figure 4.3-6) the maximum concentration contour shading is reduced to 100 times (orange) the Tier I screening value.

4.3.2 Effectiveness of SVE at Selected Monitoring Wells

In Figures 4.3-7 through 4.3-14, data from a subset of 8 monitoring wells are presented showing concentration versus depth for 1,2-DCA; TCE; PCE; and 1,1,1-TCA for each of the 10 quarters after the start of SVE operation compared with baseline 2014 data. In all of the depth-dependent plots, baseline 2014 data are shown in light blue. The three 2015 data sets show concentration changes during the active SVE phase; the six data sets from 2016 and 2017 show concentration changes during the rebound phase.

4.3.2.1 SVE-West

Figures 4.3-7 and 4.3-8 show concentration data from boreholes 54-27641and 54-24240, respectively, both within a 30-ft radius of SVE-West. These boreholes show large concentration reductions within 110 ft bgs, and mass removal appears to be especially effective in the top 80 ft bgs in borehole 54-24240, where concentration had dropped several orders of magnitude by November 2015, just before the SVE units were turned off. This region may be impacted by flow of fresh air from the atmospheric boundary being pulled toward the low-pressure region created by the SVE system. The effectiveness of the SVE is observed to decrease with depth in borehole 54-27641, especially at depths below 150 ft. The data from April 2015 show an anomalous increase in concentration at the 340-ft depth; however, this anomaly is not observed in the subsequent quarters of data, where concentrations return to values measured in the pre-SVE baseline sampling. Observed rebound in these two wells is strongest in monitoring borehole 54-24240, implying that continued vapor-phase releases from buried drums are localized closer to this well than to borehole 54-27641, where observed rebound was lower. In both cases, rebound in the upper 60 ft is noticeably higher, coincident with the depth of the waste shafts. Note that both concentration reduction and rebound of PCE is nearly constant with depth. This trend may be related to the lower vapor pressure of PCE and increased pore-water storage of this chemical.

Figure 4.3-9 shows concentration data from borehole 54-02022, located more than 150 ft from SVE-West. This monitoring well shows concentration decreases to a depth of 200 ft. Data from April 2015 are again anomalous, showing concentration increases above the pre-SVE baseline at depths below 150 ft; however, both the July 2015 and November 2015 sampling rounds show decreases in all four analytes at all depths. The strong decreases of both TCA and TCE at 200 ft bgs suggest the radius of influence (ROI) for the SVE-West extraction well may be greater than 150 ft. Rebound in this well was fairly minimal, which is expected given its distance from the source region. In this well, PCE does not recover as dramatically as in borehole 54-24240; however, suction at the larger radius to borehole 54-02022 was much lower during SVE, and pre-SVE concentrations were also lower in borehole 54-02022.

4.3.2.2 SVE-East

Figures 4.3-10 and 4.3-11 show data for boreholes 54-24243 and 54-24241, located 54 ft and 83 ft radially from SVE-East, respectively. Both show strong impacts from SVE, with concentration decreases by factors of between 1/3 to 1/100 in many ports. Both of these boreholes show strong SVE impacts to total depth. Rebound from the minimum measured concentrations for the four VOCs presented is significant at all depths, with some shallower values rising toward pre-SVE conditions, with PCE concentrations in borehole 54-24241 rebounding the most of all the constituents. One anomaly in the data is for 1,2-DCA in borehole 54-24241, where concentrations have risen nearly 4 times the pre-SVE values at ports above 100 ft bgs. A possible explanation for this increase would be leakage from a container with a relatively higher ratio of 1,2-DCA, as the other constituents in these shallow ports do not show similar increases in concentration above pre-SVE values. Note that 1,2-DCA concentrations below 100 ft bgs show little change over the course of the IM. Results from 2021 show 1,2-DCA concentrations at depths of less than 100 ft bgs have dropped to values of less than half the baseline pre-SVE values.

Borehole 54-27642 is located about 130 radial ft from SVE-East and shows reductions in concentration with greater efficiency at shallow depths (Figure 4.3-12). Borehole 54-27642 is located near the edge of the paved portion of the site and shows appreciable reductions in concentration to 175 ft bgs, with less impact observed at greater depths. The large reductions in concentration in this borehole also suggest that the 150-ft ROI may be conservative with respect to design of a corrective measures SVE system as discussed in the CME report (LANL 2011, 205756). Rebound in this well is significant, with TCE and PCE both rebounding to near pre-SVE values by August 2017. DCA[1,2] at 120 and 340 ft bgs increases above the pre-SVE concentrations, although not dramatically. TCA[1,1,1] rebounds to pre-SVE concentrations at the deepest port (340 ft), while near-surface rebound is less pronounced.

Boreholes 54-02089 and 54-24238 are approximately 70 ft and 100 ft from the SVE-East extraction well and are fairly close to the eastern disposal shafts (Figure 1.1-1). Many of the ports in these wells show increased concentrations for all analytes, particularly at the deepest 89-ft ports (Figures 4.3-13 and 4.3-14). Only in the shallowest ports are concentrations reduced by SVE and only for certain analytes (TCA in both holes, and all four analytes shown in 54-02089). The data from borehole 54-24238 are very similar to what is predicted in simulations of increased leakage from the source region and could imply a recent increase in leakage from a buried container (drum) near this well. Another hypothesis for the increasing concentrations is that suction from the SVE unit could be pulling higher existing vapor concentrations located to the north in a region with no monitoring boreholes toward the eastern SVE well. Continued monitoring at this location should be undertaken to ensure that the observed concentration increase is not a significant release that is just arriving at this location. Data from 2021 show that total VOC in these two wells is returning to values close to the baseline pre-SVE.

4.3.2.3 Gradient Reversals

In section 3.3.1 of the IMWP (LANL 2014, 261843), it was hypothesized that

> [with] maximum concentrations lower in the source regions, vapor transport will reverse direction, and VOCs will diffuse from deeper in the plume back toward the surface. This reversal of the diffusion gradient would limit deeper migration into the underlying basalt and potentially toward groundwater.

Borehole 54-27641 clearly demonstrates such a reversal in concentration gradient. Figure 4.3-7 shows that before SVE operations, concentrations were highest near the surface with lower concentrations at depth, a situation that would move mass to depth from high to low concentrations via diffusion. Thus, in Figure 4.3-7 for the 2014 baseline curve, 1,1,1-TCA mass at 150 ft bgs would diffuse downward along the concentration gradient. However, this trend has been reversed by the impacts of the SVE system. At the end of the active SVE operation in November 2015, when the primary mass transport mechanism switches from advection back to diffusion, the concentration gradient (from high to low concentration) at 150 ft bgs has reversed to an upward direction, meaning that diffusion will transport mass at 150 ft bgs following the concentration gradient toward the surface and will aid in remediation. Similar gradient reversals have been observed in borehole 54-24240 at 100 ft bgs and in borehole 54-24243 at 80 ft bgs. However, reversal of the concentration gradient is not ubiqitous, and boreholes 54-27642, 54-02022, and

54-24241 show concentration reductions at all depths without reversals of their concentration gradients over the 10-mo SVE IM.

4.4 Monitoring Well 54-24399

The deepest monitoring well at MDA L, 54-24399, installed in 2005, lies near the center of MDA L and is cased from the surface to a depth of approximately 567 ft bgs. The original plan to collect data from a 1-ft interval at the top of the uncased section (568–569 ft bgs) using a dual-packer system was abandoned after the July 2015 sampling event when the lower packer was damaged during sampling after it came in contact with vesicular basalt. Logbooks from this sampling event conclude that the sample taken was valid. Video logs of the open hole show a short section of massive basalt near the top of the uncased section followed by vesicular basalt, some having large voids and very sharp rock formations (Appendix D).

Because of the risk of damage to packers from sampling the borehole below the casing, sampling with the dual-packer system was removed from the sampling plan and a permanent single packer was installed in August 2016 (Figure 2.2-2). The new permanent packer has several benefits including (1) a simpler sampling process needing no drill rig, (2) a substantial reduction in borehole breathing due to new construction of the well head (Figure 2.2-3), and (3) the ability to maintain longer periods of packer inflation to ensure isolation of the deep basalt.

TCA[1,1,1] data collected from May 2005 through February 2022 at borehole 54-24399 are shown in Figure 4.4-1. Concentrations were measured using a variety of sampling techniques, including a dual packer that isolated a 1-ft interval near the bottom of the casing; a single packer lowered from a drill rig and set at the base of the casing; and the latest permanent packer, which has been used since August 2016. The horizontal line in the figure is the Tier I screening level for this compound calculated as simple equilibrium partitioning from the gas phase into hypothetical drinking water; the vertical line is the date of the installation of the permanent packer. Data show a high degree of variability through time, with TCA values spanning a range from a low of 13 ppbv to a high of 4800 ppbv on November 14, 2016.

Data for other VOCs are shown in Figures 4.4-2 through 4.4-5 and closely follow the same trends as 1,1,1-TCA. The concentrations of TCE; PCE; 1,2-DCA; and methylene chloride all exceed Tier I screening levels, especially in samples taken following the installation of the permanent packer.

Two other boreholes at this site are completed in the basalt and provide a limited but important data set to compare with the behavior of 54-24399. Boreholes 54-01015 and 54-01016 angle under the site from the north and approach 54-24399 to within 243 and 95 lateral feet, although ports in each do not reach the total depth of the bottom of the casing in 54-24399. Sampling ports in these boreholes are connected to the surface with Teflon tubes, with discrete locations completed in sand pack surrounded by bentonite. Data from the deep angled boreholes, shown in figures 4.4-1 through 4.4-5, show that measurements in the basalt are consistent and support the idea of a well-mixed gas in the basalt.

Borehole 54-24399 was an open conduit for 11 years (2005–2016) before installation of the permanent packer in August 2016, having a well cap that allowed significant airflow. During this time, strong flows of air out of the borehole were regularly observed, and the borehole was visited as part of tours to the site to show passive vapor extraction in action. However, airflow regularly reversed direction, pulling surface air into the deep borehole. MDA L is a staging area for transport of waste and thus often has trucks idling for hours at a time. Additionally, for installation of temporary packer systems before August 2016, a running drill rig would be parked at the open hole for each sampling event. Exhaust from these vehicles would have been pulled into the deep borehole during atmospheric pressure highs and could have added a component of vehicle exhaust (benzene, ethylbenzene, toluene, and xylenes [BTEX]) to deep samples.

To determine if 11 years of barometrically induced breathing in borehole 54-24399 caused measurable changes in the chemical composition, the ratio of 1,1,1-TCA to toluene from boreholes 54-24399 and 54-24241 were compared (Figure 4.4-6). The deep samples do show a shift to lower 1,1,1-TCA/toluene values and support the hypothesis that exhaust has impacted the deep basalt. However, installation of the new packer has greatly reduced barometric breathing to the surface through borehole 54-24399, and the exhaust signature is expected to dissipate over time. The new completion on this well, with an O-ring pulled tightly onto the top of the wellhead by the weight of 587 ft of 1-in. galvanized pipe, has reduced breathing to nearly zero. The new configuration allows more representative samples to be collected from this well.

4.4.1 2017 Deep Basalt Tracer Test

In 2017, DOE performed a tracer test in a deep vertical borehole located near the middle of Area L on the edge of the eastern source area (LANL 2016, 601622; Stauffer et al. 2019, 700871). This tracer test was designed to test the hypothesis that observed pressure variations in the basalt are caused by rapid airflow through fracture connections to the atmosphere [Neeper 2002, 098639]. The deep borehole (54-24399) is cased from the surface to 173 m (567 ft) and is open (uncased) from this depth to a total depth of 201 m (660 ft). The uncased interval lies completely within the basalt approximately 80 m (262 ft) below the Bandelier tuff and approximately 91 m (300 ft) above the regional aquifer. Recent measurements of VOC gas concentrations in this interval have been below Tier I screening levels, except for one measurement of 1,4-dioxane. This is important because measured concentrations in the deep basalt would have to rise above screening levels before any risk to groundwater could develop.

In the tracer experiment, sulfur hexafluoride (SF_6) tracer was injected into the top of the uncased open interval of borehole 54-24399, and concentrations at the upper sampling port were monitored after the injection. As predicted from simulations done before the tracer test, concentrations at the release location first dropped, then quickly rebounded. This cycle was repeated as atmospheric pressure variations moved the tracer back and forth across the monitoring point. The simulations used values for fracture and rubble zone permeability in the basalt that were based on previous experiments and observations (Stauffer and Stone 2005, 090037), and atmospheric pressure measured at a nearby weather station corrected to the elevation of the injection interval to represent a far-field boundary (outcrop). The data from the test were used to constrain outcrop distance using the measured pressure variations within the uncased section of the deep borehole. Details on the simulations used to analyze the data from this experiment can be found in Stauffer et al., 2019.

Results from the tracer test showed that barometric pumping at an outcrop located approximately 1 km from the test location could account for the observed pressure response in the borehole. Further, the SF_6 tracer data agreed with the simulated response to fluctuations in barometric pressure. Estimates of instantaneous velocity in the basalt, assuming a fracture width of 1 mm, reached as high as 1000 m/day (0.62 mi per day) for brief intervals. Such high rates of gas transport will cause dispersion, spreading gas 10–100× faster than diffusion alone. The breathing basalt represents a new conceptual model for transport at this site and helps explain the seemingly contradictory observations of low VOC concentrations measured in the basalt (<1× Tier I) at the same time that high VOC concentrations (>100× Tier 1) are measured at the base of the Bandelier tuff (N3B 2018, 700039; Stauffer et al. 2019, 700871).

4.5 Differential Pressure Measurements

Subsurface differential pressure measurements were made at pore-gas sampling ports in boreholes sampled during SVE operations. Measurements were made during the baseline sampling in August and September 2014, in April 2015, in July 2015, and in November 2015. For these measurements, one input on a digital manometer is connected to a subsurface gas sampling port, while the other input is left open to the atmosphere. The manometer then records the difference in pressure between the subsurface port and the atmosphere. Table 4.3-2 shows the results of the pressure measurements for 189 ports in the 28 boreholes for the baseline and a subset of these for the three quarterly sampling events (April 2015, July 2015, and November 2015) that occurred during SVE operations.

To evaluate these data, it is helpful to first review measurements made at MDA L in the 1990s. Neeper (2002, 098639) presents atmospheric and differential subsurface pressure data from boreholes near MDA L. These data show that the atmosphere can change pressure by more than 1.5 kPa over the span of a few days (Neeper 2002, 098639, Figure 3). Subsurface pressure changes in response to atmospheric pressure; however, pressure changes in the subsurface are shifted in time and reduced in amplitude, based on the formation's connection to the atmosphere at a particular depth. The amplitude of subsurface pressures within the Bandelier Tuff decreases, and maximum deviations from average pressure are shifted to later times with increasing depth. Neeper (2002, 098639) presents data collected from a borehole located 100 m (328 ft) to the east of the site that show almost no pressure difference between the atmosphere and a port at the depth of 11 m (36 ft). However, at depths of 77 m and 103 m (250 ft and 338 ft), the amplitude of the pressure wave is depressed, and the phase is shifted such that maximum differential pressure between atmospheric pressure and downhole pressure varies between +0.6 kPa and −0.6 kPa, with the maximum downhole deviation from average pressure occurring up to 0.33 d after the maximum atmospheric deviation.

Given the variability expected in subsurface differential pressure, it is difficult to attribute many of the measured values presented in Table 4.3-2 to the SVE systems. However, some ports at boreholes 54-24240, 54-24241, and 54-27641 show strong signals that are likely impacted by the SVE suction. Additionally, some of the shallower pressure measurements should be less impacted by shifts in magnitude and phase, allowing smaller pressure differences to be attributed to the suction from the SVE units. Further analysis using daily pressure variations at the time of the sampling could allow more refined estimates of the extent of pressure propagation from the SVE units and may reduce unexpected variability observed in data collected between April 2015 and February 2016. Such analysis requires the use of layered permeability models to separate out the effects of natural-phase shift and amplitude reduction from those caused by the SVE systems at individual ports.

4.6 Rebound Data

To more fully evaluate SVE strategies for MDA L, the Laboratory collected and analyzed data related to plume rebound following shutdown of the SVE units in November 2015. Rebound sampling is important to the development of a long-term strategy for using SVE as a vapor-plume control at MDA L. Rebound sampling also helps determine whether, and to what degree, ongoing VOC releases from the shafts are occurring. This is because very little VOC mass is adsorbed to the tuff or dissolved into pore water and therefore must be coming from the source in the shafts. Thus, repartitioning of previously released mass is unlikely to result in significant rebound. Large rebound would more likely be indicative of ongoing release from source.

For the rebound analysis, there are two types of plume rebound data collected. First, monitoring data from the surrounding boreholes can be used to see if subsurface concentrations are rebounding because of continued leakage in the source area. Second, rebound concentrations from the exhaust from the SVE units can guide development of restart intervals for long-term planning.

Quarterly and annual monitoring data for boreholes surrounding the SVE boreholes are a vital part of the rebound analysis and were collected through August 2017. However, because the SVE systems pull vapor from a large volume of the subsurface, the rebound characteristics of the SVE restarts provide data to complement point measurements of rebound gathered in the quarterly and annual subsurface vapor sampling.

For the rebound testing, the Laboratory restarted the SVE units for 2-d periods to allow integrated rebound assessment. These brief restarts were done in April, June, and September 2016. Because of an electrical issue with the SVE-East unit, rebound sampling in September 2016 was delayed until late November 2016. Based on continued higher concentrations in the SVE-East rebound samples, a single 25-d rebound test in June 2017 was performed. Concentration data (1,1,1-TCA) from the rebound tests are shown relative to the concentrations measured during active SVE in Figures 4.6-1 and 4.6-2. TCA rebound on the west side of MDA L is not as significant as on the east side. During the rebound sampling it was estimated that 5–8 lb were extracted for each 2-d test, while the 25-d test resulted in nearly 80 additional pounds of VOC removed from SVE-East. Thus, the total rebound mass removal is on the order of 110–130 lb. Rebound molar concentration ratios appear to return partway toward those seen at the beginning of the SVE IM (Figure 4.2-2).

The impact of 10 mo of SVE operation in 2015 on the subsurface plume can be seen by plotting baseline concentrations in 2014 versus concentrations in 2017 (Figure 4.6-3). The bulk of the data show that the plume in 2017 remains below measured baseline conditions. Concentrations have increased for monitoring wells 54-24238 and 54-02089. The increase is especially pronounced for 1,1,1-TCA and methylene chloride. Increases in these two compounds may suggest a leak from buried source containers (drums) near boreholes 54-24238 and 54-02089 or alternatively, migration of higher concentrations from the north towards the SVE-West borehole.

4.7 Pore-gas Monitoring Data 2019 to 2021

Results of recent pore-gas monitoring from the annual sampling campaigns of 2019 through 2021 are reported in pore-gas monitoring reports (N3B 2021, 701563; N3B 2021, 701446; N3B 2022, 702084). The last round of sampling for the 2021 campaign includes data from February 2022 due to issues with a transition in contractors.

4.7.1 Pore-gas Monitoring Data from 2019

Vapor monitoring conducted during the first sample round in 2019 included collecting 163 vapor samples for VOC analysis, along with 17 field duplicate samples and 17 field blank samples from 163 of the 168 sample ports within 28 boreholes (sentry and peripheral). Five ports were blocked and not sampled. Vapor monitoring in the second round of sampling in 2019, conducted in early January 2020, included collecting 32 vapor samples for VOC analysis, along with 7 field duplicate samples and 8 field blank samples, from 32 sample ports of the 6 sentry boreholes. Vapor samples, along with 3 field duplicate and 3 field blank samples, were also collected for tritium analysis from all 32 sample ports of 6 sentry boreholes in the second sampling round of 2019.

Validated analytical results demonstrated the presence of 34 VOCs in subsurface vapor and clearly show the 2 VOC source areas. The VOC screening evaluation identified 14 VOCs in MDA L pore gas at concentrations exceeding Tier I screening levels (based on groundwater screening levels) in the first sampling round and 14 in the second sampling round; a total of 15 different VOCs exceeded Tier I screening levels between the 2 rounds. Concentrations in the basalt were below Tier I screening levels. To cause concern for the regional aquifer, concentrations in the basalt would have to be above Tier I levels. Because borehole 54-24399 was determined to be useful in warning of issues with transport toward the regional aquifer, this borehole was added to the list of sentry boreholes, bringing the total sentry borehole count to 7.

4.7.2 Pore-gas Monitoring Data from 2020

Vapor monitoring in 2020 included collecting 36 vapor samples from 36 sample ports within the 7 sentry boreholes in each of 2 sampling rounds. Validated analytical results demonstrate the presence in subsurface vapor of 40 VOCs in the first sampling round, and 33 in the second sampling round, and confirm the 2 VOC source areas. The VOC screening evaluation identified 14 VOCs in MDA L pore gas at concentrations exceeding Tier 1 screening levels (based on groundwater screening levels) in the first sampling round and 13 in the second sampling round. During the 2020 sampling, no contaminants were found above Tier I screening levels in the basalt in borehole 54-24399.

4.7.3 Pore-gas Monitoring Data from 2021

Data from 2021 show that the SVE IM has led to overall reductions in concentration in the plume persisting more than 6 yr (Figure 4.4-1). Maximum TCE concentrations in the two source areas are clearly lower and have not rebounded to the red (100× Tier I) levels seen in 2014. The 100× Tier I red regions have also been reduced vertically as shown on the A-A’ vertical cross-sections. The lateral extent of the plume edge also shows some reductions, as seen in the top map view panels of Figure 4.4-1. In these map view panels, the width of the plume along the B-B’ and C-C’ lines is reduced, with concentrations at the edge of the plume lower in 2021 than they were in 2014. The same reduction in plume extent can be seen in the lower vertical panels, where drops in concentration from 2014 to 2021 are apparent in borehole 54-02026 on the A-A’ cross-section, in borehole 54-02031 in the B-B’ cross-section, and in borehole 54-02023 on the left side of the C-C’ cross-section. Thus, the IM objective of reducing the plume concentration and extent has been met.

Concentrations of total VOC at the deepest edge of the plume directly below the eastern source area, near the basalt/tuff interface, have dropped from nearly 250 ppmv in 2014 to just over 70 ppbv in February 2022. Although some concentrations at this interface are well above Tier I screening levels, the breathing nature of the basalt (see Section 4.5.1) provides a protective vertical zone where concentrations are well mixed and drop rapidly below the tuff. This means that high concentrations are contained within the Bandelier Tuff, satisfying the third objective of the IM.

4.7.4 Summary of Recent Pore-gas Monitoring Data from, and Relevance to, the SVE

Approximately 1200 lb of VOC mass was removed through soil vapor extraction (SVE), satisfying the first objective of the IMWP. Maximum VOC concentrations have been reduced in the core of the plume beneath the source regions, and concentrations at the lateral boundaries have dropped (Figure 4.7-1), satisfying the second objective of the IMWP. Concentrations of total VOC at the deepest edge of the plume directly below the eastern source area, near the basalt/tuff interface, have dropped from nearly 250 ppmv in 2014 to just over 70 ppmv in February 2022 (Figure 4.7-2). Although some concentrations at this interface are well above Tier I screening levels, the breathing nature of the basalt provides a protective vertical zone where concentrations are well mixed and drop rapidly below the tuff. This means that high concentrations are contained within the Bandelier Tuff, satisfying the third objective of the IM. Thus, the three objectives listed in the IMWP have been met.

The most recent data show only three instances where VOC concentrations in the basalt were significantly above Tier I screening levels.

- A single port in borehole 54-01016, at a slant depth of 481 ft, measured TCE at 1.7× the Tier I screening level. The port above this, at a slant depth of 390 ft, has a TCE concentration 0.2 × Tier I.
- The two deepest sample ports in the basalt in borehole 54-24399 show 1,4-dioxane concentrations above Tier I screening levels in the data from May 2021. The measured values are above the method detection limit (based on theoretical measurements); however, they are well below the analytical laboratory's report detection limit (based on measurement data from the analytical laboratory). Dioxane[-1,4] was not detected in the seven other ports in the basalt in boreholes 54-01015 and 54-01016 in May 2021, or in borehole 54-24399 in the second round of sampling for 2021 (February 2022).
- If future samplings continue to show high 1,4-dioxane concentrations, a focused validation of the raw data will be performed to determine if the measured detections are trustworthy.

Low VOC concentrations in the basalt are significant because the basalt lies between high concentrations of VOC in the Bandelier Tuff (to depths of 300 ft) and the regional aquifer (at 1000-ft depth). This indicates that the groundwater is currently protected by 700 ft of rock having low concentrations of VOC.

VOC measurements over the last 17 yr show overall decreasing contaminant concentrations in sample ports of both sentry and peripheral boreholes. These drops in concentration are primarily the result of the SVE operations during the IM, when more than 1200 lb of VOCs was removed from within the mesa.

5.0 NUMERICAL ANALYSIS

This section contains a brief review of previous modeling work in support of decision analysis undertaken at MDA L, followed by a description of the generation of an initial pre-SVE simulated plume corresponding to the period just before the IM was initiated in January 2015. A more complete review of previous simulation work, including references showing where simulation details can be found, is included in Appendix F. Simulation results generated in December 2014 are presented for predicted plume behavior and are then compared with those results obtained during the SVE IM. Differences between predicted and observed behavior are discussed with emphasis on how these differences impact previous recommendations for long-term corrective measures.

5.1 MDA L Vapor Plume Modeling Review

A 3-D numerical model of the VOC vapor plume in the subsurface at MDA L was developed using a site-scale numerical model. The porous flow simulator Finite Element Heat and Mass Transfer (FEHM) is used for all calculations (Zyvoloski et al. 1997, 070147). The numerical simulations account for diffusion, advection, partitioning between liquid and vapor, variable saturation and porosity, an atmospheric boundary, four discrete source release locations, an asphalt cover, and topography. Figure 5.1-1 shows the numerical 3-D model domain and the site boundary of MDA L. The numerical domain contains more than 140,000 finite-volume elements with a lateral spacing of 25 ft. The domain extends from the topographic surface to the water table and contains two high-resolution regions around the SVE boreholes.

The site-scale numerical model has evolved over many years (1999–2017) and has been used to evaluate the nature and extent of the subsurface plume at MDA L associated with waste disposal. As a surrogate for the entire plume, the contaminant with the highest subsurface concentrations (1,1,1-TCA) was selected to reduce the complexity of the simulations. The numerical model includes a 2006 SVE pilot test of less than 1-mo duration that was used to calibrate permeability at MDA L by matching flow rate versus pressure drop simultaneously with concentrations in the exhaust gas (Vrugt et al. 2008, 104951). The calibrated model parameters were then used to initiate model validation that started from the pre-SVE test in 2006 and was used to predict plume concentrations in the year 2010. Results from this effort yielded a data/model correlation coefficient (r^2) for over 150 data model pairs of greater than 90%. The ability of the model to align with data after 4 yr that include two active SVE demonstration tests provided confidence that the model captures the dominant physical transport processes at this site. The validated numerical model was next used to explore scenarios related to the possible role of SVE as a corrective measure at MDA L (LANL 2011, 205756; Stauffer et al. 2011, 255584). Previous analysis showed that SVE has the potential to effectively remove significant quantities of VOCs from the subsurface (Stauffer et al. 2007, 104950; Stauffer et al. 2007, 097871). Suggestions regarding sampling frequency and location were made based on these results to allow for rapid detection of any sudden changes in the plume (Stauffer et al. 2007, 097871). Estimates of the ROIs of the SVE pilot test wells (~37 m [120 ft]) were given and a suggested SVE system for long-term plume control was presented (LANL 2011, 205756). To judge the quality of the model throughout the modeling process, spatially dependent 1,1,1-TCA concentration data from the site and the predicted (modeled) concentrations are compared through linear regression.

5.2 November 2014 Base Simulation

The last model update, before the current SVE interim measure, was performed in 2011 for the MDA L corrective measures evaluation (CME) (LANL 2011, 205756). To generate an updated model that represents the subsurface TCA plume, the output of the 2011 CME model, which correlated well with the 2011 plume data, was used as the starting point (Behar et al. 2019, 700854). The two source regions were then assumed to leak with fixed concentrations until 2014 (Figure 5.1-1). During the fixed leakage simulations, diffusion is assumed to be the only process moving mass in the subsurface. Figure 5.2-1 shows predicted concentrations for three simulations with fixed leakage from 2011–2014; the simulations assume three different fixed source concentrations (500 ppmv, 300 ppmv, or 200 ppmv) with both the eastern and western source regions leaking with the same concentrations for a particular simulation. When the two source regions are fixed at 500 ppmv, the model generates concentrations that are higher than the data. The simulations with 200 ppmv and 300 ppmv are quite similar; however, using a least squares regression between model and data, a fixed concentration of 300 ppmv in the source regions leads to the best match between the model and data from the set of 100–1000 ppmv, run in discrete leakage steps of 100 ppmv. Also included in Figure 5.2-1 are the +30% data reproducibility bounds on either side of the model = data line. Simulated results on a plane 60 ft below the ground surface are shown in Figure 5.2-2 where the two source regions are visible with higher concentrations.

5.3 Predicted Plume Behavior Compared with Measured SVE Response

Predictions for the first 10 mo of SVE operations were used to inform the project and NMED on expected VOC mass removal rates. Estimates were on the order of less than 2000 lb of VOC production during the SVE IM. After 10 mo of SVE IM data were collected, predicted effluent concentrations from both SVE-West and SVE-East were compared with the effluent data. The effluent predictions were calculated in December 2014 before the SVE system was started in January 2015, with pumping assumed to run continuously on both east and west units for a full year. The SVE-West predictions of effluent concentration based on the previously calibrated permeabilities and assumption of 300 ppmv constant source concentration are similar to the effluent data (Figure 5.3-1). However, SVE-East effluent predictions, shown in Figure 5.3-2, are consistently higher than the measured data. The less accurate model for the SVE-East side of MDA L may be related to two unexplained differences that have been observed. First, unexplained increases in concentrations at ports in boreholes 54-02089 and 54-24243 push the data higher than the baseline. Second, the suction required at SVE-East to pull 100 scfm (25 kPa) during the 2015 IM is significantly higher than suction required in 2006 to pull the same gas flow rate (19 kPa). In addition to these unexplained issues, the initial state of the SVE pumping calculations may play a role in the data/model mismatch on the eastern side of MDA L.

To address the mismatch in the SVE-East prediction, a second calibration was performed. For this calibration, permeabilities were modified on the east side with the constraint that the suction of 25 kPa be maintained while pulling 100 scfm. Figure 5.3-3 shows the improved fit using the new calibration data. In the new calibration, the constant source was also lowered from 300 to 200 ppmv. The new calibration permeability field, suction, and flow rate were used for all remaining simulations in this report.

5.4 Predicted Plume Behavior Compared with Measured Monitoring Borehole Data

Simulated concentrations at subsurface monitoring locations are next compared with measured data. The locations of the monitoring boreholes used in the comparison are shown in Figure 5.1-1. On the west side of MDA L, borehole 54-27641 is located near the source region, and the simulation at this well is in good agreement with measured data. Figure 5.4-1 shows the evolution of 1,1,1-TCA concentrations in the subsurface, with values dropping over time to a minimum in February 2016, just after the active SVE period ended. At depths shallower than 100 ft bgs, concentrations in this borehole have rebounded to less than 30% of their original values. Model predictions track fairly closely, especially in February 2016. One exception is the simulated rebound at 180 ft bgs in February and August 2017 that is not seen in the data.

Simulated concentrations in the subsurface on the east side of MDA L are less correlated with the data, especially at depths greater than 100 ft (Figure 5.4-2). Some disconnection between the model and data is expected, given that the starting concentrations in the simulations for borehole 54-24241 are approximately 50% higher than the measured 2014 data. Also, at borehole 54-24243, which is located approximately 50 ft east of the SVE-East unit, initial model concentrations are 50% lower than measured concentrations in the 2014 baseline sampling (Figure 5.4-3). One cause of the model/data differences is the location of the simulated source leakage, which is included in the simulations to provide enough continuous leakage to maintain measured concentrations through time. The distribution of these source locations has not been varied and is meant to capture the general plume behavior. Therefore, a 100% agreement between the model and data is not expected at all points around the plume.

5.5 Simulated Rebound

Simulations of plume rebound after the 10-mo period of active SVE are next presented. These simulations are run with a leak rate equal to the simulated leak rate on January 9, 2015, just before the SVE systems were turned on. Using the new calibration that achieved a better fit to effluent versus time, the fixed leak rate was based on a constant concentration in the source regions of 200 ppmv over the period of 2010 through January 9, 2015. These simulations use the newly calibrated geological unit permeabilities for the west side of the site. As seen in Figure 5.5-1, the simulations overestimate the rebound on the east side until June 2017 when simulated rebound falls quite close to measured rebound. On the west side, simulated rebound is quite close to measured values, until September 2016 when the simulated rebound is lower than the measured values (Figure 5.5-2). This could suggest an increase in leakage from the underground source over the period of June to September 2016. Borehole 54-24240 does show an increase in 1,1,1-TCA concentrations from May 2016 through August 2017, with concentrations at the shallowest port rising from less than 50 ppmv to over 150 ppmv during this period (Figure 4.3-8).

As a whole, the rebound data show that the site is not rebounding quickly to pre-SVE conditions. Over 18 mo after the active system was shut down in November of 2015, concentrations from the SVE-East unit have recovered to approximately half of the pre-SVE condition. This is not surprising considering the continued reduction in concentration seen in data from the surrounding boreholes (Figures 4.3-7 through 4.3-14). Given the 2006 SVE Pilot Test had a long-lasting impact on the VOC plume (LANL 2011, 205756), it is reasonable to expect that concentrations at many ports will remain lower than they were at the start of the 2015 SVE IM.

However, uncertainty remains on the mass of VOC still contained in the underground source, and data from MDA L clearly show that some ports are measuring continued slow leakage from buried source containers. This is especially evident in boreholes 54-24238 and 54-02089 where concentrations have risen above the September 2014 baseline, and in the case of TCA in borehole 54-24238, where concentrations have risen from 230 ppmv to 560 ppmv (Figure 4.3-14).

5.6 Simulated Sudden Failure of Buried Drums

To address the possibility that buried drums of waste pose the potential for sudden failure, an analysis was conducted using the latest calibrated numerical model to explore scenarios of drum failure, monitoring behavior, and post-failure SVE performance. For this analysis, between one and five drums (200 L per drum) of pure liquid 1,1,1-TCA are assumed to be released suddenly. The analysis further assumes that this mass of solvent (264 kg per drum) is spread at the maximum 1,1,1-TCA vapor pressure (160,000 ppmv at 20°C) into a region of the model domain 40–80 ft bgs within the source region. A single source region on the east side was chosen to allow behavior at a range of distances to be characterized through the location of the release relative to existing monitoring boreholes (Figure 5.6-1). The release location and the boreholes chosen characterize the potential for observations and span the distances from any known location of solvent-containing drums (or containers) to an existing observation well (Table 5.6-1). This analysis should therefore provide predictions sufficient to develop a robust monitoring strategy for detecting sudden drum/container failure at MDA L. All simulations of sudden drum/container failure were initiated on June 30, 2017, following the final SVE-East rebound study.

5.6.1 Drum Failure in Absence of SVE

Next, simulation results are presented for cases where drum failure occurs with no subsequent SVE operation, and simulations are run for 10 yr to June 2027. First, the evolution of concentration in the closest monitoring borehole, 54-24238, for the case of a single 200-L drum of TCA failing is shown in Figure 5.6-2. Because this borehole is quite close to the drum failure, concentrations in the monitoring ports spike quickly to greater than 1000 ppmv (1E6 ppbv). Concentrations for the next closest monitoring borehole, 54-27642, are shown in Figure 5.6-3. In this borehole, maximum concentrations of nearly 5000 ppmv are seen in the upper 100 ft bgs within approximately 1 yr. At the furthest analyzed monitoring borehole from the release, 54-24241, concentrations increase an order of magnitude within 2 yr for ports above 100 ft bgs (Figure 5.6-4). Results for simulations with five drum failures are even more extreme and easily detected at the three example distances from the release.

Results showing the arrival at three distances resulting from one drum failing suggest that by using existing monitoring boreholes, a reasonable metric for detecting drum failure of VOC from the source area can be constructed. The distance from the release to borehole 54-24241 is the maximum distance explored and is greater than the distance from any potential release location to an existing borehole. The distance from borehole 54-27642 to the simulated sudden release is more representative of the maximum distance any leak would be from an existing borehole, and simulation results from this location suggest that a conservative metric for detection of such a release would be an increase in total VOC concentration to over 2000 ppmv within a period of 2 yr, with a trend of consistent increase with each consecutive measurement for ports to depths of 100 ft within an impacted borehole. Further, given that there are multiple monitoring boreholes immediately surrounding both the east and west shaft clusters, a logical path forward would be to assign this group of monitoring boreholes to be “sentry boreholes” and focus monitoring on these moving forward. Given the 1–2-yr time scale for a sudden release signal to arrive at the sentry boreholes, a logical interval for sampling these boreholes would be every 6 mo. Since no known source exists outside of the source locations, monitoring of peripheral boreholes could be reduced in frequency to create a sitewide plume measurement once every 2 yr.

5.6.2 Simulated SVE Remediation Following Sudden Drum Failure

In this section, results are presented that demonstrate the ability of the existing SVE-East borehole to remediate a sudden drum failure. For this simulation, a five-drum release is evaluated, with the failure happening on June 29, 2017. The saturated vapor pressure of 1,1,1-TCA is fixed in the failure region from 40 to 80 ft bgs for 166 d to generate vapor-phase mass equal to five 200-L drums. It is assumed that 3 yr are needed to notice the sudden release, stand up the remediation, and initiate SVE on June 29, 2020. SVE is allowed to run continuously for 7 yr to June 29, 2027, with a goal of remediating the sudden drum failure. This is likely a longer continuous operation than would be conducted in practice; however, the results from this simulation can guide decisions on what length of time would be appropriate for remediating a failure of this magnitude.

Figure 5.6-5 shows the results from the five-drum sudden failure simulation including 7 yr of SVE operation starting in June 2020 for borehole 54-27642. Borehole 54-27642 is 138 ft from the SVE-East unit, at the outside of the radius of influence shown in Figure 1.1-1. A dramatic increase in concentration is seen in the first year for ports to 116 ft bgs. Concentrations rise from 40 to 50 ppmv in these shallowest three ports to over 20,000 ppmv. The port at 175 ft bgs shows a more gradual rise to almost 1000 ppmv. Diffusion in the rocks leads to a slow drop in the shallow ports until the SVE system is turned on June 29, 2020. At this time, the concentrations in all ports drop quickly. By June 2022, after just 2 yr of SVE, concentrations at all ports have returned to pre-failure values.

The impact of SVE on the total plume can be seen in Figure 5.6-6, where the total 1,1,1-TCA plume mass in the vapor phase (1500 kg), largely from the five-drum failure (1351 kg), has been reduced to less than 300 kg in only 2 yr of active extraction. This simulation provides a defensible estimate for creating a plan for remediating hypothetical drum failures and shows that the site operators would have ample time to turn on the SVE system after detection.

6.0 DEVIATIONS

This section describes deviations from the IMWP (LANL 2014, 261843). The deviations discussed below include ports that could not be sampled, a reduction from 1 full year of operation, and issues with the usage of a dual-packer system in borehole 54-24399.

6.1 Sampling Ports

Several ports listed in Table 2.2-3 were found to be either fully or partially blocked. If ports were partially or fully blocked for two consecutive sampling rounds, these ports were assumed to be suspect and were removed from the sampling plan. Additionally, radiological concerns caused some ports to be temporarily removed from the sampling plan in November 2015. RCT monitoring detected gas concentrations of greater than 20 µg/m^3 in 18 ports (Table 2.2-3). However, this issue was resolved, and an RCT-approved method for sampling allowed these 18 ports to be sampled in future quarterly sampling events.

6.2 Active Extraction Duration

The SVE system was run from January 2015 to November 2015. This is a deviation from the initial plan to run the system for a full year. The decision to stop the SVE units in November 2015 was based on production of condensate from the SVE units during times when temperatures dropped below freezing. Subsurface vapor, containing both water vapor and VOC gases, condenses in the SVE system and accumulates in the 20-gal. liquid storage container (Figure 2.1-1). This liquid must be characterized because of the dissolved VOC component. Furthermore, the liquid must be removed from the storage container on a regular basis because several gallons per day can accumulate during cold weather. To avoid issues with condensate, the decision was made to shut down the SVE units in November 2015.

6.3 Deep Borehole 54-24399 Dual-Packer Failure

During the April 2015 sampling event, the dual-packer sampling system used to isolate a 1-ft interval (568–569 ft bgs) directly beneath the casing of borehole 54-24399 was badly damaged. The lower packer was shredded when it came in contact with very sharp basalt. The sharp nature of the vesicular basalt can be observed in the video log of borehole 54-24399 (Appendix D). The video log shows a limited region of massive basalt directly below the casing (less than 2 ft), followed by a large void area. To avoid further problems with packer destruction, the decision was made to install a permanent single packer.

In August 2016, a permanent single packer was installed at the bottom of the casing (566.7 ft bgs) to collect pore-gas samples in the open portion of the borehole. The permanent single packer hangs from the surface on a 1-in. steel pipe, pulling a new well cap firmly down onto an O-ring in an effort to minimize barometrically pumped flow into and out of the well. Two gas sampling ports penetrate the packer and are connected to ports on the surface well cap. The first port samples directly beneath the packer (566.7 ft bgs) while the second port ends 21 ft below the bottom of the packer at 587.8 ft bgs. A pressure transducer is mounted on the top of the packer with its pressure sampling port located directly beneath the packer at 566.7 ft bgs. The final connection on the packer top is used to connect a 50-psi nitrogen line for packer inflation.

7.0 CONCLUSIONS

The three objectives listed in the IMWP have been met.

- Approximately 1200 lb of VOC mass was removed during the IM through SVE, satisfying the first objective.
- Maximum VOC concentrations have been reduced in the core of the plume beneath the source regions and concentrations at the lateral boundaries have dropped, satisfying the second objective.
- Although concentrations at the deepest edge of the plume near the basalt/tuff interface were not changed significantly by operation of the IM SVE, the breathing nature of the basalt provides a protective vertical zone where concentrations are well mixed and drop rapidly below the tuff. This means that high concentrations are contained within the Bandelier Tuff, satisfying the third objective.

During the initial IM SVE operation in 2015, the two SVE units removed 553 kg (1217 lb) of total organic vapor mass. The mass was primarily removed from within an approximately 150-ft radius surrounding each of the extraction wells. Mass removal was higher initially and continued at a removal rate of nearly 17 lb/mo after 10 mo of operation.

Rebound of the plume after the end of the active SVE IM was slow, with most observation ports rebounding to no more than 50% of their original concentrations over more than 6 yr. Two wells in the eastern shaft cluster (54-02089 and 54-24238) showed increases in concentration above baseline sampling, which may be the result of an active leak.

The long-term ability of the SVE system to remove significant quantities of vapor-phase organics has been demonstrated, and data collected during the IM has been analyzed further as part of ongoing efforts to support the selection and design of a final remedy for MDA L. Simulations show that the current SVE boreholes are capable of remediating a sudden release of solvents and that such remediation could happen over a relatively short period (2 yr of SVE).

8.0 RECOMMENDATIONS

The following recommendations are based on 10 mo of SVE operation at MDA L followed by more than 6 yr of plume rebound, and include results from a tracer test performed in the deep Cerros del Rio basalt.

1. Conduct semiannual monitoring of boreholes located in the source region (“sentry boreholes”) to allow early detection of potential container failure. Boreholes 54-24240 and 54-27641 on the western side of MDA L are sentry boreholes. On the eastern side of MDA L, boreholes 54-24238, 54-24241, and 54-27642 and open borehole 54-24399 are sentry boreholes. Peripheral borehole 54-02089 was added to the sentry borehole sampling network in 2020 because of an increase in concentrations over the last several sampling events.
2. Monitor peripheral boreholes once every 2 yr for evidence of plume expansion or contraction.
3. Conduct semiannual monitoring of deep borehole 54-24399 to further characterize long-term trends of VOC concentrations in the basalt and to provide data needed to support the Corrective Measures Evaluation process (e.g., updating the conceptual model for transport, and developing Tier II screening levels and cleanup goals).
4. Operate the SVE units to continue mass removal. Operation of the SVE units will initially be in the spring and fall seasons, using effluent data to determine run times for each extraction cycle. The operation schedule of the SVE units will adapt to changing subsurface concentration data and will continue until a final remedy is implemented at MDA L.
5. Activate the eastern SVE system if, at any time, total VOC concentrations in any ports in the eastern sentry boreholes rise above 2000 ppmv, with a trend of consistent increase with each consecutive measurement for ports to depths of 100 ft, and adapt the eastern SVE system as necessary to run as continuously as possible until concentrations drop below 2000 ppmv.
6. Activate the western SVE system if, at any time, total VOC concentrations in any ports in the western sentry boreholes rise above 2000 ppmv with a trend of consistent increase with each consecutive measurement for ports to depths of 100 ft, and adapt the western SVE system as needed to run as continuously as possible until concentrations drop below 2000 ppmv.
7. Report all monitoring data and SVE operations details in a single report to be submitted annually to NMED. This report will replace the current MDA L Periodic Monitoring Report, and renamed to indicate the addition of the SVE operational details.

9.0 REFERENCES AND MAP DATA SOURCES

9.1 References

The following reference list includes documents cited in this report. Parenthetical information following each reference provides the author(s), publication date, and ERID, ESHID, or EMID. ERIDs were assigned by Los Alamos National Laboratory's (the Laboratory's) Associate Directorate for Environmental Management (IDs through 599999); ESHIDs were assigned by the Laboratory's Associate Directorate for Environment, Safety, and Health (IDs 600000 through 699999); and EMIDs are assigned by N3B (IDs 700000 and above).

Behar, H.R., E.E. Snyder, S. Marczak, L.J. Salazar, B. Rappe, G.F. Fordham, S.P. Chu, D.M. Strobridge, K.H. Birdsell, T.A. Miller, K.C. Rich, and P.H. Stauffer, February 2019. "An Investigation of Plume Response to Soil Vapor Extraction and Hypothetical Drum Failure," *Vadose Zone Journal,* Vol. 18, No. 1. (Behar et al. 2019, 700854)

DOE (U.S. Department of Energy), October 12, 2016. "Withdrawal of Three Corrective Measures Evaluations and Suggested Priorities for New Mexico Environment Department Review of Documents," U.S. Department of Energy letter to J. Kieling (NMED-HWB) from D. Rhodes (DOE-EM), Los Alamos, New Mexico. (DOE 2016, 601899)

LANL (Los Alamos National Laboratory), September 2005. "Investigation Report for Material Disposal Area L, Solid Waste Management Unit 54-006, at Technical Area 54," Los Alamos National Laboratory document LA-UR-05-5777, Los Alamos, New Mexico. (LANL 2005, 092591)

LANL (Los Alamos National Laboratory), November 2006. "Summary Report: 2006 In Situ Soil Vapor Extraction Pilot Study at Material Disposal Area L, Technical Area 54, Los Alamos National Laboratory," Los Alamos National Laboratory document LA-UR-06-7900, Los Alamos, New Mexico. (LANL 2006, 094152)

LANL (Los Alamos National Laboratory), September 2011. "Corrective Measures Evaluation Report for Material Disposal Area L, Solid Waste Management Unit 54-006, at Technical Area 54, Revision 2," Los Alamos National Laboratory document LA-UR-11-4798, Los Alamos, New Mexico. (LANL 2011, 205756)

LANL (Los Alamos National Laboratory), September 2014. "Interim Measures Work Plan for Soil-Vapor Extraction of Volatile Organic Compounds from Material Disposal Area L, Technical Area 54, Revision 1," Los Alamos National Laboratory document LA-UR-14-26472, Los Alamos, New Mexico. (LANL 2014, 261843)

LANL (Los Alamos National Laboratory), September 2015. "Interim Measures Progress Report for Soil-Vapor Extraction of Volatile Organic Compounds from Material Disposal Area L, Technical Area 54," Los Alamos National Laboratory document LA-UR-15-26893, Los Alamos, New Mexico. (LANL 2015, 600930)

LANL (Los Alamos National Laboratory), May 2016. "Interim Measures Progress Report for Soil-Vapor Extraction of Volatile Organic Compounds from Material Disposal Area L, Technical Area 54," Los Alamos National Laboratory document LA-UR-16-23065, Los Alamos, New Mexico. (LANL 2016, 601484)

LANL (Los Alamos National Laboratory), July 2016. "Work Plan for a Tracer Test at Material Disposal Area G, Technical Area 54," Los Alamos National Laboratory document LA-UR-16-24628, Los Alamos, New Mexico. (LANL 2016, 601622)

N3B (Newport News Nuclear BWXT-Los Alamos, LLC), August 2018. "Interim Measures Final Report for Soil-Vapor Extraction of Volatile Organic Compounds from Material Disposal Area L, Technical Area 54," Newport News Nuclear BWXT-Los Alamos, LLC, document EM2018-0008, Los Alamos, New Mexico. (N3B 2018, 700039)

N3B (Newport News Nuclear BWXT-Los Alamos, LLC), July 2021. "Periodic Monitoring Report for 2019 Vapor-Sampling Activities at Material Disposal Area L, Solid Waste Management Unit 54-006, at Technical Area 54, Revision 2," Newport News Nuclear BWXT-Los Alamos, LLC, document EM2021-0379, Los Alamos, New Mexico. (N3B 2021, 701563)

N3B (Newport News Nuclear BWXT-Los Alamos, LLC), May 2021. "Periodic Monitoring Report for 2020 Vapor-Sampling Activities at Material Disposal Area L, Solid Waste Management Unit 54-006, at Technical Area 54," Newport News Nuclear BWXT-Los Alamos, LLC, document EM2021-0242, Los Alamos, New Mexico. (N3B 2021, 701446)

N3B (Newport News Nuclear BWXT-Los Alamos, LLC), May 2022. "Periodic Monitoring Report for 2021 Vapor-Sampling Activities at Material Disposal Area L, Solid Waste Management Unit 54-006, at Technical Area 54," Newport News Nuclear BWXT-Los Alamos, LLC, document EM2022-0265, Los Alamos, New Mexico. (N3B 2022, 702084)

Neeper, D.A., 2002. "Investigation of the Vadose Zone Using Barometric Pressure Cycles," *Journal of Contaminant Hydrology,* Vol. 54, pp. 59-80. (Neeper 2002, 098639)

NMED (New Mexico Environment Department), July 17, 2014. "Approval with Modifications, Interim Measures Work Plan for Soil-Vapor Extraction of Volatile Organic Compounds from Material Disposal Area L, Technical Area 54," New Mexico Environment Department letter to P. Maggiore (DOE-NA-LA) and J.D. Mousseau (LANL) from J.E. Kieling (NMED-HWB), Santa Fe, New Mexico. (NMED 2014, 525053)

NMED (New Mexico Environment Department), July 17, 2019. "NMED Draft Comments on Interim Measures Final Report for Soil-Vapor Extraction of Volatile Organic Compounds from Material Disposal Area L, Technical Area 54," Santa Fe, New Mexico. (NMED 2019, 700515)

Stauffer, P., K. Birdsell, and W. Rice, March 7–11, 2011. "3-D Model Validation in Support of Site Closure, Material Disposal Area L, Los Alamos, NM," Paper 11545, Waste Management 2011 Conference, March 7–11, 2011, Phoenix, AZ. (Stauffer et al. 2011, 255584)

Stauffer, P.H., K.H. Birdsell, M.S. Witkowski, and J.K. Hopkins, 2005. "Vadose Zone Transport of 1,1,1-Trichloroethane: Conceptual Model Validation through Numerical Simulation," *Vadose Zone Journal,* Vol. 4, pp. 760–773. (Stauffer et al. 2005, 090537)

Stauffer, P.H., J.K. Hopkins, and T. Anderson, February 25–March 1, 2007. "A Soil Vapor Extraction Pilot Study in a Deep Arid Vadose Zone, Part 2: Simulations in Support of Decision Making Processes," Waste Management Conference 2007, February 25–March 1, 2007, Tucson, Arizona. (Stauffer et al. 2007, 104950)

Stauffer, P.H., J.K. Hopkins, T. Anderson, and J. Vrugt, July 11, 2007. “Soil Vapor Extraction Pilot Test at Technical Area 54, Material Disposal Area L: Numerical Modeling in Support of Decision Analysis,” Los Alamos National Laboratory document LA-UR-07-4890, Los Alamos, New Mexico. (Stauffer et al. 2007, 097871)

Stauffer, P.H., T. Rahn, J.P. Ortiz, L.J. Salazar, H. Boukhalfa, H.R. Behar, and E.E. Snyder, March 2, 2019. “Evidence for High Rates of Gas Transport in the Deep Subsurface,” *Geophysical Research Letters,* Vol. 46, No. 7. (Stauffer et al. 2019, 700871)

Stauffer, P.H., and W.J. Stone, 2005. “Surface Water–Groundwater Connection at the Los Alamos Canyon Weir Site: Part 2. Modeling of Tracer Test Results,” *Vadose Zone Journal,* Vol. 4, pp. 718–728. (Stauffer and Stone 2005, 090037)

Vrugt, J.A., P.H. Stauffer, T. Wöhling, B.A. Robinson, and V.V. Vesselinov, May 2008. “Inverse Modeling of Subsurface Flow and Transport Properties: A Review with New Developments,” *Vadose Zone Journal,* Vol. 7, No. 2, pp. 843–864. (Vrugt et al. 2008, 104951)

Weston (Weston Solutions, Inc.), May 2015. “Final Baseline Data Evaluation for Soil Vapor Extraction at Material Disposal Area L, Solid Waste Management Unit 54-006, at Technical Area 54,” report prepared for Los Alamos National Laboratory, Los Alamos, New Mexico. (Weston 2015, 600886)

Weston (Weston Solutions, Inc.), September 2015. “Draft Final Evaluation of Data from the First Quarter of Soil Vapor Extraction at Material Disposal Area L, Solid Waste Management Unit 54-006, at Technical Area 54,” report prepared for Los Alamos National Laboratory, Los Alamos, New Mexico. (Weston 2015, 600887)

Zyvoloski, G.A., B.A. Robinson, Z.V. Dash, and L.L. Trease, July 1997. “Summary of the Models and Methods for the FEHM Application — A Finite-Element Heat- and Mass-Transfer Code,” Los Alamos National Laboratory report LA-13307-MS, Los Alamos, New Mexico. (Zyvoloski et al. 1997, 070147)

9.2 Map Data Sources

Hypsography, 20 and 100 Foot Contour Intervals; Los Alamos National Laboratory, ENV-Environmental Remediation and Surveillance Program; 1991

Materials Disposal Areas; Los Alamos National Laboratory, ENV-Environmental Remediation and Surveillance Program; ER2004-0221; 1:2,500 Scale Data; 23 April 2004

Waste Storage Features; Los Alamos National Laboratory, ENV-Environmental Remediation and Surveillance Program, ER2005-0748; 1:2,500 Scale Data; 06 October 2005

Security fence: Security and Industrial Fences and Gates; Los Alamos National Laboratory, KSL Site Support Services, Planning, Locating and Mapping Section; 06 January 2004; as published 29 November 2010.

Paved roads: Paved Road Arcs; Los Alamos National Laboratory, KSL Site Support Services, Planning, Locating and Mapping Section; 06 January 2004; as published 29 November 2010.

Unpaved roads: Dirt Road Arcs; Los Alamos National Laboratory, KSL Site Support Services, Planning, Locating and Mapping Section; 06 January 2004; as published 29 November 2010.

Structures: Structures; Los Alamos National Laboratory, KSL Site Support Services, Planning, Locating and Mapping Section; 06 January 2004; as published 29 November 2010.

Locations: ER Project Locations; Los Alamos National Laboratory, ESH&Q Waste and Environmental Services Division, 2010-2E; 1:2,500 Scale Data; 04 October 2010.

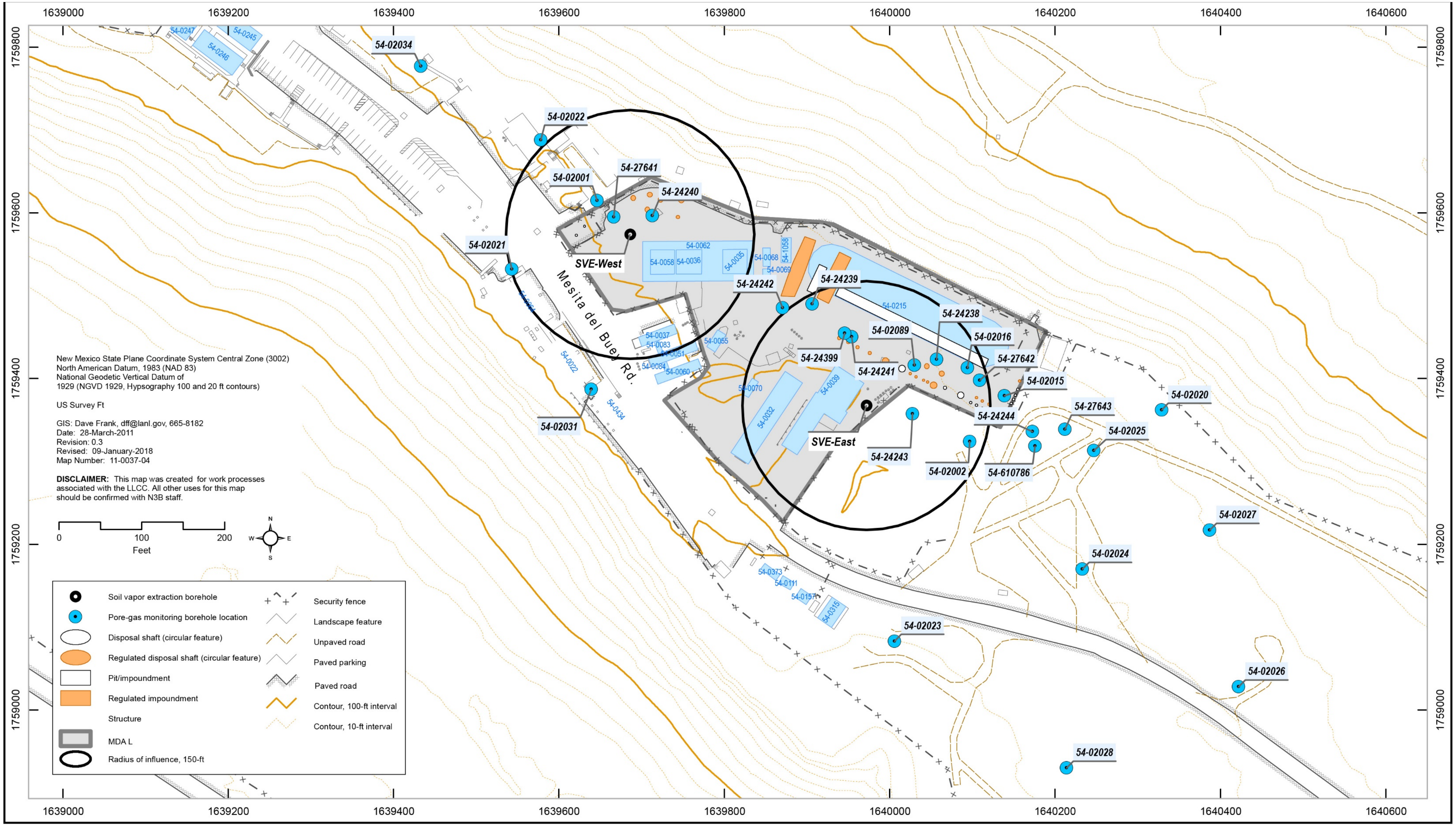

Figure 1.1-1 View of MDA L with disposal units, surface structures, pore-gas monitoring boreholes, SVE boreholes, and 150-ft ROI of extraction wells

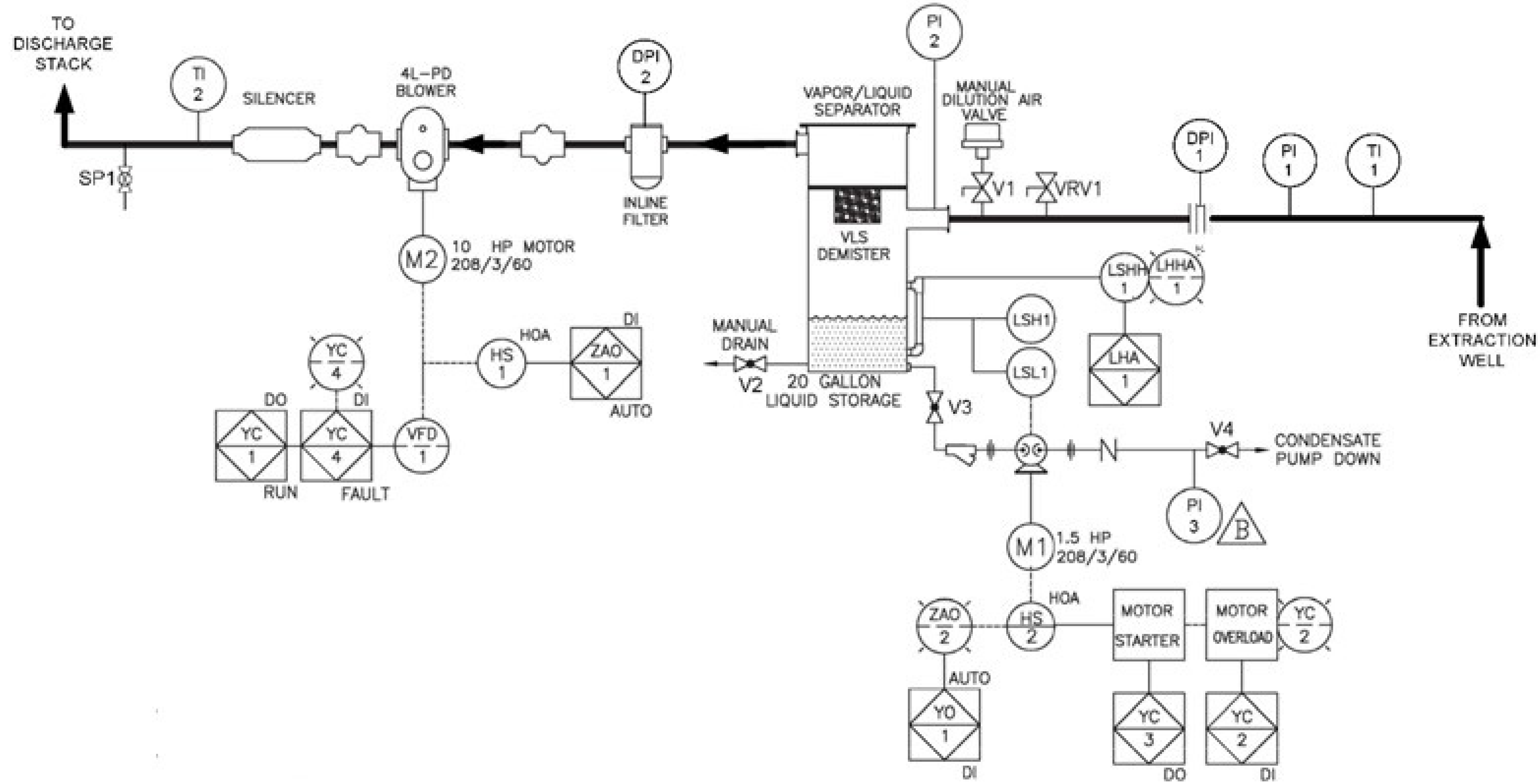

Figure 2.1-1 Diagram of SVE-East and SVE-West system piping and instrumentation

Figure 2.1-2 SVE-East unit

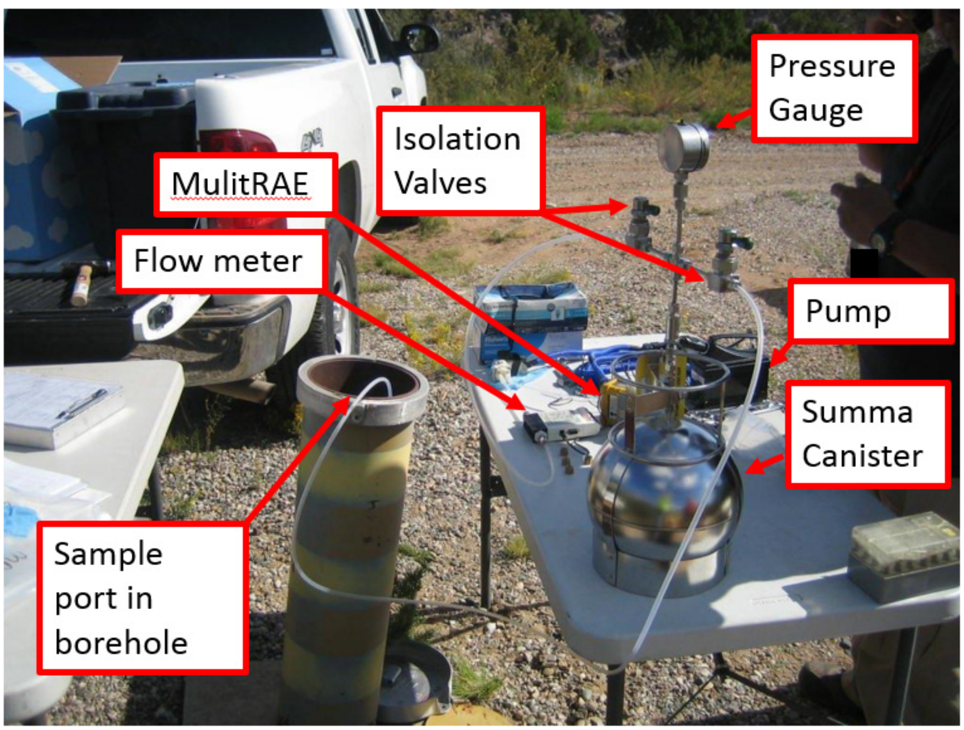

Figure 2.2-1 Subsurface sampling train

Figure 2.2-2 Permanent packer installed in borehole 54-24399 in August 2016

Figure 2.2-3 Surface completion of the permanent packer at borehole 54-24399

Figure 2.2-4 **Top of the permanent packer showing the OMEGA pressure transducer, one sample line, and the nitrogen inflation line**

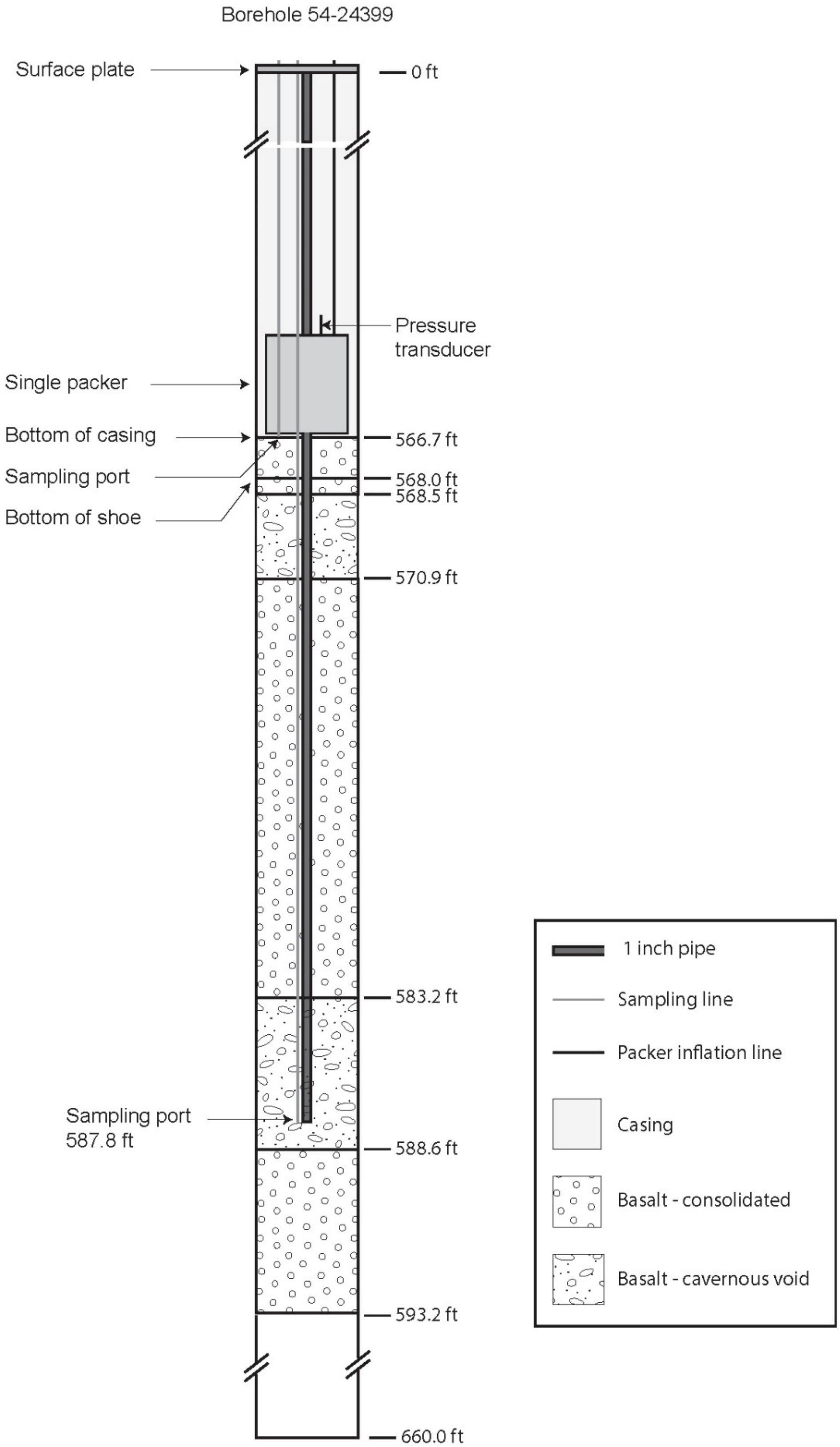

Figure 2.2-5 Schematic of the completed single packer installation in borehole 54-24399

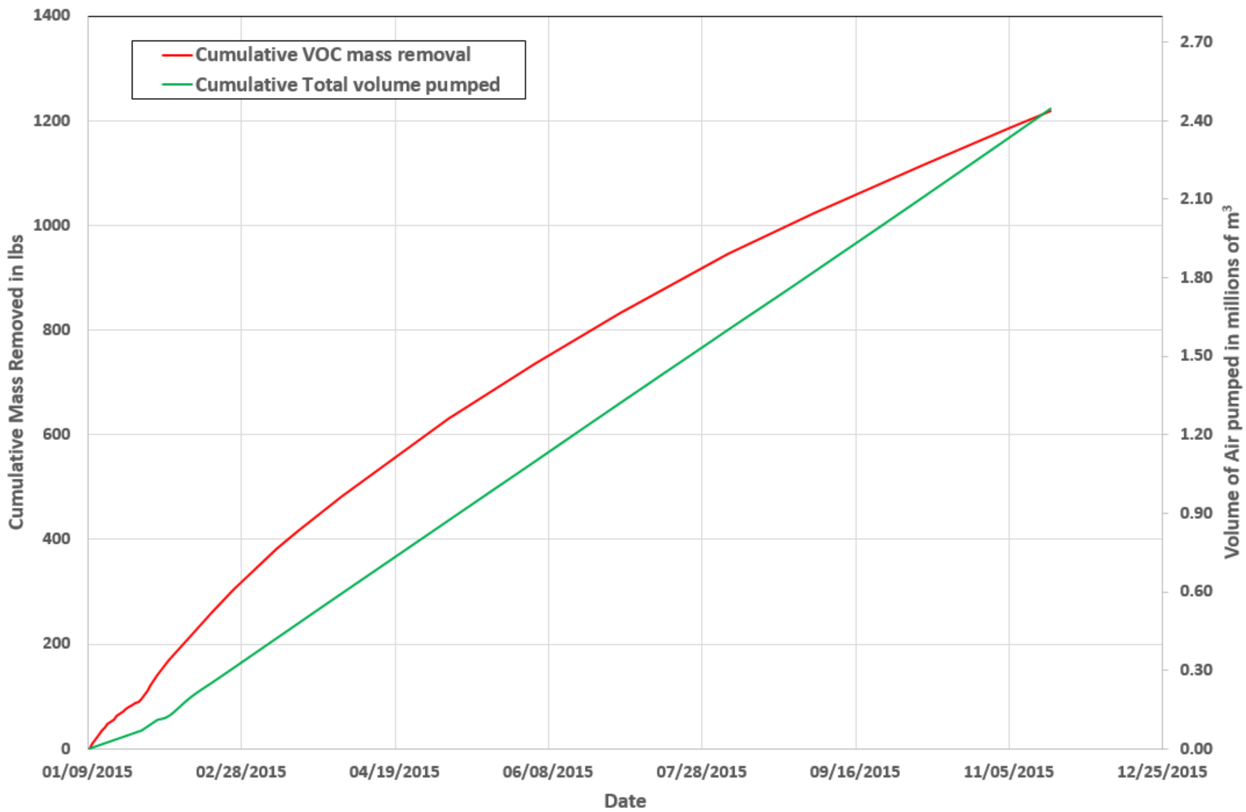

Figure 4.1-1 Cumulative mass removal and cumulative volume of pore gas pumped from the subsurface from both SVE units as a function of time

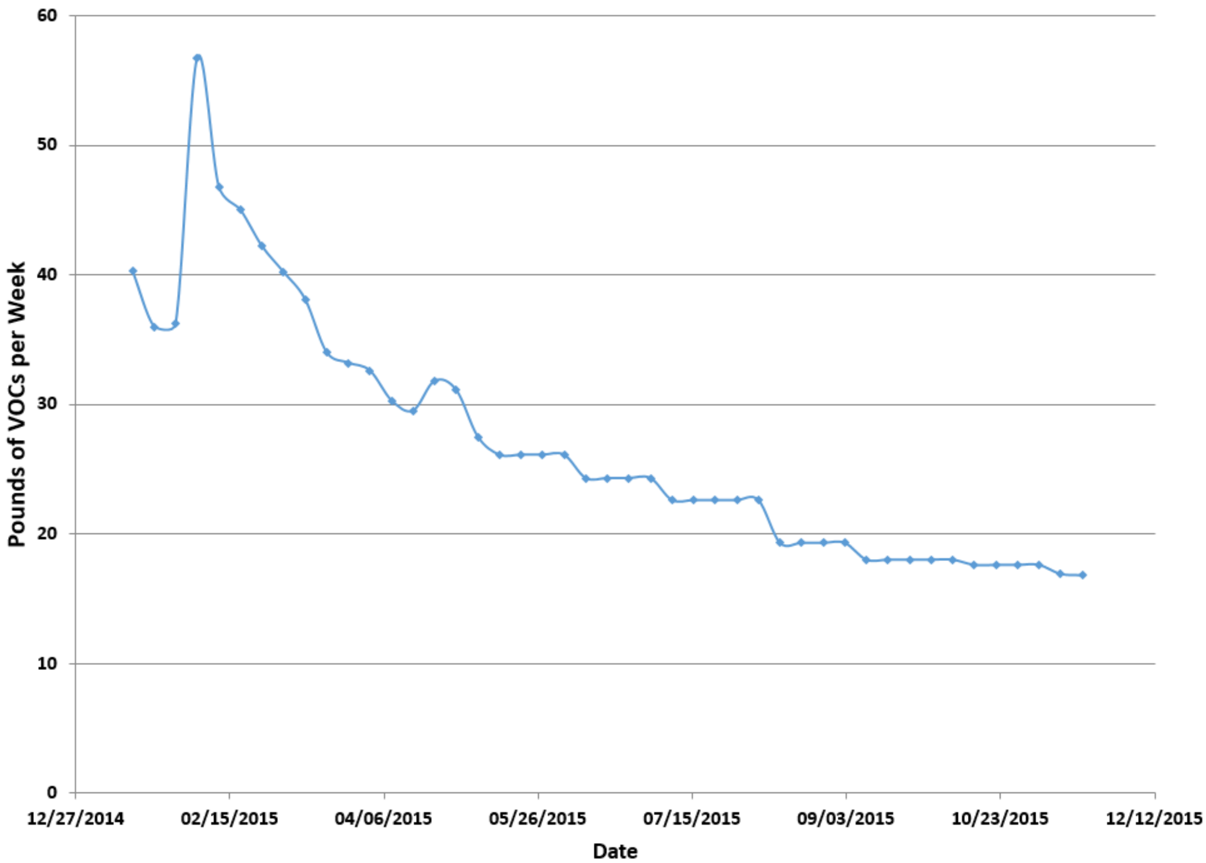

Figure 4.1-2 Weekly mass removal rate from both SVE units as a function of time

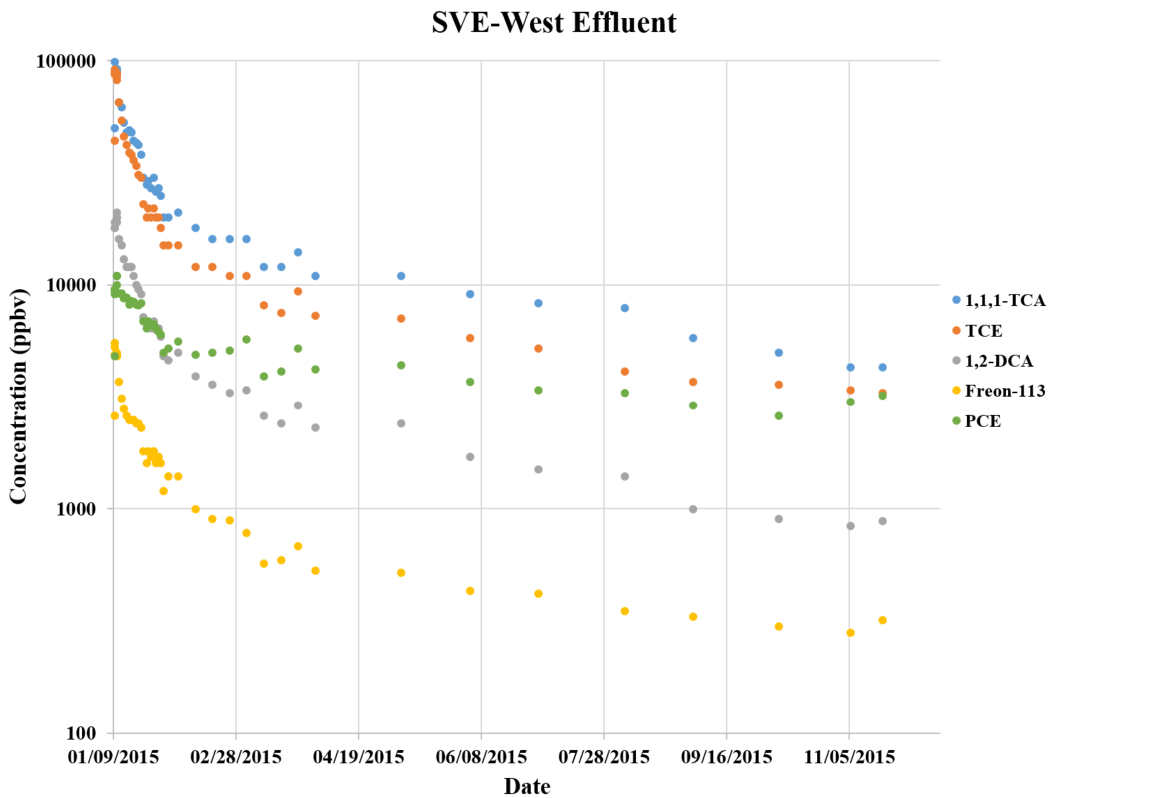

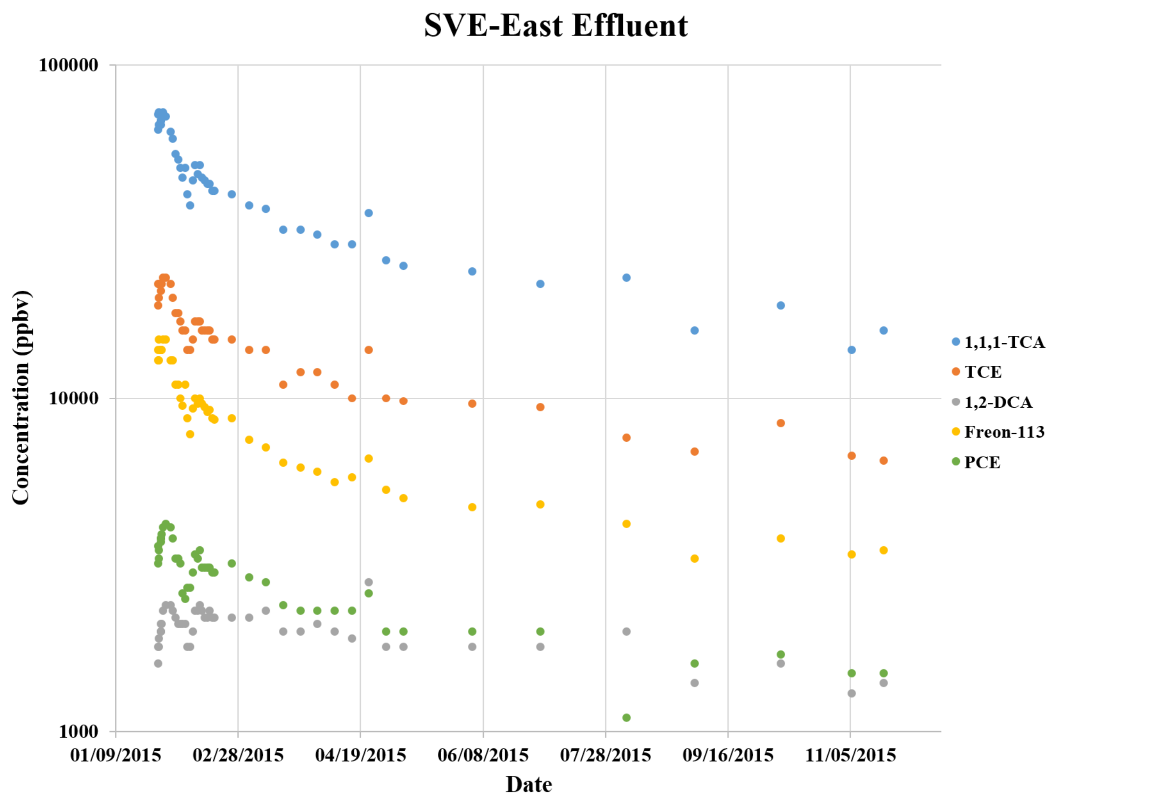

Figure 4.2-1 Effluent concentration versus time for SVE-West and SVE-East

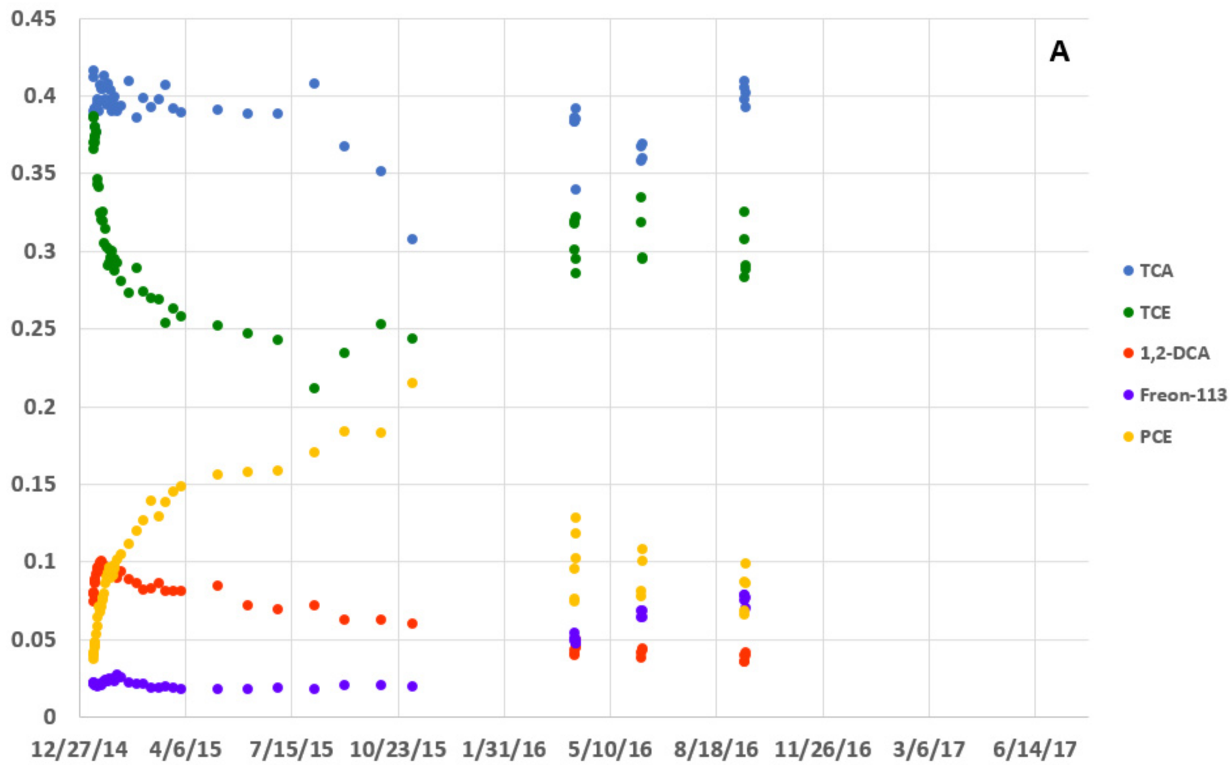

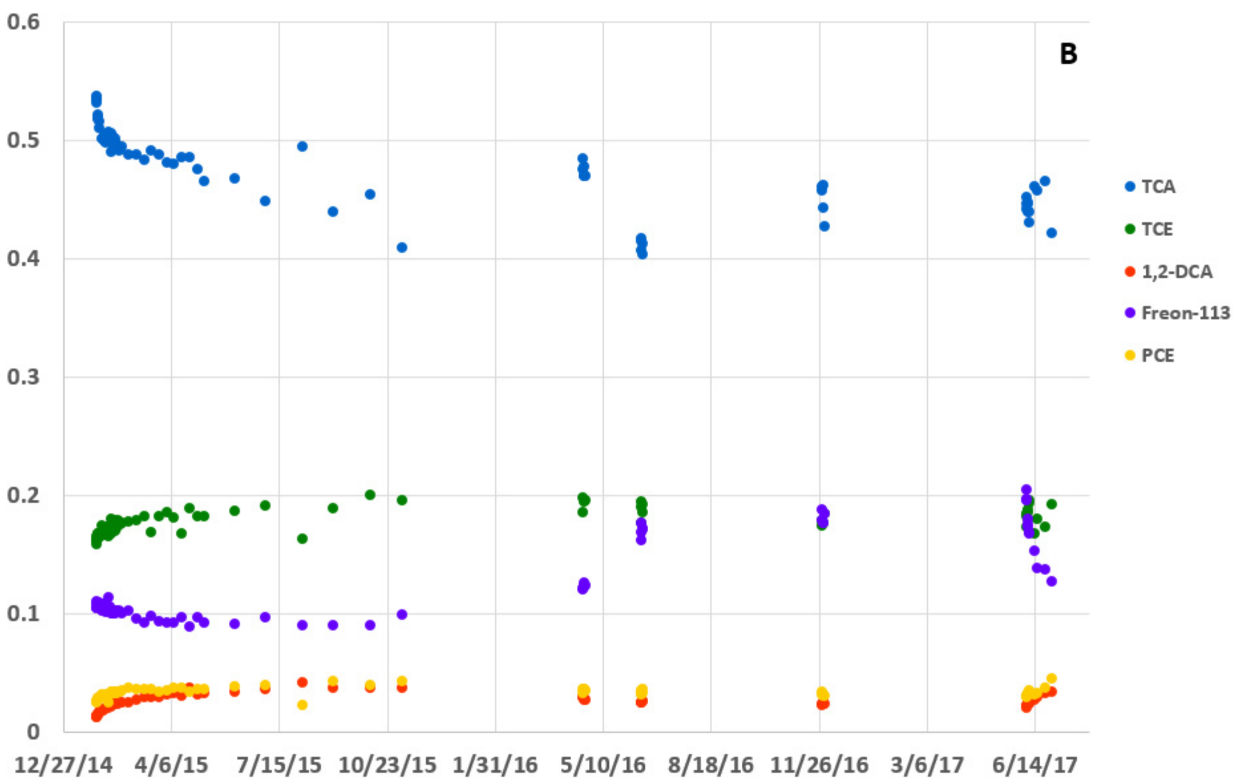

Figure 4.2-2 Effluent concentration ratios versus time for (A) SVE-West and (B) SVE-East

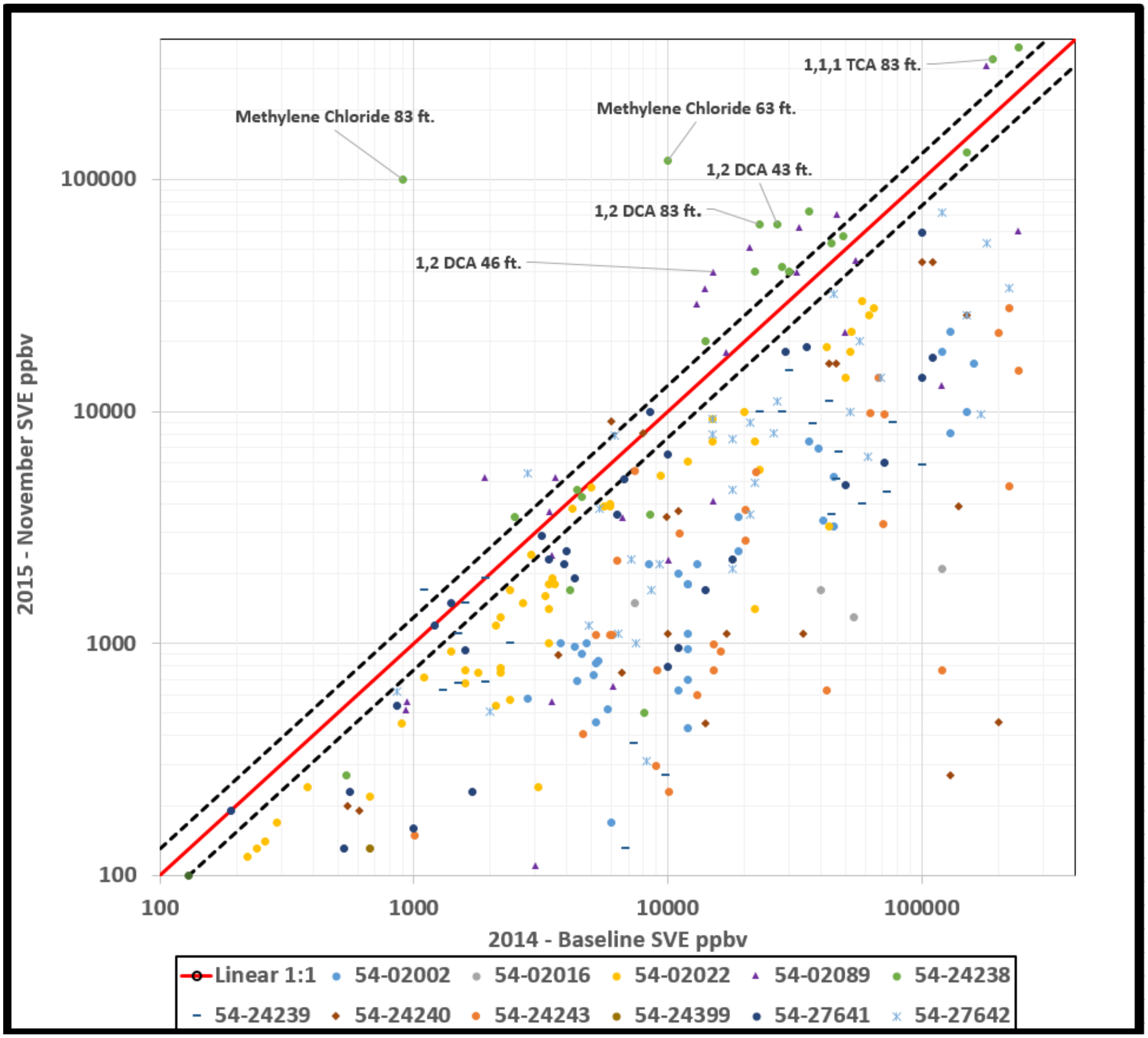

Figure 4.3-1 Comparison of subsurface VOC concentrations before SVE (baseline 2014) and after 10-plus mo of SVE pumping (November 2015)

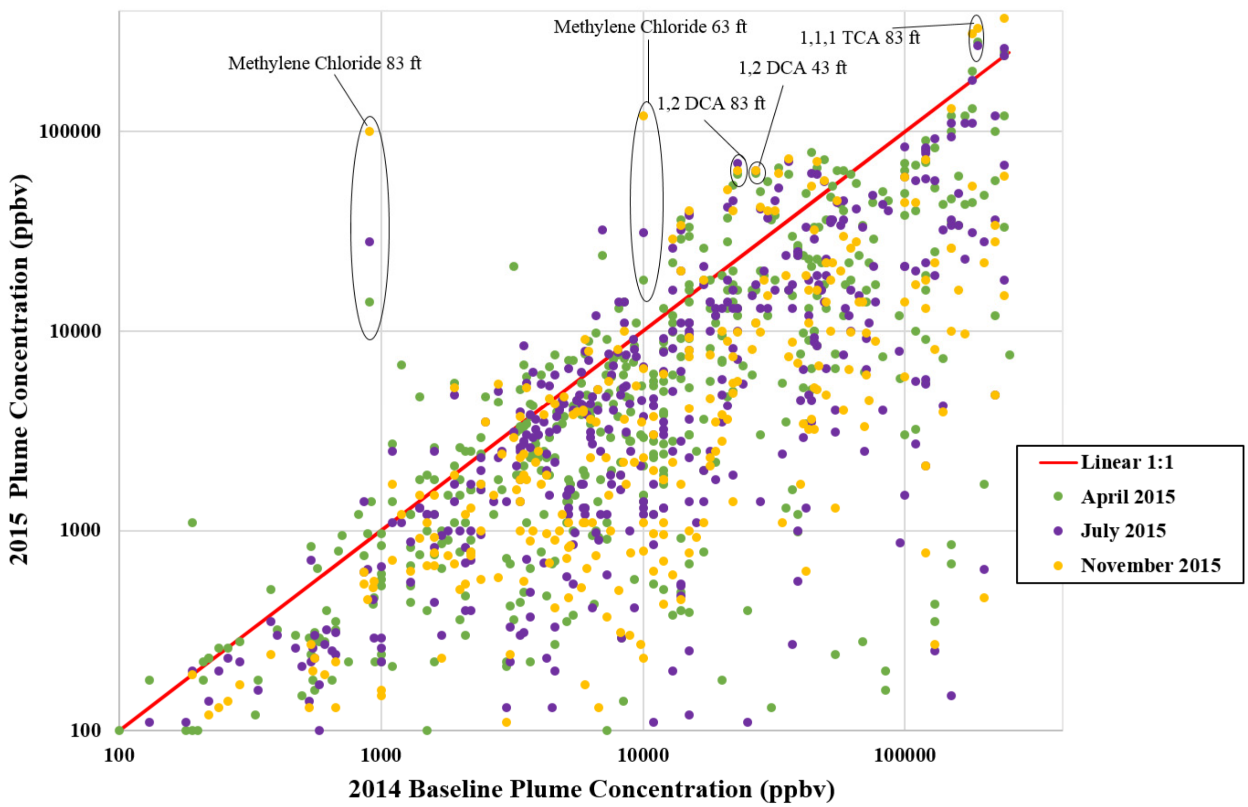

Figure 4.3-2 Comparison of post-SVE and pre-SVE subsurface VOC concentrations for seven analytes passing Tier II screening. Labeled points are all from borehole 54-24238.

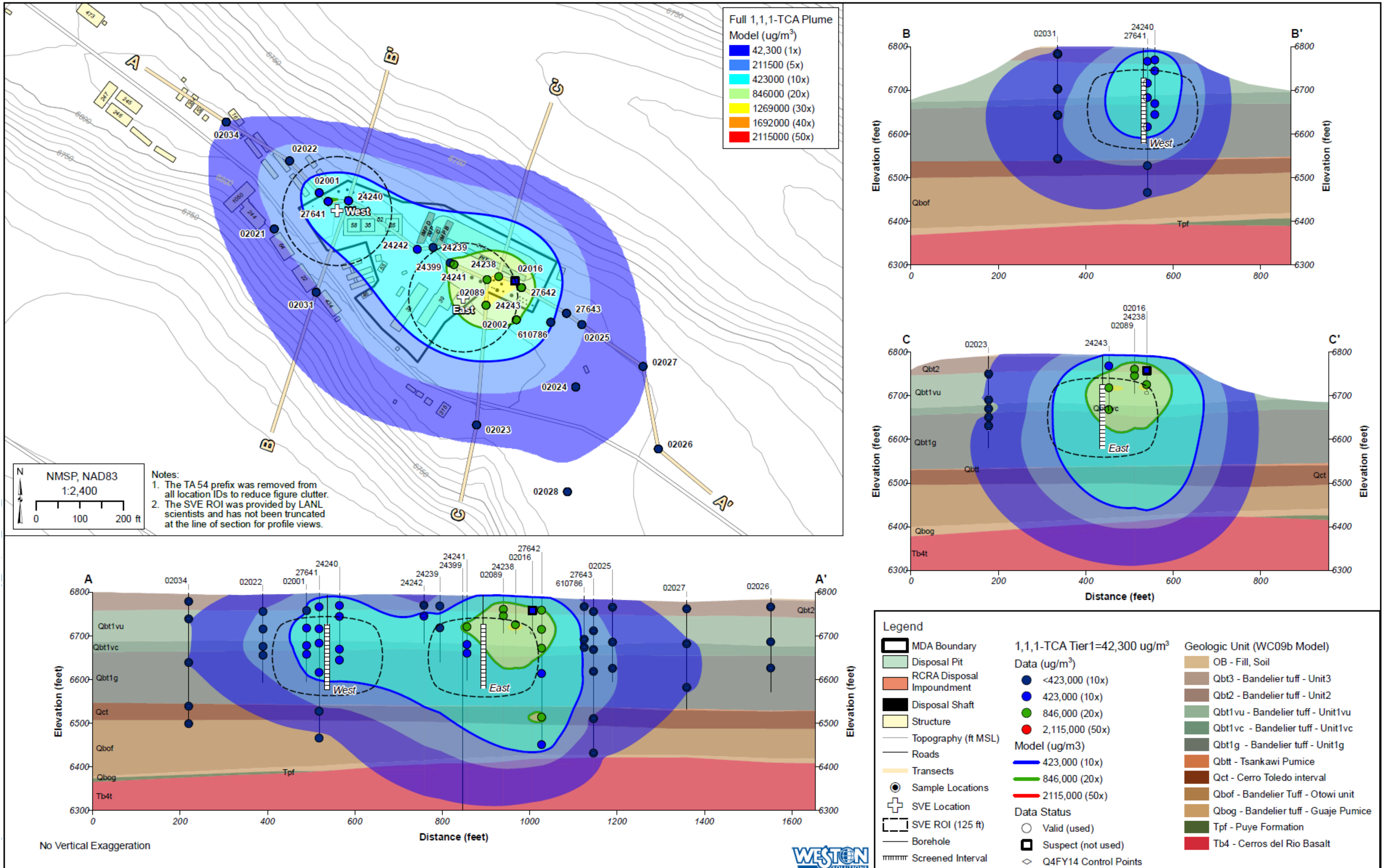

Figure 4.3-3 Baseline 2014 1,1,1-TCA plume data interpolated from borehole data

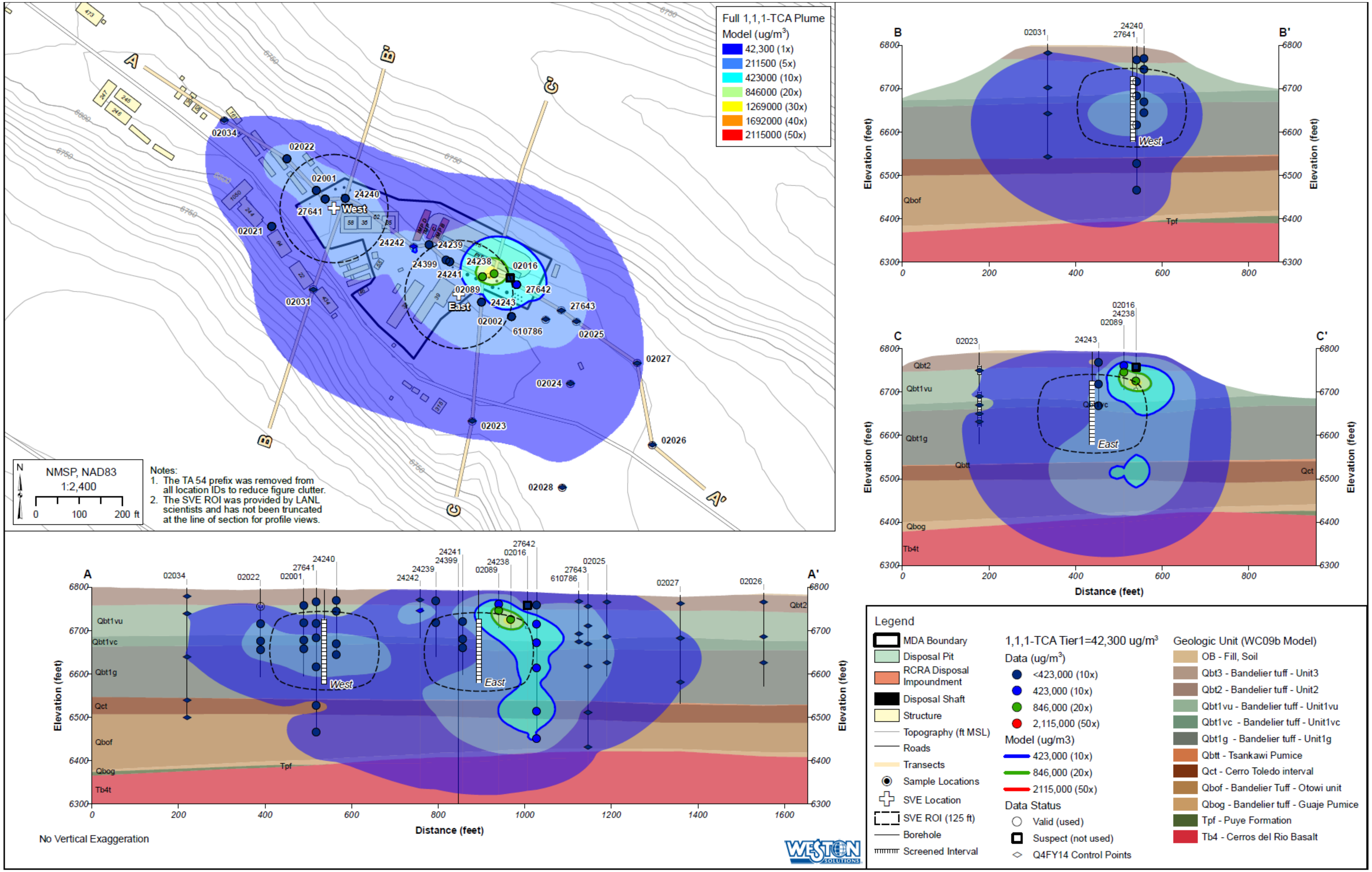

Figure 4.3-4 April 2015 1,1,1-TCA plume data interpolated from borehole data

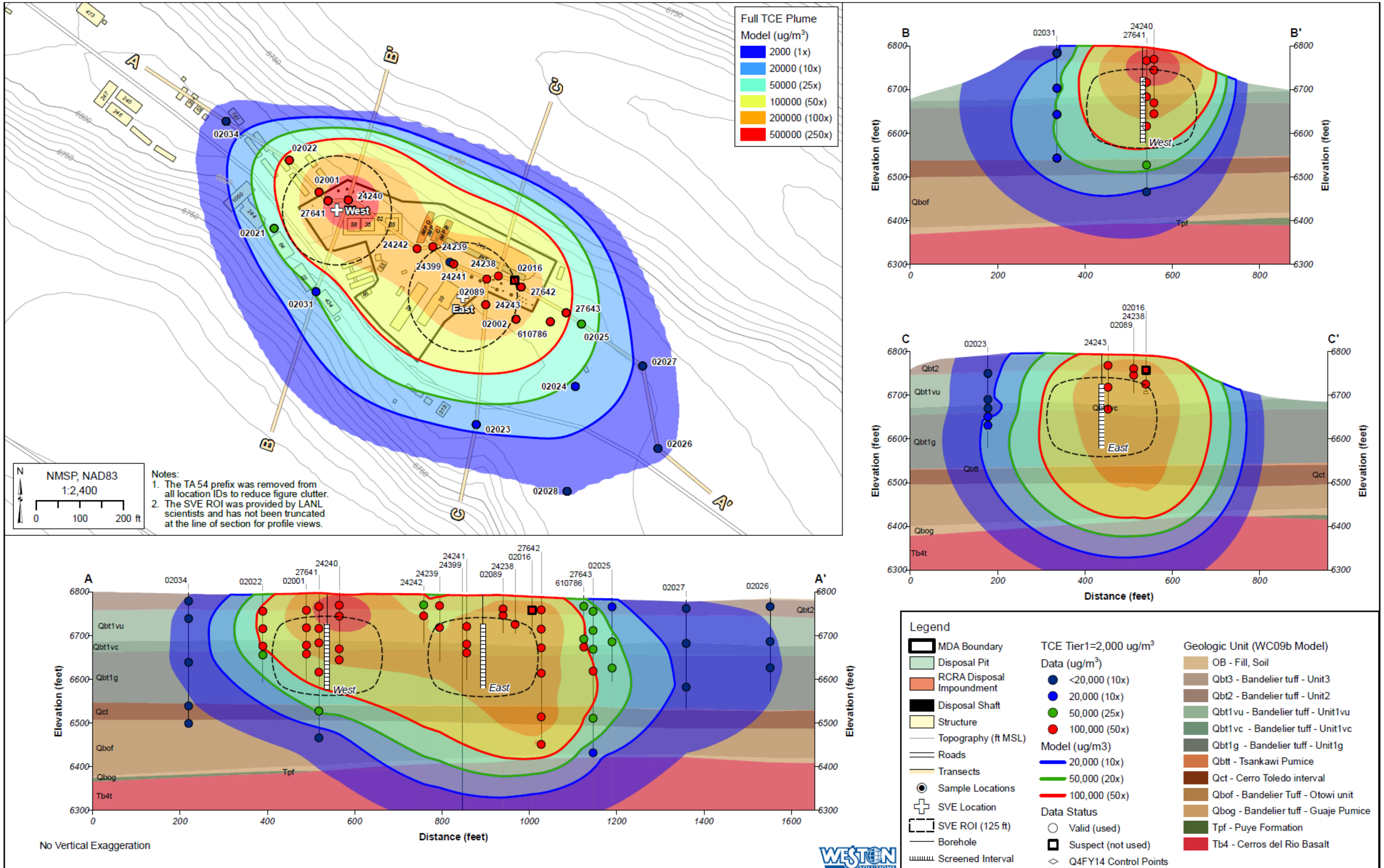

Figure 4.3-5 Baseline 2014 TCE plume data interpolated from borehole data

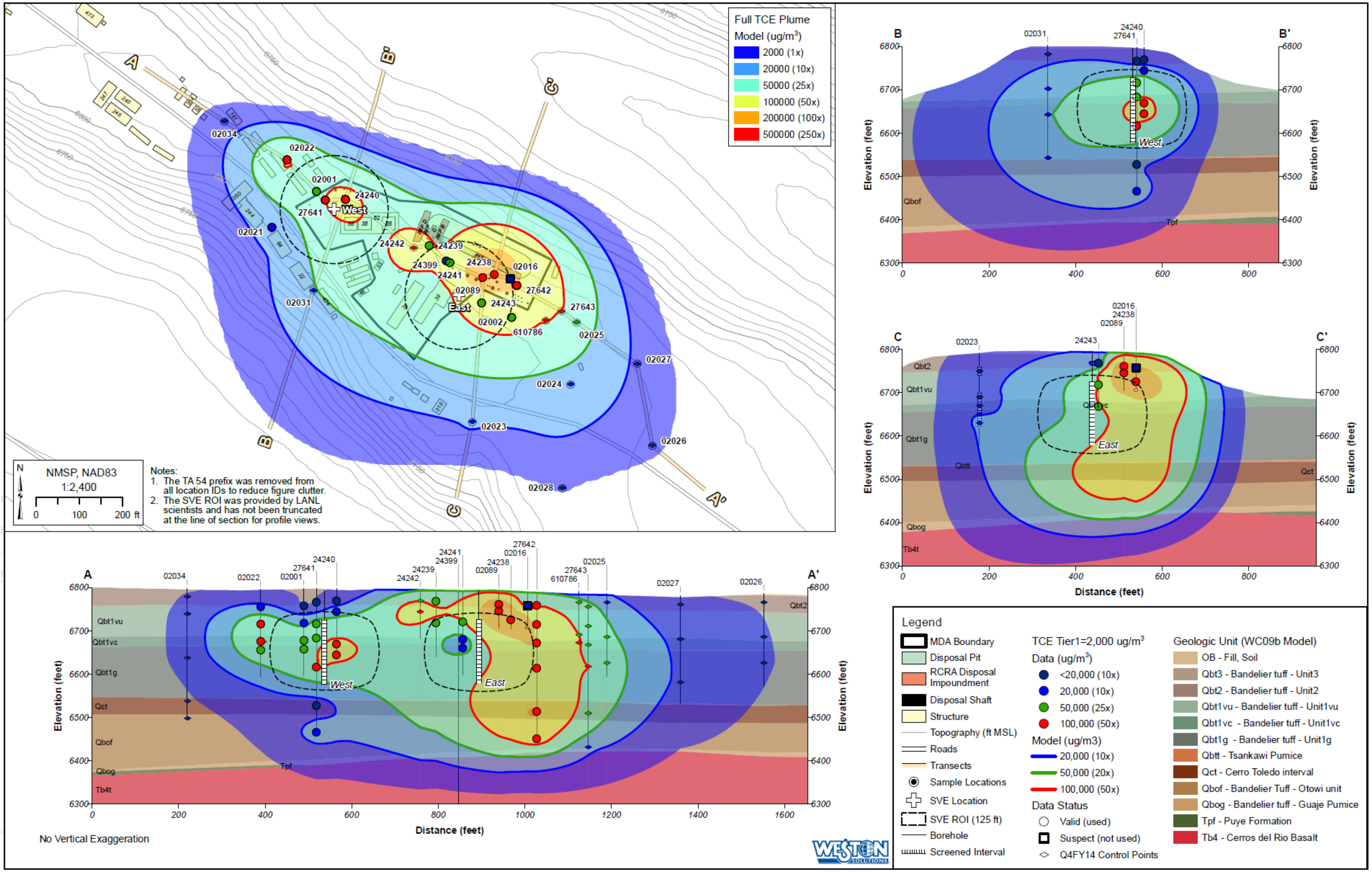

Figure 4.3-6 April 2015 TCE plume data interpolated from borehole data

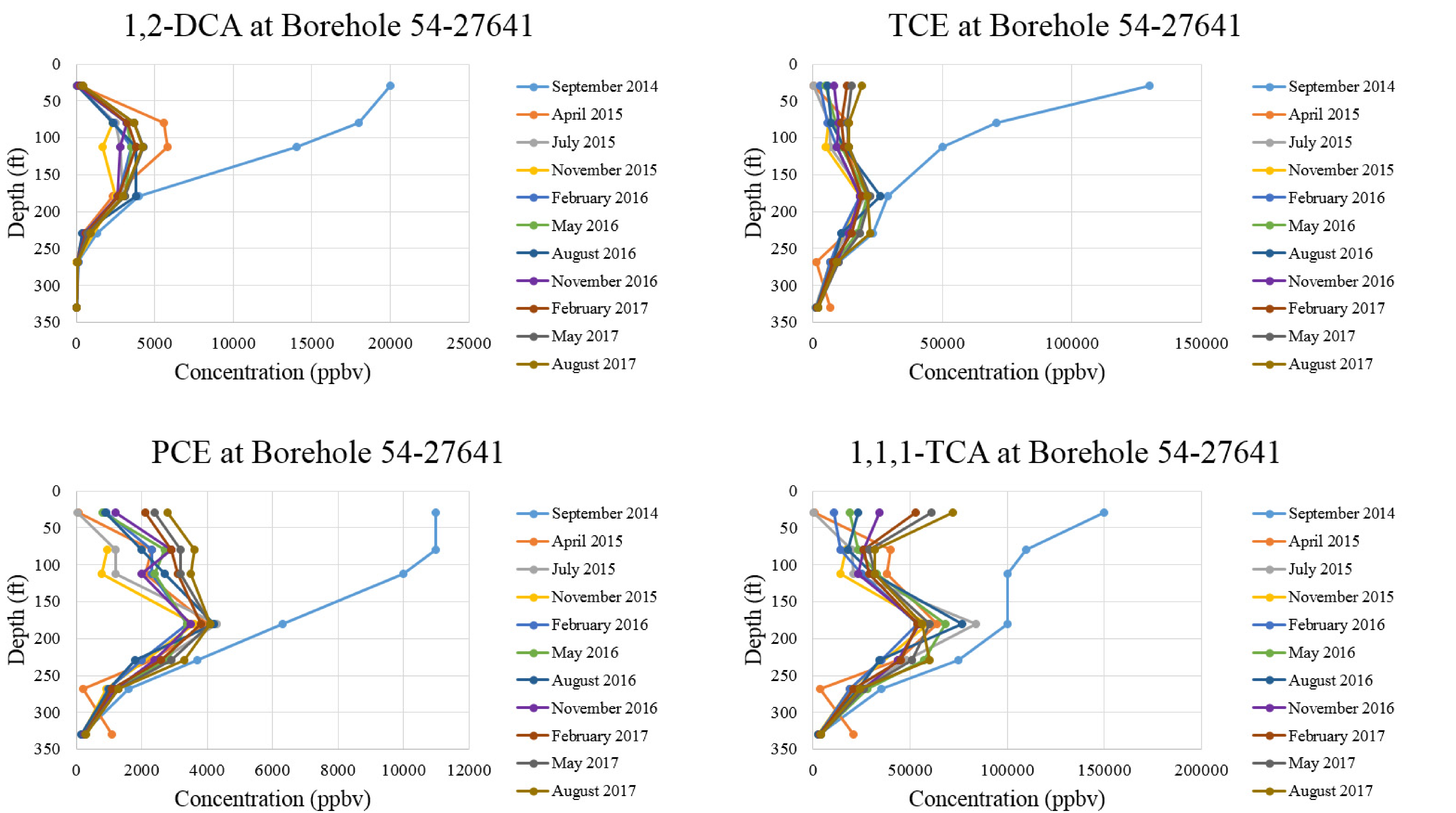

Figure 4.3-7 DCA[1,2], TCE, PCE, and 1,1,1-TCA concentration data for borehole 54-27641

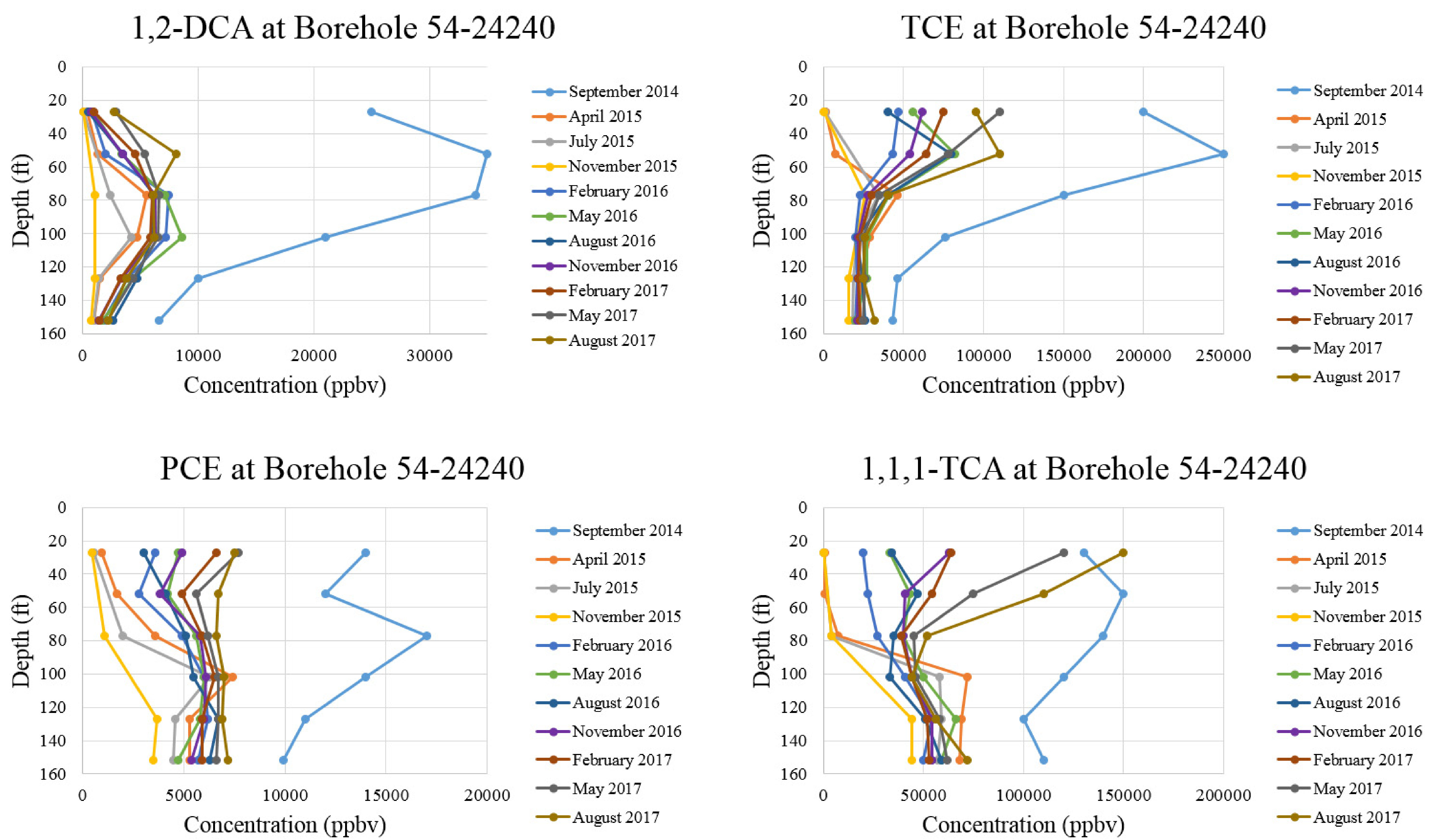

Figure 4.3-8 DCA[1,2], TCE, PCE, and 1,1,1-TCA concentration data for borehole 54-24240

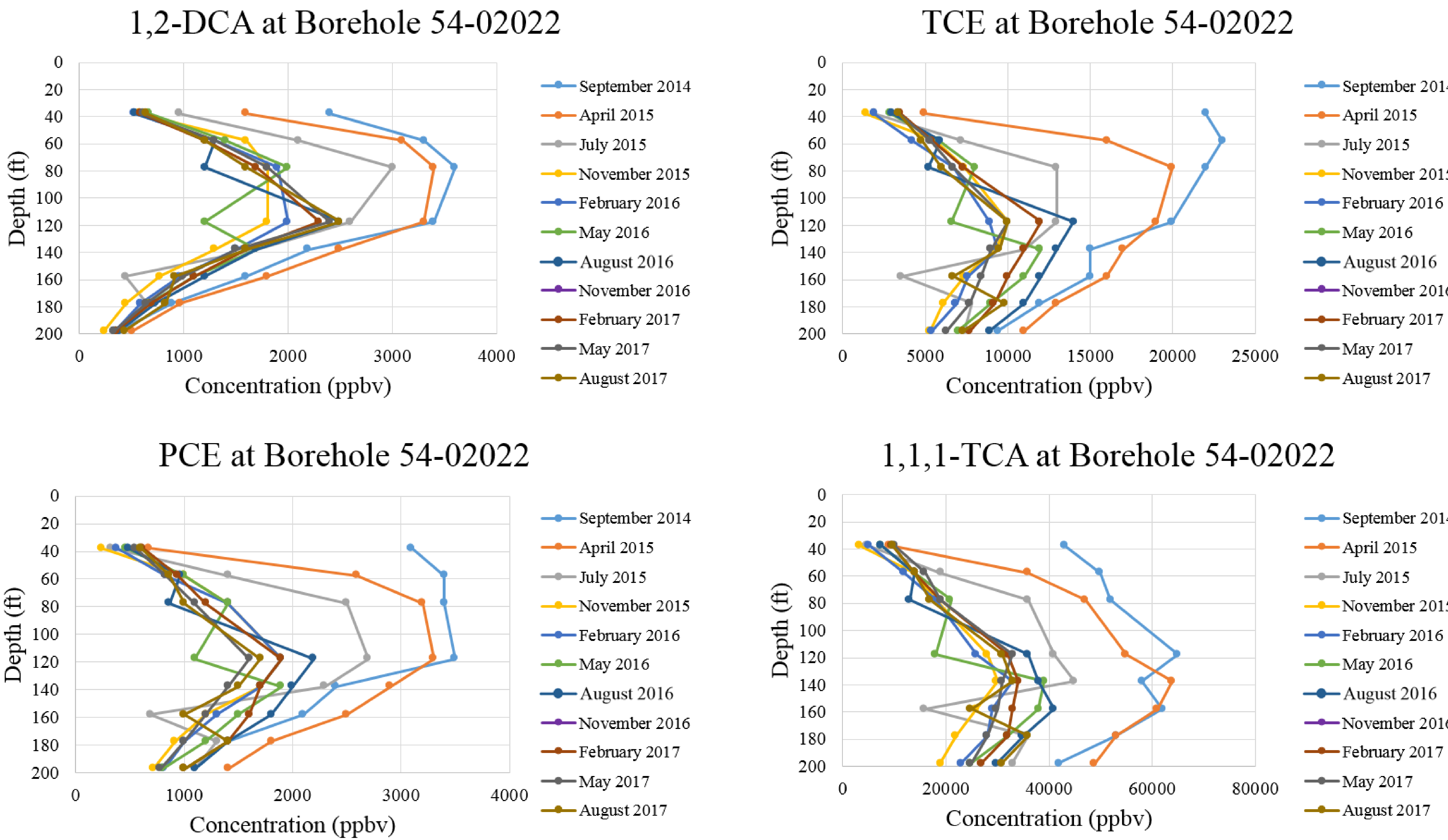

Figure 4.3-9 DCA[1,2], TCE, PCE, and 1,1,1-TCA concentration data for borehole 54-02022

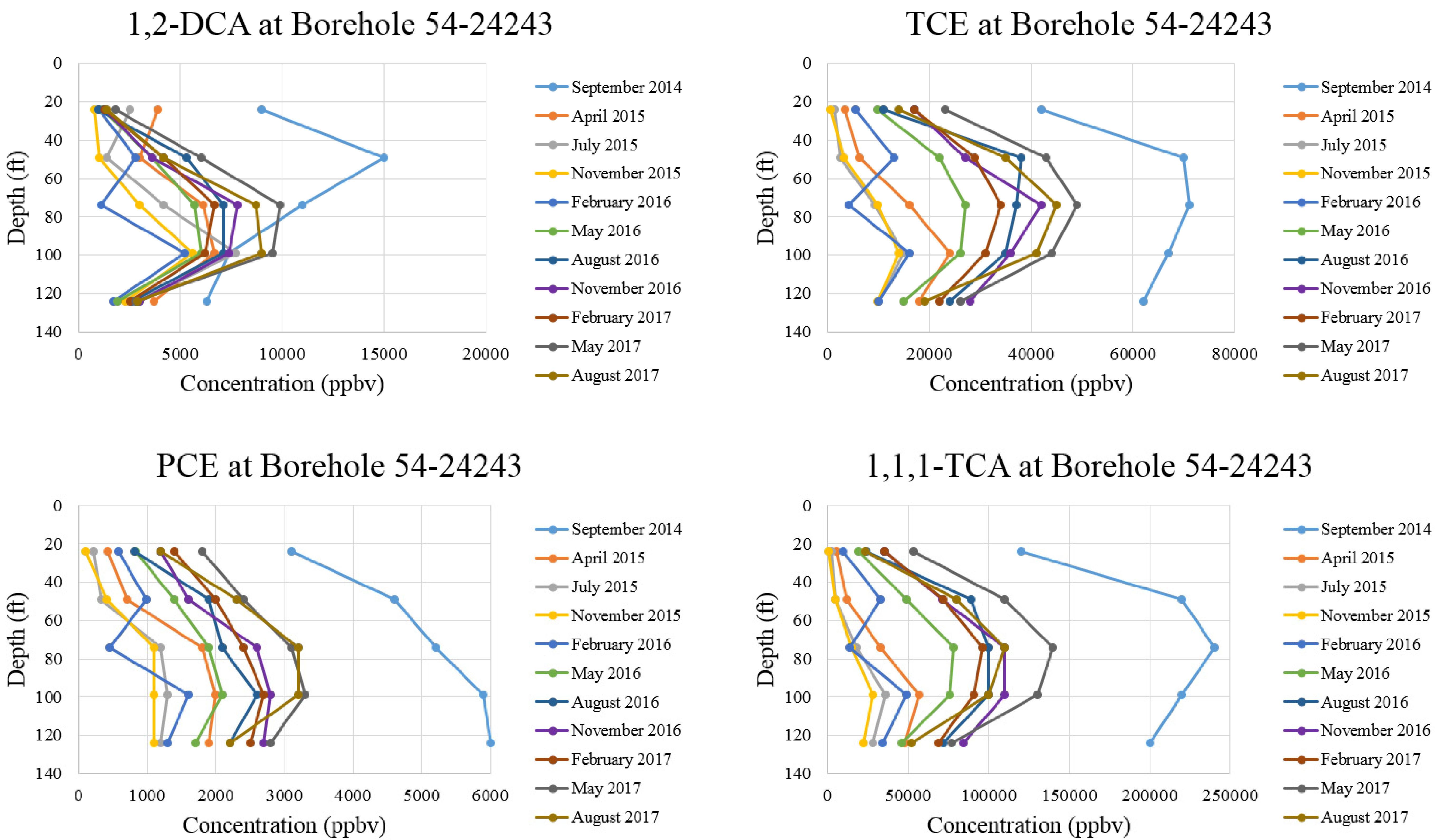

Figure 4.3-10 DCA[1,2], TCE, PCE, and 1,1,1-TCA concentration data for borehole 54-24243

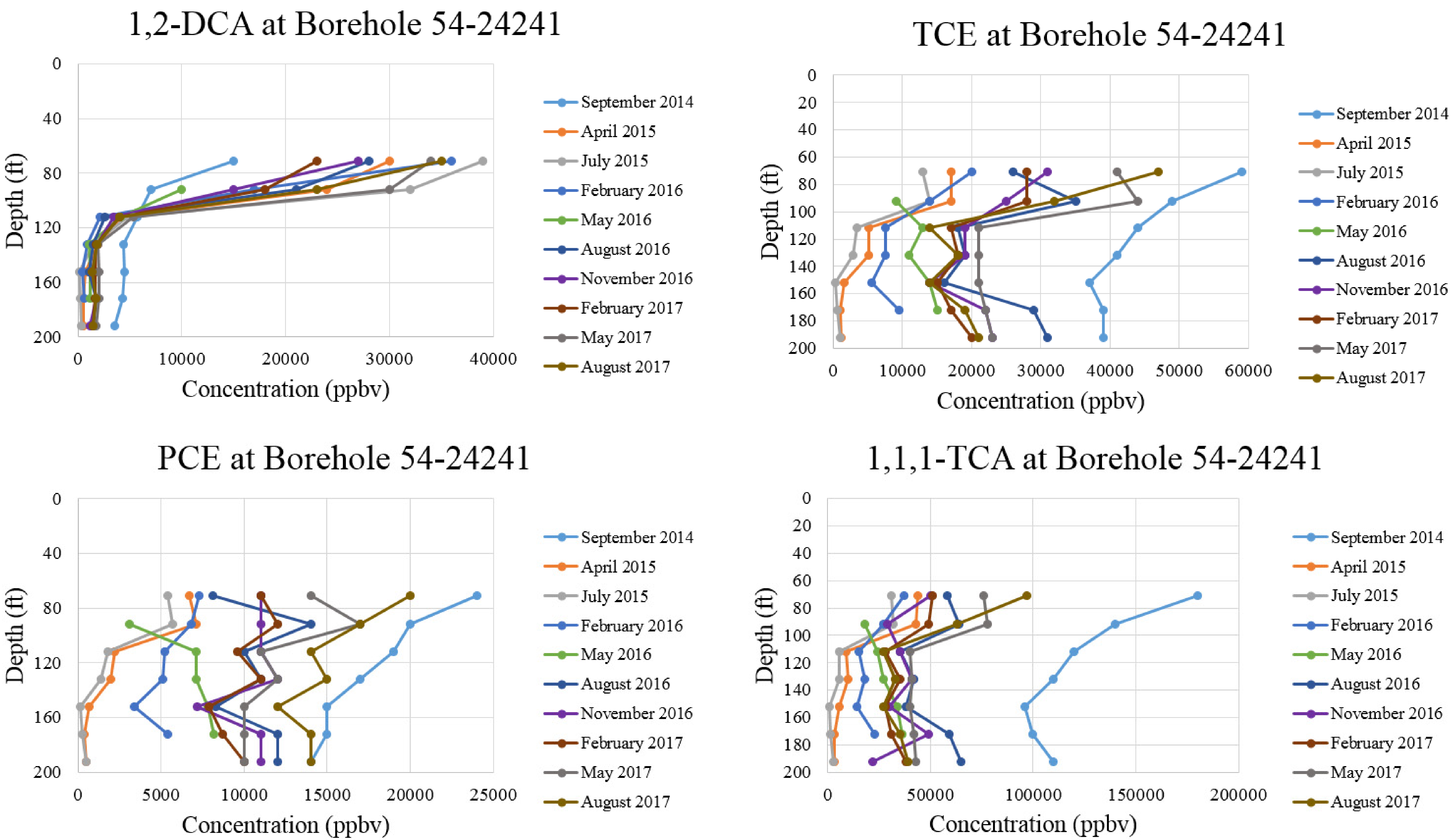

Figure 4.3-11 DCA[1,2], TCE, PCE, and 1,1,1-TCA concentration data for borehole 54-24241

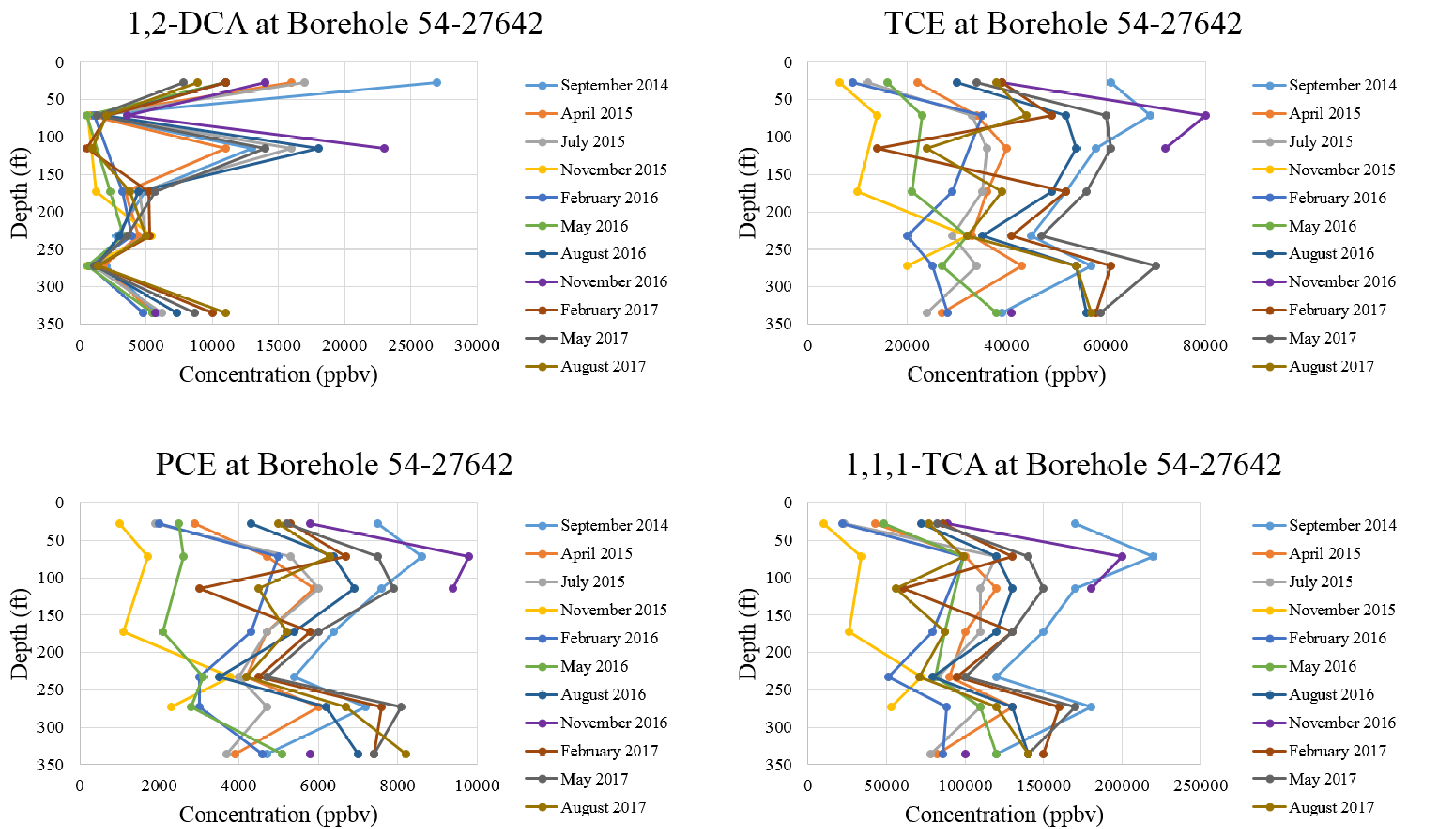

Figure 4.3-12 DCA[1,2], TCE, PCE, and 1,1,1-TCA concentration data for borehole 54-27642

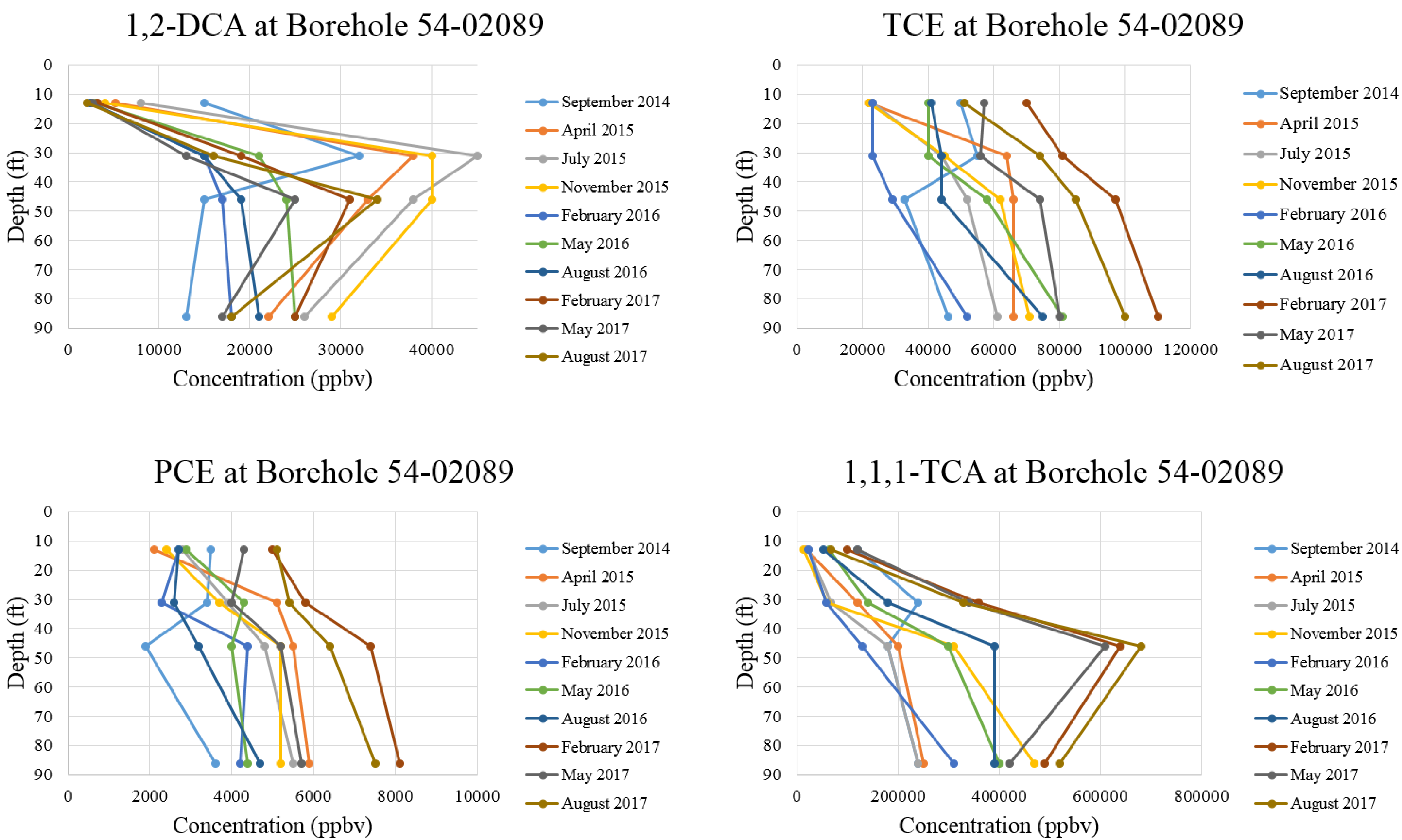

Figure 4.3-13 DCA[1,2], TCE, PCE, and 1,1,1-TCA concentration data for borehole 54-02089

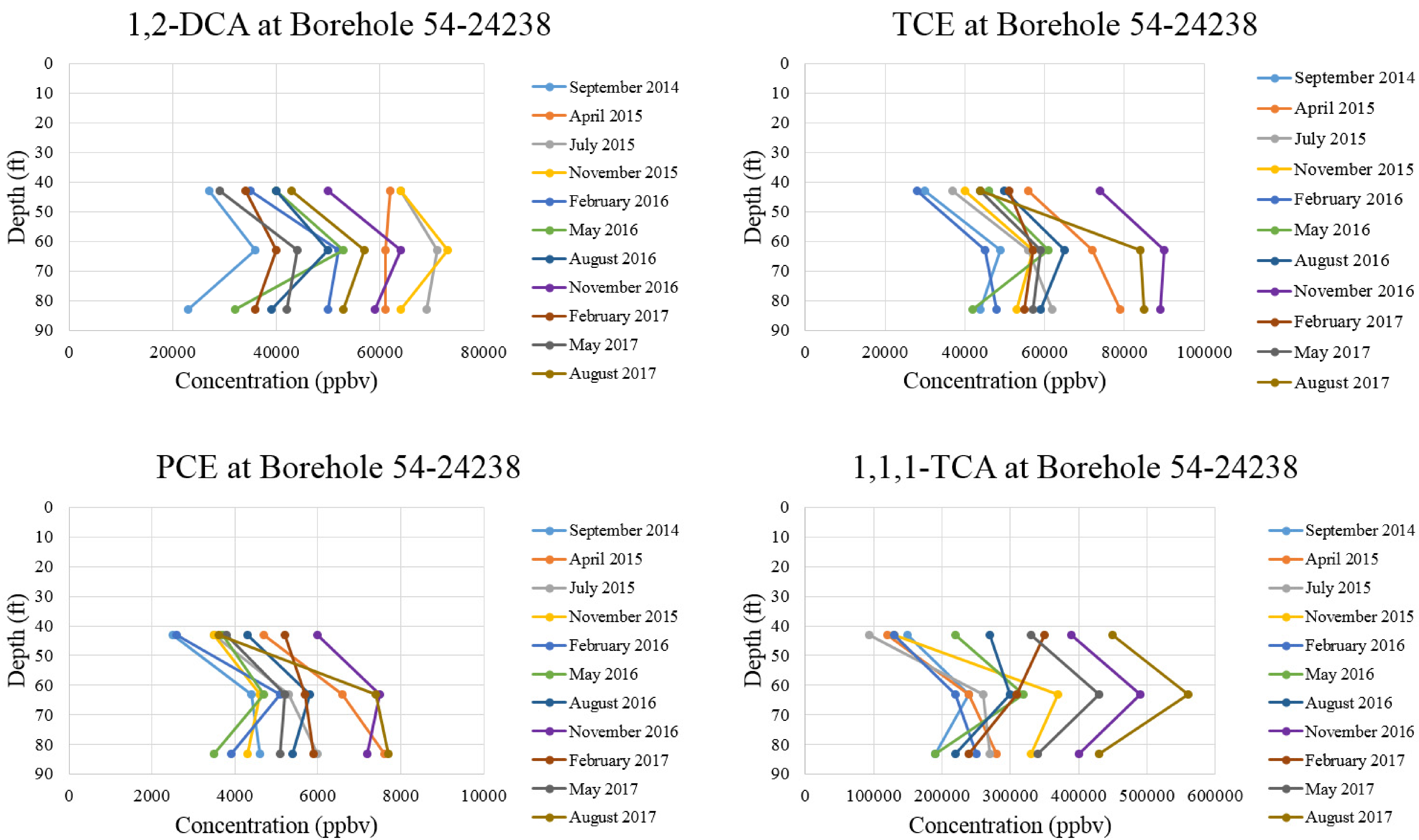

Figure 4.3-14 DCA[1,2], TCE, PCE, and 1,1,1-TCA concentration data for borehole 54-24238

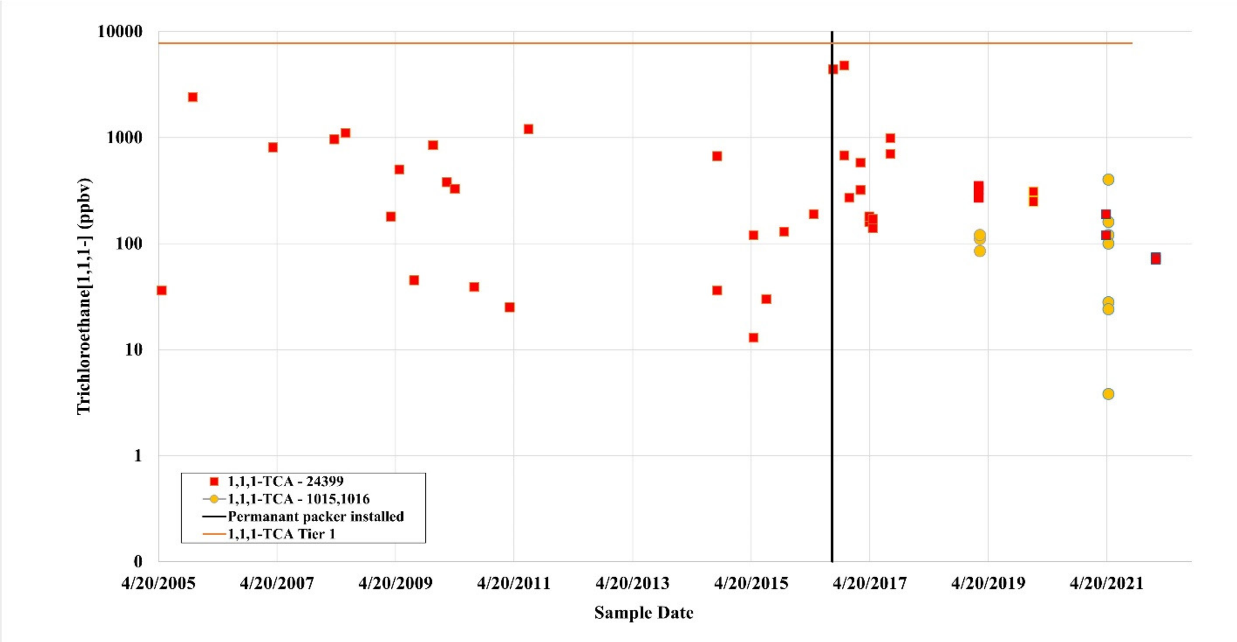

Figure 4.4-1 TCA[1,1,1] in the basalt sampled using SUMMA canisters, relative to the Tier 1 screening level

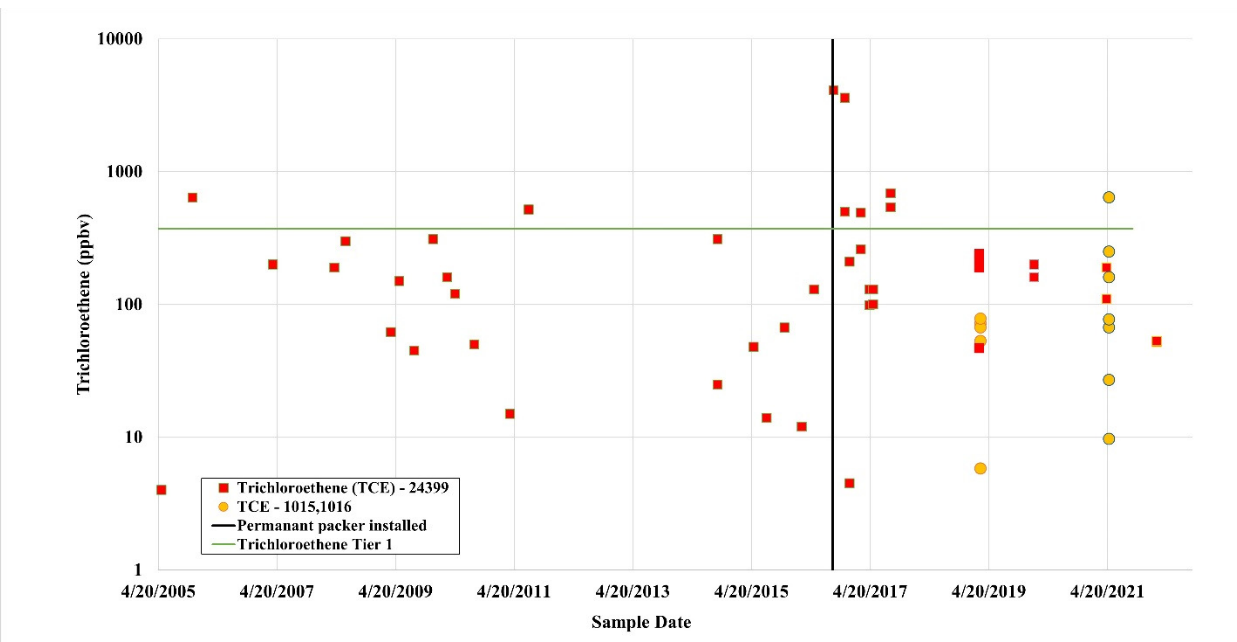

Figure 4.4-2 TCE in the basalt sampled using SUMMA canisters, relative to the Tier 1 screening level

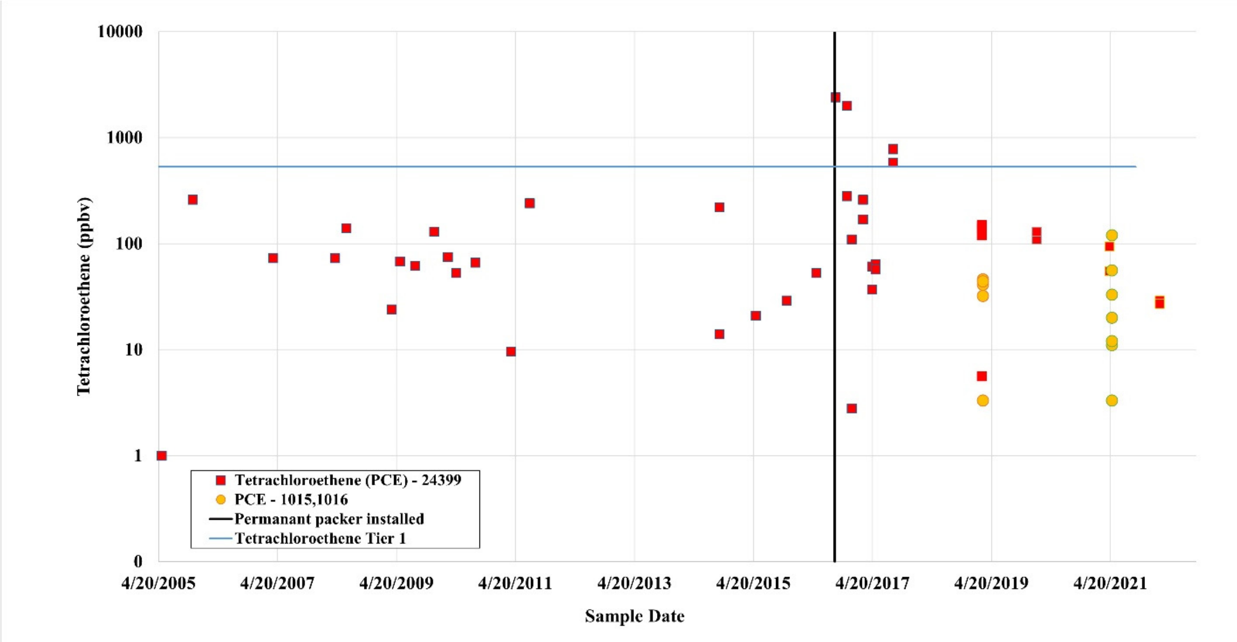

Figure 4.4-3 PCE in the basalt sampled using SUMMA canisters, relative to the Tier 1 screening level

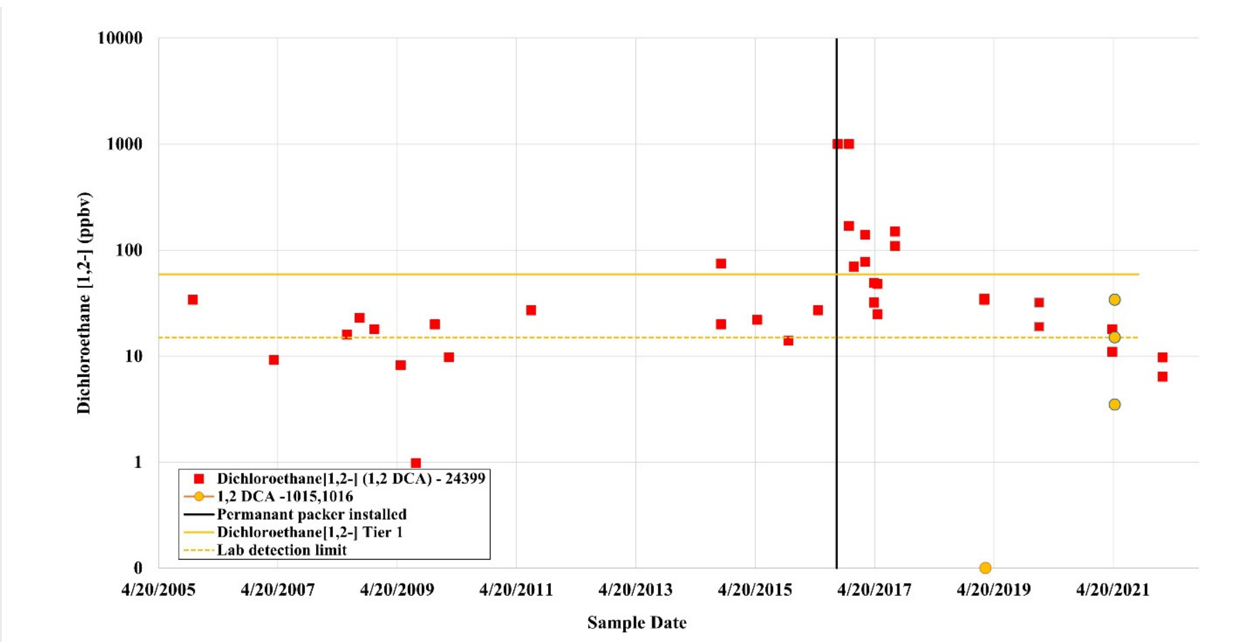

Figure 4.4-4 DCA[1,2] in the basalt sampled using SUMMA canisters, relative to the Tier 1 screening level

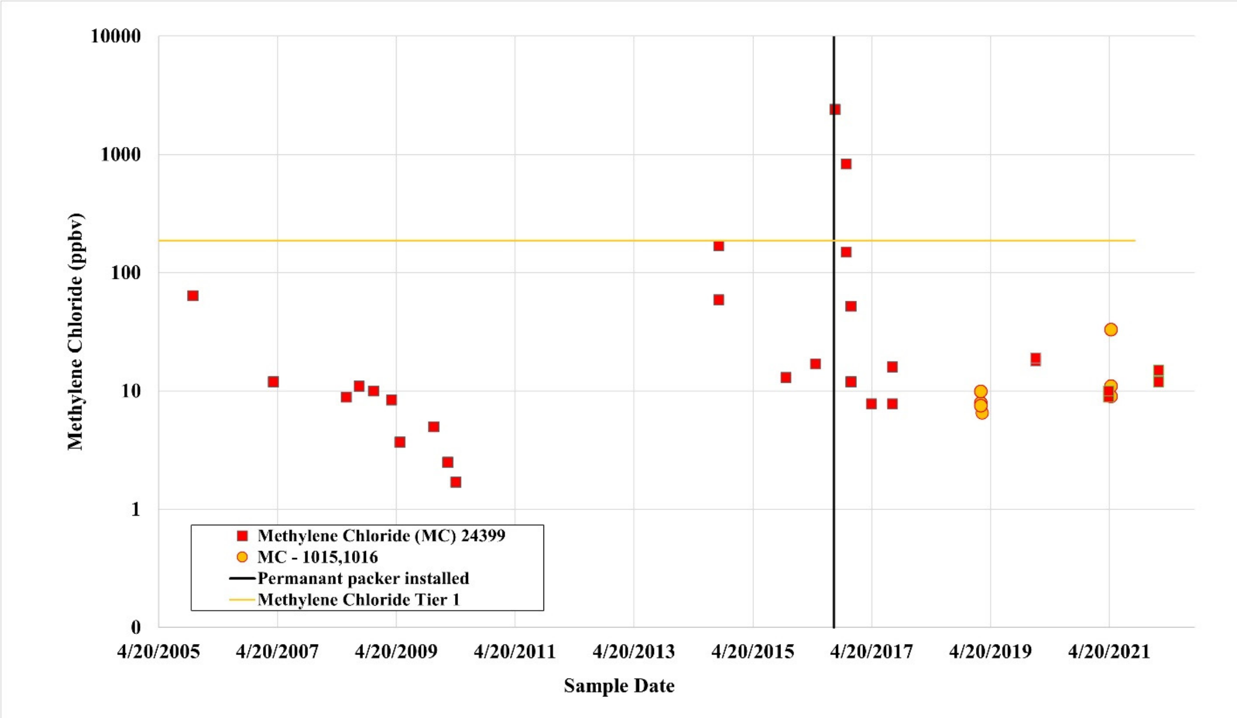

Figure 4.4-5 Methylene chloride in the basalt sampled using SUMMA canisters, relative to the Tier 1 screening level

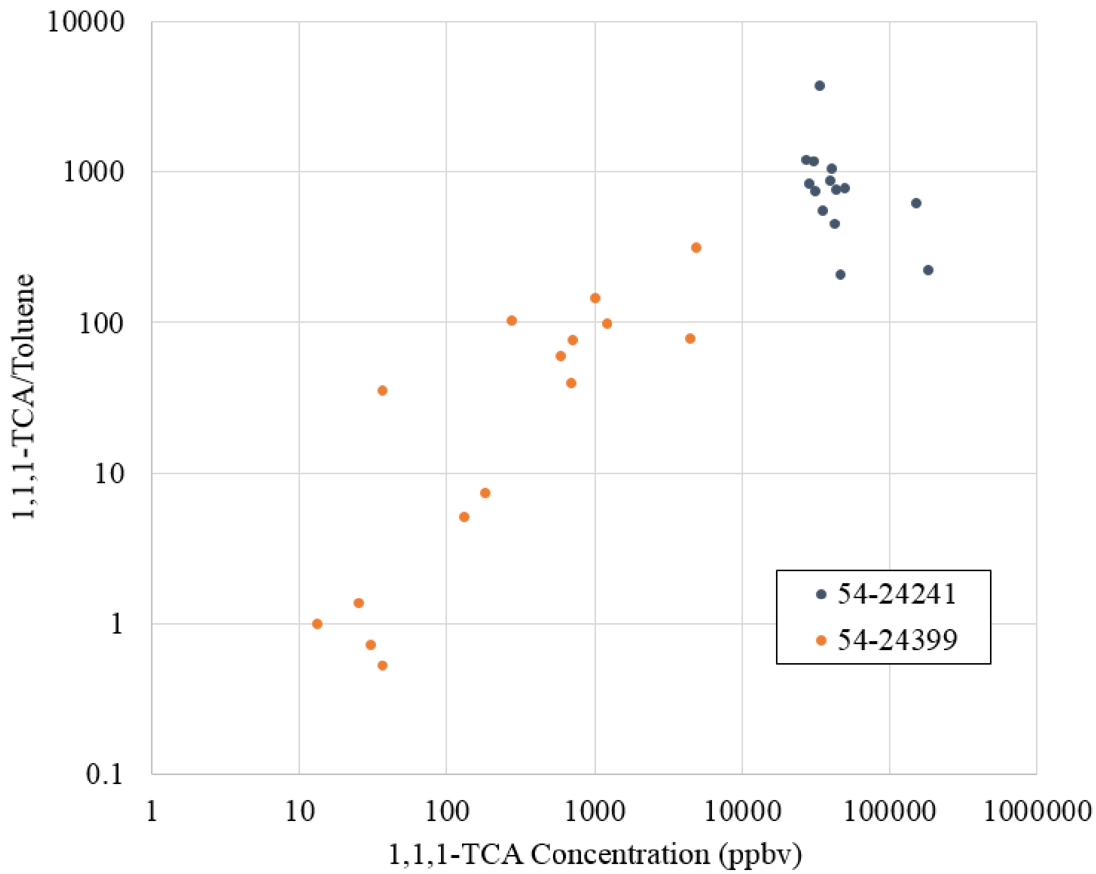

Figure 4.4-6 Ratio of 1,1,1-TCA to toluene plotted versus 1,1,1-TCA concentration comparing borehole 54-24399 with borehole 54-24241

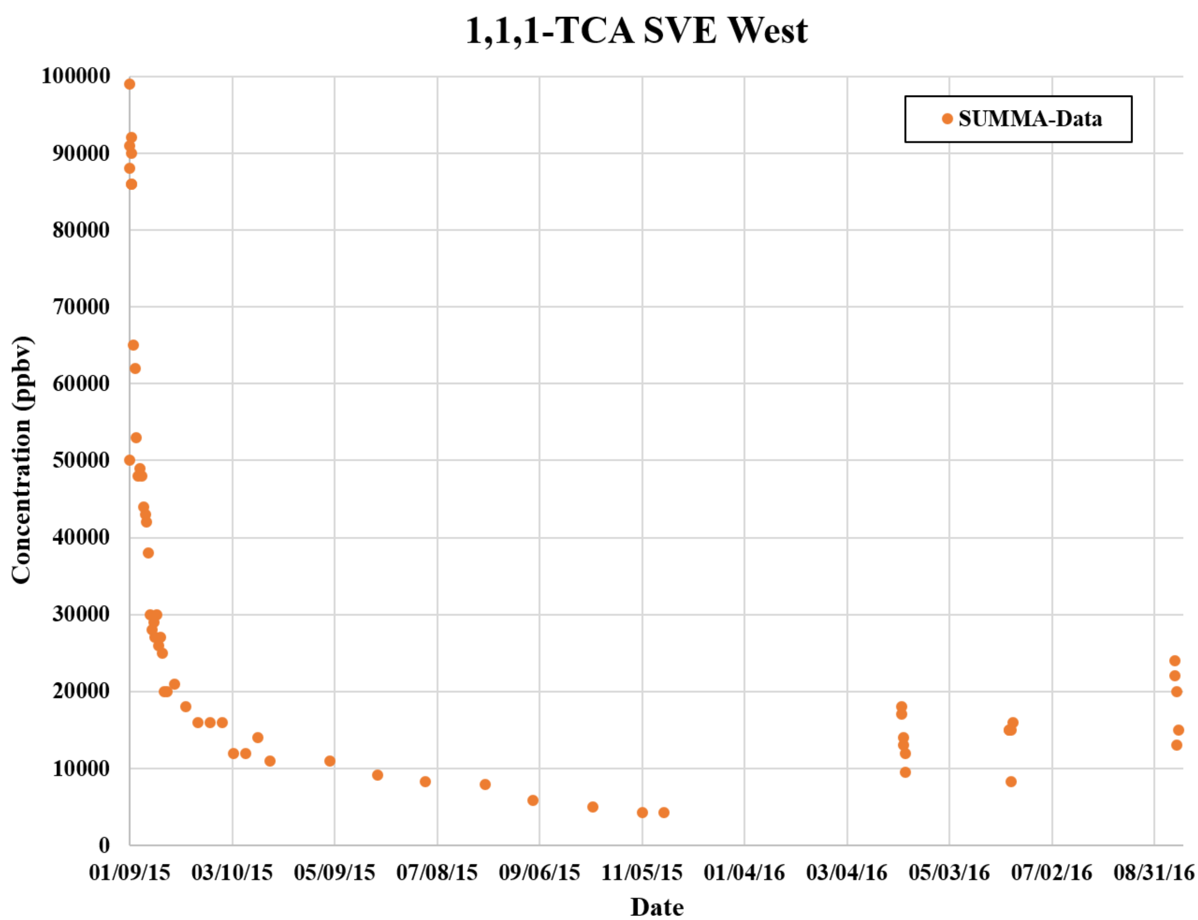

Figure 4.6-1 TCA[1,1,1] concentrations in effluent from SVE-West versus time including three short duration (2-d) rebound tests in 2016

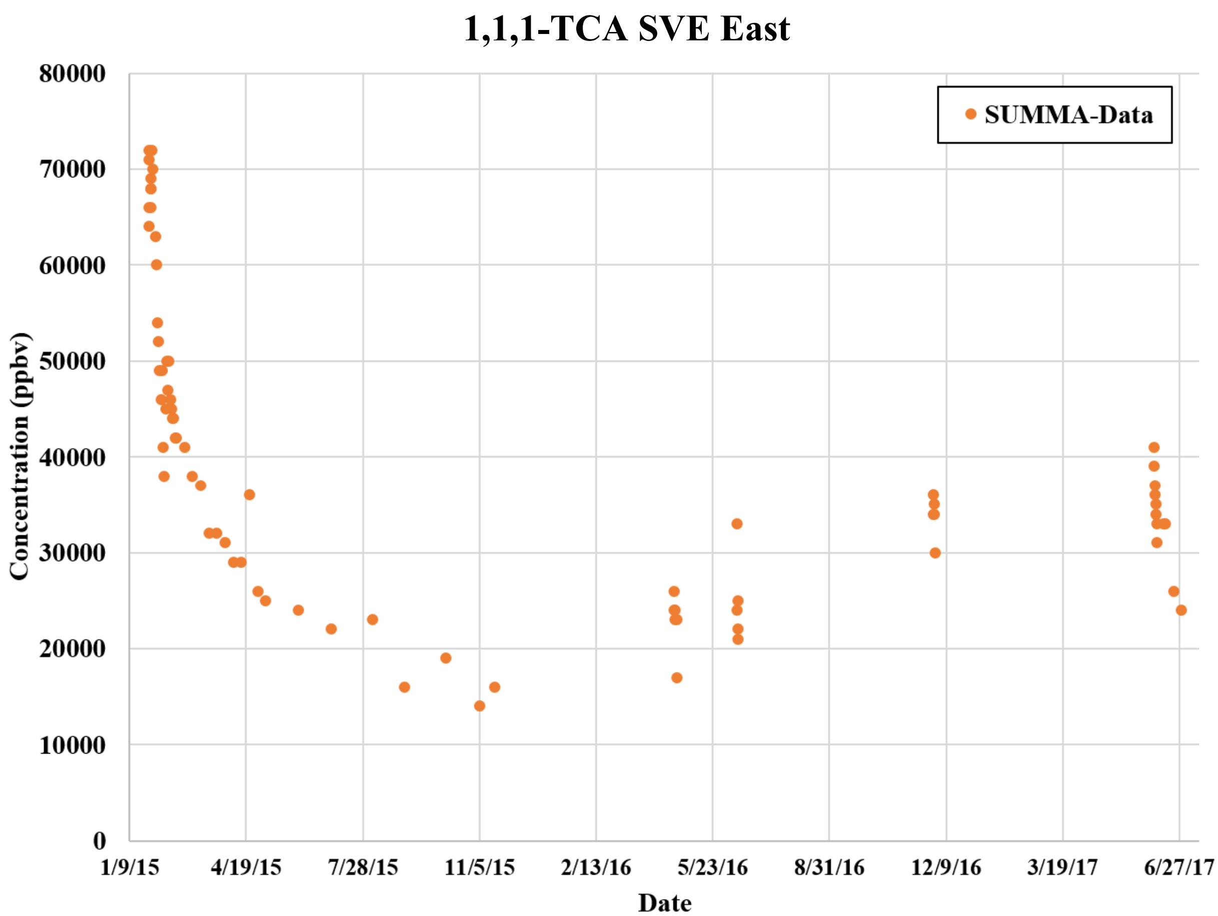

Figure 4.6-2 **Concentration in effluent from SVE-East versus time including three short duration (2-d) rebound tests in 2016 and a 25-d rebound test in June 2017**

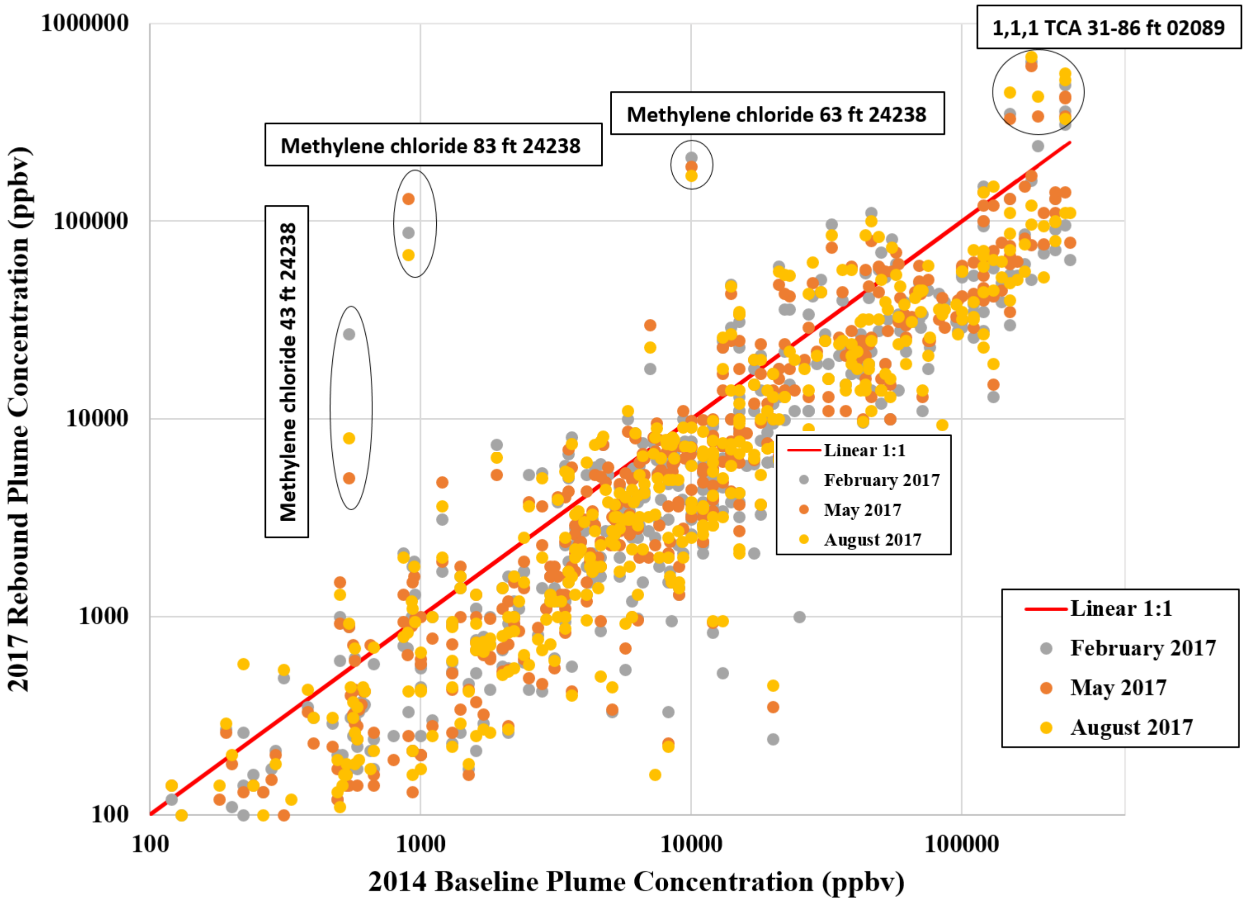

Figure 4.6-3 **Subsurface plume concentrations in 2017 versus baseline (2014) concentrations for seven analytes**

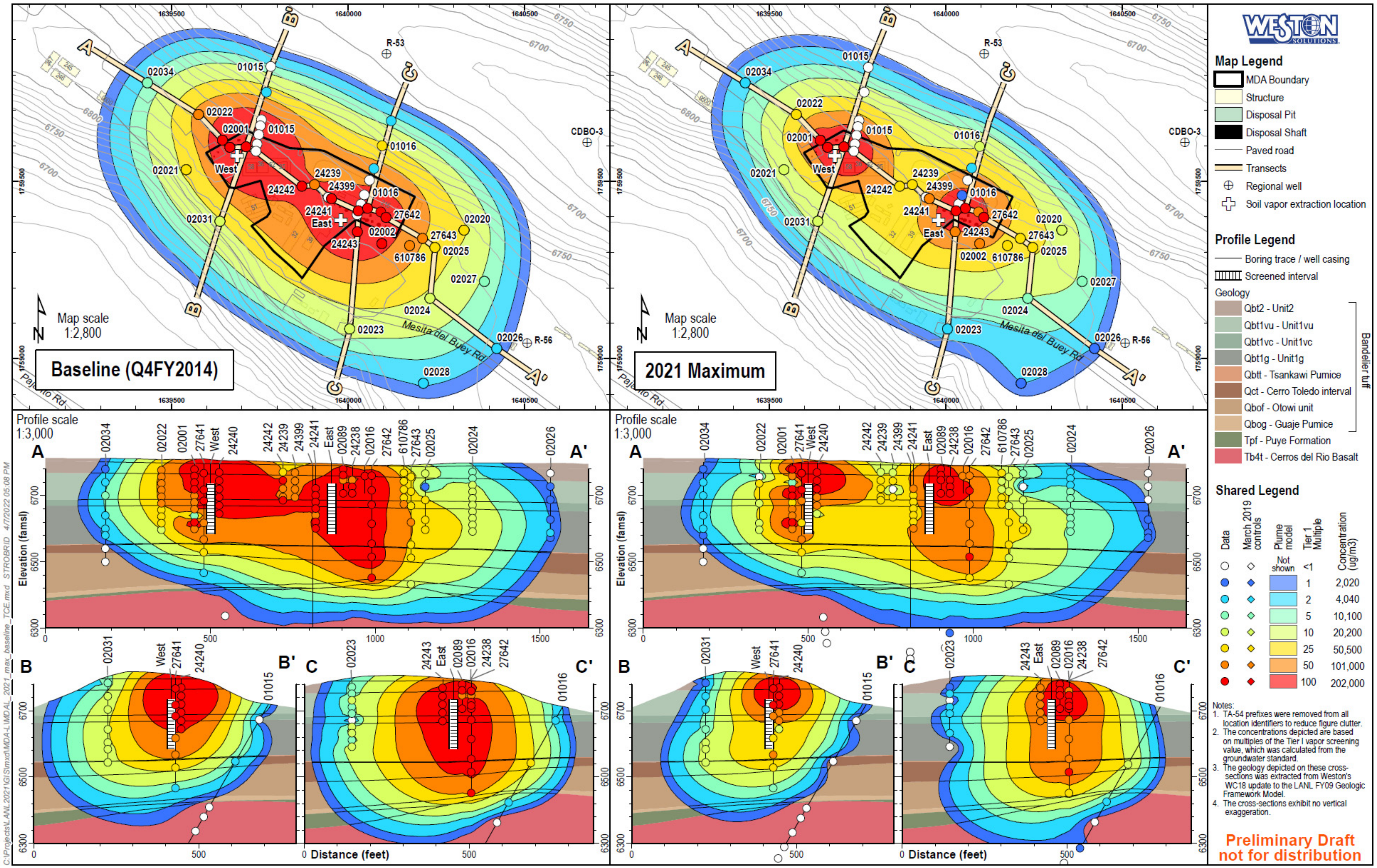

Figure 4.7-1 TCE concentration comparison from pre-SVE baseline to the maximum measured concentration at each port from the 2021 sampling

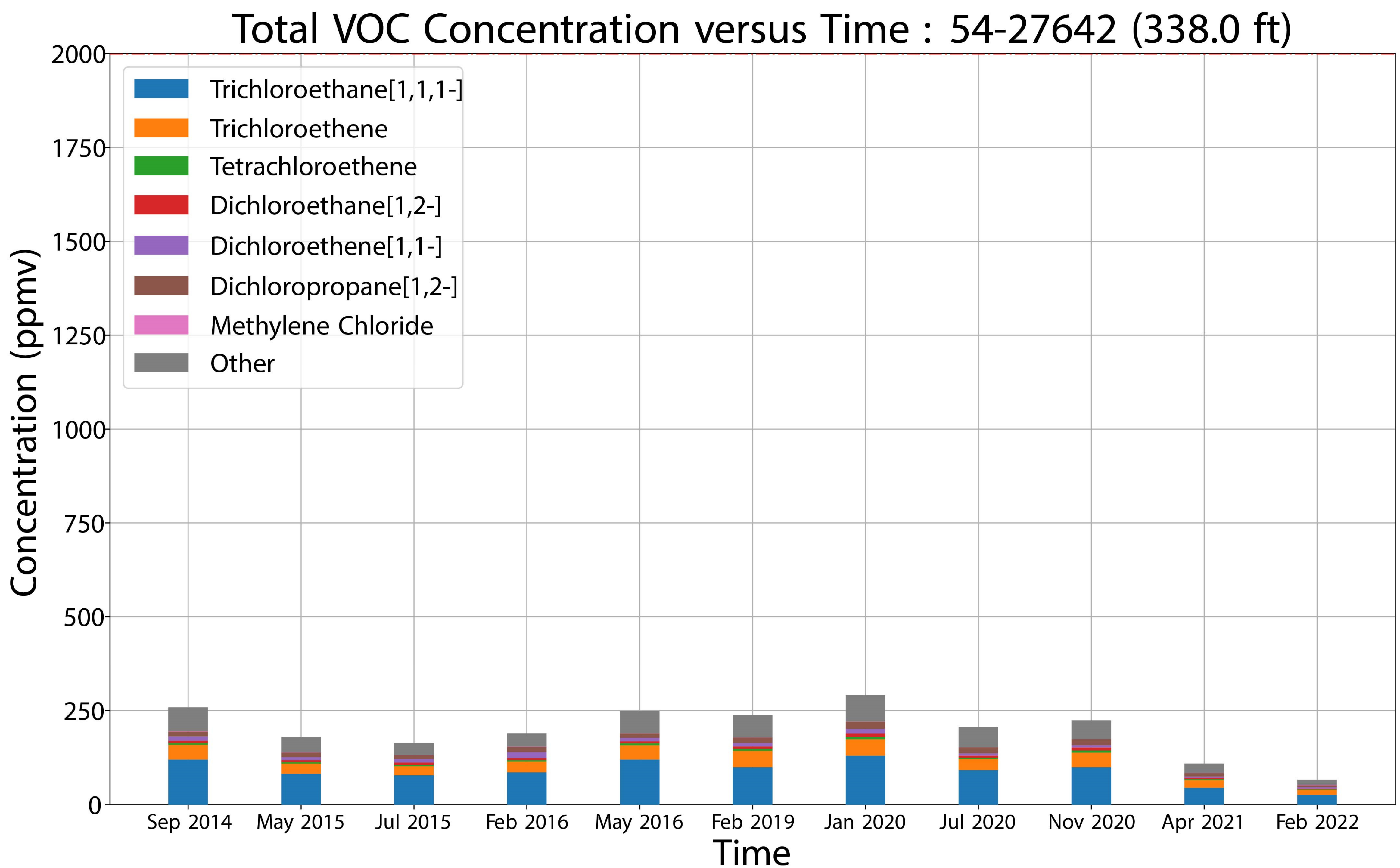

Figure 4.7-2 Total VOC concentration at the deepest monitoring port in the Bandelier Tuff beneath the eastern source area versus time

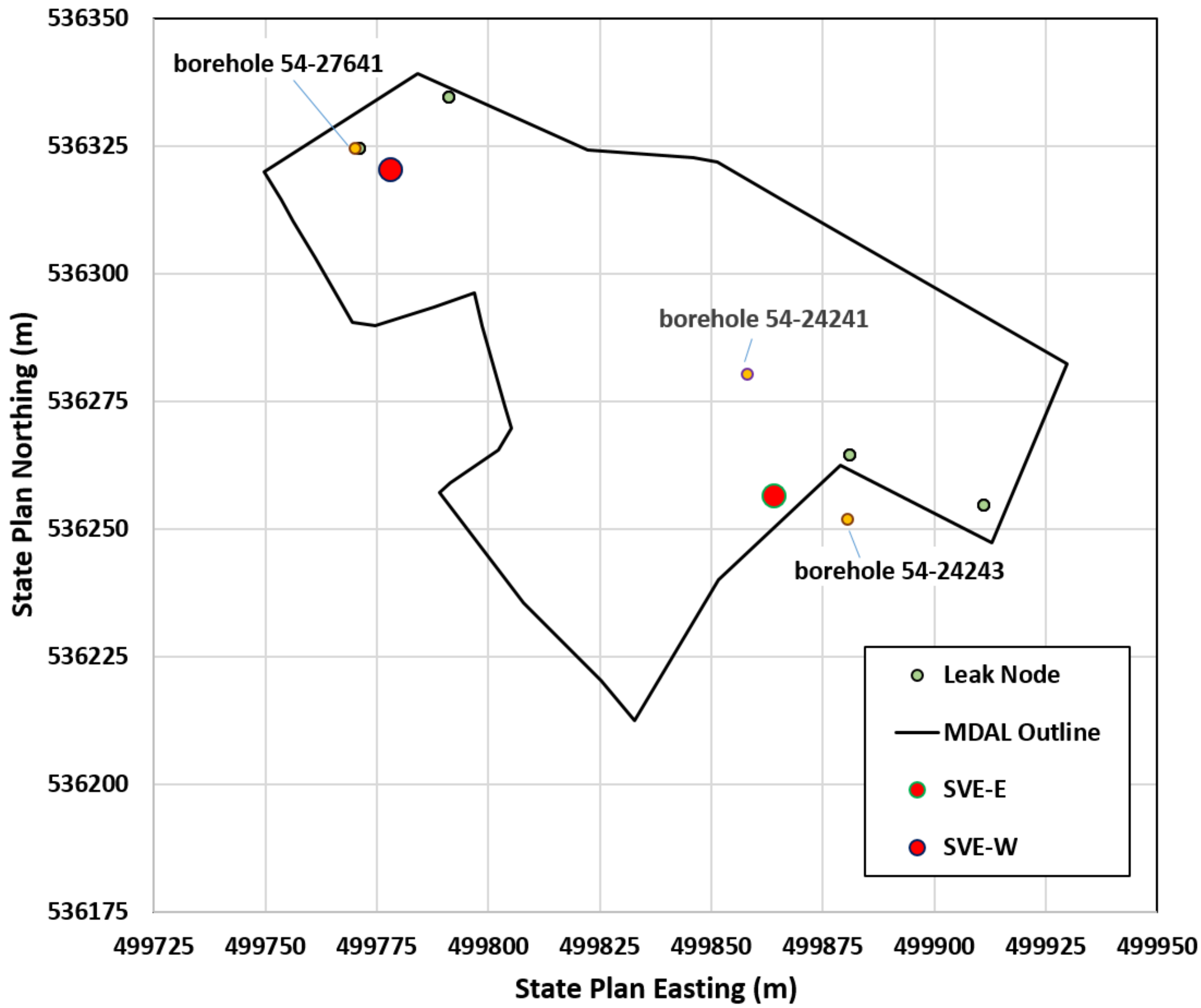

Figure 5.1-1 **Locations of the MDA L outline, example monitoring boreholes, SVE units, and simulated leaking subsurface sources**

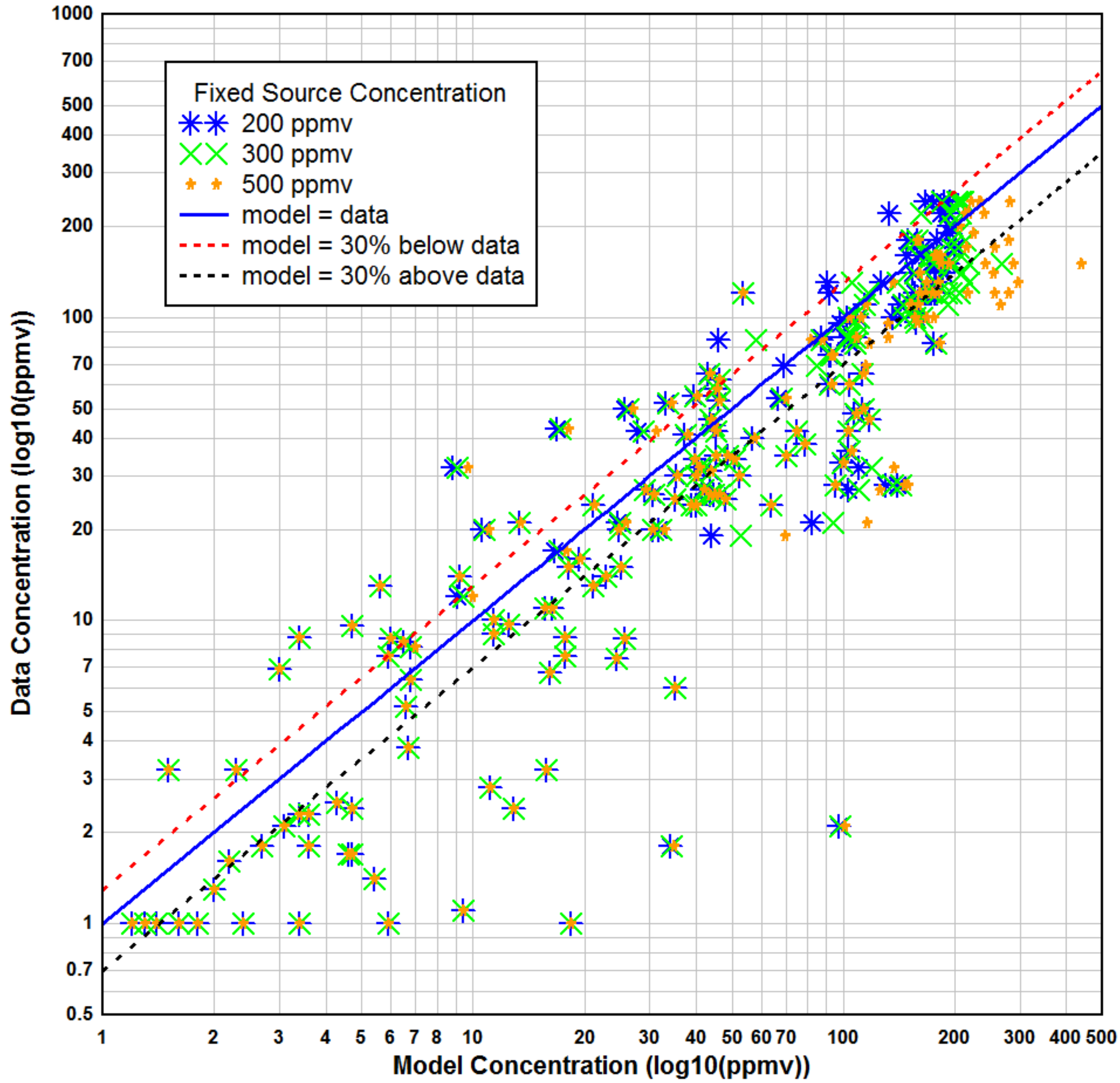

Figure 5.2-1 Simulated 1,1,1-TCA concentration compared with data for the 2014 baseline pre-SVE initial state

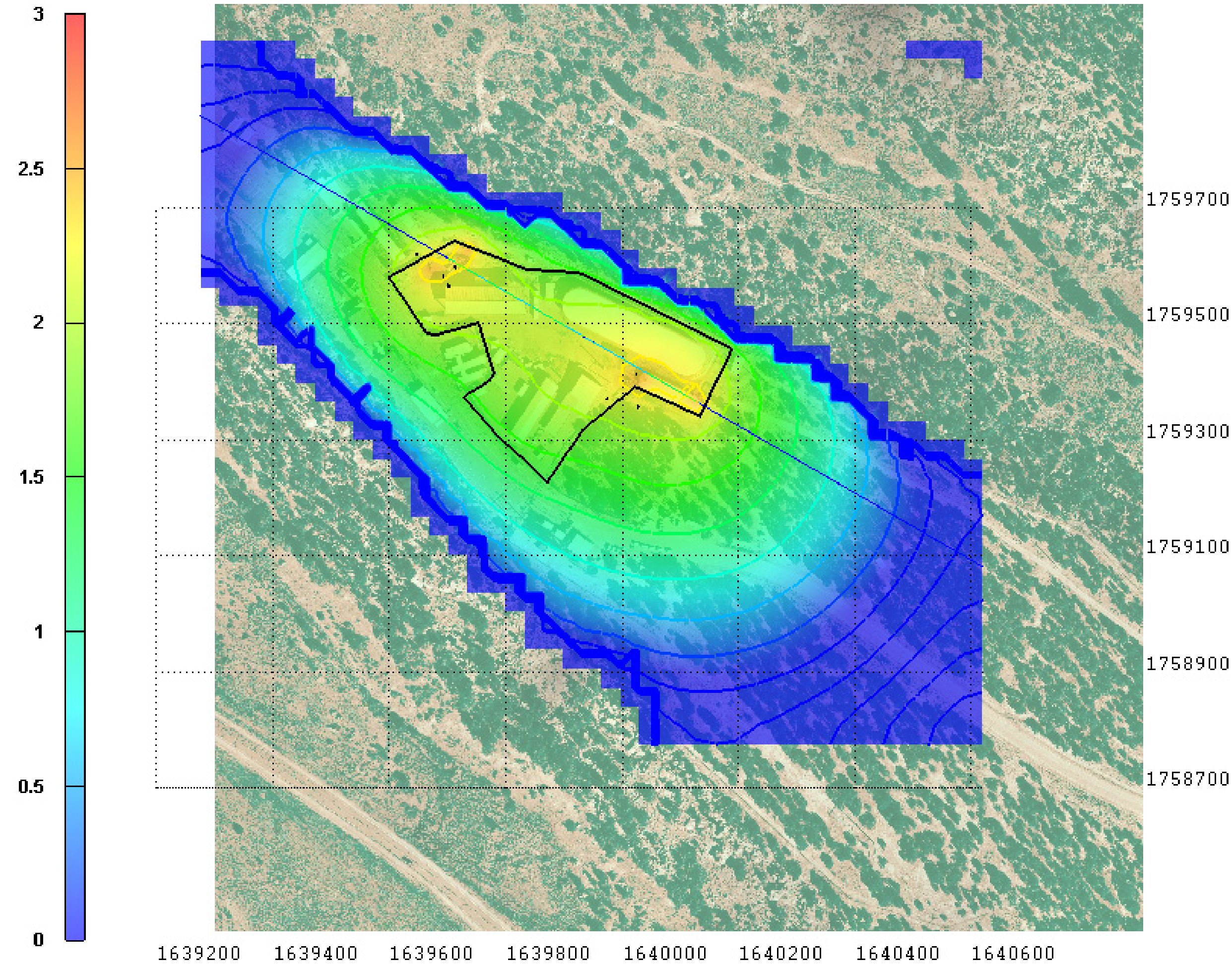

Note: X-Y units are State Plan feet while the legend shows log10 (ppmv).

Figure 5.2-2 Simulated 1,1,1-TCA concentration on a plane 60 ft below the ground surface of MDA L

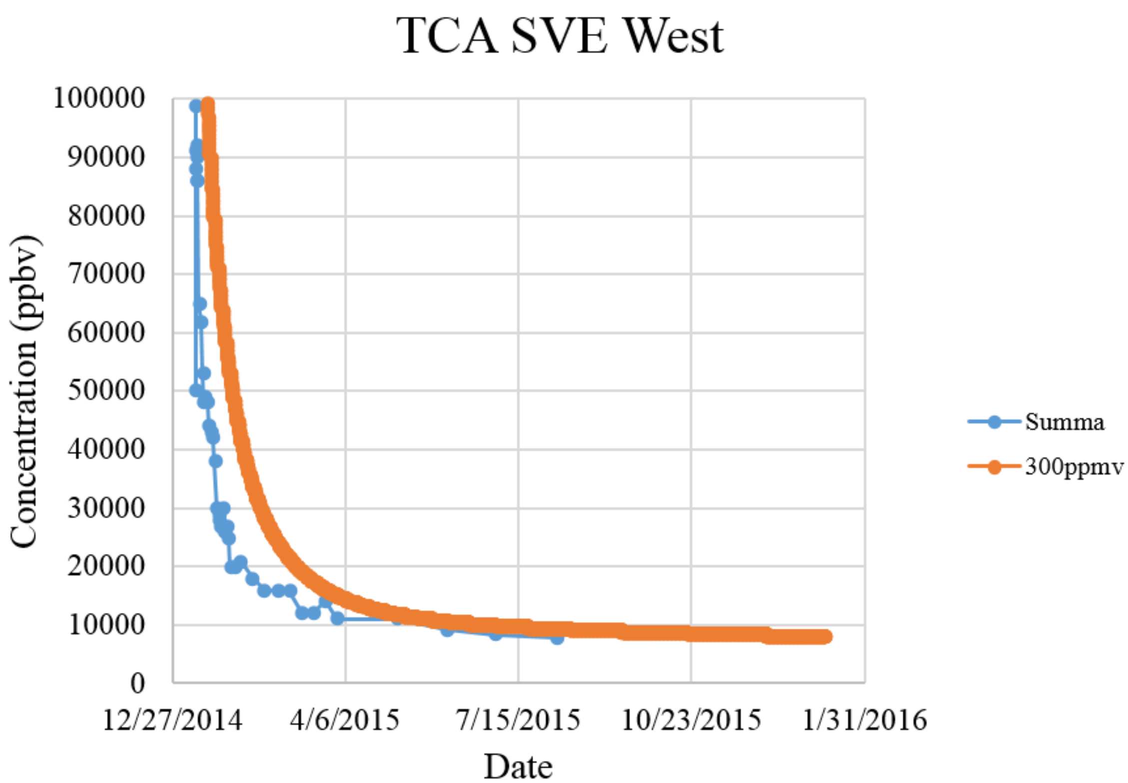

Figure 5.3-1 Predicted versus measured concentrations of 1,1,1-TCA at SVE-West

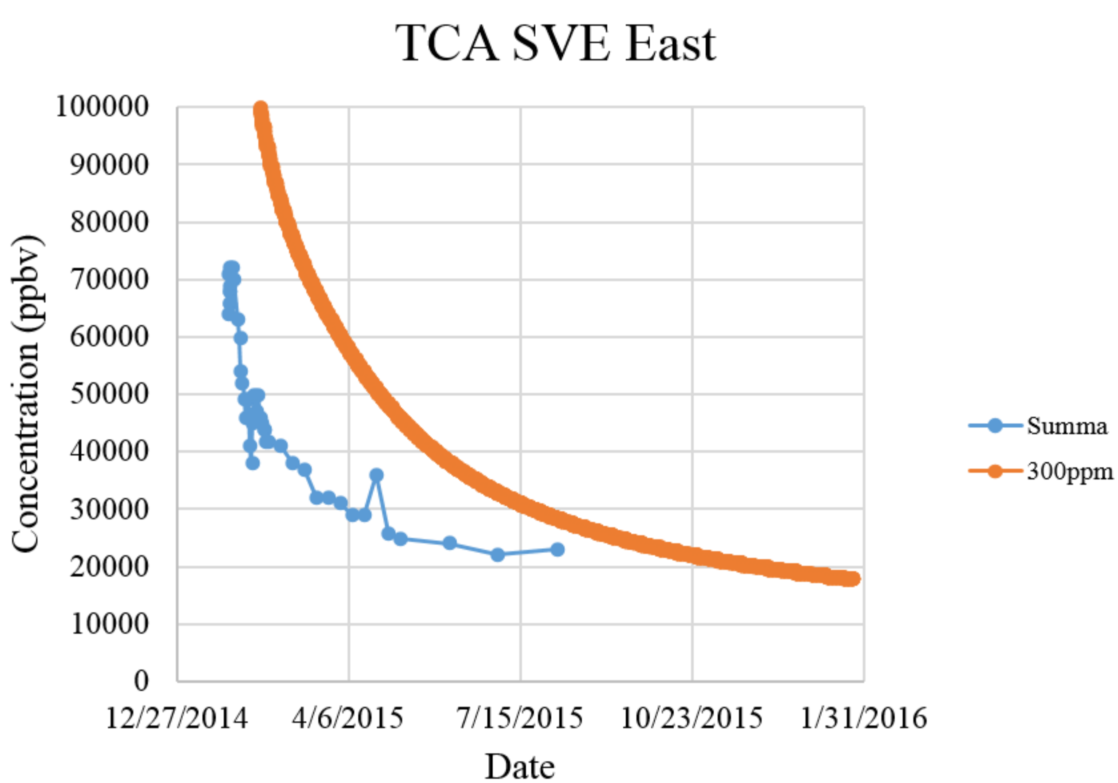

Figure 5.3-2 Predicted versus measured 1,1,1-TCA concentrations at SVE-East

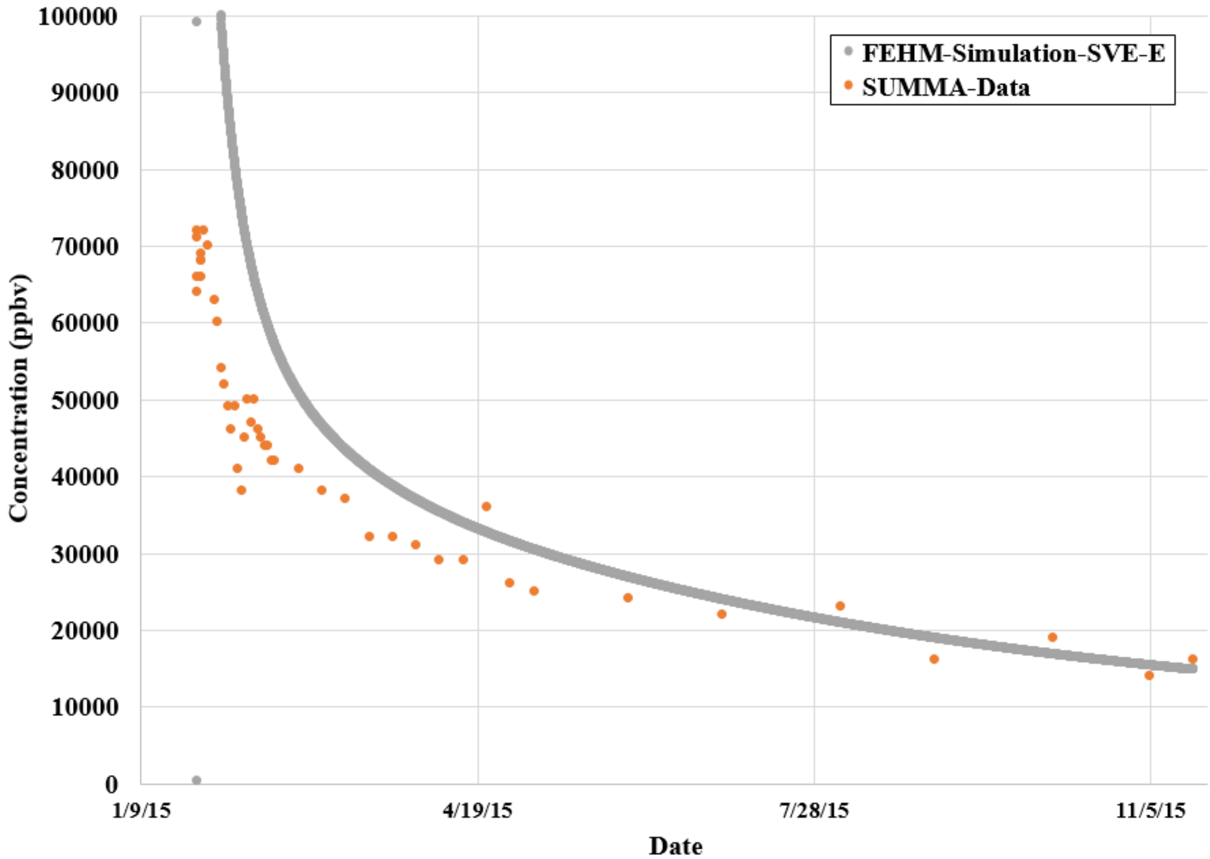

Figure 5.3-3 Predicted versus measured 1,1,1-TCA concentrations at SVE-East for the recalibrated simulation

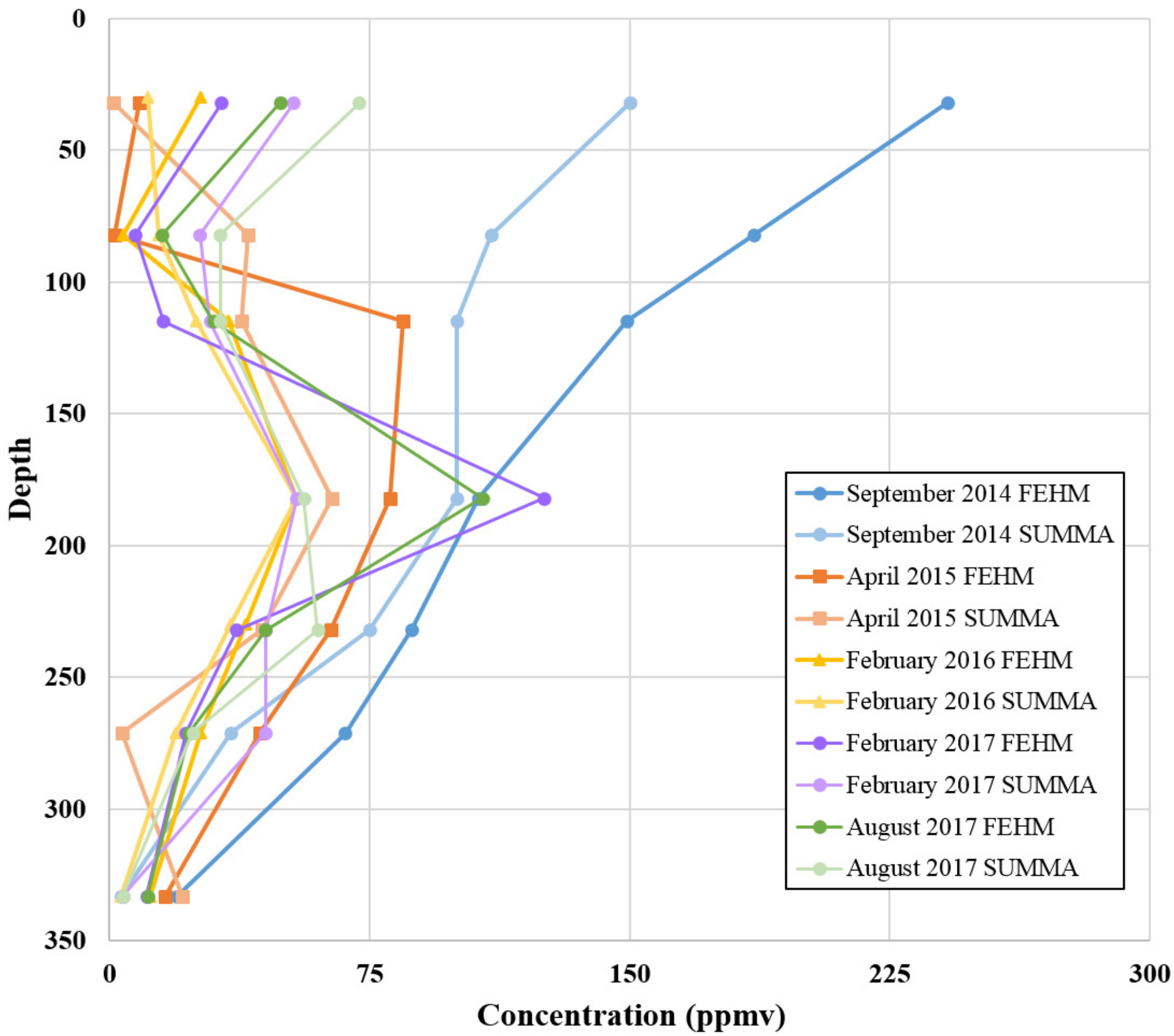

Figure 5.4-1 Simulated versus measured 1,1,1-TCA concentration in borehole 54-27641

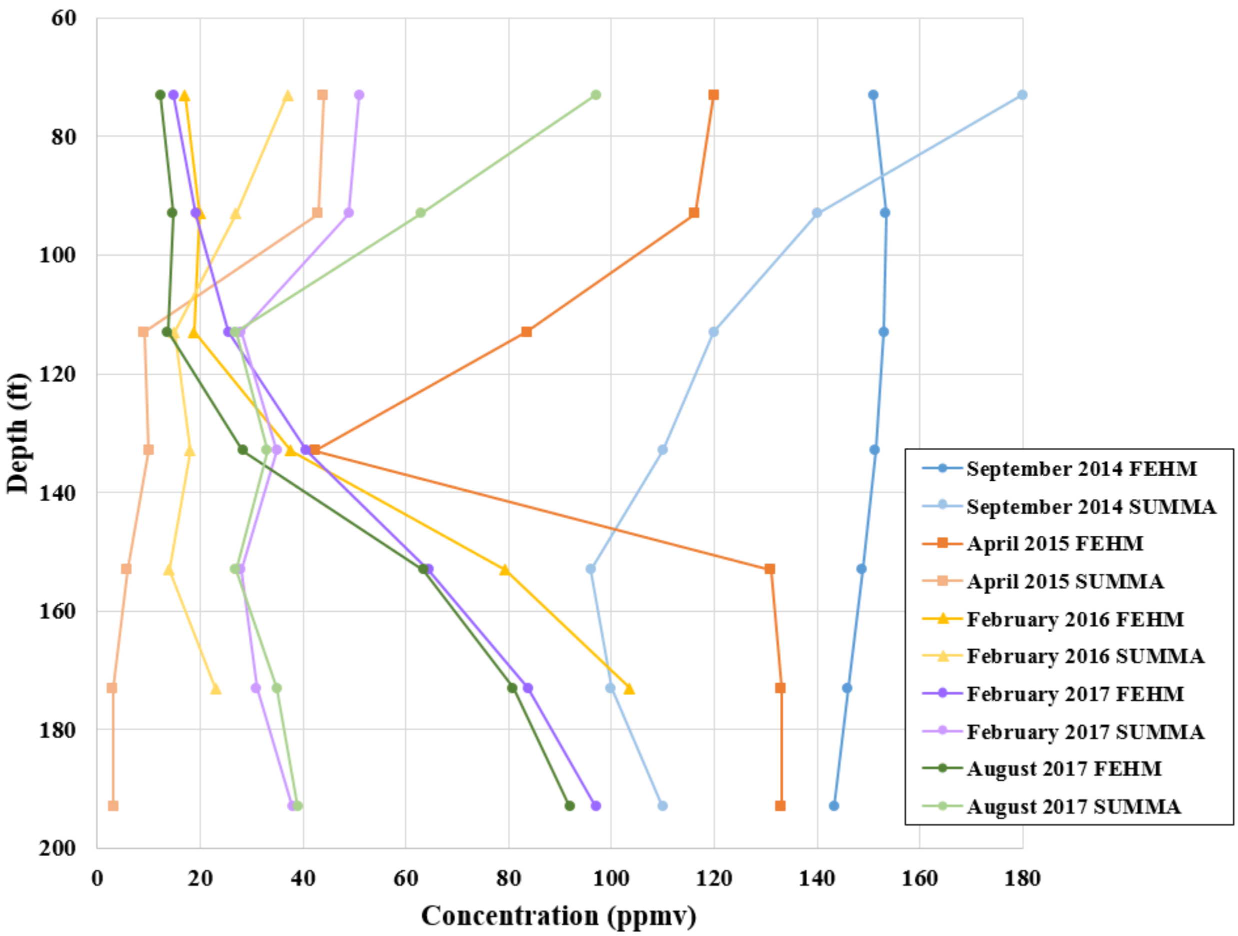

Figure 5.4-2 Simulated versus measured 1,1,1-TCA concentration in borehole 54-24241

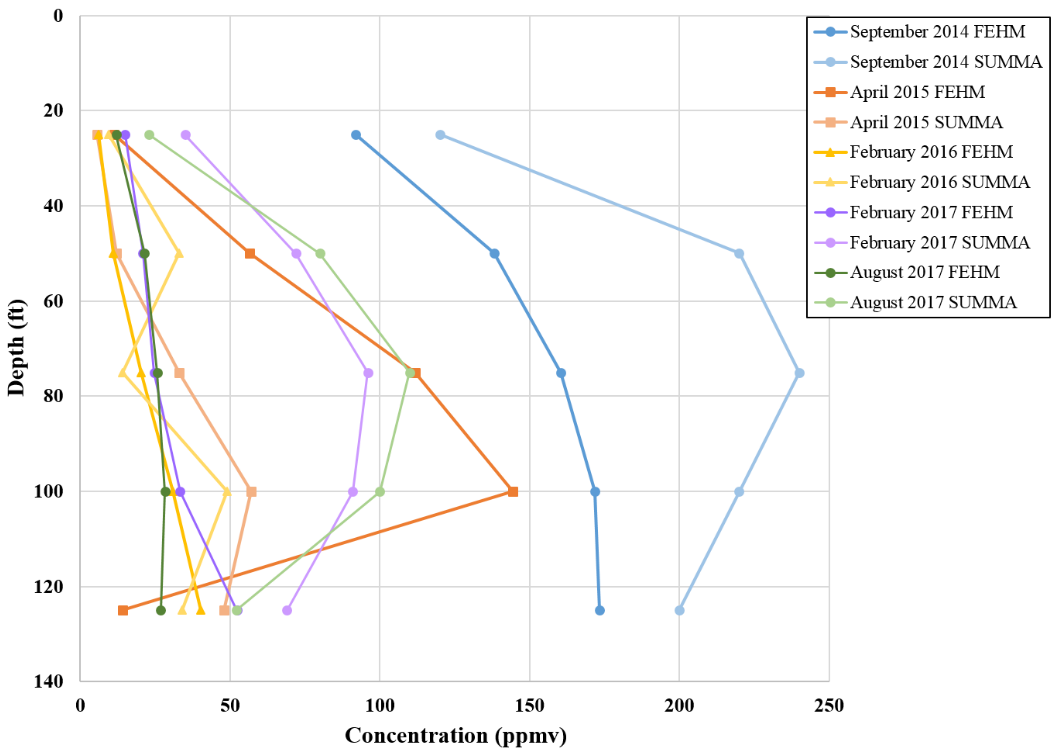

Figure 5.4-3 Simulated versus measured 1,1,1-TCA concentration in borehole 54-24243

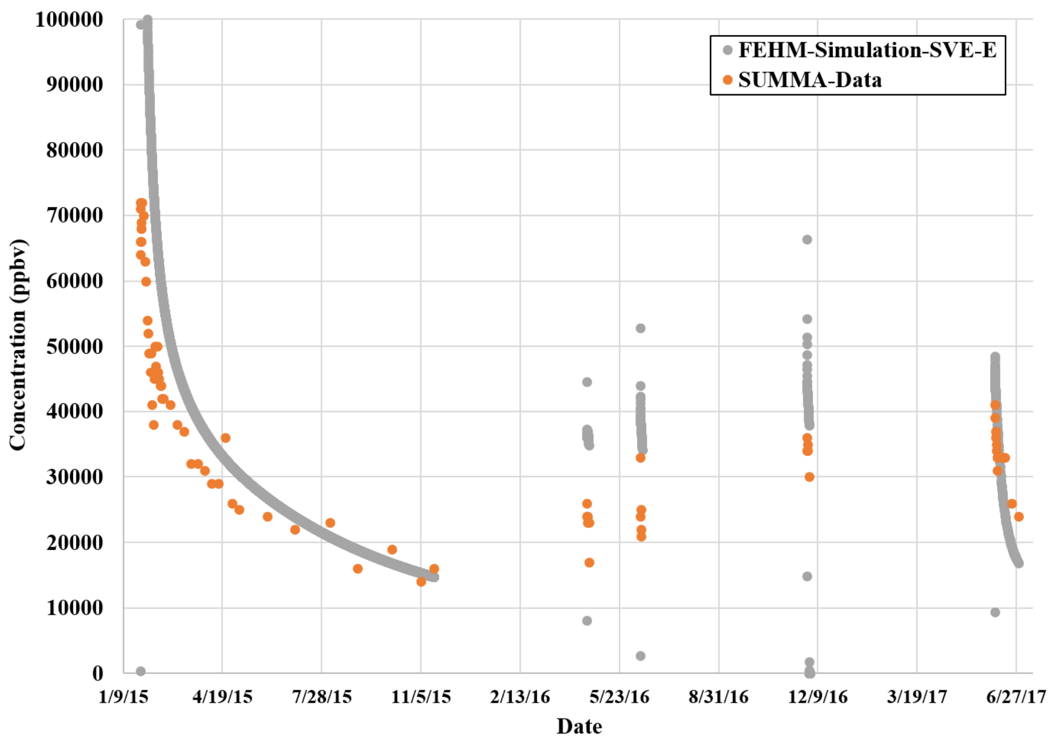

Figure 5.5-1 Simulated rebound for SVE-East compared with measured SUMMA data from SVE-East effluent

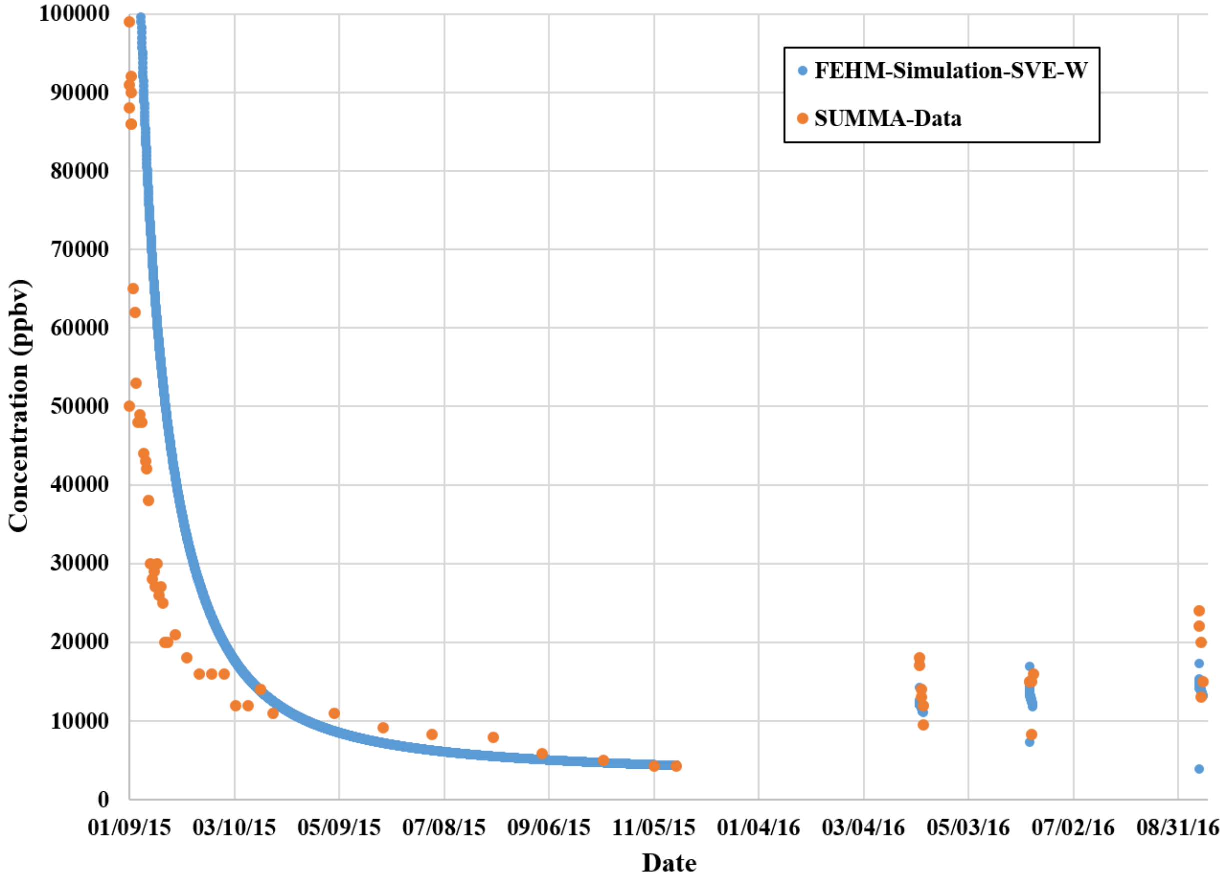

Figure 5.5-2 **Simulated active extraction concentrations and rebound for SVE-West compared with measured SUMMA data**

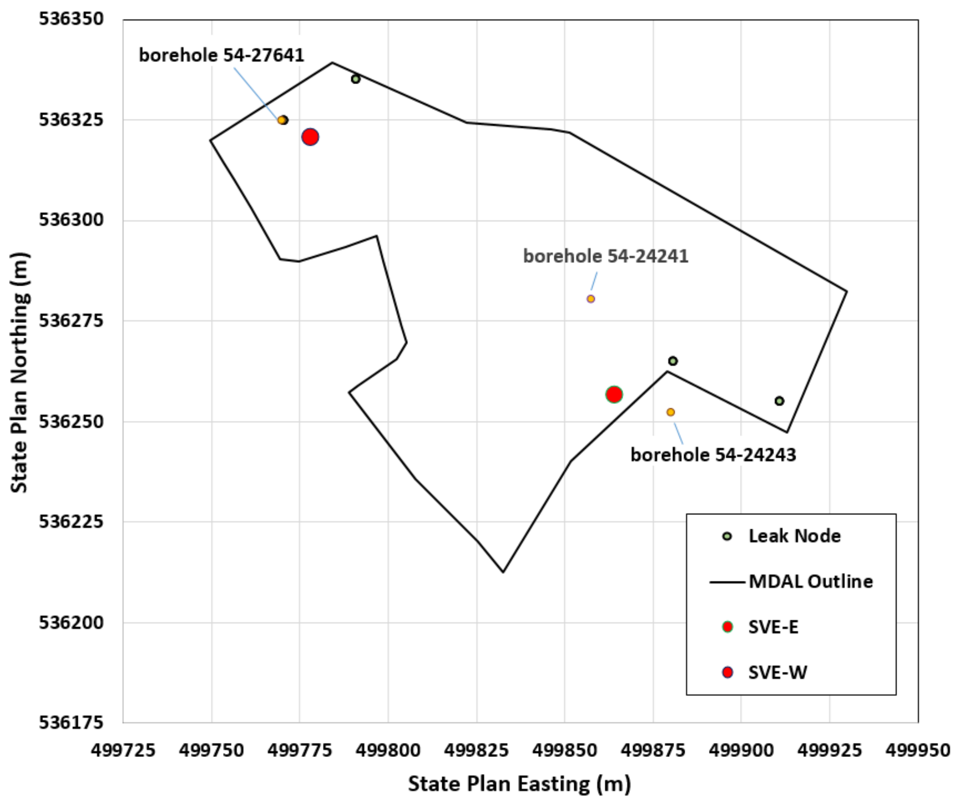

Figure 5.6-1 Location of sudden drum failure and three existing monitoring wells

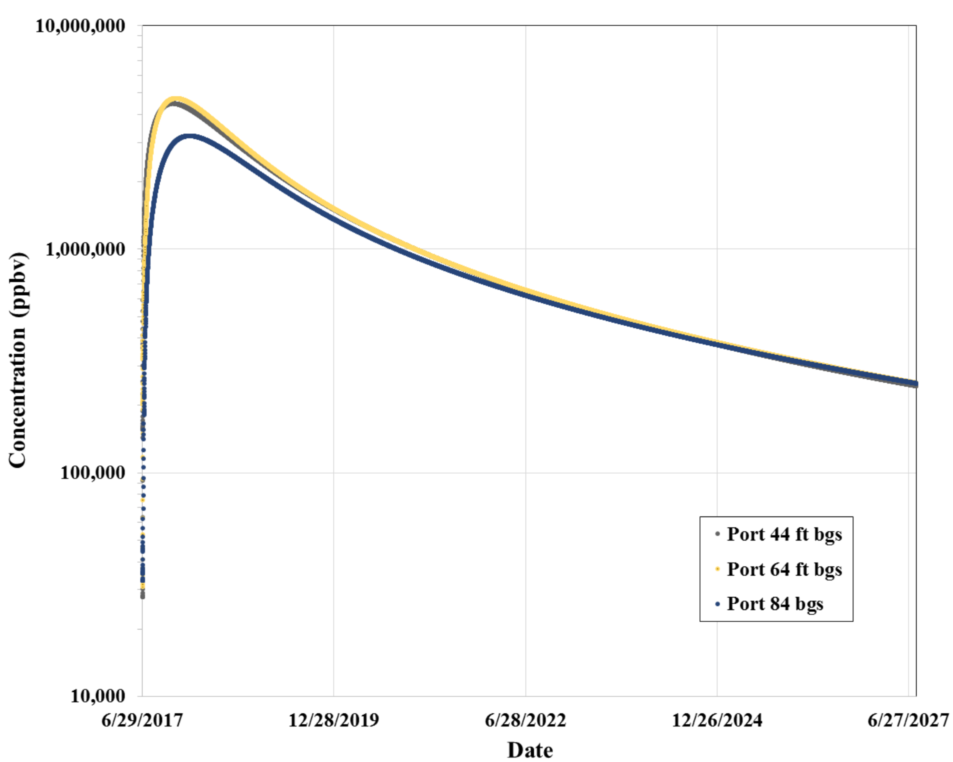

Figure 5.6-2 Borehole 54-24238 response to sudden release of 1 drum (200 L) of 1,1,1-TCA

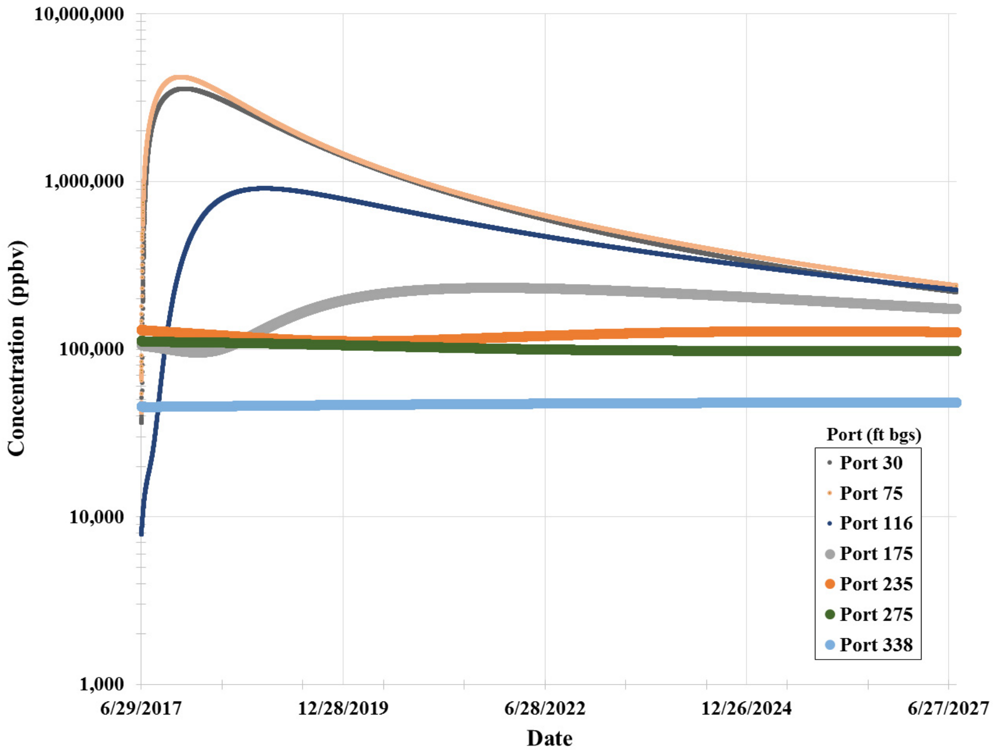

Figure 5.6-3 Borehole 54-27642 response to sudden release of 1 drum (200 L) of 1,1,1-TCA

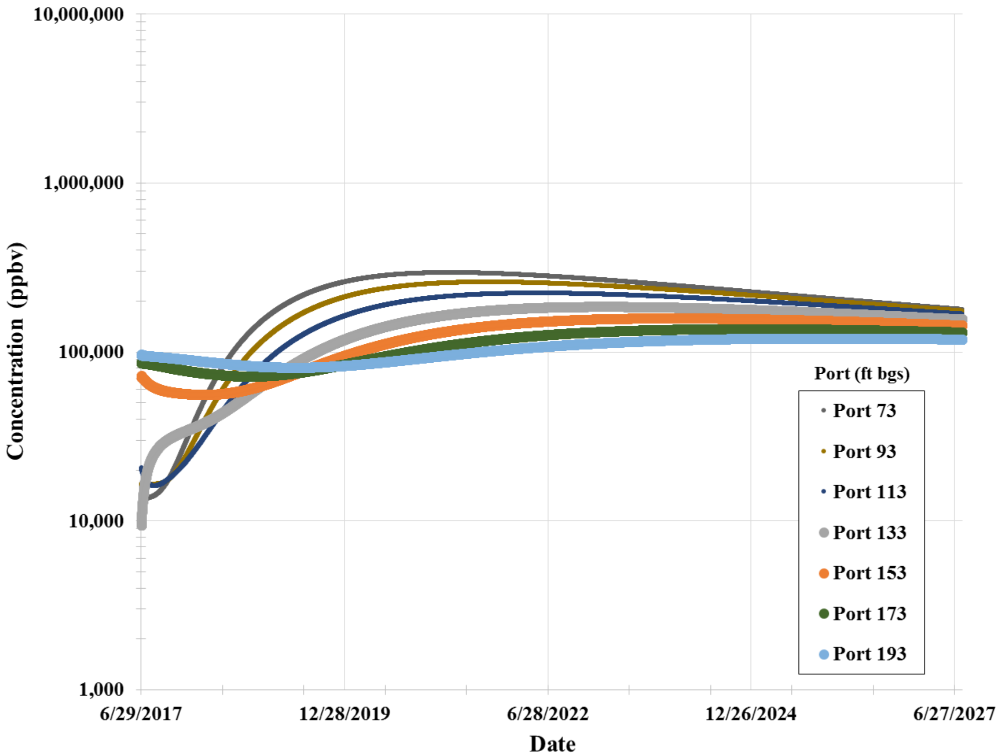

Figure 5.6-4 Borehole 54-24241 response to sudden release of 1 drum (200 L) of 1,1,1-TCA

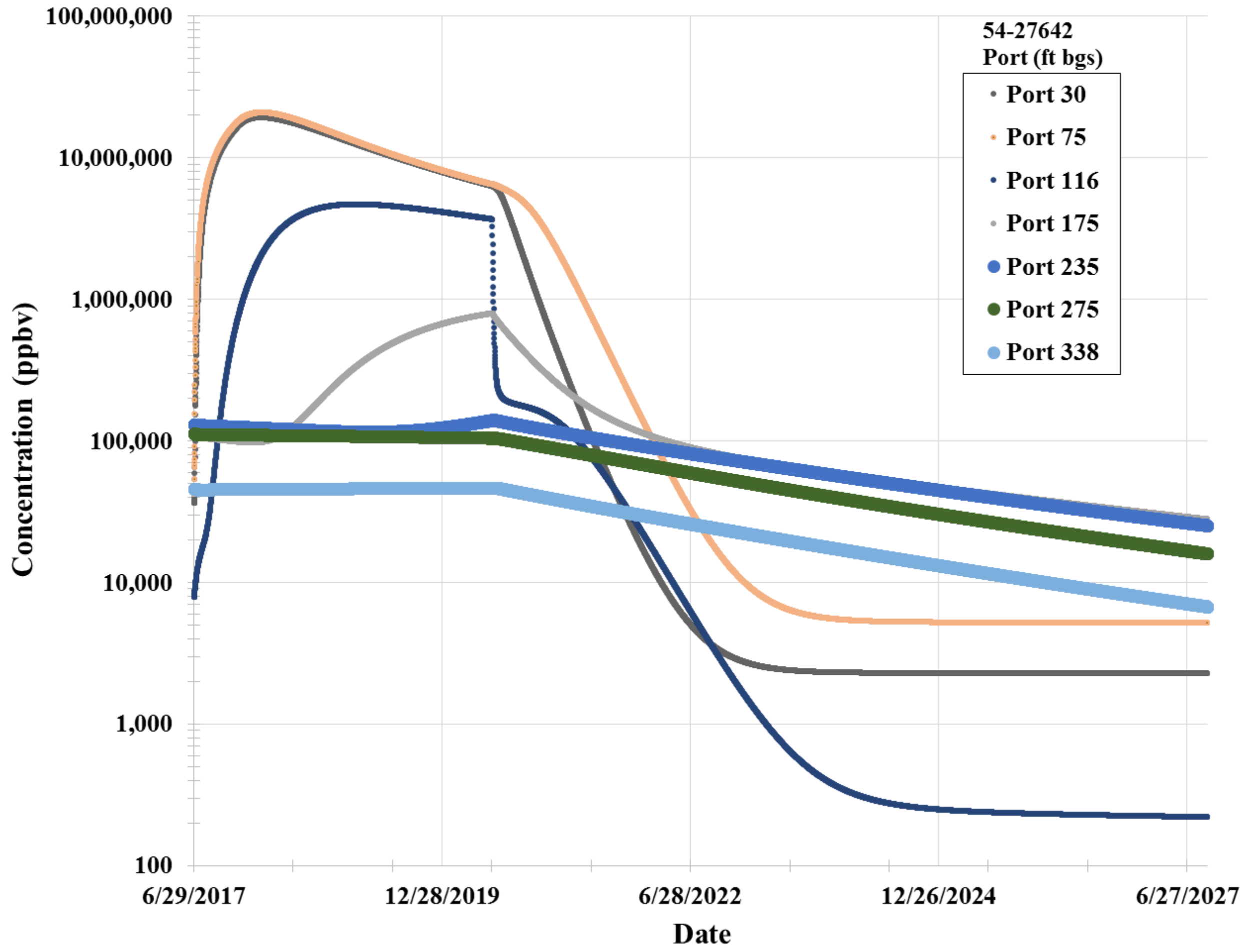

Figure 5.6-5 Concentrations in monitoring borehole 54-27642 for a simulated five-drum sudden failure of TCA followed by 7 yr of SVE

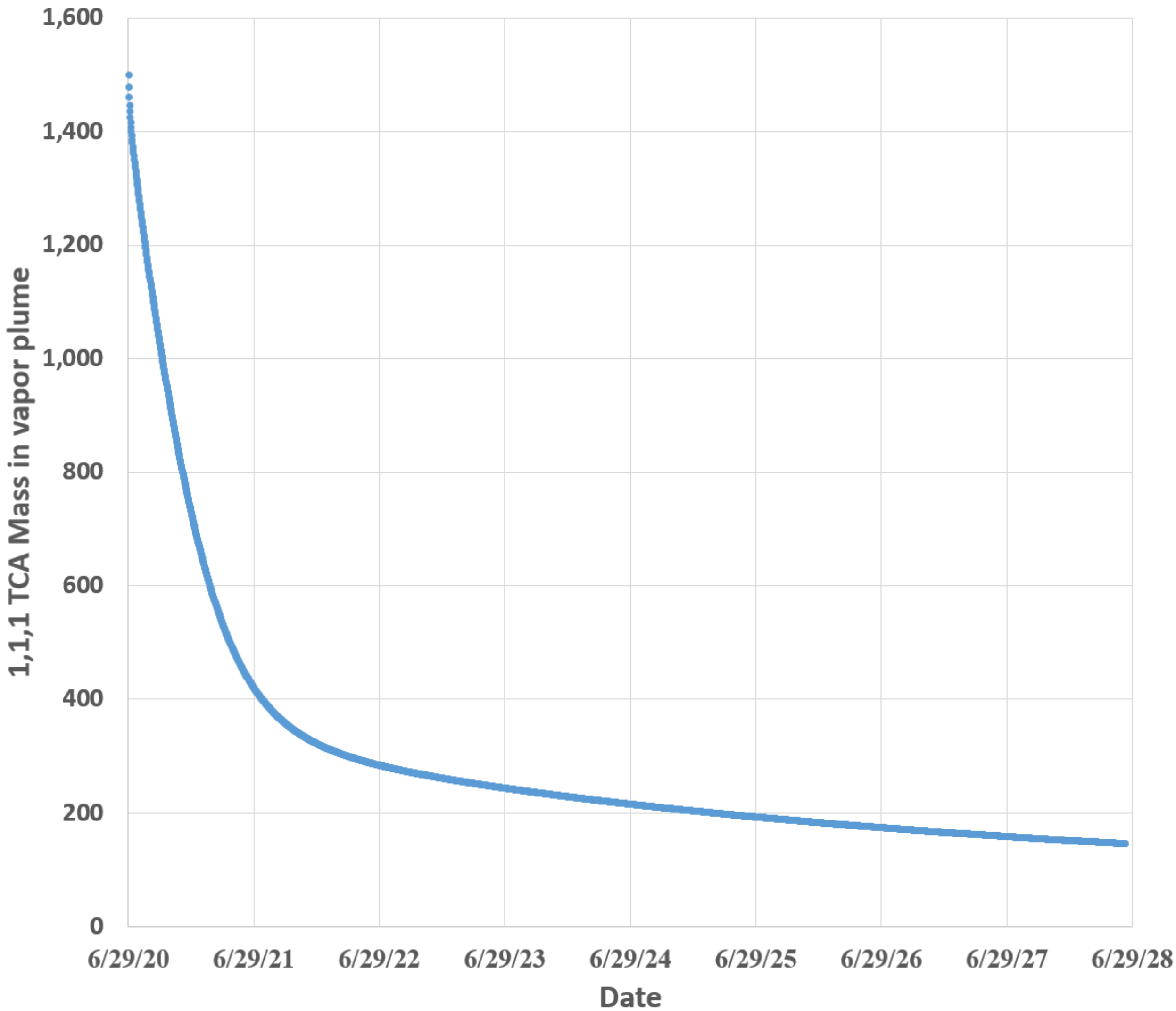

Figure 5.6-6 Mass removal by active SVE of 1,1,1-TCA versus time for the five-drum case

Table 2.2-1
List of 62 Organic Compounds Analyzed
by EPA Method TO-15 during SVE Operations

Acetone	Dioxane[1,4-]
Benzene	Ethanol
Benzyl Chloride	Ethylbenzene
Bromodichloromethane	Ethyltoluene[4-]
Bromoform	Hexachlorobutadiene
Bromomethane	Hexane
Butadiene[1,3-]	Hexanone[2-]
Butanone[2-]	Isooctane
Carbon Disulfide	Isopropylbenzene
Carbon Tetrachloride	Methyl tert-Butyl Ether
Chloro-1-propene[3-]	Methyl-2-pentanone[4-]
Chlorobenzene	Methylene Chloride
Chlorodibromomethane	n-Heptane
Chloroethane	Propanol[2-]
Chloroform	Propylbenzene[1-]
Chloromethane	Styrene
Cyclohexane	Tetrachloroethane[1,1,2,2-]
Dibromoethane[1,2-]	Tetrachloroethene
Dichloro-1,1,2,2-tetrafluoroethane[1,2-]	Tetrahydrofuran
Dichlorobenzene[1,2-]	Toluene
Dichlorobenzene[1,3-]	Trichloro-1,2,2-trifluoroethane[1,1,2-]
Dichlorobenzene[1,4-]	Trichlorobenzene[1,2,4-]
Dichlorodifluoromethane	Trichloroethane[1,1,1-]
Dichloroethane[1,1-]	Trichloroethane[1,1,2-]
Dichloroethane[1,2-]	Trichloroethene
Dichloroethene[1,1-]	Trichlorofluoromethane
Dichloroethene[cis-1,2-]	Trimethylbenzene[1,2,4-]
Dichloroethene[trans-1,2-]	Trimethylbenzene[1,3,5-]
Dichloropropane[1,2-]	Vinyl Chloride
Dichloropropene[cis-1,3-]	Xylene[1,2-]
Dichloropropene[trans-1,3-]	Xylene[1,3-]+Xylene[1,4-]

Table 2.2-2
Subsurface Vapor-Monitoring Locations, Port Depths, and Corresponding Sampling Intervals Used for Baseline and Annual Monitoring

MDA L Well	Port Depth (ft bgs)	Sampling Interval (ft length along borehole)	Status
54-01015[a]	37.6	36–46	S
54-01015[a]	165.4	182–192	S
54-01015[a]	308.3	340–352	S
54-01015[a]	333.3	375–385	S
54-01015[a]	377.7	425–435	S
54-01015[a]	426.5	480–490	S
54-01015[a]	462.1	520–530	S
54-01016[a]	30.8	30–40	S
54-01016[a]	162.2	178–190	S
54-01016[a]	274.7	318–324	S
54-01016[a]	336.3	386–396	S
54-01016[a]	414.3	473–483	RfP
54-01016[a]	459.5	530–540	RfP
54-01016[a]	517.6	592–602	S
54-02001	20	17.5–22.5	S
54-02001	40	37.5–42.5	S
54-02001	60	57.5–62.5	RfP
54-02001	80	77.5–82.5	S
54-02001	100	97.5–102.5	S
54-02001	120	117.5–122.5	S
54-02001	140	137.5–142.5	S
54-02001	160	157.5–162.5	RfP
54-02001	180	177.5–182.5	S
54-02001	200	197.5–202.5	RfP
54-02002	20	17.5–22.5	RfP
54-02002	40	37.5–42.5	S
54-02002	60	57.5–62.5	S
54-02002	80	77.5–82.5	RfP
54-02002	100	97.5–102.5	RfP
54-02002	120	117.5–122.5	S
54-02002	140	137.5–142.5	RfP
54-02002	157/160	154.5–159.5	RfP
54-02002	180	177.5–182.5	S
54-02002	200	197.5–202.5	S
54-02016	18	15.5–20.5	RfP
54-02016	31	28.5–33.5	S
54-02016	82	79.5–84.5	RfP

Table 2.2-2 (continued)

MDA L Borehole	Port Depth (ft bgs)	Sampling Interval (ft length along borehole)	Status
54-02020	20	10–30	S
54-02020	40	30–50	S
54-02020	60	50–70	S
54-02020	80	70–90	S
54-02020	95	90–110	S
54-02020	120	110–130	S
54-02020	140	130–150	S
54-02020	160	150–170	S
54-02020	180	170–190	S
54-02020	200	190–210	S
54-02021	20	10–30	S
54-02021	40	30–50	RfP
54-02021	60	50–70	RfP
54-02021	80	70–90	RfP
54-02021	100	90–110	RfP
54-02021	120	110–130	RfP
54-02021	140	130–150	S
54-02021	160	150–170	S
54-02021	180	170–190	S
54-02021	198	190–210	S
54-02022	20	17.5–22.5	RfP
54-02022	40	37.5–42.5	S
54-02022	60	57.5–62.5	S
54-02022	80	77.5–82.5	S
54-02022	100	97.5–102.5	RfP
54-02022	120	117.5–122.5	S
54-02022	140	137.5–142.5	S
54-02022	160	157.5–162.5	S
54-02022	180	177.5–182.5	S
54-02022	200	197.5–202.5	S
54-02023	20	10–30	S
54-02023	40	30–50	S
54-02023	60	50–70	S
54-02023	80	70–90	S
54-02023	100	90–110	S
54-02023	120	110–130	RfP
54-02023	140	130–149	RfP
54-02023	159	149–169	S
54-02023	180	170–190	RfP
54-02023	200	190–210	S

Table 2.2-2 (continued)

MDA L Borehole	Port Depth (ft bgs)	Sampling Interval (ft length along borehole)	Status
54-02024	20	10–30	S
54-02024	40	30–50	S
54-02024	60	50–70	S
54-02024	80	70–90	S
54-02024	100	90–110	S
54-02024	120	110–130	RfP
54-02024	140	130–150	S
54-02024	160	150–170	S
54-02024	180	170–190	S
54-02024	200	190–210	S
54-02025	20	20	S
54-02025	60	60	S
54-02025	100	100	S
54-02025	160	160	S
54-02025	190	190	S
54-02026	20	20	S
54-02026	60	60	S
54-02026	100	100	S
54-02026	160	160	S
54-02026	200	200	S
54-02026	215	215	S
54-02027	20	20	S
54-02027	60	60	S
54-02027	100	100	S
54-02027	160	160	S
54-02027	200	200	S
54-02027	220	220	S
54-02027	250	250	S
54-02028	20	20	S
54-02028	60	60	S
54-02028	100	100	S
54-02028	160	160	S
54-02028	200	200	S
54-02028	220	220	S
54-02028	250	250	S
54-02031	20	20	S
54-02031	60	60	S
54-02031	100	100	S
54-02031	160	160	S
54-02031	200	200	S
54-02031	220	220	S

Table 2.2-2 (continued)

MDA L Borehole	Port Depth (ft bgs)	Sampling Interval (ft length along borehole)	Status
54-02031	260	260	S
54-02034	20	20	S
54-02034	60	60	S
54-02034	100	100	S
54-02034	160	160	S
54-02034	200	200	S
54-02034	220	220	S
54-02034	260	260	S
54-02034	300	300	S
54-02089	13	13	S
54-02089	31	31	S
54-02089	46	46	S
54-02089	86	86	S
54-24238	44	43–45	S
54-24238	64	63–65	S
54-24238	84	83–85	S
54-24239	25	24–26	S
54-24239	50	49–51	S
54-24239	75	74–76	S
54-24239	99.5	98.5–100.5	S
54-24240	28	27–29	S
54-24240	53	52–54	S
54-24240	78	77–79	S
54-24240	103	102–104	S
54-24240	128	127–129	S
54-24240	153	152–154	S
54-24241	73	71–74	S
54-24241	93	92–94	S
54-24241	113	112–114	S
54-24241	133	132–134	S
54-24241	153	152–154	S
54-24241	173	172–174	S
54-24241	193	192–194	S
54-24242	25	24–26	S
54-24242	50	49–51	S
54-24242	75	74–76	S
54-24242	100	99–101	S
54-24242	110.5	109.5–111.5	S
54-24243	25	24–26	S
54-24243	50	49–51	S
54-24243	75	74–76	S

Table 2.2-2 (continued)

MDA L Borehole	Port Depth (ft bgs)	Sampling Interval (ft length along borehole)	Status
54-24243	100	99–101	S
54-24243	125	124–126	S
54-24399[b]	568	568	RfP
54-24399[b]	568	568-569	RfP
54-24399[b, c]	567[c]	567	S
54-24399[b, c]	588	588	S
54-27641	32	29.5–34.5	S
54-27641	82	79.5–84.5	S
54-27641	115	112.5–117.5	S
54-27641	182	179.5–184.5	S
54-27641	232	229.5–234.5	S
54-27641	271	268.5–273.5	S
54-27641	332.5	330–335	S
54-27642	30	27.5–32.5	S
54-27642	75	71.5–76.5	S
54-27642	116	114.5–119.5	S
54-27642	175	172.5–177.5	S
54-27642	235	232.5–237.5	S
54-27642	275	272.5–277.5	S
54-27642	338	335.5–340.5	S
54-27643	30	27.5–32.5	S
54-27643	74	71.5–76.5	S
54-27643	117	114.5–119.5	S
54-27643	167	164.5–169.5	S
54-27643	235	232.5–237.5	S
54-27643	275	272.5–277.5	S
54-27643	354	351.5–356.5	S
54-610786[d]	25	22.5–27.5	S
54-610786[d]	50	47.5–52.5	S
54-610786[d]	75	72.5–77.5	S
54-610786[d]	100	97.5–102.5	S
54-610786[d]	118.5	116–121	S

Notes: S = Sampled; RfP = Removed from plan.

[a] Vapor-monitoring borehole angled. Port depth is depth below ground surface. Port-depth interval is length along borehole.

[b] Open borehole below 566.7 ft bgs.

[c] Permanent packer installed August 2016.

[d] Drilled in December 2009.

Table 2.2-3
Subsurface Vapor-Monitoring Locations, Port Depths, and Corresponding Sampling Intervals Used for Quarterly Sampling within 150-ft Radius of the SVE Units

MDA L Well	Port depth (ft bgs)	Sampling Interval (ft length along borehole)	Apr-15	Jul-15	Nov-15	Feb-16	May-16	Aug-16	Nov-16	Feb-17	May-17	Aug-17	Status
54-02001	20	17.5-22.5	S	S	NS-RS	S	S	S	S	S	S	S	S
54-02001	40	37.5-42.5	S	S	NS-RS	S-PB	S	S	S	S	S	S	S
54-02001	60	57.5-62.5	NS-B	NS-B	NS	NS	NS	NS	NS	NS	NS	NS	RfP
54-02001	80	77.5-82.5	S	S	NS-RS	S	S	S	S	S	S	S	S
54-02001	100	97.5-102.5	S	S	NS-RS	S	S	S	S	S	S	S	S
54-02001	120	117.5-122.5	S	S	NS-RS	S	S	S	S	S	S	S	S
54-02001	140	137.5-142.5	S	S	NS-RS	S-PB	NS-B	S-PB	S	S	S	S	S
54-02001	160	157.5-162.5	NS-B	NS-B	NS	NS	NS	NS	NS	NS	NS	NS	RfP
54-02001	180	177.5-182.5	S	S	NS-RS	S	S	S	S	S	S	S	S
54-02001	200	197.5-202.5	NS-B	S-PB	NS-B	NS-B	NS-B	NS-B	NS-B	NS-B	NS-B	NS-B	RfP
54-02002	20	17.5-22.5	NS-B	NS-B	NS	NS	NS	NS	NS	NS	NS	NS	RfP
54-02002	40	37.5-42.5	S	S	S	S	S	S	S	S	S	S	S
54-02002	60	57.5-62.5	S	S	S	S	S	S	S	S	S	S	S
54-02002	80	77.5-82.5	S-PB	S-PB	NS	NS	NS	NS	NS	NS	NS	NS	RfP
54-02002	100	97.5-102.5	NS-B	NS-B	NS	NS	NS	NS	NS	NS	NS	NS	RfP
54-02002	120	117.5-122.5	S	S	S	S	S	S	S	S	S	S	S
54-02002	140	137.5-142.5	S-PB	S-PB	NS-B	NS-B	NS-B	NS-B	NS-B	NS-B	NS-B	NS-B	RfP
54-02002	157/160	154.5-159.5	S-PB	S-PB	NS	NS	NS	NS	NS	NS	NS	NS	RfP
54-02002	180	177.5-182.5	S	S	S	S	S	S	S	S	S	S	S
54-02002	200	197.5-202.5	S	S	S	S	S	S	S	S	S	S	S
54-02016	18	15.5-20.5	NS-B	NS-B	NS-B	NS-B	NS-B	NS-B	NS-B	NS-B	NS-B	NS-B	RfP
54-02016	31	28.5-33.5	S	S	S	S	S	S	S	S	S	S	S
54-02016	82	79.5-84.5	NS-B	NS-B	NS-B	NS-B	NS-B	NS-B	NS-B	NS-B	NS-B	NS-B	RfP

Table 2.2-3 (continued)

MDA L Well	Port depth (ft bgs)	Sampling Interval (ft length along borehole)	Apr-15	Jul-15	Nov-15	Feb-16	May-16	Aug-16	Nov-16	Feb-17	May-17	Aug-17	Status
54-02021	20	10-30	S	S	S	S	S	S	S	S	S	S	S
54-02021	40	30-50	S-PB	S-PB	NS	NS	NS	NS	NS	NS	NS	NS	RfP
54-02021	60	50-70	S	S-PB	NS	NS	NS	NS	NS	NS	NS	NS	RfP
54-02021	80	70-90	S-PB	S-PB	NS	NS	NS	NS	NS	NS	NS	NS	RfP
54-02021	100	90-110	S-PB	S-PB	NS	NS	NS	NS	NS	NS	NS	NS	RfP
54-02021	120	110-130	S-PB	S-PB	NS	NS	NS	NS	NS	NS	NS	NS	RfP
54-02021	140	130-150	S	S	S	S	S	S	S	S	S	S	S
54-02021	160	150-170	S	S	S	S	S	S	S	S	S	S	S
54-02021	180	170-190	S	S	S	S	S	S	S	S	S	S	S
54-02021	198	190-210	S	S	S	S	S	S	S	S	S	S	S
54-02022	20	17.5-22.5	NS-B	S-PB	NS	NS	NS	NS	NS	NS	NS	NS	RfP
54-02022	40	37.5-42.5	S	S	S	S	S	S	S	S	S	S	S
54-02022	60	57.5-62.5	S	S	S	S	S	S	S	S	S	S	S
54-02022	80	77.5-82.5	S	S	S	S	S	S	S	S	S	S	S
54-02022	100	97.5-102.5	NS-B	S-PB	NS	NS	NS	NS	NS	NS	NS	NS	RfP
54-02022	120	117.5-122.5	S	S	S	S	S	S	S	S	S	S	S
54-02022	140	137.5-142.5	S	S	S	S	S	S	S	S	S	S	S
54-02022	160	157.5-162.5	S	S	S	S	S	S	S	S	S	S	S
54-02022	180	177.5-182.5	S	S	S	S	S	S	S	S	S	S	S
54-02022	200	197.5-202.5	S	S	S	S	S	S	S	S	S	S	S
54-02089	13	13	S	S	S	S	S	S	S	S	S	S	S
54-02089	31	31	S	S	S	S	S	S	S	S	S	S	S
54-02089	46	46	S	S	S	S	S	S	S	S	S	S	S
54-02089	86	86	S	S	S	S	S	S	S	S	S	S	S

Table 2.2-3 (continued)

MDA L Well	Port depth (ft bgs)	Sampling Interval (ft length along borehole)	Apr-15	Jul-15	Nov-15	Feb-16	May-16	Aug-16	Nov-16	Feb-17	May-17	Aug-17	Status
54-24238	44	43-45	S	S	S	S	S	S	S	S	S	S	S
54-24238	64	63-65	S	S	S	S	S	S	S	S	S	S	S
54-24238	84	83-85	S	S	S	S	S	S	S	S	S	S	S
54-24239	25	24-26	S	S	S	S	S	S	S	S	S	S	S
54-24239	50	49-51	S	S	S	S	S	S	S	S	S	S	S
54-24239	75	74-76	S	S	S	S	S	S	S	S	S	S	S
54-24239	99.5	98.5-100.5	S	S	S	S	S	S	S	S	S	S	S
54-24240	28	27-29	S	S	S	S	S	S	S	S	S	S	S
54-24240	53	52-54	S	S	S	S	S	S	S	S	S	S	S
54-24240	78	77-79	S	S	S	S	S	S	S	S	S	S	S
54-24240	103	102-104	S	S	NS-FV	S	S	S	S	S	S	S	S
54-24240	128	127-129	S	S	S	S	S	S	S	S	S	S	S
54-24240	153	152-154	S	S	S	S	S	S	S	S	S	S	S
54-24241	73	71-74	S	S	NS-RS	S	NS-B	S	S	S	S	S	S
54-24241	93	92-94	S	S	NS-RS	S	S	S	S	S	S	S	S
54-24241	113	112-114	S	S	NS-RS	S	S	S	S	S	S	S	S
54-24241	133	132-134	S	S	NS-RS	S	S	S	S	S	S	S	S
54-24241	153	152-154	S	S	NS-RS	S	S	S	S	S	S	S	S
54-24241	173	172-174	S	S	NS-RS	S	S	S	S	S	S	S	S
54-24241	193	192-194	S	S	NS-RS	NS-B	NS-B	S	S	S	S	S	S
54-24243	25	24-26	S	S	S	S	S	S	S	S	S	S	S
54-24243	50	49-51	S	S	S	S	S	S	S	S	S	S	S
54-24243	75	74-76	S	S	S	S	S	S	S	S	S	S	S
54-24243	100	99-101	S	S	S	S	S	S	S	S	S	S	S
54-24243	125	124-126	S	S	S	S	S	S	S	S	S	S	S

Table 2.2-3 (continued)

MDA L Well	Port depth (ft bgs)	Sampling Interval (ft length along borehole)	Apr-15	Jul-15	Nov-15	Feb-16	May-16	Aug-16	Nov-16	Feb-17	May-17	Aug-17	Status
54-24399[a]	568	568	S	S	S	S	S	NS	NS	NS	NS	NS	RfP
54-24399[a]	568	568-569	S	S	NS	NS	NS	NS	NS	NS	NS	NS	RfP
54-24399[a,b]	567	567	n/a[c]	n/a	n/a	n/a	n/a	n/a	S	S	S	S	S
54-24399[a,b]	588	588	n/a	n/a	n/a	n/a	n/a	S	S	S	S	S	S
54-27641	32	29.5-34.5	S	S	NS-RS	S	S	S	S	S	S	S	S
54-27641	82	79.5-84.5	S	S	S	S	S	S	S	S	S	S	S
54-27641	115	112.5-117.5	S	S	S	S	S	S	S	S	S	S	S
54-27641	182	179.5-184.5	S	S	S	S	S	S	S	S	S	S	S
54-27641	232	229.5-234.5	S	S	NS-RS	S	S	S	S	S	S	S	S
54-27641	271	268.5-273.5	S	S	S	S	S	S	S	S	S	S	S
54-27641	332.5	330-335	S	S	S	S	S	S	S	S	S	S	S
54-27642	30	27.5-32.5	S	S	S	S	S	S	S	S	S	S	S
54-27642	75	71.5-76.5	S	S	S	S	S	S	S	S	S	S	S
54-27642	116	114.5-119.5	S	S	NS-RS	NS-B	NS-B	S	S	S	S	S	S
54-27642	175	172.5-177.5	S	S	S	S	S	S	S	S	S	S	S
54-27642	235	232.5-237.5	S	S	S	S	S	S	S	S	S	S	S
54-27642	275	272.5-277.5	S	S	S	S	S	S	S	S	S	S	S
54-27642	338	335.5-340.5	S	S	NS-RS	S	S	S	S	S	S	S	S

Notes: S (green) = Sampled; S-PB (light blue) = Sample partially blocked; NS-B (yellow) = Not sampled because port blocked; NS-RS (orange) = Not sampled because of radiological screening; NS (purple) = Not sampled; NS-FV (dark blue) = Not sampled because valve faulty; RfP (pink) = Removed from plan.

[a] Open borehole below 566.7 ft bgs.

[b] Permanent packer installed August 2016.

[c] n/a = Not applicable since these ports did not exist before August 2016.

Table 4.1-1
Mass Removed for Detected Organic Compounds during SVE Operation

Parameter Name	Cumulative Total Pounds through 2/18/2015 10:53:00 AM	Cumulative Total Pounds through 3/18/2015 10:53:00 AM	Cumulative Total Pounds through 4/18/2015 10:53:00 AM	Cumulative Total Pounds through 5/18/2015 10:53:00 AM	Cumulative Total Pounds through 6/18/2015 10:53:00 AM
Acetone	0.01	0.01	0.01	0.01	0.01
Benzene	0.12	0.22	0.31	0.39	0.48
Carbon Tetrachloride	0.58	0.92	1.22	1.49	1.72
Chlorobenzene	0.00	0.00	0.00	0.01	0.02
Chloroform	5.39	8.51	11.19	13.53	15.65
Dichlorodifluoromethane	0.48	0.74	0.96	1.15	1.33
Dichloroethane[1,1-]	4.16	6.36	8.29	9.97	11.47
Dichloroethane[1,2-]	12.16	17.48	22.52	27.03	31.06
Dichloroethene[1,1-]	5.84	9.73	13.30	16.50	19.82
Dichloropropane[1,2-]	4.13	8.08	11.50	14.62	17.50
Dioxane[1,4-]	0.22	0.60	1.15	1.73	2.39
Ethanol	0.01	0.01	0.03	0.05	0.05
Hexane	0.05	0.05	0.05	0.05	0.05
Isooctane	0.02	0.13	0.13	0.14	0.17
Methylene Chloride	2.52	4.63	6.64	8.51	10.27
n-Heptane	0.02	0.02	0.02	0.02	0.02
Tetrachloroethene	20.10	33.02	45.67	57.13	67.95
Tetrahydrofuran	0.11	0.24	0.35	0.47	0.61
Toluene	0.20	0.43	0.66	0.88	1.11
Trichloro-1,2,2-trifluoroethane[1,1,2-]	21.40	37.13	50.75	62.63	73.57
Trichloroethane[1,1,1-]	116.25	187.31	250.50	305.43	354.80
Trichloroethene	65.87	97.69	125.95	150.78	173.69
Trichlorofluoromethane	1.24	2.13	2.94	3.65	4.27
Xylene[1,3-]+Xylene[1,4-]	0.02	0.03	0.05	0.06	0.07
Total VOCs	260.88	415.49	554.20	676.23	788.08

Table 4.1-1 (continued)

Parameter Name	Cumulative Total Pounds through 7/18/2015	Cumulative Total Pounds through 8/18/2015	Cumulative Total Pounds through 9/18/2015	Cumulative Total Pounds through 10/18/2015	Cumulative Total Pounds through 11/18/2015
Acetone	0.01	0.01	0.01	0.01	0.01
Benzene	0.56	0.64	0.71	0.78	0.85
Carbon Tetrachloride	1.92	2.10	2.27	2.42	2.56
Chlorobenzene	0.03	0.05	0.06	0.06	0.07
Chloroform	17.59	19.47	21.12	22.62	24.12
Dichlorodifluoromethane	1.50	1.67	1.82	1.95	2.06
Dichloroethane[1,1-]	12.75	13.94	15.00	16.00	16.98
Dichloroethane[1,2-]	34.66	38.12	41.05	43.63	46.19
Dichloroethene[1,1-]	23.11	26.27	28.85	31.15	34.00
Dichloropropane[1,2-]	20.00	22.35	24.51	26.61	28.70
Dioxane[1,4-]	3.04	3.67	4.24	4.79	5.38
Ethanol	0.05	0.05	0.11	0.23	0.31
Hexane	0.06	0.08	0.09	0.09	0.09
Isooctane	0.19	0.19	0.19	0.19	0.19
Methylene Chloride	11.83	13.33	14.72	16.05	17.41
n-Heptane	0.04	0.07	0.09	0.09	0.09
Tetrachloroethene	77.26	85.97	94.19	102.16	110.63
Tetrahydrofuran	0.74	0.86	1.00	1.13	1.25
Toluene	1.29	1.44	1.61	1.79	1.97
Trichloro-1,2,2-trifluoroethane[1,1,2-]	83.64	93.00	101.17	109.01	117.16
Trichloroethane[1,1,1-]	399.42	441.79	477.93	510.09	540.98
Trichloroethene	193.45	211.32	227.65	243.63	259.45
Trichlorofluoromethane	4.86	5.43	5.93	6.38	6.82
Xylene[1,3-]+Xylene[1,4-]	0.11	0.16	0.20	0.21	0.21
Total VOCs	888.08	981.99	1064.50	1141.05	1217.49

Table 4.1-2
Flow Rate Data for SVE-West

Date	Time	Flow Rate (scfm)
1/9/2015	12:55	0.0
1/9/2015	12:56	99.9
1/9/2015	12:59	99.9
1/9/2015	13:01	99.9
1/9/2015	13:02	99.9
1/9/2015	13:05	99.9
1/9/2015	13:07	99.9
1/9/2015	13:09	99.9
1/9/2015	13:11	99.9
1/9/2015	13:32	99.9
1/9/2015	13:36	99.9
1/9/2015	13:37	99.9
1/9/2015	13:38	99.9
1/9/2015	13:45	99.9
1/9/2015	13:52	99.9
1/9/2015	14:01	99.9
1/9/2015	14:22	99.9
1/9/2015	14:42	99.9
1/9/2015	14:53	99.9
1/9/2015	15:05	99.9
1/9/2015	15:15	99.9
1/9/2015	15:16	99.9
1/9/2015	15:24	99.9
1/9/2015	15:34	99.9
1/9/2015	15:44	99.9
1/9/2015	15:54	99.9
1/9/2015	16:03	99.9
1/9/2015	16:05	99.9
1/9/2015	16:07	99.9
1/10/2015	9:08	99.9
1/10/2015	9:09	99.9
1/10/2015	9:10	99.9
1/10/2015	9:53	99.9
1/10/2015	9:55	99.9
1/10/2015	9:57	99.9
1/10/2015	10:41	99.9
1/10/2015	10:43	99.9

Table 4.1-2 (continued)

Date	Time	Flow Rate (scfm)
1/10/2015	10:48	99.9
1/10/2015	10:48	99.9
1/10/2015	11:35	99.9
1/10/2015	11:48	99.9
1/10/2015	11:51	99.9
1/10/2015	11:52	99.9
1/11/2015	9:02	99.9
1/11/2015	9:05	99.9
1/11/2015	9:07	99.9
1/12/2015	12:03	99.9
1/12/2015	12:05	99.9
1/12/2015	12:07	99.9
1/13/2015	8:57	99.9
1/13/2015	8:59	99.9
1/13/2015	9:00	99.9
1/14/2015	9:37	99.9
1/14/2015	9:40	99.9
1/14/2015	9:42	99.9
1/15/2015	11:36	99.9
1/15/2015	11:38	99.9
1/15/2015	11:40	99.9
1/16/2015	8:58	99.9
1/16/2015	8:59	99.9
1/16/2015	9:00	99.9
1/17/2015	9:05	99.9
1/17/2015	9:07	99.9
1/17/2015	9:09	99.9
1/18/2015	8:57	99.9
1/18/2015	8:58	99.9
1/18/2015	9:00	99.9
1/18/2015	9:02	99.9
1/19/2015	9:03	99.9
1/19/2015	9:05	99.9
1/19/2015	9:07	99.9
1/19/2015	9:09	99.9
1/20/2015	9:54	99.9
1/20/2015	9:55	99.9
1/20/2015	9:57	99.9
1/21/2015	9:54	99.9

Table 4.1-2 (continued)

Date	Time	Flow Rate (scfm)
1/21/2015	9:56	99.9
1/21/2015	9:58	99.9
1/22/2015	14:43	99.9
1/22/2015	14:44	99.9
1/22/2015	14:47	99.9
1/23/2015	9:20	100.7
1/23/2015	9:25	100.7
1/23/2015	9:28	100.7
1/24/2015	10:46	99.9
1/24/2015	10:49	99.9
1/24/2015	10:53	99.9
1/25/2015	9:40	100.3
1/25/2015	9:42	100.3
1/25/2015	9:45	100.3
1/26/2015	9:08	99.9
1/26/2015	9:11	99.9
1/26/2015	9:15	99.9
1/27/2015	10:50	99.5
1/27/2015	10:51	99.5
1/27/2015	10:52	99.5
1/28/2015	9:45	99.5
1/28/2015	9:47	99.5
1/28/2015	9:49	99.5
1/29/2015	9:02	99.6
1/29/2015	9:05	99.6
1/29/2015	9:06	99.6
1/31/2015	13:54	99.5
1/31/2015	13:55	99.5
1/31/2015	13:59	99.5
2/4/2015	10:07	99.1
2/11/2015	10:29	99.6
2/18/2015	9:58	97.8
2/25/2015	12:42	99.1
3/4/2015	9:53	100.6
3/11/2015	9:16	99.2
3/18/2015	9:05	100.1
3/25/2015	8:58	100.1
4/1/2015	10:19	99.6
4/8/2015	9:20	99.6

Table 4.1-2 (continued)

Date	Time	Flow Rate (scfm)
4/9/2015	11:43	99.2
4/14/2015	9:27	99.2
4/15/2015	9:09	99.6
4/21/2015	9:31	99.6
4/22/2015	10:33	99.6
4/28/2015	9:42	98.7
4/29/2015	9:52	99.2
5/6/2015	9:36	99.2
5/13/2015	9:58	99.7
5/20/2015	11:41	98.7
5/27/2015	9:14	98.7
6/3/2015	10:56	98.7
6/10/2015	9:23	100.0
6/17/2015	9:30	100.0
6/24/2015	11:16	100.0
7/1/2015	8:56	97.8
7/9/2015	9:48	99.5
7/15/2015	9:42	98.6
7/22/2015	9:51	97.3
7/29/2015	9:42	99.5
8/5/2015	9:45	97.3
8/12/2015	9:25	99.1
8/19/2015	15:10	98.6
8/26/2015	8:34	99.6
9/2/2015	9:17	100.0
9/9/2015	9:19	99.9
9/16/2015	11:39	99.1
9/23/2015	9:27	99.6
9/30/2015	8:56	100.1
10/7/2015	9:18	100.1
10/14/2015	8:19	100.1
10/22/2015	9:46	100.5
10/28/2015	10:55	99.7
11/5/2015	10:58	99.7
11/12/2015	9:23	101.1
11/17/2015	12:37 PM	99.7
11/18/2015	10:54	99.7

Note: Standard conditions for the orifice flow meter are 60°F and 14.7 psi (21.1°C and 101.3 kPa).

Table 4.1-3
Flow Rate Data for SVE-East

Date	Time	Flow Rate (scfm)
1/26/2015	10:20	0.0
1/26/2015	10:21	95.6
1/26/2015	10:25	95.6
1/26/2015	10:30	95.6
1/26/2015	10:34	95.6
1/26/2015	10:57	95.6
1/26/2015	11:01	95.6
1/26/2015	11:03	95.6
1/26/2015	11:18	95.6
1/26/2015	11:21	95.6
1/26/2015	11:27	95.6
1/26/2015	11:31	95.6
1/26/2015	11:41	95.6
1/26/2015	11:47	95.6
1/26/2015	11:55	95.6
1/26/2015	12:01	95.6
1/26/2015	12:05	95.6
1/26/2015	13:59	95.6
1/26/2015	14:06	95.6
1/26/2015	14:10	95.6
1/26/2015	14:15	95.6
1/26/2015	14:20	95.6
1/26/2015	14:24	95.6
1/26/2015	14:29	95.6
1/26/2015	14:31	95.6
1/26/2015	14:44	95.6
1/26/2015	14:47	95.6
1/26/2015	14:53	95.6
1/26/2015	15:02	95.6
1/26/2015	15:10	95.6
1/26/2015	15:17	95.6
1/26/2015	15:19	95.6
1/26/2015	15:21	95.6
1/27/2015	11:17	94.6
1/27/2015	11:19	94.6
1/27/2015	11:21	94.6
1/27/2015	12:18	94.6

Table 4.1-3 (continued)

Date	Time	Flow Rate (scfm)
1/27/2015	12:20	94.6
1/27/2015	12:22	94.6
1/27/2015	13:57	94.6
1/27/2015	13:59	94.6
1/27/2015	14:00	94.6
1/27/2015	14:55	94.6
1/27/2015	14:57	94.6
1/27/2015	14:59	94.6
1/27/2015	15:45	94.6
1/27/2015	15:50	94.6
1/27/2015	15:52	94.6
1/27/2015	15:54	94.6
1/28/2015	10:20	94.4
1/28/2015	10:21	94.4
1/28/2015	10:23	94.4
1/29/2015	10:12	94.4
1/29/2015	10:13	94.4
1/29/2015	10:15	94.4
1/31/2015	14:37	93.6
1/31/2015	14:40	93.6
1/31/2015	14:41	93.6
2/1/2015	8:51	94.1
2/1/2015	8:54	94.1
2/1/2015	8:57	94.1
2/2/2015	9:40	93.6
2/2/2015	9:42	93.6
2/2/2015	9:46	93.6
2/4/2015	10:07	93.4
2/5/2015	8:51	96.0
2/6/2015	10:23	100.6
2/7/2015	9:34	98.9
2/8/2015	9:21	98.9
2/9/2015	9:58	96.3
2/10/2015	9:34	98.0
2/11/2015	9:47	97.4
2/12/2015	9:00	97.4
2/13/2015	9:03	97.4
2/14/2015	8:58	98.0
2/15/2015	8:58	98.0

Table 4.1-3 (continued)

Date	Time	Flow Rate (scfm)
2/17/2015	9:39	98.4
2/18/2015	9:25	98.0
2/25/2015	13:18	98.2
3/4/2015	10:41	98.5
3/11/2015	9:47	98.5
3/18/2015	9:39	98.5
3/25/2015	9:21	98.5
4/1/2015	9:21	96.2
4/8/2015	9:45	97.7
4/9/2015	12:13	97.3
4/14/2015	9:55	96.6
4/15/2015	9:34	97.7
4/21/2015	9:58	96.6
4/22/2015	10:49	98.6
4/28/2015	10:05	97.3
4/29/2015	10:19	97.3
5/6/2015	10:10	97.3
5/13/2015	10:30	97.7
5/20/2015	11:59	96.8
5/27/2015	9:40	97.3
6/3/2015	11:48	98.0
6/10/2015	9:45	98.0
6/17/2015	9:45	97.3
6/24/2015	11:37	97.3
7/1/2015	9:15	97.1
7/9/2015	10:28	97.0
7/15/2015	10:02	96.6
7/22/2015	10:14	95.5
7/29/2015	10:08	98.0
8/5/2015	10:06	97.1
8/12/2015	9:47	93.4
8/19/2015	15:25	93.4
8/26/2015	8:49	96.1
9/2/2015	9:37	96.8
9/9/2015	9:36	96.4
9/16/2015	11:56	96.8
9/23/2015	9:45	97.3
9/30/2015	9:13	97.3
10/7/2015	9:49	98.4

Table 4.1-3 (continued)

Date	Time	Flow Rate (scfm)
10/14/2015	8:39	98.4
10/22/2015	10:09	98.2
10/28/2015	11:15	100.1
11/5/2015	11:30	100.3
11/12/2015	9:42	100.1
11/17/2015	13:18	102.4
11/18/2015	11:30	99.4

Note: Standard conditions for the orifice flow meter are 60°F and 14.7 psi (21.1°C and 101.3 kPa).

Table 4.3-1
MDA L CME Tier I+II Screening Calculations

VOC	Henry's Law Constant[a] (dimensionless)	Groundwater SL (µg/L)	Source of Groundwater SL	Tier I Pore-Gas Concentrations Corresponding to Groundwater Standard (µg/m³)	MDA L–Specific Tier II Calculated Pore-Gas Screening Concentrations (µg/m³)
Acetone	0.0016	22,000	EPA regional SL	35,200	104,000,000
Benzene	0.228	5	EPA MCL	1140	34,900
Butanone[2-]	0.0023	7100	EPA regional SL	16,330	553,000
Carbon Tetrachloride	1.1	5	EPA MCL	5500	74,200
Chlorobenzene	0.13	100	EPA MCL	13,000	440,000
Chloroform	0.15	100	NMWQCC	15,000	508,000
Cyclohexane	6.1	13,000	EPA regional SL	79,300,000	496,000,000
Dichlorodifluoromethane	14	390	EPA regional SL	5,460,000	30,900,000
Dichloroethane[1,1-]	0.23	25	NMWQCC	5750	185,000
Dichloroethane[1,2-]	0.048	5	EPA MCL	240	8,120
Dichloroethene[1,1-]	1.1	5	NMWQCC	5500	58,800
Dichloroethene[trans-1,2-]	0.38	100	EPA MCL	38,000	789,000
Dichloropropane[1,2-]	0.12	5	EPA MCL	600	20,300
Dioxane[1,4-]	0.0002	61	EPA regional SL	12.2	413
Ethanol	na[b]	na	na	na	na
Ethylbenzene	0.323	700	EPA MCL	226,100	6,540,000
Ethyltoluene[4-]	na	na	na	na	na
Hexane	74	880	EPA regional SL	65,120,000	344,000,000
Methanol	0.00019	18,000	EPA regional SL	3420	116,000
Methylene Chloride	0.13	5	EPA MCL	650	22,000
Styrene	0.11	100	EPA MCL	11,000	372,000
Tetrachloroethene	0.72	5	EPA MCL	3600	70,500
Tetrahydrofuran	na	na	na	na	na
Toluene	0.272	750	NMWQCC	204,000	6,070,000
Trichloro-1,2,2-trifluoroethane[1,1,2-]	22	59,000	EPA regional SL	1,298,000,000	7,540,000,000
Trichloroethane[1,1,1-]	0.705	60	NMWQCC	42,300	700,000
Trichloroethane[1,1,2-]	0.034	5	EPA MCL	170	5,760
Trichloroethene	0.4	5	EPA MCL	2000	48,100
Trichlorofluoromethane	4	1300	EPA regional SL	5,200,000	37,400,000
Trimethylbenzene[1,2,4-]	0.25	15	EPA regional SL	3750	127,000
Trimethylbenzene[1,3,5-]	0.36	370	EPA regional SL	133,200	3,900,000

Table 4.3-2
Differential Pressure Data at
Sampling Ports Monitored during SVE Operations

Well	Port Depth (ft bgs)	Sampling Interval (ft length along borehole)	Static Pressure (kPa)			
			Baseline 2014	April 15	July 15	November 15
54-01015[a]	37.6	36–46	-0.106	—[b]	—	—
54-01015[a]	165.4	182–192	-0.180	—	—	—
54-01015[a]	308.3	340–352	0.011	—	—	—
54-01015[a]	333.3	375–385	-0.119	—	—	—
54-01015[a]	377.7	425–435	-0.126	—	—	—
54-01015[a]	426.5	480–490	-0.122	—	—	—
54-01015[a]	462.1	520–530	0.000	—	—	—
54-01016[a]	30.8	30–40	-0.056	—	—	—
54-01016[a]	162.2	178–190	0.021	—	—	—
54-01016[a]	274.7	318–324	0.020	—	—	—
54-01016[a]	336.3	386–396	0.016	—	—	—
54-01016[a]	414.3	473–483	0.010	—	—	—
54-01016[a]	459.5	530–540	0.000	—	—	—
54-01016[a]	517.6	592–602	0.010	—	—	—
54-02001	20	17.5–22.5	-0.063	-0.314	-0.206	NS-RS[c]
54-02001	40	37.5–42.5	-0.035	-0.545	-0.253	NS-RS
54-02001	60	57.5–62.5	0.000	NS-B[d]	NS-B	NS[e]
54-02001	80	77.5–82.5	-0.113	-0.855	-0.694	NS-RS
54-02001	100	97.5–102.5	-0.038	-0.349	-0.267	NS-RS
54-02001	120	117.5–122.5	-0.167	-0.989	-0.639	NS-RS
54-02001	140	137.5–142.5	-0.380	-1.034	-0.622	NS-RS
54-02001	160	157.5–162.5	0.000	NS-B	NS-B	NS
54-02001	180	177.5–182.5	-0.022	0.317	-0.210	NS-RS
54-02001	200	197.5–202.5	-0.037	NS-B	-0.214	NS
54-02002	20	17.5–22.5	NS-B	NS-B	NS	NS
54-02002	40	37.5–42.5	-0.025	-0.828	0.527	0.565
54-02002	60	57.5–62.5	-0.014	-0.174	0.153	0.187
54-02002	80	77.5–82.5	-0.020	-0.379	NS	NS
54-02002	100	97.5–102.5	NS-B	NS-B	NS	NS
54-02002	120	117.5–122.5	-0.021	-0.746	0.525	0.583
54-02002	140	137.5–142.5	0.000	NS-B	NS-B	NS
54-02002	157/160	154.5–159.5	0.000	NS	0.495	NS
54-02002	180	177.5–182.5	0.100	0.016	0.000	0.00
54-02002	200	197.5–202.5	0.000	-1.092	0.440	0.439
54-02016	18	15.5–20.5	NS-B	NS-B	NS-B	NS

Table 4.3-2 (continued)

Well	Port Depth (ft bgs)	Sampling Interval (ft length along borehole)	Static Pressure (kPa)			
			Annual	April 15	July 15	November 15
54-02016	31	28.5–33.5	0.041	-0.057	-0.061	0.102
54-02016	82	79.5–84.5	NS-B	NS-B	NS-B	NS
54-02020	20	10–30	-0.041	—	—	—
54-02020	40	30–50	-0.068	—	—	—
54-02020	60	50–70	-0.100	—	—	—
54-02020	80	70–90	-0.129	—	—	—
54-02020	95	90–110	-0.146	—	—	—
54-02020	120	110–130	-0.147	—	—	—
54-02020	140	130–150	-0.154	—	—	—
54-02020	160	150–170	-0.157	—	—	—
54-02020	180	170–190	-0.159	—	—	—
54-02020	200	190–210	0.012	—	—	—
54-02021	20	10–30	-0.044	-0.070	-0.098	-0.028
54-02021	40	30–50	-0.053	-0.075	-0.112	NS
54-02021	60	50–70	-0.250	-0.082	-0.306	NS
54-02021	80	70–90	-0.128	-0.075	-0.155	NS
54-02021	100	90–110	-0.216	-0.093	-0.253	NS
54-02021	120	110–130	0.000	-0.056	-0.227	NS
54-02021	140	130–150	-0.239	-0.120	-0.303	-0.616
54-02021	160	150–170	-0.103	-0.079	-0.110	-0.173
54-02021	180	170–190	-0.269	-0.127	-0.282	-0.697
54-02021	198	190–210	-0.271	0.042	-0.173	-1.129
54-02022	20	17.5–22.5	-0.041	NS-B	NS-B	NS
54-02022	40	37.5–42.5	-0.055	-0.177	-0.173	0.025
54-02022	60	57.5–62.5	-0.070	-0.200	-0.192	0.00
54-02022	80	77.5–82.5	-0.101	-0.207	-0.243	-0.023
54-02022	100	97.5–102.5	-0.142	NS-B	NS-B	NS
54-02022	120	117.5–122.5	-0.126	-0.247	-0.259	-0.097
54-02022	140	137.5–142.5	-0.085	-0.239	-0.200	-0.219
54-02022	160	157.5–162.5	-0.041	-0.229	-0.185	-0.289
54-02022	180	177.5–182.5	0.000	-0.212	-0.146	-0.336
54-02022	200	197.5–202.5	0.020	-0.200	-0.127	-0.354
54-02023	20	10–30	0.011	—	—	—
54-02023	40	30–50	0.017	—	—	—
54-02023	60	50–70	0.178	—	—	—
54-02023	80	70–90	0.051	—	—	—
54-02023	100	90–110	0.072	—	—	—

Table 4.3-2 (continued)

Well	Port Depth (ft bgs)	Sampling Interval (ft length along borehole)	Static Pressure (kPa)			
			Annual	April 15	July 15	November 15
54-02023	120	110–130	0.018	—	—	—
54-02023	140	130–149	0.079	—	—	—
54-02023	159	149–169	0.151	—	—	—
54-02023	180	170–190	0.033	—	—	—
54-02023	200	190–210	0.204	—	—	—
54-02024	20	10–30	-0.035	—	—	—
54-02024	40	30–50	-0.034	—	—	—
54-02024	60	50–70	-0.047	—	—	—
54-02024	80	70–90	-0.092	—	—	—
54-02024	100	90–110	-0.132	—	—	—
54-02024	120	110–130	-0.146	—	—	—
54-02024	140	130–150	-0.164	—	—	—
54-02024	160	150–170	-0.182	—	—	—
54-02024	180	170–190	-0.193	—	—	—
54-02024	200	190–210	-0.203	—	—	—
54-02025	20	20	-23.000	—	—	—
54-02025	60	60	0.110	—	—	—
54-02025	100	100	-0.151	—	—	—
54-02025	160	160	-0.174	—	—	—
54-02025	190	190	-0.185	—	—	—
54-02026	20	20	0.000	—	—	—
54-02026	60	60	-0.017	—	—	—
54-02026	100	100	-0.100	—	—	—
54-02026	160	160	-0.217	—	—	—
54-02026	200	200	-0.258	—	—	—
54-02026	215	215	-0.277	—	—	—
54-02027	20	20	0.010	—	—	—
54-02027	60	60	-0.017	—	—	—
54-02027	100	100	-0.112	—	—	—
54-02027	160	160	-0.162	—	—	—
54-02027	200	200	-0.170	—	—	—
54-02027	220	220	-0.173	—	—	—
54-02027	250	250	-0.166	—	—	—
54-02028	20	20	0.000	—	—	—
54-02028	60	60	0.000	—	—	—
54-02028	100	100	0.010	—	—	—
54-02028	160	160	0.068	—	—	—

Table 4.3-2 (continued)

Well	Port Depth (ft bgs)	Sampling Interval (ft length along borehole)	Static Pressure (kPa)			
			Annual	April 15	July 15	November 15
54-02028	200	200	0.086	—	—	—
54-02028	220	220	0.085	—	—	—
54-02028	250	250	0.076	—	—	—
54-02031	20	20	0.000	—	—	—
54-02031	60	60	0.041	—	—	—
54-02031	100	100	0.101	—	—	—
54-02031	160	160	0.106	—	—	—
54-02031	200	200	0.207	—	—	—
54-02031	220	220	0.145	—	—	—
54-02031	260	260	0.235	—	—	—
54-02034	20	20	-0.029	—	—	—
54-02034	60	60	-0.063	—	—	—
54-02034	100	100	-0.041	—	—	—
54-02034	160	160	0.210	—	—	—
54-02034	200	200	0.243	—	—	—
54-02034	220	220	0.247	—	—	—
54-02034	260	260	0.272	—	—	—
54-02034	300	300	0.318	—	—	—
54-02089	13	13	-0.017	-0.049	-0.107	0.106
54-02089	31	31	-0.015	-0.047	-0.107	0.102
54-02089	46	46	-0.024	-0.047	-0.121	0.117
54-02089	86	86	-0.044	-0.192	-0.291	0.314
54-24238	44	43–45	-0.020	-1.728	-0.150	0.017
54-24238	64	63–65	-0.024	-0.258	-0.278	0.293
54-24238	84	83–85	0.011	0.105	0.000	0.324
54-24239	25	24–26	-0.024	0.033	-1.509	0.023
54-24239	50	49–51	-0.029	0.047	0.010	0.146
54-24239	75	74–76	0.064	0.028	-0.029	0.015
54-24239	99.5	98.5–100.5	0.103	-0.233	-0.022	0.095
54-24240	28	27–29	0.000	-0.244	-0.227	-0.208
54-24240	53	52–54	-0.013	-0.897	-0.838	-0.846
54-24240	78	77–79	-0.060	-2.053	-1.983	-1.946
54-24240	103	102–104	-0.116	-1.652	-1.488	-1.405
54-24240	128	127–129	-0.143	-1.187	-0.988	-0.883
54-24240	153	152–154	-0.167	-0.654	-0.435	-0.300
54-24241	73	71–74	-0.127	-0.802	-0.394	NS-RS
54-24241	93	92–94	-0.150	-1.035	-0.565	NS-RS

Table 4.3-2 (continued)

Well	Port Depth (ft bgs)	Sampling Interval (ft length along borehole)	Static Pressure (kPa)			
			Annual	April 15	July 15	November 15
54-24241	113	112–114	-0.180	-1.283	-0.695	NS-RS
54-24241	133	132–134	-0.233	-1.320	-0.659	NS-RS
54-24241	153	152–154	-0.278	-1.409	-0.124	NS-RS
54-24241	173	172–174	-0.282	-1.398	-0.566	NS-RS
54-24241	193	192–194	-0.288	-1.292	-0.585	NS-RS
54-24242	25	24–26	-0.048	—	—	—
54-24242	50	49–51	-0.203	—	—	—
54-24242	75	74–76	-0.112	—	—	—
54-24242	100	99–101	-0.053	—	—	—
54-24242	110.5	109.5–111.5	-0.213	—	—	—
54-24243	25	24–26	0.073	-0.115	-0.129	0.146
54-24243	50	49–51	0.075	-0.145	-0.180	0.139
54-24243	75	74–76	0.109	-0.330	-0.395	0.240
54-24243	100	99–101	0.176	-0.888	-0.961	-0.020
54-24243	125	124–126	0.179	-1.064	-1.253	1.017
54-24399[f]	561.5–565.5	561.5–565.5	n/a[g]	n/a	n/a	n/a
54-24399[f]	568–608	568–608	n/a	n/a	n/a	n/a
54-24399[f]	568–569	568–569	n/a	n/a	n/a	n/a
54-27641	32	29.5–34.5	-0.035	-0.283	-0.300	NS-RS
54-27641	82	79.5–84.5	-0.059	-3.844	-3.919	-3.805
54-27641	115	112.5–117.5	-0.169	-1.169	-1.319	-0.966
54-27641	182	179.5–184.5	-0.178	-0.067	-0.420	-0.053
54-27641	232	229.5–234.5	-0.164	0.053	-0.320	NS-RS
54-27641	271	268.5–273.5	-0.164	0.141	-0.227	-0.257
54-27641	332.5	330–335	-0.175	0.151	-0.195	-0.277
54-27642	30	27.5–32.5	-0.028	-0.094	-0.050	0.066
54-27642	75	71.5–76.5	-0.035	-0.667	-0.264	0.300
54-27642	116	114.5–119.5	0.000	-0.761	-0.480	NS-RS
54-27642	175	172.5–177.5	0.049	-0.985	-0.285	0.191
54-27642	235	232.5–237.5	0.038	-0.793	-0.154	0.701
54-27642	275	272.5–277.5	0.000	-0.722	-0.236	0.485
54-27642	338	335.5–340.5	-0.028	-0.526	-0.088	NS-RS
54-27643	30	27.5–32.5	0.018	—	—	—
54-27643	74	71.5–76.5	0.050	—	—	—
54-27643	117	114.5–119.5	0.129	—	—	—
54-27643	167	164.5–169.5	0.251	—	—	—
54-27643	235	232.5–237.5	0.279	—	—	—

Table 4.3-2 (continued)

Well	Port Depth (ft bgs)	Sampling Interval (ft length along borehole)	Static Pressure (kPa)			
			Annual	April 15	July 15	November 15
54-27643	275	272.5–277.5	0.276	—	—	—
54-27643	354	351.5–356.5	0.133	—	—	—
54-610786[h]	25	22.5–27.5	0.000	—	—	—
54-610786[h]	50	47.5–52.5	0.000	—	—	—
54-610786[h]	75	72.5–77.5	-0.020	—	—	—
54-610786[h]	100	97.5–102.5	-0.044	—	—	—
54-610786[h]	118.5	116–121	-0.053	—	—	—

[a] Vapor-monitoring borehole angled. Port depth is depth below ground surface. Port-depth interval is length along borehole.

[b] — = Not measured as part of quarterly sampling.

[c] NS-RS = Not sampled because of radiological concerns.

[d] NS-B = Not sampled because port blocked.

[e] NS = Not sampled because previous rounds port blocked or partially blocked.

[f] Open borehole below 565.5 ft bgs.

[g] n/a = Not applicable for packer system.

[h] Drilled in December 2009.

Table 5.6-1
Distances from Example Observation Points to SVE-East and Sudden Drum Failure Location

Well	Distance from SVE-East	Distance from Sudden Release
54-27642	41.9 m (138 ft)	14.2 m (47 ft)
54-24238	29.7 m (98 ft)	7.7 m (25 ft)
54-24241	24.5 m (80 ft)	36.6 m (120 ft)

Appendix A

Spreadsheet Containing Dwyer Orifice Plate Calculations
(on CD included with this document)

Appendix B

Analytical Suites and Results
(on CD included with this document)

Appendix C

Example Calculations for Effluent Mass Removal

This appendix explains calculations of the total mass of volatile organic compounds (VOCs) being removed in the soil-vapor extraction (SVE) effluent. The numbers presented below are not exact measurements, but they are representative of the data collected during SVE operation at Material Disposal Area L, Technical Area 54, at Los Alamos National Laboratory. The example calculations are a simplified description of several Excel macros that combine both flow and concentration data to create graphs of mass removal versus time.

C-1.0 INITIALIZATION OF THE CALCULATION

For both SVE-East and SVE-West, one data point was added and set 1 min before start time and with flow "0." The concentration at the 1 min before start time is assumed to be equal to the first measured concentration.

C-2.0 GENERATING FLOW RATE VERSUS TIME

Air-flow data, in standard cubic feet per minute (scfm), from both SVE-East and SVE-West are loaded into a spreadsheet. Next, data on flow are numerically integrated over discrete time intervals using the trapezoid method to create volumes associated with each time interval (in m^3). Example air-flow data for SVE-West is included in Table C-2.0-1.

Table C-2.0-1
SVE-West Example Air-Flow Data

Time	1/9/2015 12:55	1/9/2015 12:56	1/16/2015 8:58	1/26/2015 9:08	2/25/2015 12:42	2/28/2015 12:42
Flow (scfm)	0	99.9	98.3	101	99.8	99.9

The partial volume pumped for each time interval is calculated using the following formula:

Partial volume = (flow1 + flow2)/2 * time difference * 0.0283168 m^3/ft^3,

where 0.0283168 is a recalculation factor from standard cubic feet to m^3.

For the first data point, this leads to the expression,

Partial volume = (0+99.9)/2 * (1/9/2015 12:56:00 PM - 1/9/2015 12:55:00 PM) * 0.0283168

Partial volume = 45.95 cfm * 1 min = 1.41 m^3 (for time 1/9/2015 12:56:00 PM).

This calculation is repeated for all five pairs of data in Table C-2.0-1 and leads to the values in Table C-2.0-2 (values are rounded to whole numbers).

Table C-2.0-2
SVE-West, Volumes Pumped for Discrete Time Intervals

Time	1/9/2015 12:55	1/9/2015 12:56	1/16/2015 8:58	1/26/2015 9:08	2/25/2015 12:42	2/28/2015 12:42
Flow	0	99.9	98.3	101	99.8	99.9
(Flow1+flow2)/2 (scfm)		50	99	100	100	100
Time difference		1	9842	14,410	43,414	4320
Partial volume (m³)		**1**	**27,619**	**40,662**	**123,426**	**12,215**

Total volume pumped is calculated by adding partial volumes:

- For 1/9/2015 12:56:00 PM: total volume = 1
- For 1/16/2015 8:58:00 AM: total volume = 1 + 27,619 = 27,620
- For 1/26/2015 9:08 AM: total volume = 1 + 27,619 + 40,662 = 27,620 + 40,662 = 68,282 and so on.

The results of the calculated total volume pumped at discrete times is included in Table C-2.0-3.

Table C-2.0-3
SVE-West, Integrated Total Volume Pumped at Discrete Times

Time	1/9/2015 12:55	1/9/2015 12:56	1/16/2015 8:58	1/26/2015 9:08	2/25/2015 12:42	2/28/2015 12:42
Flow	0	99.9	98.3	101	99.8	99.9
(Flow1+flow2)/2 (scfm)		50	99	100	100	100
Time difference		1	9842	14,410	43,414	4320
Partial volume (m³)		1	27,619	40,662	123,426	12,215
Total volume (m³)		**1**	**27,620**	**68,282**	**191,708**	**203,923**

C-3.0 INTERPOLATING CONCENTRATION VERSUS TIME TO THE FLOW DATA

To obtain total mass on the compound 1,1,1-trichloroethane (1,1,1-TCA) in this example, the concentration data versus time have to be interpolated to the total volume scale because concentration data were not collected at every flow rate measurement. Concentrations at discrete times for SVE-West are included in Table C-3.0-1.

Table C-3.0-1
SVE-West, Effluent Concentration at Discrete Times

Time	1/9/2015 12:55	1/9/2015 14:24	1/16/2015 9:04	1/26/2015 9:19	2/25/2015 12:46
Concentration (µg/m³)	479,833	479,833	261,727	141,769	87,242.3

The volume pumped at the start,1 min, is equal to 0. For the next data point (at 1/9/2015 14:24), linear interpolation is used.

To use linear interpolation, two points were selected from Table C-2.0-3, one immediately before and one immediately after the interpolation point. For the interpolated point at 1/9/2015 14:24, these points are 1/9/2015 12:56 and 1/16/2015 8:58. Initially, the equation of the line passing through these points is calculated: y = ax + b. At the end of interpolation step, the equation of this line and the time value for interpolated point to find the interpolated total volume are used.

If time is marked as “x” and total volume as “y,” the equations are

a = (y2-y1)/(x2-x1),

b = y1-a*x1,

and finally

$y_c = a*x_c+b$.

For the example listed above,

a = (27620-1)/(1/16/2015 8:58:00 AM–1/9/2015 12:56:00 PM) = 4040.98

b = 1-4040.98*(1/9/2015 12:56:00 PM) = −169776018.10

y_c = 4040.98*(1/9/2015 2:24:00 PM)−169776018.10 = 248

Note: In the explanation above, dates as values of x are used. Within Excel, “date values” are used to remove any problems with incorporating dates into equations. Calculations explained above are repeated for three more points from Table C-3.0-1, and the results are included in Table C-3.0-2.

Table C-3.0-2
SVE-West, Effluent Concentration at Discrete Times

Time	1/9/2015 12:55	1/9/2015 14:24	1/16/2015 9:04	1/26/2015 9:19	2/25/2015 12:46
Concentration (µg/m^3)	479,833	479,833	261,727	141,769	87,242.3
Total volume pumped (m^3)	0	248	27,637	68,313	191,719

Table C-3.0-3 presents values of the linear coefficients used in the interpolation for each point in Table C-3.0-2.

Table C-3.0-3
SVE-West Flow Volume Integration

Time	1/9/2015 12:55	1/9/2015 12:56	1/16/2015 8:58	1/26/2015 9:08	2/25/2015 12:42	2/28/2015 12:42
Flow (scfm)	0	99.9	98.3	101	99.8	99.9
(Flow1+flow2)/2 (scfm)		50	99	100	100	100
Time difference		1	9842	14,410	43,414	4320
Partial volume (m^3)		1	27,619	40,662	123,426	12,215
Total volume (m^3)		1	27,620	68,282	191,708	203,923
		a	4040.98354	4063.37821	4093.919934	4071.666667
		b	-169,776,018.10	-1,707,17,050.49	-172,000,730.78	-171,064,746.59

C-4.0 CALCULATION OF MASS REMOVAL SVE-WEST

Data from Table C-3.0-2 may be numerically integrated leading to the total mass of 1,1,1-TCA contained in the effluent stream removed from SVE-West as a function of time mapped to discrete points in time.

Partial mass removed = (concentration1+concentration2)/2*(volume2 − volume1)*1e-9 * 2.20462, where 1e-9 is recalculation factor from µg to kg, and '2.20462" is recalculation factor from kg to lb.

Total mass removed is integrated numerically as the sum of the partial masses.

For time "1/9/2015 2:24:00 PM," the partial mass removed = (479,833 + 479,833)/2*(248-0)*1e-9*2.20462 = 0.3 lb.

Results of the volume-concentration time alignment and mass removal integration for SVE-West are presented in Table C-4.0-1.

Table C-4.0-1
SVE-West, Volume-Concentration Integration of 1,1,1-TCA Mass Removal

Time	1/9/2015 12:55	1/9/2015 14:24	1/16/2015 9:04	1/26/2015 9:19	2/25/2015 12:46
Concentration (µg/m^3)	479,833	479,833	261,727	141,769	87,242.3
Total volume pumped (m^3)	0	248	27,637	68,313	191,719
Partial mass removed (lb)	0	0.3	22.4	18.1	31.2
Total mass removed (lb)	0	0.3	22.7	40.8	72

C-5.0 CALCULATION OF MASS REMOVAL SVE-EAST

The same calculation pattern is used to calculate mass numbers for the SVE-East unit. The results are presented in Tables C-5.0-1 and C-5.0-2.

Table C-5.0-1
SVE-East Flow Interpolation Coefficients

Time	1/26/2015 10:20	1/26/2015 10:21	1/27/2015 11:17	2/25/2015 13:18	2/28/2015 13:42
Flow	0	99.5	98.6	98.5	99.1
(Flow1+flow2)/2		50	99	99	99
Time difference		1	1496	41,881	4344
Partial volume (m^3)		1	4196	116,874	12,153
Total volume (m^3)		1	4197	121,071	133,224
		a	4038.930481	4018.494305	4028.618785
		b	-169,757,988.92	-168,899,026.40	-169,324,867.60

Table C-5.0-2
SVE-East Volume-Concentration Integration of 1,1,1-TCA Mass Removal

Time	1/26/2015 10:20	1/26/2015 11:12	1/27/2015 12:27	2/25/2015 13:20
Concentration (µg/m³)	348,969	348,969	370,780	223,558
Total volume pumped (m³)	0	144	4392	121,077
Partial mass removed (lb)	0	0.1	3.4	76.4
Total mass removed (lb)	0	0.1	3.5	79.9

C-6.0 CALCULATION OF COMBINED SVE-WEST PLUS SVE-EAST MASS REMOVAL

To calculate the total amount of 1,1,1-TCA removed, SVE-West and SVE-East numbers have to be added. Again, interpolation and data alignment are necessary because there are no total mass removed data at the same times for SVE-West and SVE-East.

The SVE-West unit was always sampled and recorded first, so the dates from the SVE-West unit are used as interpolation dates. For each interpolation date, two time points from SVE-East are used, one immediately before (1/27/2015 12:27) and one immediately after (2/25/2015 13:20). Using the interpolation formulas from section 3.0, the following is derived:

a = (79.9-3.5)/(2/25/2015 13:20-1/27/2015 12:27) = 2.6311

b = 3.5-2.6311*(1/27/2015 12:27:00 PM) = -110587.45

Results for interpolation coefficients are listed in Table C-6.0-1.

Table C-6.0-1
Interpolation Coefficients for the Combined Mass Removal

Time	1/26/2015 10:20	1/26/2015 11:12	1/27/2015 12:27	2/25/2015 13:20
Concentration (µg/m³)	348,969	348,969	370,780	223,558
Total volume pumped (m³)	0	144	4392	121,077
Partial mass removed (lb)	0	0.1	3.4	76.4
Total mass removed (lb)	0	0.1	3.5	79.9
	a	2.769230769	3.231683168	2.631143424
	b	-116,391.96	-135,829.05	-110,587.45

When Tables C-4.0-1 and C-6.0-1 are compared, the only date from Table C-4.0-1 when both units, West and East, were operational is 2/25/2015 12:46:00 PM. The amount of 1,1,1-TCA SVE-East removed at 2/25/2015 12:46:00 PM can be calculated using this date and “a” and “b” coefficients from Table C-6.0-1.

yc = a*(2/25/2015 12:46:00 PM)+b = 2.631143424*(2/25/2015 12:46:00 PM)-110587.45 = 79.8 lb

By adding SVE-West and SVE-East (East after interpolation), the total amount of the 1,1,1-TCA removed by both units is (72 +79.8 = 151.8). Table C-6.0-2 presents the combined total mass of 1,1,1-TCA removed by both units.

Table C-6.0-2
Integration of Combined Mass Removal

Time	1/9/2015 12:55	1/9/2015 14:24	1/16/2015 9:04	1/26/2015 9:19	2/25/2015 12:46
Concentration (µg/m^3)	479,833	479,833	261,727	141,769	87,242.3
Total volume pumped (m^3)	0	248	27,637	68,313	191,719
Partial mass removed (lb)	0	0.3	22.4	18.1	31.2
Total mass removed West (lb)	0	0.3	22.7	40.8	72
Total mass removed East (lb)*	0	0	0	0	79.8
East + West (lb)	0	0.3	22.7	40.8	151.8

* The first four columns for the East unit list “0” because SVE-East was not operational on 1/9/2015.

The flow data were integrated each time new SUMMA data were obtained. The calculation pattern for concentrations, as described above, is repeated for each detected analyte. (The analyte does not have to be detected in all SUMMA samples; single detection will trigger the calculations described above.) The total “East+West lb” values were added together to obtain total value of VOC removed.

Appendix D

Video Log of Borehole 54-24399
(on DVD included with this document)
(Note that the depths indicated in the video are inaccurate because of cable stretch)

Appendix E

Flow Rate Data for SVE-West and SVE-East
(on CD included with this document)

Appendix F

Modeling Details

F-1.0 INTRODUCTION

This appendix summarizes the development of the three-dimensional (3-D) site-specific flow and transport model for Material Disposal Area (MDA) L. Details on parameters used in the simulations can be found in the references contained in this appendix.

F-2.0 DATA ANALYSIS THROUGH SIMULATION

To form a more complete picture of processes affecting transport of volatile organic compounds (VOCs) to the groundwater at Area L, results have been compiled from a group of studies that combine site data with numerical models, each providing clues to vapor transport beneath Area L (Neeper 2002, 098639; Stauffer et al. 2005, 090537; LANL 2006, 094152; Anderson et al. 2007, 702070; Stauffer et al. 2007, 104950; Vrugt et al. 2008, 104951; LANL 2011, 205756; Stauffer et al. 2011, 255584; Neeper and Stauffer 2012, 601587; Snyder et al. 2017, 702064; Stauffer et al. 2017, 602792; N3B 2018, 700039; Behar et al. 2019, 700854; Stauffer et al. 2019, 700871; Stauffer et al. 2022, 702065). By combining inferences from results of all of these studies, more robust conclusions can be drawn than would be possible based on any single study.

F-2.1 Numerical Simulation Tool

The Finite Element Heat and Mass (FEHM) code is used for all simulation-based analysis of the Area L plume (Zyvoloski et al. 1994, 054420; Dash et al. 2015, 702067; Zyvoloski et al. 2015, 702066) (https://fehm.lanl.gov/) in conjunction with results from a deep basalt tracer test (Stauffer et al. 2017, 602792; Stauffer et al. 2019, 700871). FEHM, developed at Los Alamos National Laboratory (LANL), has been used successfully to simulate barometrically-pumped contaminant transport in fractured rock (Neeper and Stauffer 2012, 601587; Stauffer et al. 2017, 602792; Bourret et al. 2019, 702060; Harp et al. 2019, 702068; Stauffer et al. 2019, 700871). FEHM simulates gas advection coupled to tracer transport using a standard form of the advection-dispersion equation (Zyvoloski et al. 1994, 054420; Johnson et al. 2019, 702061; Johnson et al. 2019, 702062). FEHM has been extensively validated against analytical solutions for a wide variety of multiphase flow and transport problems (Dash et al. 2015, 702067).

The current MDA L soil-vapor extraction (SVE) model assumes no flow of liquid water during the period of the simulations. This assumption is based on very low infiltration fluxes inferred on the dry mesas of the Pajarito Plateau. Water in the porous formations is included to allow Henry's Law partitioning of VOC into the pore water; however, the relative permeability of the water is set to a very low value to ensure no flow of liquid water. All calcuations are isothermal.

The top boundary of the model is assigned an average barometric pressure and a fixed concentration of zero VOC to represent the infinite sink of the atmosphere. This boundary allows air to flow into the domain as simulated suction on the extraction holes drops the presssure in the subsurface. The bottom and side boundaries below the atmosphere are no-flow with respect to gas and water. The SVE suction is simulated by fixing the measured pressure at the top of the extraction borehole and allowing the fixed suction to propagate to depth in an open borehole, with a very high permeability set to approximate the pressure drop calculated for pipe flow. The rocks in the model are single porosity, with the basalt simulated as having a very low porosity and high permeability. Calibration was done to estimate permeability as described in Vrugt et al., 2008 (104951). In 2015 the east side was manually recalibrated to better match data from the 2015 SVE testing. Permeability is annotated in the input decks presented at the end of this appendix.

For the basalt tracer simulations, both rubble and massive basalt are included based on video logs and drilling logs.

F-2.2 1975-2000 Plume Growth

The initial work on understanding processes at Area L involved calibrating plume growth from 1975 through 2000 (Stauffer et al. 2005, 090537). This work used a 3-D mesh with dimensions of 411 m (1348 ft) long in the east-west direction by 290 m (951 ft) wide in the north-south direction (Figure F-1). From the land surface, units of the Bandelier tuff (Qbt 2 down to the Guaje Pumice) overlay the Cerros del Rio Basalt. The computational mesh extends well beyond the edge of the VOC plume to reduce the impact of boundaries on the simulation results. The mesh has 25,456 nodes and extends vertically from the ground surface to the water table (Stauffer et al. 2005, 090537). The mesh resolution is 15 m (49 ft) horizontally and 1 to 25 m (3 to 82 ft) vertically.

This study found that higher initial leakage from the source regions was required to push the plume to depth, followed by a period of lower leakage where concentrations in the source remained in the range of nearly 3000 ppmv. Under non-pumping conditions, the simulations show that plume size is primarily controlled by diffusion away from the two shaft fields, with the atmosphere and pore water acting as sinks. This work highlighted the need to include (1) the asphalt barrier on the surface of Area L, (2) a zero-concentration atmospheric boundary following the topography of the mesa, (3) diffusion as a function of water content and porosity, and (4) partitioning of VOC into the liquid phase.

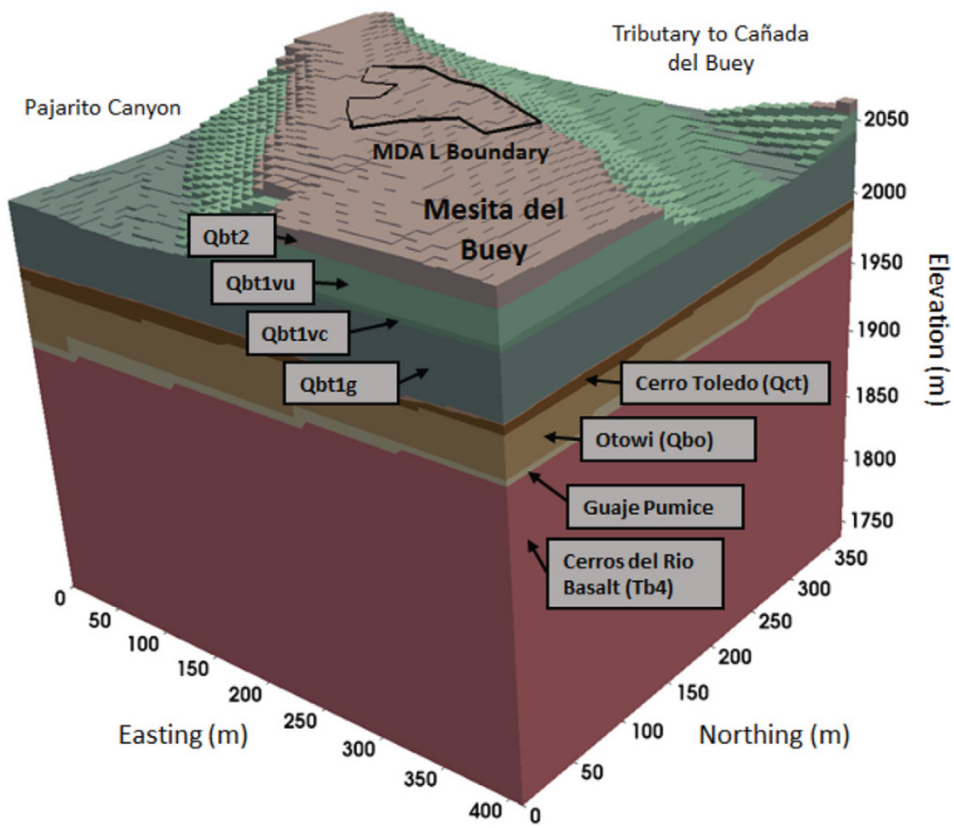

Figure F-1 Computational domain including topography and geologic units (Stauffer et al. 2017, 602792)

F-2.3 2006 SVE Pilot Test and 2007 Modeling

In 2006, DOE undertook a pilot SVE test at Area L (LANL 2006, 094152; Anderson et al. 2007, 702070). This test used two SVE boreholes, one located near the east source area (SVE-East) and the other near the west source area (SVE-West). The 0.2 m (8 in.) boreholes were auger-drilled to 61 m (200 ft) and cased to 18 m (60 ft), with the remaining 43 m (140 ft) of the borehole open (no casing) to pull gas from within the mesa. Two industrial vacuum units pulled 170 standard cubic meters per hour during the SVE testing for a period of 45 days. The test removed over 350 kg of VOC mass from the mesa.

A new, high-resolution 3-D computational mesh of the site was created in a 2007 modeling study, with 10 m (33 ft) lateral spacing and 1 m (3 ft) vertical spacing to greater depth, such that the final mesh has 140,000 nodes. The new computational mesh includes two high-resolution extraction boreholes. This mesh was used to determine the permeability structure of the subsurface under vacuum conditions and to provide data for SVE system designs included in a Corrective Measures Evaluation (CME) report (Stauffer et al. 2007, 104950; Vrugt et al. 2008, 104951).

Results from the numerical analysis showed that the radius of influence of the SVE system was a minimum of 38 m (125 ft) in the more permeable units, and that, in the absence of significant new leakage, operation of the SVE for a few months every few years would maintain low concentrations in the source regions. Further, analysis of significant leakage, simulated by sudden release of up to ten 200-L (53 gal.) drums, showed that such a release could be detected in the semiannual vapor sample collection in the current monitoring boreholes located near the source regions, which would give ample warning to activate the SVE system.

F-2.4 2011 MDA L Corrective Measures Evaluation update

The last model update before the current SVE interim measure was performed in 2011 for the MDA L CME (LANL 2011, 205756). During this update, lower leakage rates were found to fit the plume growth following the 2006 SVE Pilot test through 2011.

F-2.5 2015 Interim Measure SVE

In 2015, DOE implemented an Interim Measure (IM) SVE at Area L (LANL 2014, 261843; LANL 2015, 600930).

Subsurface parameters and methods developed from previous studies were used to analyze the IM data using the FEHM simulation framework (Stauffer et al. 2005, 090537; Anderson et al. 2007, 702070; Stauffer et al. 2007, 104950; Vrugt et al. 2008, 104951; LANL 2011, 205756; Stauffer et al. 2011, 255584; Neeper and Stauffer 2012, 601587). This generated a pre-IM vapor plume at MDA L that matches the pre-SVE vapor concentrations of the major plume constituent, 1,1,1-trichloroethane (TCA), in the subsurface.

The simulations of the 2015 SVE IM were able to capture the mass removal from both the SVE-East and SVE-West boreholes, while maintaining the observed suction at the top of the extraction wellbores (N3B 2018, 700039). Further, simulated concentrations at monitoring boreholes were in good agreement with the concentrations measured in field sample collection. Finally, simulated rebound also matched the observed rebound. These results provide confidence that the simulations are capturing the major physical processes in the subsurface at Area L.

The MDA L site model, calibrated to the 2015 SVE IM data, was then used to explore hypothetical scenarios of future drum failure (Behar et al. 2019, 700854). Prior to implementation of Resource

Conservation and Recovery Act (RCRA) regulations in 1982-1983, waste drums were not required to contain absorbent material, so the shafts may contain full drums of liquid solvents (Anderson et al. 2007, 702070). Failure of waste drums could release significant quantities of VOCs, leading to deep penetration of the plume and a future threat to groundwater. An analysis of waste drum corrosion based on data from a nearby dry mesa site suggests that the Area L drums will develop pinhole leaks through time, with a mean failure period on the order of 55 yr after burial, with all drums failing by 85 yr (Behar et al. 2019, 700854). The shape of the calculated Poisson failure distribution suggests that drum failure due to corrosion is likely to increase in the next 10 yr.

The simulations used conservative, worst-case assumptions in which drum failure is assumed to happen instantaneously and that each failed drum releases 200 L of pure TCA (264 kg = 582 lb) into the mesa. The simulated hypothetical release of 1, 5, and 10 drums occurs over a depth of 12 to 24 m, with source concentrations fixed at the saturated vapor pressure of TCA (160,000 ppmv). The fixed source concentration rapidly pushes mass into the mesa and requires 1, 159, and 482 days, respectively, to reach 1, 5, and 10 drums equivalent mass of TCA (Stauffer et al. 2017, 602792). The resulting plume was then allowed to migrate under diffusive transport. Impacts of SVE at different times after drum failure were simulated, and the simulated concentrations in nearby sentry boreholes were monitored. Sections 4.0 and 5.0 of this appendix include annotated input decks for one of the drum failure scenarios, including parameters used across the IM simulations.

F-2.6 2016 Deep Basalt Tracer Test

In 2016, DOE performed a tracer test in a deep vertical borehole located near the middle of Area L on the edge of the eastern source area (LANL 2015, 600930; Stauffer et al. 2019, 700871), designed to test the hypothesis that observed pressure variations in the basalt are caused by rapid airflow through fracture connections to the atmosphere (LANL 2006, 094152). The deep borehole (54-24399) is cased from the surface to 173 m (567 ft) and is open (uncased) from this depth to a total depth of 201 m (660 ft). The uncased interval lies completely within the basalt, approximately 80 m (262 ft) below the Bandelier tuff and approximately 91 m (300 ft) above the regional aquifer. Recent measurements of VOC gas concentrations in this interval have been below New Mexico Environment Department groundwater protection screening levels. This is important because measured concentrations in the deep basalt would have to rise above screening levels before any risk to groundwater could develop.

Sulfur hexafluoride (SF_6) tracer was injected into the top of the uncased open interval and concentrations at the upper sampling port were monitored after the injection. As predicted from simulations done before the tracer test, concentrations at the release location first dropped, then quickly rebounded. This cycle was repeated as atmospheric pressure variations moved the tracer back and forth across the monitoring point. Fracture and rubble zone permeability in the basalt were based on previous experiments and observations (LANL 2016, 601622), and the simulations were driven by measured atmospheric pressure at a far-field boundary (outcrop). The data from the test were used to better constrain outcrop distance, using the measured pressure variations within the uncased section of the deep borehole.

Results from the tracer test showed that barometric pumping at an outcrop located approximately 1 km (0.6 mi) from the test location could account for the observed pressure response in the borehole. Further, the data from the SF_6 tracer test were well fit by the simulated response to variations in barometric pressure pushing the initial tracer spike back and forth across the sample location. Estimates of instantaneous velocity in the basalt, assuming a fracture width of 1 mm, reached as high as 1000 m/day (0.6 mi per day) for brief intervals. Such high rates of gas transport will cause dispersion, spreading gas 10–100× faster than diffusion alone. The breathing basalt represents a new conceptual model for transport at this site and helps explain the seemingly contradictory observations of low VOC concentrations measured in the basalt (< 1× Tier I) at the same time that high VOC concentrations

(>100× Tier 1) are measured at the base of the Bandelier tuff (Stauffer et al. 2005, 090537; Behar et al. 2019, 700854; Stauffer et al. 2019, 700871).

F-3.0 EXAMPLE INPUT DECK FOR FEHM, PRE-SVE 3 YEAR RUN

This input deck is for the 5-drum failure scenario and includes calibrated permeability and diffusion coefficients for the various rock layers at MDA L. Notes are added in red text.

```
-24 0 0        2
 -23 0 0        2
 -14 0 0        2 title: Area L
text
Run 5 drum failure

airwater                      isothermal simulation with air and water, no water vapor simulated
2
 15 0.08
zonn
file
/scratch/er/stauffer/L/Grid/tetv7_material_kay.zone
zonn
file
/scratch/er/stauffer/L/Grid/Split_East_perm.zone
#  7 = Basalt; 10 = Guaje Pumice;
#  11=Otowi; 12=Cerro Toledo;13=Qbtt
#  14=Tsh-1g;  23=Tsh-1vc; 24=1vu; 16=Tsh2;
#         East side add 50 (66 is Tsh2 East)      Permeability on East and West are independently
calibrated
#
#  West side is first in the well model 142708 - 143042
#  East side is next                    143043 - 143377
well                                    Wellbores are embedded 2D radial with sub meter resolution
wellmodel
2 1
1 4  67  0
1     127. 246.  2070. 0.08 0.  0.  2.
-67   127. 246.  2004. 0.08 0.  0.  2.

2 4  67  0
1     213. 182.  2071. 0.08 0.  0.  2.
-67   213. 182.  2005. 0.08 0.  0.  2.

wellend

perm
1     0 0     1.75E-13  1.75E-13  1.75E-13
-66   0 0     1.00E-13 1.00E-13  1.00E-13
-74   0 0     1.00E-13 1.00E-13  1.00E-13
-73   0 0     1.28E-11 1.28E-11  1.28E-11
-64   0 0     1.00E-13 1.00E-13  1.00E-13
-62   0 0     1.00E-13 1.00E-13  1.00E-13
-63   0 0     1.00E-13 1.00E-13  1.00E-13
```

```
-61   0 0     1.00E-13 1.00E-13  1.00E-13   _______ Here and above are East Side permeabilities
-16   0 0      7.83E-13  7.83E-13  5.53E-13
-24   0 0      7.22E-12  7.22E-12  2.41E-12
-23   0 0      1.23E-13  1.23E-13  6.89E-13
-14   0 0      1.21E-13  1.21E-13  6.18E-13                    West side perms
-12   0 0      6.03E-13  6.03E-13  6.03E-13
-13   0 0      6.03E-13  6.03E-13  6.03E-13
-11   0 0      1.81E-13  1.81E-13  1.81E-13
142709 142814 5   5.e-19     5.e-19      5.e-19               Well casing is basically impermeable
143044 143149 5   5.e-19     5.e-19      5.e-19
142713 142883 5   1.00e-04   1.00e-04    1.00e-04               Wellbores have almost no resistance
143048 143338 5   1.00e-04   1.00e-04    1.00e-04
142708 142708 1   5.e-19     5.e-19      5.e-19               Well tops are plugged to stop inflow
143043 143043 1   5.e-19     5.e-19      5.e-19

# - 2035 and below in West hole is cement (142883)  116 ft open hole cased to 68.0 ft 142814
# - 2011 and below in East hole is cement (143338)  196.5 ft open hole cased to 68.5 ft 143149
rlp
  2   0.0  0.0  0.0  0.0
 -1   0.0  1.0  1.e-5 0.001

     1      0 0     2
  143708 143377 5     2
  0
rock                                      Final column are the porosities of the rock units
   1 0  0   1400.   1000.   1.00
 -66 0  0   1400.   1000.   0.41
 -74 0  0   1400.   1000.   0.49
 -73 0  0   1400.   1000.   0.49
 -64 0  0   1400.   1000.   0.46
 -63 0  0   1400.   1000.   0.45
 -62 0  0   1400.   1000.   0.45
 -61 0  0   1400.   1000.   0.44
 -60 0  0   1400.   1000.   0.44
 -57 0  0   1800.   1200.   0.1
 -16 0  0   1400.   1000.   0.41
 -24 0  0   1400.   1000.   0.49
 -23 0  0   1400.   1000.   0.49
 -14 0  0   1400.   1000.   0.46
 -13 0  0   1400.   1000.   0.45
 -12 0  0   1400.   1000.   0.45
 -11 0  0   1400.   1000.   0.44
 -10 0  0   1400.   1000.   0.44
 -7  0  0   1800.   1200.   0.1

pres
   1  0  0  0.08   0.05    2
  0
#  Top=6  Bottom=5
zonn
file
/scratch/er/stauffer/L/Grid/tetv7_material_kay.zone
```

```
zonn
file
/scratch/er/stauffer/L/Grid/tetv7_True_TOP_bottom.zone
#-------------------------------------------------------
#  East flow is -2001  node:143048    0.05775 kg/s
#  West flow is -1001  node:142713    0.05775 kg/s
#  -2001  0 0  0.05387  -1   1e5
#  -1001  0 0  0.06208  -1   1e5
perm
142708 142708 1   1.e-19    1.e-19    1.e-19
143043 143043 1   1.e-19    1.e-19    1.e-19

flow
  129905 129905 1  -5.e-13 0.0 0
  129934 129934 1  -5.e-13 0.0 0
  132566 132566 1  -5.e-13 0.0 0
  132594 132594 1  -5.e-13 0.0 0          VERY Small flow rates are applied in the leaking source
  139038 139038 1  -5.e-13 0.0 0          to mimic the rate of release in the diffusion only simulations
  139061 139061 1  -5.e-13 0.0 0          This needs to be done to prevent large leakage
  130136 130136 1  -5.e-13 0.0 0
  130108 130108 1  -5.e-13 0.0 0
  132787 132787 1  -5.e-13 0.0 0
  132760 132760 1  -5.e-13 0.0 0
  139220 139220 1  -5.e-13 0.0 0
  139195 139195 1  -5.e-13 0.0 0
  142708 142708 1  0.80016E-01 -1  1.e7
  143043 143043 1  0.80006E-01 -1  1.e7
  0
flow              Atmospheric pressure is fixed along the land surface of the model
file
/scratch/er/stauffer/L/Grid/top_pres_grav.macro
#-------------------------------------------------------
time                              Simulation is restarted from 903 days and ends at 1998 days allowing
 1.   1998. 40000    1  1999  7    the drum failure to diffuse for 3 years with NO SVE
  10.   -1.4   1.  1   730.
  0 0 0 0
ctrl
 -3   1.e-06  40  100 gmres
 1  0 0     2
   0    0    0    0
 1.0   3  1.
 7   1.4  1.e-9  1.
 0    1
finv
iter
 1.e-3 1.e-3 1.e-3 -1.e-3 1.2
 0 0 0 0  19400.
sol
 +1   -1
Node                          These nodes are output to the out-file and his-files
 69
  125193        118839 111407 101341 91834   82258   72682
```

```
  135137         123130 105721 79028   48704   31148   21572
  131754         125196 119960
  136730         130804 123091 115221 104226
  132595
  130836
  128073
  125161
  122080
  16825          24805   37573   98219   107203 130867
  16822          26398   39166   98216   107200 131751
  16784          26360   37532   98178   107162 130837
  16740          26316   37488   98134   107118 131691
  129905
  129934
  132566
  132594
  139038
  139061
  130136
  130108
  132787
  132760
  139220
  139195
  142713 143048 142708 143043 142838 142014
#-----------------------------
hist
press
concentration
global
liquid
vapor
end
#-----------------------------
cont
tec 1000    3650.
liquid
pres
velocity
sat
temp
conc
vec
vapor
formatted
geom
xyz
endavs
#-------- set tracer stuff,
# Zone 1=Asphalt, 2=East Source,  4=West                Review of zone definitions
#  5=bottom , 6= top
#  7 = Basalt; 10 = Guaje Pumice;
```

```
#  11=Ottowi; 12=Cerro Toledo;13=Qbtt
#  14=Tsh-1g;  23=Tsh-1vc; 24=1vu; 16=Tsh2;
#          East side add 50 (66 is Tsh2 East)
zonn
file
/scratch/er/stauffer/L/Grid/areal_1985.zone
perm
  -1 0 0  1.35E-14  1.35E-14  1.35E-14
  -6 0 0  1.e-11 1.e-11 1.e-11

trac
 0  1  1.e-6  1.0
 0. 627375.  1.e8  1.e8
 50  1.4  1.   5.0  1
 1
-2
0  0 0 1  1.e-9  1.e-22 1.e-22 1.e-22     water diffusion and dispersion for model 1
0  0 0 1  3.e-6  1.e-19 1.e-19 1.e-19       gas diffusion and dispersion for model 1
0  0 0 1  1.e-9  1.e-22 1.e-22 1.e-22
0  0 0 1  2.e-6  1.e-19 1.e-19 1.e-19
0  0 0 1  1.e-9  1.e-22 1.e-22 1.e-22
0  0 0 1  1.e-6  1.e-19 1.e-19 1.e-19
0  0 0 1  1.e-9  1.e-22 1.e-22 1.e-22
0  0 0 1  5.e-7  1.e-19 1.e-19 1.e-19
0  0 0 1  1.e-9  1.e-22 1.e-22 1.e-22     water diffusion and dispersion for model 5
0  0 0 1  1.e-14 1.e-19 1.e-19 1.e-19      gas diffusion and dispersion for model 5

   1 0 0       1
 -66 0 0       1
 -74 0 0       2
 -73 0 0       2      Different diffusion coefficients are assigned to the different rock types
 -64 0 0       2      The number 2 here refers to the second line in the list directly above
 -63 0 0       4       with 3e-6 m2/s gas phase diffusion
 -62 0 0       4
 -61 0 0       4
 -60 0 0       4
 -57 0 0       1
 -16 0 0       1

 -13 0 0       4
 -12 0 0       4
 -11 0 0       4
 -10 0 0       4
  -7 0 0       1
  -1 0 0       5
  -6 0 0       3
 142709 142804 5 5
 143044 143139 5 5
 -1000 0 0      5

  1 62. 0.                        Henry’s partitioning for TCA
  1  0  0    1.e-19
```

```
 -6      0 0  -1.e-19        0.  390000.
  132595 132595 1  -5.52   902.0034  903.0034
  130836 130836 1  -5.52   902.0034  903.0034  High concentrations are fixed in the drum failure region
  128073 128073 1  -5.52   902.0034  903.0034    for one day to input the correct amount of mass
  125161 125161 1  -5.52   902.0034  903.0034      5 drums x 200 liters TCE per drum
  122080 122080 1  -5.52   902.0034  903.0034
  129905 129905 1 1.05E+05  0.   1.e6
  129934 129934 1 7.82E+04  0.   1.e6
  132566 132566 1 1.11E+05  0.   1.e6
  132594 132594 1 8.54E+04  0.   1.e6
  139038 139038 1 1.57E+05  0.   1.e6      Concentration in the very low flow coming into the leaking
  139061 139061 1 1.40E+05  0.   1.e6       shafts recreates the leakage rate of the diffusion only case
  130136 130136 1 1.19E+05  0.   1.e6
  130108 130108 1 9.44E+04  0.   1.e6
  132787 132787 1 1.01E+05  0.   1.e6
  132760 132760 1 8.03E+04  0.   1.e6
  139220 139220 1 1.75E+05  0.   1.e6
  139195 139195 1 1.64E+05  0.   1.e6
  139086 139086 1  2.50e4  0.   1.e6
  135164 135164 1  2.50e4  0.   1.e6
  130866 130866 1  2.50e4  0.   1.e6
  118841 118841 1  2.50e4  0.   1.e6
  0
stop
```

F-4.0 EXAMPLE INPUT DECK FOR FEHM, SVE EAST TURNED ON FOR 7 YEARS

This input deck is for the 5-drum failure scenario and includes calibrated permeability and diffusion coefficients for the various rock layers at MDA L. Notes are added in red text.

```
title: Area L
text
Run from Try63-2014 313 days of SVE from Jan26 2015  modified leakage

airwater
2
 15 0.08
zonn
file
/scratch/er/stauffer/L/Grid/tetv7_material_kay.zone
zonn
file
/scratch/er/stauffer/L/Grid/Split_East_perm.zone
#  7 = Basalt; 10 = Guaje Pumice;
#  11=Otowi; 12=Cerro Toledo;13=Qbtt
#  14=Tsh-1g;  23=Tsh-1vc; 24=1vu; 16=Tsh2;
#          East side add 50 (66 is Tsh2 East)
#
#  West side is first in the well model 142708 - 143042
#  East side is next                    143043 - 143377
well
```

```
wellmodel
2 1
1 4  67  0
1     127. 246.  2070. 0.08 0.  0.  2.
-67   127. 246.  2004. 0.08 0.  0.  2.

2 4  67  0
1     213. 182.  2071. 0.08 0.  0.  2.
-67   213. 182.  2005. 0.08 0.  0.  2.

wellend

perm
1     0 0      1.75E-13  1.75E-13  1.75E-13
-66   0 0      1.00E-13 1.00E-13  1.00E-13
-74   0 0      1.00E-13 1.00E-13  1.00E-13
-73   0 0      1.28E-11 1.28E-11  1.28E-11
-64   0 0      1.00E-13 1.00E-13  1.00E-13
-62   0 0      1.00E-13 1.00E-13  1.00E-13
-63   0 0      1.00E-13 1.00E-13  1.00E-13
-61   0 0      1.00E-13 1.00E-13  1.00E-13
-16   0 0       7.83E-13  7.83E-13  5.53E-13
-24   0 0       7.22E-12  7.22E-12  2.41E-12
-23   0 0       1.23E-13  1.23E-13  6.89E-13
-14   0 0       1.21E-13  1.21E-13  6.18E-13
-12   0 0       6.03E-13  6.03E-13  6.03E-13
-13   0 0       6.03E-13  6.03E-13  6.03E-13
-11   0 0       1.81E-13  1.81E-13  1.81E-13
142709 142814 5   5.e-19     5.e-19      5.e-19
143044 143149 5   5.e-19     5.e-19      5.e-19
142713 142883 5   1.00e-04   1.00e-04    1.00e-04
143048 143338 5   1.00e-04   1.00e-04    1.00e-04
142708 142708 1   5.e-19     5.e-19      5.e-19
143043 143043 1   5.e-19     5.e-19      5.e-19

# - 2035 m and below in West hole is cement (142883)  116 ft open hole cased to 68.0 ft 142814
# - 2011 m and below in East hole is cement (143338)  196.5 ft open hole cased to 68.5 ft 143149
rlp
  2   0.0  0.0  0.0  0.0
 -1   0.0  1.0  1.e-5 0.001

      1      0 0     2
  143708 143377 5     2
  0
rock
   1 0  0   1400.   1000.   1.00
 -66 0  0   1400.   1000.   0.41
 -74 0  0   1400.   1000.   0.49
 -73 0  0   1400.   1000.   0.49
 -64 0  0   1400.   1000.   0.46
 -63 0  0   1400.   1000.   0.45
 -62 0  0   1400.   1000.   0.45
```

```
 -61 0  0   1400.   1000.   0.44
 -60 0  0   1400.   1000.   0.44
 -57 0  0   1800.   1200.   0.1
 -16 0  0   1400.   1000.   0.41
 -24 0  0   1400.   1000.   0.49
 -23 0  0   1400.   1000.   0.49
 -14 0  0   1400.   1000.   0.46
 -13 0  0   1400.   1000.   0.45
 -12 0  0   1400.   1000.   0.45
 -11 0  0   1400.   1000.   0.44
 -10 0  0   1400.   1000.   0.44
 -7  0  0   1800.   1200.   0.1

pres
   1  0  0  0.08   0.05    2
  0
#  Top=6  Bottom=5
zonn
file
/scratch/er/stauffer/L/Grid/tetv7_material_kay.zone
zonn
file
/scratch/er/stauffer/L/Grid/tetv7_True_TOP_bottom.zone
#-------------------------------------------------------
#  East flow is -2001  node:143048     0.05775 kg/s
#  West flow is -1001  node:142713     0.05775 kg/s
#  -2001  0 0  0.05387  -1   1e5
#  -1001  0 0  0.06208  -1   1e5
perm
142708 142708 1   1.e-19     1.e-19     1.e-19

flow
   -2001  0 0  0.05387  -1   1e5
  129905 129905 1  -5.e-13 0.0 0
  129934 129934 1  -5.e-13 0.0 0
  132566 132566 1  -5.e-13 0.0 0
  132594 132594 1  -5.e-13 0.0 0
  139038 139038 1  -5.e-13 0.0 0
  139061 139061 1  -5.e-13 0.0 0
  130136 130136 1  -5.e-13 0.0 0
  130108 130108 1  -5.e-13 0.0 0
  132787 132787 1  -5.e-13 0.0 0
  132760 132760 1  -5.e-13 0.0 0
  139220 139220 1  -5.e-13 0.0 0
  139195 139195 1  -5.e-13 0.0 0
  142708 142708 1  0.80016E-01 -1  1.e7
  143043 143043 1  0.80006E-01 -1  1.e7
  0
flow
file
/scratch/er/stauffer/L/Grid/top_pres_grav.macro
#-------------------------------------------------------
```

FLOW at the SVE E wellhead is driven by fixed measured pressure of 0.05387 MPa

```
time
  1.   4900.  40000    1  1999  7
   10.   -1.4   1.  1   365.
   0 0 0 0
ctrl
  -3   1.e-06  40  100 gmres
  1  0 0     2
    0    0    0    0
  1.0   3  1.
  7   1.4  1.e-9  1.
  0    1
finv
iter
  1.e-3 1.e-3 1.e-3 -1.e-3 1.2
  0 0 0 0  19400.
sol
 +1   -1
node
 69
   125193          118839 111407 101341 91834   82258   72682
   135137          123130 105721 79028   48704   31148   21572
   131754          125196 119960
   136730          130804 123091 115221 104226
   132595
   130836
   128073
   125161
   122080
   16825           24805   37573   98219   107203 130867
   16822           26398   39166   98216   107200 131751
   16784           26360   37532   98178   107162 130837
   16740           26316   37488   98134   107118 131691
   129905
   129934
   132566
   132594
   139038
   139061
   130136
   130108
   132787
   132760
   139220
   139195
   142713 143048 142708 143043 142838 142014
#-----------------------------
hist
press
concentration
global
liquid
vapor
```

```
end
#-----------------------------
cont
tec 1000    365.
time
liquid
pres
velocity
sat
temp
conc
vec
vapor
formatted
geom
xyz
endavs
#-------- set tracer stuff,
# Zone 1=Asphalt, 2=East Source,  4=West
#  5=bottom , 6= top
#  7 = Basalt; 10 = Guaje Pumice;
#  11=Ottowi; 12=Cerro Toledo;13=Qbtt
#  14=Tsh-1g;  23=Tsh-1vc; 24=1vu; 16=Tsh2;
zonn
file
/scratch/er/stauffer/L/Grid/areal_1985.zone
perm
  -1 0 0  1.35E-14  1.35E-14  1.35E-14
  -6 0 0  1.e-11 1.e-11 1.e-11

trac
 0  1  1.e-6  1.0
 0. 627375.  1.e8  1.e8
 50  1.4  1.   5.0  1
 1
-2
0  0 0 1  1.e-9  1.e-22 1.e-22 1.e-22
0  0 0 1  3.e-6  1.e-19 1.e-19 1.e-19
0  0 0 1  1.e-9  1.e-22 1.e-22 1.e-22
0  0 0 1  2.e-6  1.e-19 1.e-19 1.e-19
0  0 0 1  1.e-9  1.e-22 1.e-22 1.e-22
0  0 0 1  1.e-6  1.e-19 1.e-19 1.e-19
0  0 0 1  1.e-9  1.e-22 1.e-22 1.e-22
0  0 0 1  5.e-7  1.e-19 1.e-19 1.e-19
0  0 0 1  1.e-9  1.e-22 1.e-22 1.e-22
0  0 0 1  1.e-14 1.e-19 1.e-19 1.e-19

   1 0 0        1
 -66 0 0        1
 -74 0 0        2
 -73 0 0        2
 -64 0 0        2
```

```
-63 0 0     4
-62 0 0     4
-61 0 0     4
-60 0 0     4
-57 0 0     1
-16 0 0     1
-24 0 0     2
-23 0 0     2
-14 0 0     2
-13 0 0     4
-12 0 0     4
-11 0 0     4
-10 0 0     4
 -7 0 0     1
 -1 0 0     5
 -6 0 0     3
142709 142804 5 5
143044 143139 5 5
-1000 0 0     5

 1 62. 0.
 1  0  0   1.e-19

-6     0 0  -1.e-19       0.  390000.
 129905 129905 1 1.05E+05  0.   1.e6
 129934 129934 1 7.82E+04  0.   1.e6
 132566 132566 1 1.11E+05  0.   1.e6
 132594 132594 1 8.54E+04  0.   1.e6
 139038 139038 1 1.57E+05  0.   1.e6
 139061 139061 1 1.40E+05  0.   1.e6
 130136 130136 1 1.19E+05  0.   1.e6
 130108 130108 1 9.44E+04  0.   1.e6
 132787 132787 1 1.01E+05  0.   1.e6
 132760 132760 1 8.03E+04  0.   1.e6
 139220 139220 1 1.75E+05  0.   1.e6
 139195 139195 1 1.64E+05  0.   1.e6
 139086 139086 1  2.50e4  0.   1.e6
 135164 135164 1  2.50e4  0.   1.e6
 130866 130866 1  2.50e4  0.   1.e6
 118841 118841 1  2.50e4  0.   1.e6
 0
stop
```

F-5.0 EXAMPLE OUTPUT FOR FEHM, SVE EAST TURNED ON FOR 7 YEARS

The output at 1615 days after the start of SVE is shown below, annotated in red.

```
Time Step      1615

                Timing Information
        Years            Days         Step Size (Days)
```

```
    9.89185489         3613.00000         1.00000000
Cpu Sec for Time Step =  0.6538     Current Total =     2732.

                 Equation Performance
Number of N-R Iterations:          2
 Avg # of Linear Equation Solver Iterations:   0.5
 Number of Active Nodes:     71688.
 Total Number of Iterations, N-R:       3230 , Solver:       2742
 Phase Changes This Time Step:        0 Total           0
 Nodes Liq Phase:        0 change        0
 Nodes Two Phase:   143377 change        0
 Nodes Gas Phase:        0 change        0
 Number of restarted time steps           0
                 Largest Residuals
 EQ1 R=  0.1486E-08 node=     42 x= 410.0     y= 0.000     z= 1737.
 EQ2 R=  0.1984E-12 node=  18227 x= 400.0     y= 150.0     z= 1954.

                 Nodal Information (Water)
                                          source/sink
  Node   P (MPa)     E (MJ)    L sat     Temp (C)     (kg/s)
 125193   0.7762E-01  0.00     0.150       15.000    0.000
 118839   0.7665E-01  0.00     0.150       15.000    0.000
 111407   0.7542E-01  0.00     0.150       15.000    0.000
 101341   0.7488E-01  0.00     0.150       15.000    0.000
  91834   0.7562E-01  0.00     0.150       15.000    0.000
  82258   0.7648E-01  0.00     0.150       15.000    0.000
  72682   0.7721E-01  0.00     0.150       15.000    0.000
 135137   0.7922E-01  0.00     0.600E-01   15.000    0.000
 123130   0.7822E-01  0.00     0.150       15.000    0.000
 105721   0.7721E-01  0.00     0.150       15.000    0.000
  79028   0.7788E-01  0.00     0.150       15.000    0.000
  48704   0.7880E-01  0.00     0.150       15.000    0.000
  31148   0.7929E-01  0.00     0.400       15.000    0.000
  21572   0.7994E-01  0.00     0.350       15.000    0.000
 131754   0.7880E-01  0.00     0.600E-01   15.000    0.000
 125196   0.7820E-01  0.00     0.150       15.000    0.000
 119960   0.7775E-01  0.00     0.150       15.000    0.000
 136730   0.7905E-01  0.00     0.600E-01   15.000    0.000
 130804   0.7805E-01  0.00     0.150       15.000    0.000
 123091   0.7687E-01  0.00     0.150       15.000    0.000
 115221   0.7582E-01  0.00     0.150       15.000    0.000
 104226   0.7502E-01  0.00     0.150       15.000    0.000
 132595   0.7874E-01  0.00     0.600E-01   15.000    0.000
 130836   0.7855E-01  0.00     0.150       15.000    0.000
 128073   0.7825E-01  0.00     0.150       15.000    0.000
 125161   0.7795E-01  0.00     0.150       15.000    0.000
 122080   0.7764E-01  0.00     0.150       15.000    0.000
  16825   0.8046E-01  0.00     0.202E-01   15.000    0.000
  24805   0.7969E-01  0.00     0.350       15.000    0.000
  37573   0.7906E-01  0.00     0.400       15.000    0.000
  98219   0.7695E-01  0.00     0.150       15.000    0.000
 107203   0.7687E-01  0.00     0.150       15.000    0.000
```

130867	0.7872E-01	0.00	0.150	15.000	0.000
16822	0.8053E-01	0.00	0.203E-01	15.000	0.000
26398	0.7968E-01	0.00	0.350	15.000	0.000
39166	0.7900E-01	0.00	0.400	15.000	0.000
98216	0.7497E-01	0.00	0.150	15.000	0.000
107200	0.7484E-01	0.00	0.150	15.000	0.000
131751	0.7850E-01	0.00	0.150	15.000	0.000
16784	0.8043E-01	0.00	0.202E-01	15.000	0.000
26360	0.7958E-01	0.00	0.350	15.000	0.000
37532	0.7910E-01	0.00	0.400	15.000	0.000
98178	0.7728E-01	0.00	0.150	15.000	0.000
107162	0.7720E-01	0.00	0.150	15.000	0.000
130837	0.7885E-01	0.00	0.150	15.000	0.000
16740	0.8043E-01	0.00	0.203E-01	15.000	0.000
26316	0.7940E-01	0.00	0.350	15.000	0.000
37488	0.7868E-01	0.00	0.400	15.000	0.000
98134	0.7510E-01	0.00	0.150	15.000	0.000
107118	0.7500E-01	0.00	0.150	15.000	0.000
131691	0.7819E-01	0.00	0.150	15.000	0.000
129905	0.7901E-01	0.00	0.150	15.000	-0.000
129934	0.7805E-01	0.00	0.150	15.000	-0.000
132566	0.7921E-01	0.00	0.600E-01	15.000	-0.000
132594	0.7842E-01	0.00	0.600E-01	15.000	-0.000
139038	0.7970E-01	0.00	0.600E-01	15.000	-0.000
139061	0.7931E-01	0.00	0.600E-01	15.000	-0.000
130136	0.8009E-01	0.00	0.150	15.000	-0.000
130108	0.8010E-01	0.00	0.150	15.000	-0.000
132787	0.8007E-01	0.00	0.150	15.000	-0.000
132760	0.8007E-01	0.00	0.150	15.000	-0.000
139220	0.8002E-01	0.00	0.600E-01	15.000	-0.000
139195	0.8001E-01	0.00	0.600E-01	15.000	-0.000
142713	0.7993E-01	0.00	0.600E-01	15.000	0.000
143048	0.5387E-01	0.00	0.600E-01	15.000	-0.000
142708	0.8002E-01	0.00	0.600E-01	15.000	-0.000
143043	0.8001E-01	0.00	0.600E-01	15.000	-0.000
142838	0.8017E-01	0.00	0.600E-01	15.000	0.000
142014	0.7993E-01	0.00	0.600E-01	15.000	0.000

Nodal Information (Vapor)

	Air(Vapor)		source/sink	
Node	P (MPa)	Cap P (MPa)	Liq P (MPa)	Air(vp) (kg/s)
125193	0.7762E-01	0.000	0.7762E-01	0.000
118839	0.7665E-01	0.000	0.7665E-01	0.000
111407	0.7542E-01	0.000	0.7542E-01	0.000
101341	0.7488E-01	0.000	0.7488E-01	0.000
91834	0.7562E-01	0.000	0.7562E-01	0.000
82258	0.7648E-01	0.000	0.7648E-01	0.000
72682	0.7721E-01	0.000	0.7721E-01	0.000
135137	0.7922E-01	0.000	0.7922E-01	0.000
123130	0.7822E-01	0.000	0.7822E-01	0.000
105721	0.7721E-01	0.000	0.7721E-01	0.000
79028	0.7788E-01	0.000	0.7788E-01	0.000

48704	0.7880E-01	0.000	0.7880E-01	0.000
31148	0.7929E-01	0.000	0.7929E-01	0.000
21572	0.7994E-01	0.000	0.7994E-01	0.000
131754	0.7880E-01	0.000	0.7880E-01	0.000
125196	0.7820E-01	0.000	0.7820E-01	0.000
119960	0.7775E-01	0.000	0.7775E-01	0.000
136730	0.7905E-01	0.000	0.7905E-01	0.000
130804	0.7805E-01	0.000	0.7805E-01	0.000
123091	0.7687E-01	0.000	0.7687E-01	0.000
115221	0.7582E-01	0.000	0.7582E-01	0.000
104226	0.7502E-01	0.000	0.7502E-01	0.000
132595	0.7874E-01	0.000	0.7874E-01	0.000
130836	0.7855E-01	0.000	0.7855E-01	0.000
128073	0.7825E-01	0.000	0.7825E-01	0.000
125161	0.7795E-01	0.000	0.7795E-01	0.000
122080	0.7764E-01	0.000	0.7764E-01	0.000
16825	0.8046E-01	0.000	0.8046E-01	0.000
24805	0.7969E-01	0.000	0.7969E-01	0.000
37573	0.7906E-01	0.000	0.7906E-01	0.000
98219	0.7695E-01	0.000	0.7695E-01	0.000
107203	0.7687E-01	0.000	0.7687E-01	0.000
130867	0.7872E-01	0.000	0.7872E-01	0.000
16822	0.8053E-01	0.000	0.8053E-01	0.000
26398	0.7968E-01	0.000	0.7968E-01	0.000
39166	0.7900E-01	0.000	0.7900E-01	0.000
98216	0.7497E-01	0.000	0.7497E-01	0.000
107200	0.7484E-01	0.000	0.7484E-01	0.000
131751	0.7850E-01	0.000	0.7850E-01	0.000
16784	0.8043E-01	0.000	0.8043E-01	0.000
26360	0.7958E-01	0.000	0.7958E-01	0.000
37532	0.7910E-01	0.000	0.7910E-01	0.000
98178	0.7728E-01	0.000	0.7728E-01	0.000
107162	0.7720E-01	0.000	0.7720E-01	0.000
130837	0.7885E-01	0.000	0.7885E-01	0.000
16740	0.8043E-01	0.000	0.8043E-01	0.000
26316	0.7940E-01	0.000	0.7940E-01	0.000
37488	0.7868E-01	0.000	0.7868E-01	0.000
98134	0.7510E-01	0.000	0.7510E-01	0.000
107118	0.7500E-01	0.000	0.7500E-01	0.000
131691	0.7819E-01	0.000	0.7819E-01	0.000
129905	0.7901E-01	0.000	0.7901E-01	-0.5000E-12
129934	0.7805E-01	0.000	0.7805E-01	-0.5000E-12
132566	0.7921E-01	0.000	0.7921E-01	-0.5000E-12
132594	0.7842E-01	0.000	0.7842E-01	-0.5000E-12
139038	0.7970E-01	0.000	0.7970E-01	-0.5000E-12
139061	0.7931E-01	0.000	0.7931E-01	-0.5000E-12
130136	0.8009E-01	0.000	0.8009E-01	-0.5000E-12
130108	0.8010E-01	0.000	0.8010E-01	-0.5000E-12
132787	0.8007E-01	0.000	0.8007E-01	-0.5000E-12
132760	0.8007E-01	0.000	0.8007E-01	-0.5000E-12
139220	0.8002E-01	0.000	0.8002E-01	-0.5000E-12
139195	0.8001E-01	0.000	0.8001E-01	-0.5000E-12

142713	0.7993E-01	0.000	0.7993E-01	0.000
143048	**0.5387E-01**	**0.000**	**0.5387E-01**	**0.5815E-01**
142708	0.8002E-01	0.000	0.8002E-01	-0.1045E-11
143043	0.8001E-01	0.000	0.8001E-01	-0.4283E-10
142838	0.8017E-01	0.000	0.8017E-01	0.000
142014	0.7993E-01	0.000	0.7993E-01	0.000

Pressure in the SVE East wellhead fixed to measured values produces a mass flow of 0.058 kg/s approx. equal to the measured 100 scfm outflow

Global Mass Balances (Vapor)
Vapor discharge this time step: 0.502468E+04 kg
Total vapor discharge: 0.811583E+07 kg

Net kg vapor discharge (total out-total in): 0.549644E+05
Conservation Error: 0.133368E-02

Global Water & Air Balances
Total water in system at this time: 0.182389E+10 kg
Total mass of steam in system at this time: 0.000000E+00 kg
Total Air(gas) in system at this time: 0.870246E+07 kg

Water discharge this time step: 0.000000E+00 kg (0.000000E+00 kg/s)
Water input this time step: 0.000000E+00 kg (0.000000E+00 kg/s)
Total water discharge: 0.000000E+00 kg (0.000000E+00 kg/s)
Total water input: 0.000000E+00 kg (0.000000E+00 kg/s)

Air(gas) discharge this time step: 0.502468E+04 kg (0.581560E-01 kg/s)
Air(gas) input this time step: 0.501684E+04 kg (**0.580653E-01 kg/s**) Gas outflow is dominated
Total air(gas) discharge: 0.811583E+07 kg (0.259987E-01 kg/s) by SVE at 100 scfm
Total air(gas) input: 0.806086E+07 kg (0.258226E-01 kg/s)

Net kg water discharge (total out-total in): 0.000000E+00
Net kg air discharge (total out-total in): 0.549644E+05
Conservation Errors: 0.000000E+00 (water), 0.133368E-02 (air)

****

Solute information at time = 3613.00 days
Num of solute timesteps 2 Avg tstep = 0.500000 SAI Iter = 6460 Tot SAI iter 5219680

Nodal Information (Tracer)
Solute output information, species number 1

Node	an	anl	anv	src/sink mol/s	sinkint	equation residual
125193	0.39032E-07	0.39032E-07	0.19485E-04	0.0000	0.0000	0.14126E-17
118839	0.68992E-07	0.68992E-07	0.34877E-04	0.0000	0.0000	0.13389E-17
111407	0.91310E-07	0.91310E-07	0.46914E-04	0.0000	0.0000	-0.15531E-17
101341	0.16417E-06	0.16417E-06	0.84960E-04	0.0000	0.0000	-0.79525E-14
91834	0.19564E-05	0.19564E-05	0.10025E-02	0.0000	0.0000	0.25791E-15
82258	0.22168E-05	0.22168E-05	0.11232E-02	0.0000	0.0000	0.28035E-15
72682	0.23677E-05	0.23677E-05	0.11883E-02	0.0000	0.0000	0.28241E-15
135137	0.16273E-06	0.16273E-06	0.79595E-04	0.0000	0.0000	0.28747E-18
123130	0.36708E-06	0.36708E-06	0.18185E-03	0.0000	0.0000	0.32861E-17
105721	0.17381E-07	0.17381E-07	0.87229E-05	0.0000	0.0000	-0.50625E-16
79028	0.33355E-05	0.33355E-05	0.16595E-02	0.0000	0.0000	0.64488E-15

48704	0.32236E-05	0.32236E-05	0.15853E-02	0.0000	0.0000	0.68511E-15
31148	0.22012E-05	0.22012E-05	0.10757E-02	0.0000	0.0000	0.59679E-15
21572	0.96302E-06	0.96302E-06	0.46683E-03	0.0000	0.0000	0.27121E-15
131754	0.56369E-07	0.56369E-07	0.27720E-04	0.0000	0.0000	0.32102E-18
125196	0.77548E-07	0.77548E-07	0.38428E-04	0.0000	0.0000	0.10741E-17
119960	0.86461E-07	0.86461E-07	0.43093E-04	0.0000	0.0000	0.22116E-17
136730	0.10062E-06	0.10062E-06	0.49324E-04	0.0000	0.0000	0.40395E-20
130804	0.24507E-06	0.24507E-06	0.12168E-03	0.0000	0.0000	0.38151E-19
123091	0.41653E-06	0.41653E-06	0.20996E-03	0.0000	0.0000	0.29415E-18
115221	0.46577E-06	0.46577E-06	0.23803E-03	0.0000	0.0000	0.12635E-17
104226	0.40286E-07	0.40286E-07	0.20809E-04	0.0000	0.0000	-0.40472E-15
132595	0.25062E-06	0.25062E-06	0.12334E-03	0.0000	0.0000	0.17698E-18
130836	0.28265E-06	0.28265E-06	0.13945E-03	0.0000	0.0000	0.29978E-18
128073	0.32445E-06	0.32445E-06	0.16067E-03	0.0000	0.0000	0.56571E-18
125161	0.34675E-06	0.34675E-06	0.17237E-03	0.0000	0.0000	0.10170E-17
122080	0.35738E-06	0.35738E-06	0.17836E-03	0.0000	0.0000	0.17436E-17
16825	0.23183E-06	0.23183E-06	0.11166E-03	0.0000	0.0000	0.56114E-16
24805	0.11886E-05	0.11886E-05	0.57792E-03	0.0000	0.0000	0.34447E-15
37573	0.22281E-05	0.22281E-05	0.10921E-02	0.0000	0.0000	0.61054E-15
98219	0.94902E-06	0.94902E-06	0.47792E-03	0.0000	0.0000	0.18449E-15
107203	0.12662E-07	0.12662E-07	0.63829E-05	0.0000	0.0000	-0.24198E-16
130867	0.59513E-07	0.59513E-07	0.29297E-04	0.0000	0.0000	0.40573E-18
16822	0.19577E-06	0.19577E-06	0.94202E-04	0.0000	0.0000	0.36156E-16
26398	0.10553E-05	0.10553E-05	0.51324E-03	0.0000	0.0000	0.23546E-15
39166	0.17644E-05	0.17644E-05	0.86547E-03	0.0000	0.0000	0.25492E-15
98216	0.12286E-05	0.12286E-05	0.63500E-03	0.0000	0.0000	0.16184E-15
107200	0.25108E-07	0.25108E-07	0.13000E-04	0.0000	0.0000	-0.60665E-16
131751	0.15210E-07	0.15210E-07	0.75082E-05	0.0000	0.0000	0.61773E-18
16784	0.26262E-06	0.26262E-06	0.12652E-03	0.0000	0.0000	0.64797E-16
26360	0.15927E-05	0.15927E-05	0.77548E-03	0.0000	0.0000	0.44165E-15
37532	0.26796E-05	0.26796E-05	0.13128E-02	0.0000	0.0000	0.68841E-15
98178	0.93399E-06	0.93399E-06	0.46835E-03	0.0000	0.0000	0.17682E-15
107162	0.54207E-07	0.54207E-07	0.27208E-04	0.0000	0.0000	-0.54463E-16
130837	0.24944E-06	0.24944E-06	0.12259E-03	0.0000	0.0000	0.76147E-18
16740	0.20508E-06	0.20508E-06	0.98803E-04	0.0000	0.0000	0.54243E-16
26316	0.10762E-05	0.10762E-05	0.52520E-03	0.0000	0.0000	0.35340E-15
37488	0.16143E-05	0.16143E-05	0.79506E-03	0.0000	0.0000	0.50832E-15
98134	0.15091E-05	0.15091E-05	0.77862E-03	0.0000	0.0000	0.27927E-15
107118	0.13668E-06	0.13668E-06	0.70616E-04	0.0000	0.0000	-0.56717E-15
131691	0.21728E-06	0.21728E-06	0.10768E-03	0.0000	0.0000	0.28774E-19
129905	0.42194E-05	0.42194E-05	0.20693E-02	-0.52500E-07	-7.3256	0.13253E-17
129934	0.23916E-05	0.23916E-05	0.11873E-02	-0.39100E-07	-5.4559	0.13366E-18
132566	0.35788E-05	0.35788E-05	0.17508E-02	-0.55500E-07	-7.7442	0.65497E-18
132594	0.20406E-05	0.20406E-05	0.10084E-02	-0.42700E-07	-5.9582	0.62926E-19
139038	0.29126E-05	0.29126E-05	0.14161E-02	-0.78500E-07	-10.954	0.13602E-18
139061	0.17746E-05	0.17746E-05	0.86707E-03	-0.70000E-07	-9.7675	0.14045E-19
130136	0.23333E-05	0.23333E-05	0.11289E-02	-0.59500E-07	-8.3024	0.29455E-17
130108	0.26924E-05	0.26924E-05	0.13026E-02	-0.47200E-07	-6.5861	0.12296E-16
132787	0.23895E-05	0.23895E-05	0.11564E-02	-0.50500E-07	-7.0466	0.21289E-17
132760	0.29706E-05	0.29706E-05	0.14377E-02	-0.40150E-07	-5.6024	0.99031E-17
139220	0.43694E-05	0.43694E-05	0.21159E-02	-0.87500E-07	-12.209	0.18676E-17
139195	0.47203E-05	0.47203E-05	0.22860E-02	-0.82000E-07	-11.442	0.11512E-17

```
142713  0.23342E-05  0.23342E-05  0.11316E-02  0.0000      0.0000      0.41852E-15
143048  0.14510E-06  0.14510E-06  0.10437E-03  0.60689E-05  9909.9     0.16201E-21  TCA leaving
142708  0.11876E-04  0.11876E-04  0.57513E-02  0.0000      0.0000      0.59401E-15    in mol/s
143043  0.17704E-06  0.17704E-06  0.85748E-04  0.0000      0.0000      0.29663E-16
142838  0.73738E-06  0.73738E-06  0.35641E-03  0.0000      0.0000      0.12566E-12
142014  0.10417E-06  0.10417E-06  0.50502E-04  0.0000      0.0000      0.45990E-17

 initial mass =                  0.114451E+05 mol        Initial plume TCA in moles
 current mass =                  0.154815E+04 mol
 total injected mass =           0.983938E+02 mol ( 0.705150E-06 mol/s)  TCA leaking from drums
 total produced mass =           0.999538E+04 mol ( 0.616227E-05 mol/s)
 total mass produced by reaction =  -0.000000E+00 mol
 net mass balance =              0.964205E-03 mol
-------------------------------------------------------------------------------------------------
*******************************************************************
```

F-6.0 REFERENCES

Anderson, T., B. Stewart, P. Mark, P.H. Stauffer, and J.K. Hopkins, February 25–March 1, 2007. “A Soil Vapor Extraction Pilot Study in a Deep Arid Vadose Zone, Part 1: Field Study Summary,” Waste Management Conference 2007, February 25–March 1, 2007, Tucson, Arizona. (Anderson et al. 2007, 702070)

Behar, H.R., E.E. Snyder, S. Marczak, L.J. Salazar, B. Rappe, G.F. Fordham, S.P. Chu, D.M. Strobridge, K.H. Birdsell, T.A. Miller, K.C. Rich, and P.H. Stauffer, February 2019. “An Investigation of Plume Response to Soil Vapor Extraction and Hypothetical Drum Failure,” *Vadose Zone Journal,* Vol. 18, No. 1. (Behar et al. 2019, 700854)

Bourret, S.M., E.M. Kwicklis, T.A. Miller, and P.H. Stauffer, March 2019. “Evaluating the Importance of Barometric Pumping for Subsurface Gas Transport Near an Underground Nuclear Test Site,” *Vadose Zone Journal,* Vol. 18, No. 1. (Bourret et al. 2019, 702060)

Dash, Z.V., B.A. Robinson, R.J. Pawar, and S. Chu, December 14, 2015. “Software Validation Report for the FEHM Application Version 3.1 - 3.X,” Los Alamos National Laboratory document LA-UR-15-27776, Los Alamos, New Mexico. (Dash et al. 2015, 702067)

Harp, D.R., J.P. Ortiz, and P.H. Stauffer, July 2019. “Identification of Dominant Gas Transport Frequencies during Barometric Pumping of Fractured Rock,” *Scientific Reports,* Vol. 9, Article 9537. (Harp et al. 2019, 702068)

Johnson, P.J., S. Otto, D.J. Weaver, B. Dozier, T.A. Miller, A.B. Jordan, N.G. Hayes-Rich, and P.H. Stauffer, February 2019. “Heat-Generating Nuclear Waste in Salt: Field Testing and Simulation,” *Vadose Zone Journal,* Vol. 18, No. 1. (Johnson et al. 2019, 702061)

Johnson, P.J., G.A. Zyvoloski, and P.H. Stauffer, November 2018. “Impact of a Porosity-Dependent Retention Function on Simulations of Porous Flow,” *Transport in Porous Media,* Vol. 127, 1, pp. 211-232. (Johnson et al. 2019, 702062)

LANL (Los Alamos National Laboratory), November 2006. "Summary Report: 2006 In Situ Soil Vapor Extraction Pilot Study at Material Disposal Area L, Technical Area 54, Los Alamos National Laboratory," Los Alamos National Laboratory document LA-UR-06-7900, Los Alamos, New Mexico. (LANL 2006, 094152)

LANL (Los Alamos National Laboratory), September 2011. "Corrective Measures Evaluation Report for Material Disposal Area L, Solid Waste Management Unit 54-006, at Technical Area 54, Revision 2," Los Alamos National Laboratory document LA-UR-11-4798, Los Alamos, New Mexico. (LANL 2011, 205756)

LANL (Los Alamos National Laboratory), September 2014. "Interim Measures Work Plan for Soil-Vapor Extraction of Volatile Organic Compounds from Material Disposal Area L, Technical Area 54, Revision 1," Los Alamos National Laboratory document LA-UR-14-26472, Los Alamos, New Mexico. (LANL 2014, 261843)

LANL (Los Alamos National Laboratory), September 2015. "Interim Measures Progress Report for Soil-Vapor Extraction of Volatile Organic Compounds from Material Disposal Area L, Technical Area 54," Los Alamos National Laboratory document LA-UR-15-26893, Los Alamos, New Mexico. (LANL 2015, 600930)

LANL (Los Alamos National Laboratory), July 2016. "Work Plan for a Tracer Test at Material Disposal Area G, Technical Area 54," Los Alamos National Laboratory document LA-UR-16-24628, Los Alamos, New Mexico. (LANL 2016, 601622)

N3B (Newport News Nuclear BWXT-Los Alamos, LLC), August 2018. "Interim Measures Final Report for Soil-Vapor Extraction of Volatile Organic Compounds from Material Disposal Area L, Technical Area 54," Newport News Nuclear BWXT-Los Alamos, LLC, document EM2018-0008, Los Alamos, New Mexico. (N3B 2018, 700039)

Neeper, D.A., 2002. "Investigation of the Vadose Zone Using Barometric Pressure Cycles," *Journal of Contaminant Hydrology,* Vol. 54, pp. 59-80. (Neeper 2002, 098639)

Neeper, D.A., and P.H. Stauffer, May 2012. "Transport by Oscillatory Flow in Soils with Rate-Limited Mass Transfer: 1. Theory," *Vadose Zone Journal,* Vol. 11, No. 2. (Neeper and Stauffer 2012, 601587)

Snyder, E., S. Marczak, L. Salazar, G. Fordham, S. Chu, D. Strobridge, K. Birdsell, K. Rich, and P. Stauffer, March 5–9, 2017. "The Impact of Soil Vapor Extraction at Material Disposal Area L, Los Alamos National Laboratory - 17155," Waste Management 2017 Conference, March 5–9, 2017, Phoenix, Arizona. (Snyder et al. 2017, 702064)

Stauffer, P., H.R. Behar, D. Diehl, J. Hopkins, K. Ocker, E. Snyder, and C. Rodriguez, March 6–10, 2022. "3-D Numerical Modeling for Decision Support, Material Disposal Area L, LANL, NM, USA - 22037," Waste Management 2022 Conference, March 6–10, 2022, Phoenix, Arizona. (Stauffer et al. 2022, 702065)

Stauffer, P., K. Birdsell, and W. Rice, March 7–11, 2011. "3-D Model Validation in Support of Site Closure, Material Disposal Area L, Los Alamos, NM," Paper 11545, Waste Management 2011 Conference, March 7–11, 2011, Phoenix, AZ. (Stauffer et al. 2011, 255584)

Stauffer, P.H., K.H. Birdsell, M.S. Witkowski, and J.K. Hopkins, 2005. "Vadose Zone Transport of 1,1,1-Trichloroethane: Conceptual Model Validation through Numerical Simulation," *Vadose Zone Journal,* Vol. 4, pp. 760–773. (Stauffer et al. 2005, 090537)

Stauffer, P.H., J.K. Hopkins, and T. Anderson, February 25–March 1, 2007. "A Soil Vapor Extraction Pilot Study in a Deep Arid Vadose Zone, Part 2: Simulations in Support of Decision Making Processes," Waste Management Conference 2007, February 25–March 1, 2007, Tucson, Arizona. (Stauffer et al. 2007, 104950)

Stauffer, P.H., T. Rahn, J.P. Ortiz, L. Salazar, H. Boukalfa, and E. Snyder, December 21, 2017. "A Gas Transport Tracer Test in the Deep Cerros Del Rio Basalts, Mesita del Buey, Los Alamos NM," Los Alamos National Laboratory document LA-UR-17-31351, Los Alamos, New Mexico. (Stauffer et al. 2017, 602792)

Stauffer, P.H., T. Rahn, J.P. Ortiz, L.J. Salazar, H. Boukhalfa, H.R. Behar, and E.E. Snyder, March 2, 2019. "Evidence for High Rates of Gas Transport in the Deep Subsurface," *Geophysical Research Letters,* Vol. 46, No. 7. (Stauffer et al. 2019, 700871)

Vrugt, J.A., P.H. Stauffer, T. Wöhling, B.A. Robinson, and V.V. Vesselinov, May 2008. "Inverse Modeling of Subsurface Flow and Transport Properties: A Review with New Developments," *Vadose Zone Journal,* Vol. 7, No. 2, pp. 843–864. (Vrugt et al. 2008, 104951)

Zyvoloski, G.A., B.A. Robinson, Z.V. Dash, S. Kelkar, H.S. Viswanathan, R.J. Pawar, P.H. Stauffer, T.A. Miller, and S. Chu, December 14, 2015. "Software Users Manual (UM) for the FEHM Application Version 3.1 - 3.X," Los Alamos National Laboratory document LA-UR-12-24493, Los Alamos, New Mexico. (Zyvoloski et al. 2015, 702066)

Zyvoloski, G.A., B.A. Robinson, Z.V. Dash, and L.L. Trease, March 30, 1995. "Models and Methods Summary for the FEHMN Application," Los Alamos National Laboratory document LA-UR-94-3787, Los Alamos, New Mexico. (Zyvoloski et al. 1994, 054420)

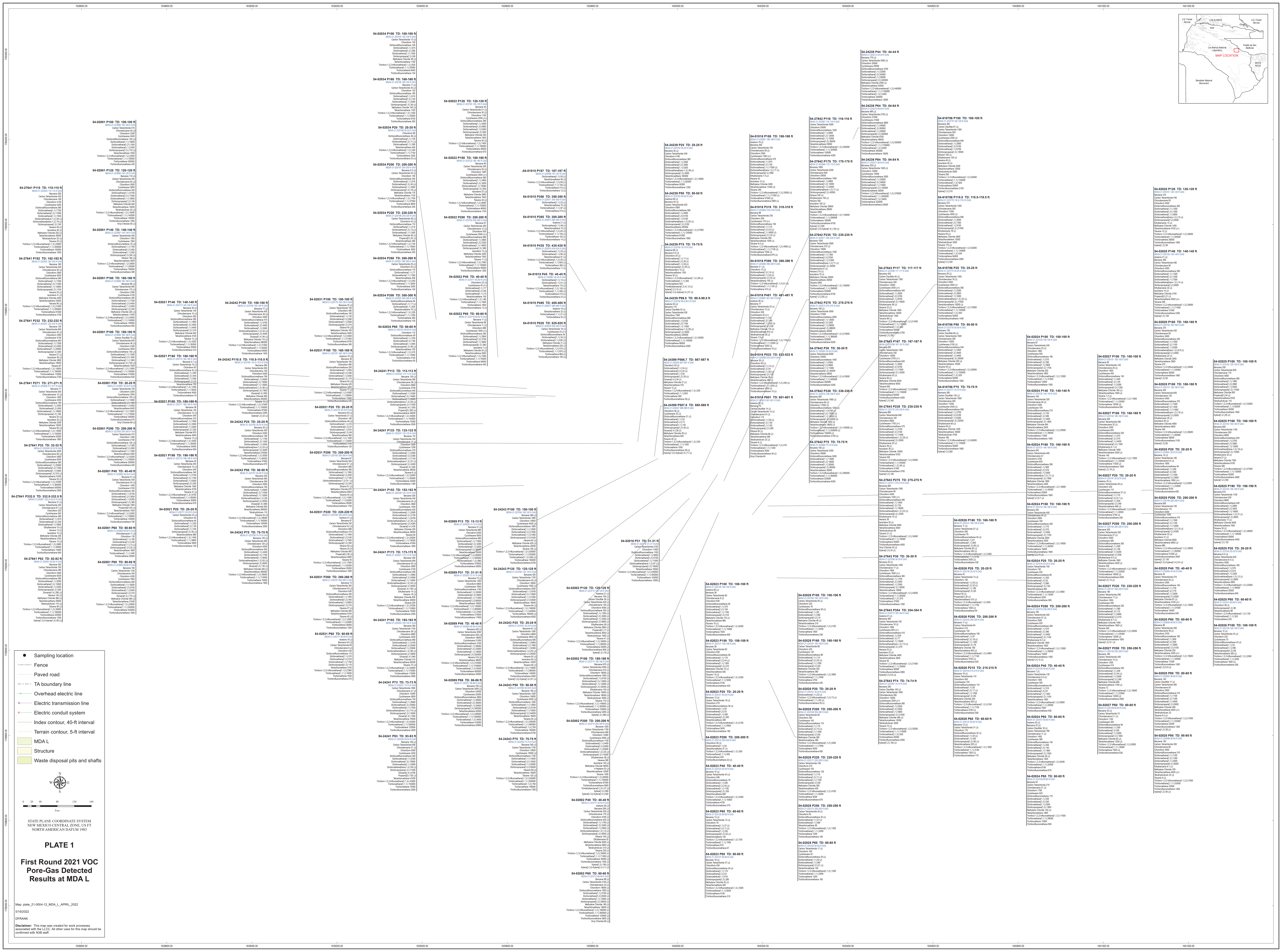
Sampling location
Fence
Paved road
TA boundary line
Overhead electric line
Electric transmission line
Electric conduit system
Index contour, 40-ft interval
Terrain contour, 5-ft interval
MDA L
Structure
Waste disposal pits and shafts
N
W
E
S
0 20 40 80 120 160
Feet
STATE PLANE COORDINATE SYSTEM
NEW MEXICO CENTRAL ZONE, US FT
NORTH AMERICAN DATUM 1983
PLATE 1
First Round 2021 VOC Pore-Gas Detected Results at MDA L
Map: plate_21-0004-12_MDA_L_APRIL_2022
5/16/2022
DFRANK
Disclaimer: This map was created for work processes associated with the LLCC. All other uses for this map should be confirmed with N3B staff.
MAP LOCATION